Special Issue in Honor of the 65th Birthday of Professor Imre J. Rudas

Foreword

This special issue of *Acta Polytechnica Hungarica* is dedicated to Professor Imre J. Rudas on the occasion of his 65th birthday and in recognition of his outstanding contributions to computational intelligence, robotics with special emphasis on robot control, soft computing, computer-aided process planning, fuzzy control and fuzzy sets. The issue can be considered as a complement to the edited volume *J. Fodor and R. Fullér (Eds.), Advances in Soft Computing, Intelligent Robotics and Control (Topics in Intelligent Engineering and Informatics, vol. 8) (Springer-Verlag, Berlin, Heidelberg, 2014)*. The manuscripts were submitted in response to direct invitations from the Editor-in-Chief, containing contributions from some of Imre's past collaborators. The guest editors are grateful to the authors for their excellent work.

It is almost impossible to summarize in a short foreword the accomplishments of the honoree. At the age of 65 he is an author of books, book chapters, journal papers, conference proceedings papers, all together over 700 scientific publications in the mentioned fields.

Professor Imre J. Rudas graduated from Bánki Donát Polytechnic, Budapest in 1971, received the Master Degree in Mathematics from the Eötvös Loránd University, Budapest, the Ph.D. in Robotics from the Hungarian Academy of Sciences in 1987, while the Doctor of Science degree from the Hungarian Academy of Sciences in 2004. He received his first Doctor Honoris Causa degree from the Technical University of Košice, Slovakia and the second one from "Politehnica" University of Timisoara, Romania.

He founded Acta Polytechnica Hungarica, an international peer-reviewed scientific journal, which started to own impact factor after 6 years of its existence. He is the founder of seven IEEE sponsored international conference and symposium series. He is the only rector in the Hungarian higher-education who could establish a new university (Óbuda University) by upgrading an existing institution (Budapest Tech), through the fulfillment of high standards.

Imre is a Fellow of IEEE, Senior Administrative Committee member of IEEE Industrial Electronics Society, member of Board of Governors of IEEE SMC Society. He was the Chair of IEEE Hungary Section, Vice-President of IFSA (International Fuzzy System Association), the President of Hungarian Fuzzy Association for ten years, Steering Committee Member of the Hungarian Robotics Association and the John von Neumann Computer Society.He serves as an associate editor of diverse scientific journals, member of various national and international scientific committees.

His present areas of research activity are Computational Cybernetics, Robotics with special emphasis on Robot Control, Soft Computing, Computer-aided Process Planning, Fuzzy Control and Fuzzy Sets. He has published books, more than 700 papers in books, various scientific journals and international conference proceedings. Imre J. Rudas' personal qualities of commitment, integrity, leadership and initiate leave lasting impression on his colleagues, students and friends.

The present issue is a collection of 15 papers written by respectable experts of the fields. Professor Rudas's wide spectrum of interests is reflected in the variety of these contributions, dealing with three major topics: intelligent robotics; fundamental aspects of soft computing; and issues and methods of applied mathematics.

We wish Imre the best of health, energy and happiness in the years ahead, and we count on his activities and contributions to scientific projects for many years to come.

János Fodor and Róbert Fullér

Guest editors

Loop Shifting and Non-Conservative qLPV Design

József Bokor[1] and Zoltán Szabó[2]

[1] MTA-BME Control Engineering Research Group, Computer and Automation Research Institute, Hungarian Academy of Sciences, Hungary; e-mail: bokor@sztaki.hu

[2] Computer and Automation Research Institute, Hungarian Academy of Sciences, Hungary; e-mail: szaboz@sztaki.hu

Abstract: As an extension of the robust H_∞ theory, the time domain design based on linear matrix inequalities (LMI) is a conceptually simple and efficient framework to obtain qLPV controllers. However, the constructed scheduling variables are not always suitable for an efficient implementation. This paper investigates the possibility of constructing the scheduling block of a qLPV controller explicitly, i.e., in the form of a linear fractional transformation (LFT). It is shown here that if both the primary and dual multiplier LMI equations lead to maximal indefinite subspaces and a coupling condition holds, the problem can be solved and a constructive algorithm results to build the desired scheduling variables.

Keywords: Linear Fractional Transform; robust control; qLPV design

1 Introduction and Motivation

In modern control design a quasi-linear parameter varying (qLPV) description is frequently used [1]. The approach is based on the possibility of rewriting the plant in a form in which nonlinear terms can be hidden by using suitably defined scheduling variables by maintaining the linear structure of the model. An advantage is that in the entire operational interval nonlinear systems can be defined and a well-developed linear system theory, to analyze and design nonlinear control systems, can be used.

The models are augmented with performance specifications and uncertainties. Weighting functions are applied to the performance signals to meet performance specifications and guarantee a good tradeoff between performance results. The uncertainties are modeled by both un-modeled dynamics and parametric uncertainties. As a result of this construction a linear fractional transformation (LFT) interconnection structure, which is the basis of control design, is achieved. In this particular structure, also known as a $M-\Delta$ configuration, where the

parameter-varying terms (scheduling variables) are located in the diagonal of the Δ operator and the time invariant part is described by the linear operator M.

In the design of robust linear parameter varying controllers, the LMI-based linear time invariant (LTI) robust control design framework has a central role, [2], [7], [8], [9], [10], [16], [17]. As opposed to the gain scheduling technique these approaches provide a design algorithm that starts from an analysis equation that guarantees a certain (quadratic) performance level and the designed controller is supposed to fulfill the robust stability and performance requirements. Therefore, qLPV models with linear matrix inequalities (LMI), as the main design tool, seem to be the most efficient approach to achieve robust and non-conservative results.

While the main steps of the quadratic robust design are well-known, there are still a lot of questions concerning the practical construction. Many of the methods, in order to keep the design linear, restrict the multipliers of the scheduling variables to a predefined set, which makes these methods conservative in general.

In this paper, the control design problem is set in the framework presented in [9], [10], [11], that strongly exploits the available LMI techniques. As opposed to the gain scheduling technique these approaches provide a design algorithm that starts from an analysis equation that guarantees a certain (quadratic) performance level and the designed controller is supposed to fulfill the robust stability and performance requirements. The method has a certain level of conservatism due to the use of constant multipliers; however it can be the starting point of more elaborate designs [12].

Our interest in this method is motivated by both theoretical and practical issues. On a theoretical level this method is a direct extension of the $\mathcal{H}_\infty$ design theory to an LPV context. The LTI part of the controller and the scheduling block of the controller are obtained through a similar extension process as the controller itself in the original $\mathcal{H}_\infty$ setting. However, the extension related to the scheduling block is related to indefinite matrices that makes the process more challenging.

On the practical side the problem concerns the scheduling variables of the controller. In the general setting, i.e., when there are no restrictions imposed on certain blocks of the multipliers, the construction of the scheduling block involves an on-line computation of a spectral subspace of a time-varying matrix, which is a computationally demanding task for the implementation. It is preferred to obtain this block in an explicit form, e.g., as an LFT of the original scheduling variables. Thus, a post-processing method, like the tensor product transformation method [13] is needed.

The aim of the paper is to investigate the possibility of constructing the scheduling block of a LPV controller explicitly. It is shown that if both the primary and dual multiplier LMI equations leads to maximal indefinite subspaces and admits a common "loop-shifting", then the problem can be solved. Once this common "loop-shifting" exists, the proposed approach is constructive and an algorithm is also provided to build the desired block of scheduling variables.

For the sake of completeness, Section 2 provides a short overview of the classical LPV controller construction presented in [9] and [10]. The analysis and the development of the proposed method are contained in Section 3. The main idea exploited in the paper resembles the idea of the loop-shift in the classical control design; this motivates the title of the section. The analysis also contains clarifications and additions concerning the original problem setting treated in [9] and [10] that might help the deeper understanding of the different conditions involved in these algorithms.

2 Problem Setup

In this section we summarize the basic setup according to [10] and to ease the understanding we barrow the notations from that paper. Accordingly, the open loop generalized plant is defined as:

$$\begin{pmatrix} \dot{x}(t) \\ z_u(t) \\ z_p(t) \\ y(t) \end{pmatrix} = \begin{pmatrix} A & B_u & B_p & B \\ C_u & D_{uu} & D_{up} & E_u \\ C_p & D_{pu} & D_{pp} & E_p \\ C & F_u & F_p & 0 \end{pmatrix} \begin{pmatrix} x(t) \\ w_u(t) \\ w_p(t) \\ u(t) \end{pmatrix} \tag{1}$$

$$\begin{pmatrix} w_u(t) \\ z_u(t) \end{pmatrix} \in \mathcal{S}(\Delta(t)) \subset \mathbb{R}^{m_u+k_u}$$

while the output--feedback LPV controller for (1) is described as

$$\begin{pmatrix} \dot{x}_c(t) \\ u(t) \\ z_c(t) \end{pmatrix} = \begin{pmatrix} A_c & B_{c1} & B_{c2} \\ C_{c1} & D_{c11} & D_{c12} \\ C_{c2} & D_{c21} & D_{c22} \end{pmatrix} \begin{pmatrix} x_c(t) \\ y(t) \\ w_c(t) \end{pmatrix} \tag{2}$$

$$\begin{pmatrix} w_c(t) \\ z_c(t) \end{pmatrix} \in \mathcal{S}_c(\Delta(t)) \subset \mathbb{R}^{m_c+k_c},$$

where the on-line measured parameter satisfy $\Delta(t) \in \nabla$. As opposed to the original setting it is assumed that $\mathcal{S}(\Delta)$ and $\mathcal{S}_c(\Delta)$ admit the explicit description $Im\begin{pmatrix} \Delta \\ I_{k_u} \end{pmatrix}$ and $Im\begin{pmatrix} \Delta_c \\ I_{k_c} \end{pmatrix}$, respectively. Under the standing hypothesis of well-posedness and of continuity these assumptions do not restrict the generality.

The controller should fulfill the quadratic $\mathcal{H}_\infty$ performance, where the performance index γ is an indicator on the quality of the controller.

Theorem 1 (LPV analysis) *There exist a controller (2) such that closed-loop system is well-posed and stable if and only if there exist* X, Y, *multipliers* $P = \begin{pmatrix} Q & S \\ S^T & R \end{pmatrix}$ *and* $\tilde{P} = \begin{pmatrix} \tilde{Q} & \tilde{S} \\ \tilde{S}^T & \tilde{R} \end{pmatrix}$ *with* $P > 0$ *on* $\mathcal{S}(\Delta)$ *and* $\tilde{P} < 0$ *on* $\mathcal{S}(\Delta)^{\perp}$ *for all* $\Delta \in \nabla$ *that satisfy the matrix inequalities*

$$\begin{pmatrix} X & I \\ I & Y \end{pmatrix} \geq 0 \tag{3}$$

$$\Psi^T \begin{pmatrix} * & & & \\ & * & & \\ & & * & \\ & & & \end{pmatrix}^T \begin{pmatrix} 0 & X & 0 & 0 & 0 & 0 \\ X & 0 & 0 & 0 & 0 & 0 \\ 0 & 0 & Q & S & 0 & 0 \\ 0 & 0 & S^T & R & 0 & 0 \\ 0 & 0 & 0 & 0 & Q_p & S_p \\ 0 & 0 & 0 & 0 & S_p^T & R_p \end{pmatrix} \begin{pmatrix} I & 0 & 0 \\ A & B_u & B_p \\ 0 & I & 0 \\ C_u & D_{uu} & D_{up} \\ 0 & 0 & I \\ C_p & D_{pu} & D_{pp} \end{pmatrix} \Psi < 0, \tag{4}$$

$$\Phi^T \begin{pmatrix} * & & & \\ & * & & \\ & & * & \\ & & & \end{pmatrix}^T \begin{pmatrix} 0 & Y & 0 & 0 & 0 & 0 \\ Y & 0 & 0 & 0 & 0 & 0 \\ 0 & 0 & \tilde{Q} & \tilde{S} & 0 & 0 \\ 0 & 0 & \tilde{S}^T & \tilde{R} & 0 & 0 \\ 0 & 0 & 0 & 0 & \tilde{Q}_p & \tilde{S}_p \\ 0 & 0 & 0 & 0 & \tilde{S}_p{}^T & \tilde{R}_p \end{pmatrix} \begin{pmatrix} -A^T & -C_u^T & -C_p^T \\ I & 0 & 0 \\ -B_u^T & -D_{uu}^T & -D_{pu}^T \\ 0 & I & 0 \\ -B_p^T & -D_{up}^T & -D_{pp}^T \\ 0 & 0 & I \end{pmatrix} \Phi > 0, \tag{5}$$

where $\Phi = \mathrm{Ker}\begin{pmatrix} B^T & E_u^T & E_p^T \end{pmatrix}$ and $\Psi = \mathrm{Ker}\begin{pmatrix} C & F_u & F_p \end{pmatrix}$.

Usually conditions $R > 0$ and $\tilde{Q} < 0$ are also imposed. These conditions follow if we require that 0ha. In the original construction $\Delta_c(0) = 0$ is also supposed in order to get to the necessary inertia conditions, however, this requirement is not a natural one.

Controller synthesis starts with the solution of the analysis LMIs of Theorem 1 which usually involves a relaxation step, resulting in the matrices X, Y and $P, \tilde{P}$.

Then the Lyapunov matrix X_e of the closed-loop system can be obtained as

$$X_e = \begin{pmatrix} X & Z \\ Z^* & [Z^*(X - Y^{-1})Z]^{-1} \end{pmatrix}, \tag{6}$$

where $\mathrm{Im}Z = \mathrm{Im}(X - Y^{-1})$. The multiplier $\mathcal{P}$, corresponding to the scheduling variables, can be obtained from P and $\tilde{P}$ as follows:

$$P_e := \begin{pmatrix} P & UT \\ (UT)^T & T^T[U^T(P - \tilde{P}^{-1})U]^{-1}T \end{pmatrix}. \tag{7}$$

U is an orthogonal matrix such that $\mathrm{Im}U = \mathrm{Im}(P - \tilde{P}^{-1})$ and T is a suitable nonsingular matrix, for additional details see [10].

The LTI part of the LPV controller can be obtained by solving the quadratic matrix inequality:

$$\begin{pmatrix} I_m \\ \mathcal{C} + \mathcal{A}\mathcal{X}\mathcal{B} \end{pmatrix}^T \mathcal{M} \begin{pmatrix} I_m \\ \mathcal{C} + \mathcal{A}\mathcal{X}\mathcal{B} \end{pmatrix} < 0, \tag{8}$$

where $\mathcal{C} \in \mathbb{R}^{n\times m}$, $\mathcal{A} \in \mathbb{R}^{n\times k}$, $\mathcal{B} \in \mathbb{R}^{l\times m}$ are matrices that depend on the system matrices of the generalized plant M. The unknown is $\mathcal{X} = \begin{pmatrix} A_c & B_c \\ C_c & D_c \end{pmatrix} \in \mathbb{R}^{k\times l}$ and the multiplier $\mathcal{M}$ is assembled from X_e, P_e and the performance multiplier $P_p = \begin{pmatrix} -\gamma I & 0 \\ 0 & I \end{pmatrix}$. A numerically reliable algorithm and a parametrization of the solutions of this inequality was given by the authors in [14].

2.1 Scheduling Variables

The most delicate point of the algorithm is the construction of the scheduling variables. If we have for the blocks $Q < 0$ and $\tilde{R} > 0$ the multipliers P and $\tilde{P}$ of Theorem 1, then there is an explicit construction [9].

The key point is that the extended multiplier should inherit this property. This indeed is possible by setting

$$P_e := \begin{pmatrix} P & T \\ T^T & T^T N T \end{pmatrix}, \tag{9}$$

with $N = (P - \tilde{P}^{-1})^{-1}$ and $T = (T_1\ T_2)$ having the blocks $T_1 = TW, T_2 = T\widetilde{W}$, where $W = \begin{pmatrix} I \\ 0 \end{pmatrix}$, $\widetilde{W} = \begin{pmatrix} 0 \\ I \end{pmatrix}$.

These blocks are chosen to fulfill the conditions

$$T_1^T (N - WQ^{-1}W^T) T_1 < 0, \tag{10}$$

$$T_2^T (N - \widetilde{W}R^{-1}\widetilde{W}^T) T_2 > 0. \tag{11}$$

By permuting the blocks of P_e one has the partitioning $\begin{pmatrix} Q_e & S_e \\ S_e^T & R_e \end{pmatrix}$ with $Q_e < 0$ and $R_e > 0$. The scheduling block Δ_c of the controller can be obtained from the condition

$$\begin{pmatrix} U_{11} & U_{12} & (W_{11} + \Delta)^T & W_{21}^T \\ U_{21} & U_{22} & W_{12}^T & (W_{22} + \Delta_c)^T \\ W_{11} + \Delta & W_{12} & V_{11} & V_{12} \\ W_{21} & W_{22} + \Delta_c & V_{21} & V_{22} \end{pmatrix} > 0,$$

where

$$U = R_e - S_e^T Q_e^{-1} S_e,\ V = -Q_e^{-1},\ W = Q_e^{-1} S_e,$$

as

$$\Delta_c = -W_{22} + \begin{pmatrix} W_{21} & V_{21} \end{pmatrix} \begin{pmatrix} U_{11} & W_{11}^T + \Delta^T \\ W_{11} + \Delta & V_{11} \end{pmatrix}^{-1} \begin{pmatrix} U_{12} \\ W_{12} \end{pmatrix}, \tag{12}$$

for additional details see [9].

We remark here, that the condition $\Delta_c(0)$ is not supposed and does not hold in general. Thus condition $R_e > 0$ is a simple choice that facilitates the design. Also, note the size of the scheduling block which is twice the original. This is not surprising if one recalls that in an LPV setting, both the state feedback and the observer gain, is parameter varying. Putting together the two blocks one can arrive to the size from (12). For the dynamics we do not meet this effect, since the state feedback has no dynamics.

Since $R > 0$ and $\tilde{Q} < 0$ is always imposed for the design the relevant conditions are $Q < 0$ and $\tilde{R} > 0$ to use this scheme. For a convex relaxation scheme, i.e., when the relevant LMIs are imposed at the vertices of the polytope defined by the scheduling variables, these conditions should hold. For the role of the choice of the convex-hull and other related relaxations schemes that can also be applied [13]. The choice of a proper relaxation scheme is the corner-stone of a successful control design, thus to decrease conservatism one should use multipliers with an indefinite Q.

The procedure to construct the scheduling variables in the general case is described in [10], and unfortunately, is quite involved. Since it involves projections on an eigenspace of a parameter varying matrix, the scheduling variable is not in explicit form, that is actually a linear fractional transform (LFT), as in Eq. (12). Therefore it is a quest for extend the applicability of this simple design for a more general setting. In what follows a partial answer to this problem will be given.

3 Loop Shifting

The starting LMI for obtaining the scheduling variables is

$$\begin{pmatrix} \Delta & 0 \\ 0 & \Delta_c \\ I & 0 \\ 0 & I \end{pmatrix}^T \begin{pmatrix} Q_e & S_e \\ S_e^T & R_e \end{pmatrix} \begin{pmatrix} \Delta & 0 \\ 0 & \Delta_c \\ I & 0 \\ 0 & I \end{pmatrix} > 0, \tag{13}$$

i.e., $\begin{pmatrix} \overline{\Delta} \\ I \end{pmatrix}^T P_e \begin{pmatrix} \overline{\Delta} \\ I \end{pmatrix} > 0$ with $\overline{\Delta} = \begin{pmatrix} \Delta & 0 \\ 0 & \Delta_c \end{pmatrix}$ having a block diagonal structure, and $\begin{pmatrix} \overline{\Delta} \\ I \end{pmatrix}$ being a maximal positive subspace.

With a maximal negative subspace of P_e of the form $\begin{pmatrix} I \\ \Gamma \end{pmatrix}$, i.e., for which

$\begin{pmatrix} I \\ \Gamma \end{pmatrix}^T P_e \begin{pmatrix} I \\ \Gamma \end{pmatrix} < 0$ one can apply a "loop shift" of the scheduling block defined by $\widehat{\Delta} = \overline{\Delta}(I - V\overline{\Delta})^{-1}$ according to the transformation

$$\begin{pmatrix} \widehat{\Delta} \\ I \end{pmatrix} \sim \begin{pmatrix} I & 0 \\ -V & I \end{pmatrix} \begin{pmatrix} \overline{\Delta} \\ I \end{pmatrix} = \begin{pmatrix} \overline{\Delta} \\ I - V\overline{\Delta} \end{pmatrix}.$$

The multiplier transforms to

$$\tilde{P}_e = \begin{pmatrix} I & 0 \\ V & I \end{pmatrix}^T P_e \begin{pmatrix} I & 0 \\ V & I \end{pmatrix} = \begin{pmatrix} \tilde{Q}_e & \tilde{S}_e \\ \tilde{S}_e^T & R_e \end{pmatrix}$$

with $\tilde{Q}_e < 0$, as desired.

In order to be able to exploit this fact the "loop shift" should be defined for all $\overline{\Delta}$ and V should be block diagonal with the same pattern as $\overline{\Delta}$, i.e., $V = \begin{pmatrix} V_p & 0 \\ 0 & V_c \end{pmatrix}$. If we can construct such a V, then the scheduling variable can be obtained by using the following potential algorithm:

- build the transformed multiplier $\tilde{P}_e$ with the transformed variables $\widetilde{\Delta} = \Delta(I - V_p \Delta)^{-1}$ and $\widetilde{\Delta}_c = \Delta_c(I - V_c \Delta_c)^{-1}$
- with this $\tilde{P}_e$ construct the shifted scheduling variable $\widetilde{\Delta}_c$ according to (12) with $\Delta \to \widetilde{\Delta}$
- transform back the scheduling variable, i.e., $\Delta_c = \widetilde{\Delta}_c(I + V_c \widetilde{\Delta}_c)^{-1}$

Observe that $\widetilde{\Delta}_c$ is an LFT and thus Δ_c is also an LFT using, in general, a repeated block $\begin{pmatrix} \Delta & 0 \\ 0 & \Delta^T \end{pmatrix}$. To obtain the matrices that define this LFT is a standard computation and it is omitted for brevity.

3.1 A Maximal Condition

First, we would like to describe when a block diagonal matrix V exists with the desired properties. Let us suppose that V_p is fixed and the question is whether exists a V_c such that

$$\begin{pmatrix} I & 0 \\ 0 & I \\ V_p & 0 \\ 0 & V_c \end{pmatrix}^T P_e \begin{pmatrix} I & 0 \\ 0 & I \\ V_p & 0 \\ 0 & V_c \end{pmatrix} < 0.$$

But this is exactly a problem of type (8), with

$$C = \begin{pmatrix} V_p & 0 \\ 0 & 0 \end{pmatrix}, \quad A = \begin{pmatrix} 0 \\ I \end{pmatrix}, \quad B = \begin{pmatrix} I \\ 0 \end{pmatrix}$$

and variable $X = V_c$, whose solvability condition is given by the Elimination

lemma, see the Appendix.

By applying the conditions of the lemma a short computation reveals that the equation is solvable if and only if

$$\begin{pmatrix} I \\ V_p \end{pmatrix}^T P \begin{pmatrix} I \\ V_p \end{pmatrix} < 0, \text{ and } \begin{pmatrix} -V_p^* \\ I \end{pmatrix}^T \tilde{P} \begin{pmatrix} -V_p^* \\ I \end{pmatrix} > 0, \tag{14}$$

where P and $\tilde{P}$ are the solution multipliers of the analysis equations.

Remark 1 *Observe that applying the same technique for the original problem* (13) *one can obtain as the solvability condition*

$$\begin{pmatrix} \Delta \\ I \end{pmatrix}^T P \begin{pmatrix} \Delta \\ I \end{pmatrix} > 0, \text{ and } \begin{pmatrix} I \\ -\Delta^* \end{pmatrix}^T \tilde{P} \begin{pmatrix} I \\ -\Delta^* \end{pmatrix} > 0, \tag{15}$$

i.e., exactly the design conditions, as expected.

Actually, we obtain a slightly different result from that from [10]. This analysis ensures the existence of a scheduling variable $\Delta_c(\Delta)$ for any extension compatible with P and $\tilde{P}$ and not only for those obtained with a diagonalizing T in (7) as in the original construction. Moreover, $\mathcal{S}_c(\Delta) = \begin{pmatrix} \Delta_c(\Delta) \\ I \end{pmatrix}$, can always be assumed without restricting the generality. Since this is a constant Lyapunov function design, continuity of $\Delta_c(\Delta)$ does not play any role concerning stability and performance guarantee.

By using a dimension count argument, from the obtained inequalities (15) and the design requirements for P and $\tilde{P}$ it follows that:

Lemma 1 *For the loop shifting algorithm it is necessary that there exists a* V_p *satisfying* (15) *and* $\begin{pmatrix} \Delta \\ I \end{pmatrix}$ *and* $\begin{pmatrix} I \\ -\Delta^* \end{pmatrix}$ *be maximal positive (negative) subspaces of* P *and* $\tilde{P}$*, respectively.*

Paper [10] gives an algorithm that constructs $\Delta_c(\Delta)$ (and not $\mathcal{S}_c(\Delta)$) if either one of the subspaces is maximal. That algorithm is also hard to implement. However, in order to apply our proposed method, it is necessary that both subspaces be maximal and to exist a V_p fulfilling (14).

In what follows, it will be shown that this condition is also sufficient if V_p also satisfies (15): then it turns out a loop shift of Δ is sufficient and a slightly simplified algorithm can be obtained.

The following lemma is a consequence of the Separation Theorems, see the Appendix.

Lemma 2 *Let* $P \in \mathbb{F}^{(m+n)\times(m+n)}$ *be a symmetric or Hermitian matrix with inertia* $in(P) = (m, 0, n)$ *and let us consider the problem* $\begin{pmatrix} I \\ \Delta \end{pmatrix}^* P \begin{pmatrix} I \\ \Delta \end{pmatrix} < 0.$

Then for any fixed solution Δ_0 the matrix $I - \Delta_0^* \Delta$ is nonsingular for all

solutions Δ.

This lemma ensures that if we find a Δ_0 with the properties

$$\begin{pmatrix} I \\ -\Delta_0^* \end{pmatrix}^* P \begin{pmatrix} I \\ -\Delta_0^* \end{pmatrix} < 0, \quad \begin{pmatrix} \Delta_0 \\ I \end{pmatrix}^* P \begin{pmatrix} \Delta_0 \\ I \end{pmatrix} > 0,$$

then the choice $V_p = -\Delta_0^*$ will define a loop shift which is well defined for all Δ of interest.

In what follows it will be shown that under the maximality hypothesis such a Δ_0 always exists and it can be computed.

3.2 Existence of V_p

In order to improve readability, some basic facts on maximal negative subspaces and some notations are placed in the Appendix.

Lemma 3 *There exists* $V_0 \in \mathbb{F}^{n\times m}$ *which satisfies the inequalities*

$$\begin{pmatrix} I \\ V_0 \end{pmatrix}^* P \begin{pmatrix} I \\ V_0 \end{pmatrix} < 0, \quad \begin{pmatrix} -V_0^* \\ I \end{pmatrix}^* P \begin{pmatrix} -V_0^* \\ I \end{pmatrix} > 0. \tag{16}$$

Proof: The matrix P can be written in the factorized form $P = U^* \Lambda J \Lambda U$, where U is a unitary matrix, $\Lambda = \mathrm{diag}(|\Lambda_-|^{1/2}, \Lambda_+^{1/2})$ and $J = \mathrm{diag}(-I, I)$.

The second inequality is equivalent to $\begin{pmatrix} I \\ V_0 \end{pmatrix}^* P^{-1} \begin{pmatrix} I \\ V_0 \end{pmatrix} < 0$.

Obviously $P^{-1} = U^* \Lambda^{-1} J \Lambda^{-1} U$ consequently, V_0, if exists, has the form

$$V_0 = T_{(\Lambda U)^{-1}}(L_1) = T_{(\Lambda^{-1}U)^{-1}}(L_2) = T_{U^*\Lambda^{-1}}(L_1) = T_{U^*\Lambda}(L_2) = T_{U^*}(T_{\Lambda^{-1}}(L_1)) = T_{U^*}(T_\Lambda(L_2)).$$

This means that $L_1 = T_{\Lambda^2}(L_2)$. Since there exists arbitrary small contraction in the domain of T_{U^*}, we can choose a contraction $L_0 \in dom(T_{U^*})$, such that $L_1 = T_\Lambda(L_0)$ and $L_2 = T_{\Lambda^{-1}}(L_0)$ are also contractions. With the choice $V_0 = T_{U^*}(L_0)$ inequalities (16) is satisfied.

The question is, however, whether there exists a matrix V_p which satisfies both the inequalities (15) and (14). Unfortunately, this is a more complex question.

As in the proof of Lemma 3 consider the factorization $P = U_P^* \Lambda_P J_P \Lambda_P U_P$ and $\tilde{P} = U_{\tilde{P}}^* \Lambda_{\tilde{P}} J_{\tilde{P}} \Lambda_{\tilde{P}} U_{\tilde{P}}$ where U_P and $U_{\tilde{P}}$ are unitary matrices. The existence of a V_p with the desired properties is guaranteed if there is a contraction $L_{0,p} \in dom(T_{U_P^*})$ and also a contraction $L_{0,\tilde{p}} \in dom(T_{U_{\tilde{P}}^*})$ such that $V_p = T_{U_P^*}(L_{0,p}) = T_{U_{\tilde{P}}^*}(L_{0,\tilde{p}})$.

This is fulfilled if $L_{0,p} = T_{U_P}(T_{U_{\tilde{P}}^*}(L_{0,\tilde{p}})) = T_{U_P U_{\tilde{P}}^*}(L_{0,\tilde{p}})$.

Corollary 1 *There exists a* V_p *that fulfills both the inequalities* (15) *and* (14) *if and only if*

$$T_{U_P U_{\tilde{P}}^*}[T_{\Lambda_{\tilde{P}}}(\mathcal{K}) \cap T_{\Lambda_{\tilde{P}}^{-1}}(\mathcal{K})] \cap [T_{\Lambda_P}(\mathcal{K}) \cap T_{\Lambda_{\tilde{P}}^{-1}}(\mathcal{K})] \neq \emptyset, \tag{17}$$

where $\mathcal{K} = \{K \mid K \|< 1\}$.

This means that if $T_{U_P U_{\tilde{P}}^*}$ maps $\lambda\mathcal{K}$ far from the origin, where $T_{\Lambda_{\tilde{P}}}(\mathcal{K}) \cap T_{\Lambda_{\tilde{P}}^{-1}}(\mathcal{K}) \subset \lambda\mathcal{K}$ then such a transformation does not exists.

3.3 Construction Algorithm

If condition of Corollary 1 is fulfilled there exists a V_p that makes possible the transform

$$P = \begin{pmatrix} Q & S \\ S^T & R \end{pmatrix} \mapsto \bar{P} = \begin{pmatrix} \bar{Q} & \bar{S} \\ \bar{S}^T & R \end{pmatrix},$$

$$\tilde{P} = \begin{pmatrix} \tilde{Q} & \tilde{S} \\ \tilde{S}^T & R \end{pmatrix} \mapsto \hat{P} = \begin{pmatrix} \tilde{Q} & \hat{S} \\ \hat{S}^T & \hat{R} \end{pmatrix}$$

with $\bar{Q} < 0$ and $\hat{R} > 0$.

With $\bar{P}$ and $\hat{P}$ one can build, using the extension process decribed in (10) and (11), a $\tilde{P}_e$ that leads to a solution $\Delta_c(\widetilde{\Delta})$ by using (12).

Note that Δ_c can be always put into an LFT form based on the single block $\begin{pmatrix} \Delta & 0 \\ 0 & \Delta^T \end{pmatrix}$.

Thus we can conclude this paper with summarizing the main result:

Proposition 1 *For the loop shifting algorithm to be applicable it is necessary and sufficient that* $\begin{pmatrix} \Delta \\ I \end{pmatrix}$ *and* $\begin{pmatrix} I \\ -\Delta^* \end{pmatrix}$ *be maximal positive (negative) subspaces of* P *and* $\tilde{P}$*, respectively, and that there exists a matrix* V_p *which satisfies both the inequalities* (15) *and* (14)*.*

If the conditions of the proposition are fulfilled then the scheduling variables of the controller can be obtained using the following algorithm:

- Compute the transformed matrices
$$\bar{P} = \begin{pmatrix} I & 0 \\ V_p & I \end{pmatrix}^T P \begin{pmatrix} I & 0 \\ V_p & I \end{pmatrix}, \quad \hat{P} = \begin{pmatrix} I & -V_p^* \\ 0 & I \end{pmatrix}^T \tilde{P} = \begin{pmatrix} I & -V_p^* \\ 0 & I \end{pmatrix}$$
- Build the transformed multiplier $\tilde{P}_e$ by the method given in (10) and (11).
- With this $\tilde{P}_e$ construct the scheduling variable Δ_c according to the formula (12) with $\Delta \to \widetilde{\Delta}$, where $\widetilde{\Delta} = \Delta(I - V_p \Delta)^{-1}$.

4 Appendix

For the sake of completeness in this section we summarize the basic results that are used in the separation framework, i.e., in the context of this paper, the LMI approach to the robust control design. These results are formulated in the finite dimensional case, i.e., for matrices. Nevertheless, such assertions can be formulated in a more general operator setting as well.

4.1 Elimination Lemma

A fundamental result of the LMI framework in the derivation of the design equations is the Elimination lemma. The conditions of the lemma lead directly to the analysis equations that are the starting point for any controller design.

Lemma 4 *Let* $Q = Q^T$ *be a non-singular matrix with inertia* $in(Q) = (m, 0, n)$ *and let us consider the quadratic matrix inequality*

$$\begin{pmatrix} I \\ C + AXB \end{pmatrix}^T Q \begin{pmatrix} I \\ C + AXB \end{pmatrix} < 0. \tag{18}$$

This inequality has a solution if and only if

$$B^* \begin{pmatrix} I \\ C \end{pmatrix}^T Q \begin{pmatrix} I \\ C \end{pmatrix} B < 0 \tag{19}$$

and

$$A_\perp \begin{pmatrix} -C^T \\ I \end{pmatrix}^T Q^{-1} \begin{pmatrix} -C^T \\ I \end{pmatrix} A_\perp^* > 0. \tag{20}$$

Here $A_\perp$ denotes a matrix with $A_\perp A = 0$ and $A_\perp A_\perp^* > 0$ while B denotes an arbitrary basis matrix such that $BB = 0$ and that $B^*B > 0$. For a proof see, e.g., [5], [10].

4.2 Separation Lemma

Theorem 2 *Let* $B \in \mathbb{F}^{n\times m}$ *be a fixed matrix and* $\boldsymbol{\Delta} \subset \mathbb{F}^{m\times n}$ *a compact set of matrices. Then the following are equivalent:*

- $I - B\Delta$ *is nonsingular for all* $\Delta \in \boldsymbol{\Delta}$
- $I - \Delta B$ *is nonsingular for all* $\Delta \in \boldsymbol{\Delta}$
- There exists an indefinite matrix $P \in \mathbb{F}^{(n+m)\times(n+m)}$

with $in(P) = (n, 0, m)$ such that

$$\begin{pmatrix} B \\ I \end{pmatrix}^* P \begin{pmatrix} B \\ I \end{pmatrix} > 0 \text{ and } \begin{pmatrix} I \\ \Delta \end{pmatrix}^* P \begin{pmatrix} I \\ \Delta \end{pmatrix} < 0, \ \forall \Delta \in \boldsymbol{\Delta}.$$

For a proof of this theorem see, e.g., [7].

The duality lemma ensures the simultaneous inequalities

$$\begin{pmatrix}\Delta\\ I\end{pmatrix}^* P \begin{pmatrix}\Delta\\ I\end{pmatrix} > 0 \;\; and \;\; \begin{pmatrix} I\\ -\Delta^*\end{pmatrix}^* P^{-1} \begin{pmatrix} I\\ -\Delta^*\end{pmatrix} < 0$$

for any $\Delta \in \mathbf{\Delta}$, however, at the same time

$$\begin{pmatrix} I\\ -\Delta^*\end{pmatrix}^* P \begin{pmatrix} I\\ -\Delta^*\end{pmatrix} < 0$$

does not hold in a general case. If it happens that there is a Δ_0 that also fulfills this inequality, the Separation lemma guarantees the invertability of $I + \Delta_0^* \Delta$ for all $\Delta \in \mathbf{\Delta}$.

4.3 Indefinite Maximal Subspaces

The following result describes the maximal negative graph subspaces of a symmetric matrix P, i.e., all the matrices Z such that

$$\begin{pmatrix} I_q\\ Z\end{pmatrix}^* P \begin{pmatrix} I_q\\ Z\end{pmatrix} < 0, \tag{21}$$

where $P \in \mathbb{F}^{(q+p)\times(q+p)}$ with inertia $in(P_s) = (q, 0, p)$.

Theorem 3 *Let $\mathcal{M}$ be a symmetric matrix such that there is a nonsingular matrix M for which $P = M^{-T} J M^{-1}$, where $J = diag(-I_m, I_n)$. Then all solutions of* (21) *are given by*

$$Z = T_M(K) \tag{22}$$

for K is an arbitrary contraction ($\| K \| < 1$) in $\mathrm{dom}(T_M)$.

For a matrix M partitioned as

$$M = \begin{pmatrix} M_{11} & M_{12}\\ M_{21} & M_{22}\end{pmatrix} \tag{23}$$

the Möbius transformation T_M is defined by the equation

$$T_M(L) = (M_{21} + M_{22}L)(M_{11} + M_{12}L)^{-1} \tag{24}$$

for $L \in \mathrm{dom}(T_M) = \{L : (M_{11} + M_{12}L)^{-1}\}$.

Thus, the parametrization relies on describing $\mathrm{dom}(T_M)$

An exhaustive description of the set $\mathcal{X}_{M_{11},M_{12}} = \{X \mid M_{11} + M_{12}X \;\; nonsingular\}$ can be done by using the generalized singular value decomposition (GSVD), however, for our purposes it is sufficient the following result, based on the more familiar singular value decomposition (SVD).

Consider the SVD of A as $A = U_A \Sigma_A V_A^*$ with

$$U_A = (U_a \quad U_{as}), \quad \Sigma_A = \begin{pmatrix}\Sigma_a & 0\\ 0 & 0_{as}\end{pmatrix}, \quad V_A = (V_a \quad V_{as}). \tag{25}$$

and that of $B = U_B \Sigma_B V_B^*$ with

$$U_B = (U_b \quad U_{bs}), \Sigma_B = \begin{pmatrix} \Sigma_b & 0 \\ 0 & 0_{bs} \end{pmatrix}, V_B = (V_a \quad V_{bs}). \tag{26}$$

With these notations one has:

Lemma 5 *The matrices*

$$X_0(\gamma) = V_B \begin{pmatrix} 0 & \gamma \Sigma_b U_b^* U_{as} \\ 0 & 0 \end{pmatrix} V_A^*. \tag{27}$$

make $A + BX_0(\gamma)$ nonsingular for every $\gamma \neq 0$.

Moreover, for $\gamma^* \leq \frac{1}{||B||}$ the matrix $X_0(\gamma)$ is contraction for all $|\gamma| < \gamma^*$.

More details on the construction and the proofs can be found in [14]. A general overview on indefinite matrix analysis can be found in [4].

Conclusions

This paper investigates the possibility of constructing the scheduling block of a qLPV controller explicitly, i.e., in form of an LFT. It was shown that if both the primary and dual equations lead to maximal indefinite subspaces and a coupling condition holds, then the problem can be solved. In addition, a constructive algorithm was provided to build the needed scheduling variables. Currently, an efficient test of the coupling condition is under investigation.

The efficient construction of the scheduling block, in a general case, i.e., under the nonrestrictive inertia conditions of the full-block S-procedure, is still an open problem and it is the subject to future research.

Acknowledgement

The research has been conducted as part of the project TÁMOP-4.2.2.A-11/1/KONV-2012-0012: Basic research for the development of hybrid and electric vehicles. The Project is supported by the Hungarian Government and co-financed by the European Social Fund.

References

[1] A. Packard and G. Balas. Theory and Application of Linear Parameter Varying Control Techniques. *American Control Conference, Workshop I, Albuquerque, New Mexico*, 1997

[2] P. Gahinet and P. Apkarian. An LMI-based Parametrization of All H_∞ Controllers with Applications. *Proceedings of the 32nd IEEE Conference on Decision and Control*, pp. 656-661, 1993

[3] P. Gahinet, P. Apkarian, and M. Chilali. Affine Parameter Dependent Lyapunov Functions and Real Parameter Uncertainty. *IEEE Transactions on Automatic Control*, Vol. 41, pp. 436-442, 1996

[4] I. Gohberg, P. Lancaster and L. Rodman. *Indefinite Linear Algebra and Applications*. Birkhauser, 2005

[5] A. Helmersson. IQC Synthesis Based on Inertia Constraints. *Proceedings of the 14th IFAC World Congress, Bejing, China,* pp. 163-168, 1998

[6] T. Iwasaki and R. E. Skelton. All Controllers for the General H_∞ Control Problem: LMI Existence Conditions and State Space Formulas. *Automatica*, 300 (8):0 1307-1317, 1994

[7] T. Iwasaki. *Recent Advances on LMI Methods in Control*, chapter Control Synthesis for Well-Posedness of Feedback Systems, pp. 229-247, SIAM, 2000

[8] T. Iwasaki and G. Shibata. LPV System Analysis via Quadratic Separator for Uncertain Implicit Systems. *IEEE Transactions on Automatic Control*, Vol. 46, pp. 1195-1208, 2001

[9] C. W. Scherer. *Recent Advances on LMI Methods in Control*, chapter Robust Mixed Control and LPV Control with Full Block Scalings, pp. 187-208, SIAM, 2000

[10] C. W. Scherer. LPV Control and Full Block Multipliers. *Automatica*, 270 (3):0 325-485, 2001

[11] C. W. Scherer and S. Weiland. *Linear Matrix Inequalities in Control*, Dutch Institute of Systems and Control (DISC) 2005

[12] J. Veenman and C. W. Scherer. On Robust LPV Controller Synthesis: A Dynamic Integral Quadratic Constraint based Approach, *49th IEEE Conference on Decision and Control, Atlanta, GA, USA*, 2010

[13] Z. Szabó, P. Gáspár and J. Bokor, A Novel Control-oriented Multi-Affine qLPV Modeling Framework, *Proc. of the 18th Mediterranean Conference on Control and Automation, Marrakech, Maroc*, pp. 1019-1024, 2010

[14] Z. Szabó, Zs. Biró and J. Bokor. All Controllers for an LPV Robust Control Problem,' *Proceedings of the 7th IFAC Symposium on Robust Control Design, Aalborg, Denmark*, 2012

[15] F. Wu, X. H. Yang, A. Packard, and G. Becker, Induced $\mathbb{L}^2$ Norm Control for LPV Systems with Bounded Parameter Variation Rates. *International Journal of Nonlinear and Robust Control*, Vol. 6, pp. 983-998, 1996

[16] F. Wu. A Generalized LPV System Analysis and Control Synthesis Framework. *International Journal of Control*, 740 (7):0 745-759, 2001

[17] F. Wu and B. Lu. On Convexified Robust Control Synthesis. *Automatica*, 400 (6):0 1003-1010, 2004

[18] F. Wu and K. Dong. Gain Scheduling Control of LFT Systems Using Parameter Dependent Lyapunov Functions. *Automatica*, Vol. 42, pp. 39-50, 2006

Causal Analysis of the Emergent Behavior of a Hybrid Dynamical System

Marcel Kvassay[1], Ladislav Hluchý[1], Peter Krammer[1], Bernhard Schneider[2]

[1] Institute of Informatics, Slovak Academy of Sciences
Dubravska cesta 9, 845 07 Bratislava, Slovakia
e-mails: {marcel.kvassay, hluchy.ui, peter.krammer}@savba.sk

[2] EADS Deutschland GmbH
Landshuter Straße 26, 85716 Unterschleißheim, Germany
e-mail: bernhard.schneider@cassidian.com

Abstract: This paper reviews selected concepts and principles of structural causal analysis and adapts them for exploratory analysis of a hybrid dynamical system whose continuous dynamics are described by ordinary nonlinear differential equations. The proposed method employs partial derivatives in order to calculate "causal partitions" of the system's state variables, which make it possible to quantify the extent to which various causes can be considered "responsible" for the emergent behavior of the simulated system. Causal partitions can be processed by machine learning techniques (e.g. clustering and classification), and so facilitate meaningful interpretations of the observed emergent behaviors. The method is applied to the simulated emotions of fear and anger in humans, in a hybrid agent-based model of human behavior in the context of EDA project EUSAS.

Keywords: Hybrid system; Causal analysis; Emergent behavior; Agent-based simulation; Human behavior modeling

1 Introduction

This article is a report of work in progress extending our earlier paper [3]. From one point of view it can be considered a case study of one hybrid dynamical system. From a wider perspective, it is an attempt to introduce a new kind of analysis inspired by structural causality into the field of simulation studies. We demonstrate how structural causality facilitates meaningful interpretations of the emergent behaviors of complex systems and helps pinpoint their causes.

The paper is organized as follows: the rest of the Introduction provides a brief outline of structural causal analysis, while Section 2 adapts and applies its principles to the hybrid system under consideration. Section 3 details the

simulation scenario selected for the experimental verification of the proposed approach. Section 4 describes the clustering and classification methods used to analyze the data and establish the relevance of causal partitions. Section 5 discusses these findings, proposes further improvements to our approach, and presents the first tentative results after the improvements were implemented.

1.1 An Outline of Structural Causal Analysis

Causality is one of the perennial topics in philosophy. Relatively recently, it has matured into a mathematical theory with significant applications in various fields of science. Although there are several competing accounts of causation, this paper focuses primarily on the comprehensive structural approach formulated by Judea Pearl and others [9, 1, 2], which subsumes and unifies the probabilistic, manipulative, counterfactual, and other specialized approaches. This section broadly follows the account given by Pearl in [9, 8, 11]. A detailed guide on how to perform structural causal analysis in practice is provided in [10].

According to Pearl[1] in his seminal book on causality [9], causal analysis can be applied to systems described by equations of the form

$$x_k = f_k(pa_k, u_k), \quad k = 1 \ldots n, \tag{1}$$

where pa_k stands for the set of "parent variables" of x_k directly determining its value through an autonomous mechanism captured by f_k, and u_k stands for the effect of omitted factors. The autonomy of the mechanisms means any of them can be changed by external intervention without affecting the others. A set of such equations is called a "structural model." If, in addition, each variable (apart from the error terms u_k) appears on the left-hand side of some equation, then the model is called a "causal model." The error variables u_k are also termed *exogenous* or *background*; they are simply considered as given. The variables x_k are termed *endogenous*, i.e. determined by the equations within the system. A given value-assignment to the background variables constitutes a *world* or *context* in which the solution to the model equations is sought. In this paper, we restrict our attention to the recursive systems (systems without feedback loops), which possess a unique solution for each context. The equality sign in structural equations is endowed with directionality and is closer to the assignment operator in programming languages than to the standard algebraic symbol of equality.

Each causal model is associated with a causal diagram – a directed graph in which, for each equation, arrows point from u_i and the parent variables in pa_i toward their child, the dependent variable x_i. In fact, certain questions are more easily answered from the diagram than from the equations. In order to illustrate

[1] J. Pearl, *Causality: Models, Reasoning and Inference* 2nd Ed. 2009, p. 27 © Judea Pearl 2000, 2009, published by Cambridge University Press, reproduced with permission

this, here is an example with three pairs of equations reproduced from the Epilogue[2] to J. Pearl's book on causality [9]:

$$Y = 2X \qquad (2a)$$
$$Z = Y + 1$$

$$X = Y/2 \qquad (2b)$$
$$Y = Z - 1$$

$$2X - 2Y + Z - 1 = 0 \qquad (2c)$$
$$2X - 2Y - 3Z + 3 = 0$$

These three pairs are algebraically equivalent, in the sense of having the same solutions, but only the first two pairs (2a) and (2b) qualify as structural models. While each equation in the third pair (2c) can be expressed as a linear combination of the equations in the preceding pairs, neither qualifies as structural, because it is not clear which variable is the dependent one (the child) and which are the independent ones (its parents). Moreover, even the first two pairs (2a) and (2b) do not describe the same causal model: their circuit representations using adders and multipliers shown in Fig. 1 make it obvious that the flow of causality in the second pair (Fig. 1b) is reversed with respect to the first (Fig. 1a). As such, we get different predictions from these two models concerning hypothetical interventions, e.g. "What happens if we set the value of the middle variable *Y* to *0*?"

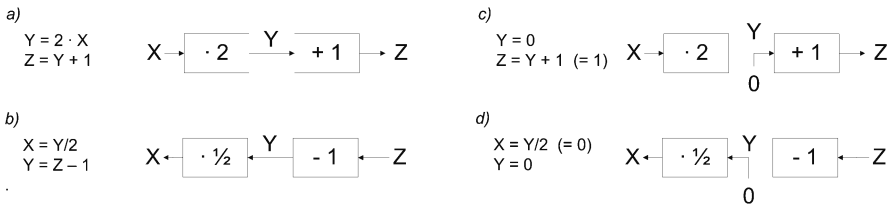

Figure 1

Circuit representations of equations (2a) and (2b) before and after an external intervention – setting Y to 0 (adapted from J. Pearl, *Causality: Models, Reasoning and Inference* 2nd Ed. 2009, pp. 416-7 © Judea Pearl 2000, 2009, published by Cambridge University Press, reproduced with permission)

In the first pair (2a), manipulating *Y* will affect *Z*, while in the second (2b), manipulating *Y* will affect *X* and leave *Z* unconstrained. This is shown both graphically and symbolically in Fig. 1c and 1d. Symbolically, the external intervention on *Y* means replacing the equation in which *Y* is the dependent variable with a new equation, in this case a straightforward value substitution *Y = 0*. The modified equations are then solved algebraically in order to determine the

[2] J. Pearl, *Causality: Models, Reasoning and Inference* 2nd Ed. 2009, pp. 416-7 © Judea Pearl 2000, 2009, published by Cambridge University Press, reproduced with permission

response of the model to the intervention. The first model (Fig. 1c) gives $Z = 1$, while the second gives $X = 0$ (Fig. 1d). In this way the structural approach provides a clear and unambiguous definition of causality. In Pearl's own words: "*Y* is a cause of *Z* if we can change *Z* by manipulating *Y*, namely, if after surgically removing the [original structural] equation for *Y*, the solution for *Z* will depend on the new value we substitute for *Y*." In contrast, the third pair of equations (2c) provides no causal structure or "intervention" guidance at all: it simply represents two general constraints on three variables, without telling us how the variables influence each other.

The directionality of causality has been one of the main obstacles to capturing causality satisfactorily in purely logical and purely statistical frameworks. The notion of cause can be further refined by distinguishing the necessary and sufficient aspects of causation, and the type-level from token-level causation. Another important concept linked with the token-level causation is that of an "actual cause" [1, 2]. For the purposes of this paper, however, these distinctions are not crucial. We shall therefore proceed with an example taken from [11], which demonstrates the use of structural models for various kinds of inference and for evaluating the effects of interventions.

The example, titled "The Impatient Firing Squad," analyses a fictitious scene just before the execution of a prisoner. The firing squad comprises a Captain and two riflemen. For the purposes of this analysis, the situation is modeled by 5 binary propositional variables: *U* ("Court orders the execution"), *C* ("Captain gives the signal"), *A* ("Rifleman-A shoots"), *B* ("Rifleman-B shoots"), and *D* ("The prisoner dies"). It is assumed that both the riflemen are law-abiding (i.e. they will only shoot if the Captain gives the signal) and competent (i.e. if any of them shoots, the prisoner will die). Likewise, the captain will signal only if ordered to do so by the court. These dependencies, expressed in the form of Boolean structural equations, lead to the following causal model:

$$C = U \tag{3a}$$

$$A = C \tag{3b}$$

$$B = C \tag{3c}$$

$$D = A \vee B \tag{3d}$$

In this model, *U* is *exogenous*, because it does not have its own structural equation in which it would appear on the left-hand side. Because this is a recursive system without feedback loops, the value of *U* uniquely determines the values of the remaining (*endogenous*) variables *C, A, B, D*. The causal diagram associated with this model is depicted in Fig. 2a.

It is obvious that in this model there exist just two consistent truth valuations of its variables: either they are all true, or they are all false, which greatly simplifies the task of evaluating the truth or falsity of the following "test" sentences:

S1: $A \Rightarrow D$ ("If rifleman-A shot, the prisoner is dead.")

S2: $\neg D \Rightarrow \neg C$ ("If the prisoner is alive, then the Captain did not signal.")

S3: $A \Rightarrow B$ ("If rifleman-A shot, then rifleman-B shot as well.")

S4: $\neg C \Rightarrow D_A$ ("If the captain gave no signal and rifleman-A decides to shoot, the prisoner will die.")

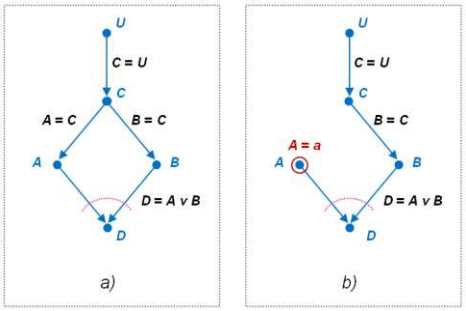

Figure 2
Causal diagrams for "The Impatient Firing Squad" example: a) original model, b) modified model after intervention (adapted from [11])

S1 is prospective inference from causes to effects (prediction), S2 retrospective or diagnostic inference from effects and back to causes (abduction), and S3 inference through common causes (transduction). Sentences S1 – S3 do not involve modifications of the original model and can be proved by purely logical means. Taking advantage of the fact that either all the variables are true, or they are all false, it is enough to check the truth values of S1 – S3 in these two settings. Since they all hold in both, we can conclude that they are entailed in the model.

S4 ("action") is an instance of "true" causal thinking – it is like prediction except that it must be evaluated in a modified model. S4 states that rifleman-A shoots *without Captain's signal*, which implies that the equation (3b) no longer holds. This is graphically depicted in Fig. 2b, where the link between C (the Captain's signal) and A (the rifleman-A's shot) is severed. Instead, the variable A is assigned the value representing the rifleman-A's new behavior: $A = True$. At the same time, S4 stipulates that the Captain did not signal, i.e. $C = False$ ($\neg C$ for short). Since S4 does not indicate any departure from the norm for the Captain, we assume that (3a) holds, i.e. U is false. Likewise, by (3c), B is false as well. However, equation (3d) still makes D_A true because $A = True$ (the subscript "$_A$" in "D_A" denotes the value of D in the minimally modified model, in which the equation for A was replaced with substitution $A = True$). In this modified setting, S4 holds, because both its antecedent and its consequent are true. It needs to be kept in mind that, while evaluating S4, no other hypothetical modifications to the original causal model besides those explicitly stipulated by S4 are permitted.

This example also illustrates the distinction between *events* and *actions*. In the context of the model (3a) – (3d), if rifleman-A shoots in response to Captain's signal, it is an event, not an action. Events represent model variables assuming particular values from their allowed range. Thus, if the equations (3a) – (3d) yield the result "*A = True*", this would denote the event "Rifleman-A shoots," while "*A = False*" would denote the event "Rifleman-A does not shoot." The term "action" (or "intervention") is reserved for happenings that entail the modification of the model itself. For example, in the "action" sentence S4, the rifleman-A's decision to shoot *without Captain's signal* implies a disruption of one of the causal mechanisms – equation (3b) – and its replacement by another (in this case by a straightforward value substitution "*A = True*"). This is different from *A* assuming the value "*True*" under "normal" conditions described by (3a) – (3d).

These principles can be used to analyze dynamic situations as well. For dynamic analysis, however, the state variables describing the system need to be discretized with respect to time. Pearl in [9] and [11] provides an example of two forest fires advancing toward a house. In that example, the discretization is both temporal and spatial, since the changing state of the forest over time is conceptualized as a directed graph (causal diagram), in which each node represents the state of one patch of forest at a certain location x and time t. Pearl demonstrates a technique of "causal beams" through which it is possible to determine which of the two forest fires is the *actual cause* of the destruction of the house. This dynamic example hints at the potential value of structural causal analysis for simulation studies in general. In the model of human emotions that we analyze below, we apply these principles to ordinary nonlinear differential equations and the discrete dynamics that comprise our hybrid system.

2 Causal Analysis of a Hybrid System

The first point that needs to be addressed is whether our human behavior model (described in more detail in section 2.1) meets the criteria set for structural causal models. The main difference is that this model includes a particular kind of ordinary nonlinear differential equations with first derivatives with respect to time t on the left-hand side. In general, following the notation used in the definition (1), such equations can be written as

$$dy_k/dt = g_k\,(pa_k', u_k) \qquad k = 1 \ldots n \tag{5}$$

where the function g_k can be nonlinear. Another difference is that the dependent variable y_k typically influences its own time derivative, i.e. it belongs to its own "parent set": $y_k \in pa_k'$. In order for such models to qualify as "causal", the differential equations need to be converted into difference equations, e.g. by replacing the derivatives with difference quotients:

$$(y_{k,j} - y_{k,j-1})/(t_j - t_{j-1}) = g_k\,(pa'_{k,j},\, u_{k,j}) \qquad k = 1\ldots n,\ j = 1\ldots m \tag{6}$$

where k indexes the original variables y_k and j indexes the discretized moments of time t_j, so that $y_{k,j}$ stands for the value of variable y_k at time t_j. Denoting $t_j - t_{j-1}$ as Δt, this can be rewritten as

$$y_{k,j} = y_{k,j-1} + \Delta t \,.\, g_k\,(pa'_{k,j},\, u_{k,j}) \qquad k = 1\ldots n,\ j = 1\ldots m \tag{7}$$

In this form the relationship to (1) becomes clear. Variable $y_{k,j}$ at the left-hand side of (7) corresponds to the variable x_k in (1), which means that in this "structural form" the value of a given variable y_k at a given point of time t_j is considered a separate "structural" variable, distinct from the value of the same variable y_k at other points in time. Similarly, the whole right-hand side of (7) corresponds to $f_k\,(pa_k, u_k)$ of (1). Thus the relationship between the parent sets of (1) and (7) can be formulated as $pa_k = pa'_{k,j} \cup \{y_{k,j-1}\}$. Most importantly, in this form the parent set of the variable $y_{k,j}$ no longer contains this variable, but only the preceding values of y_k in time, which are now considered different variables. Thus, after the discretization, no "structural" variable depends on itself. Therefore we can conclude that our human behavior model, after the discretization, does qualify as a structural causal model, as defined in [9]. Because we are interested in developing a general method for causal analysis of this kind of systems, we shall not go into details of our equations for *fear* and *anger*, but rather show a numerical solution for the general case. Yet, in order to understand our simulation experiments, an overview of the dynamics of our simulated agents will be helpful.

2.1 Internal Dynamics of Civilian Agents

A simplified diagram of our model is shown in Fig. 3. It represents the key factors affecting the behavior of civilian agents in the simulation scenario chosen for our case study. This model was used in project EUSAS financed by 20 nations under the *Joint Investment Program Force Protection* of the European Defence Agency. Interested readers can refer to a detailed exposition with a motivating example given in [5, 4]. Below we provide a brief summary of the model.

In line with the PECS modeling methodology [14, 13] used in project EUSAS, the agent behaviors are conceptualized as sequences of atomic, uninterruptible actions, e.g. one step in a certain direction, a single provocation or a single threat. Each behavior pattern is activated when its triggering motive becomes the strongest. For aggressive behaviors, the typical (but not the sole) triggering motive is *anger*, for fearful ones (such as withdrawal or flight to safety) the motive is *fear*. Regarding the dynamics of the simulated motives *fear* and *anger*, a convenient starting point is the top left corner of Fig. 3: the number of people surrounding the agent, their actions and other events in the vicinity affect the agent's motives (*fear*, *anger*) as well as its other internal parameters (*arousal*, *readiness for aggression*). Besides events and actions, there is also a direct *social influence* of other agents on the agent's *fear*, *anger* and *readiness for aggression*.

This is modeled according to Latané's formula of strength, physical proximity and the number of influencing agents [7].

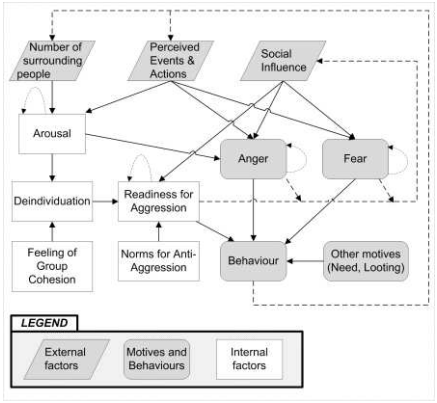

Figure 3
Sociopsychological model for the emergence of collective aggression in the form of a causal diagram

The internal *arousal* of the agent depends on the number of people in the vicinity and the violence of their actions. Speaking qualitatively, the higher the number and the more violent their actions, the sharper the increase of the agent's arousal. *De-individuation* means the agent considers himself a part of the crowd and no longer a separate individual, so the higher the agent's arousal and the more he feels a part of the group, the higher the de-individuation. *Readiness for aggression (RFA)* is jointly affected by the norms for anti-aggression, de-individuation and social influence as follows: (a) the higher the norms for anti-aggression, the lower the *RFA*; (b) the higher the de-individuation, the higher the *RFA*; and (c) the more social influence tends towards aggression, the higher the *RFA*. Psychological theories make aggression depend primarily on the *RFA*: without it, even a very angry person would not behave aggressively.

In [4] we tried to answer the question whether, in a scenario with this model, indirect social influence of nearby people was more important than external events in shaping the civilian agents' behavior. The answer provided by the causal summary of the scenario indicated that external events were more important. In this paper we revisit the same scenario (see section 3 for details) with another, more difficult problem: while experimenting, we have noticed that for a particular parameter setting, the emergent collective behavior of the civilians developed along two sharply diverging trajectories. In some cases, almost all of them got afraid and left the scene, while in others, almost all got angry and joined the attack on the security forces. Because our model incorporates an element of randomness, a certain variation of the emergent behavior of the civilians was to be expected, but the extreme variation that we witnessed was unusual and called for an explanation. Since the leading question was "Why is this happening?" it provided a welcome opportunity to test the relevance and practical utility of our approach.

2.2 Causal Partitioning – A Brief Outline

Following [4], we shall briefly illustrate causal partitioning on motive *fear*. Its continuous dynamics is driven by the equation

$$dF/dt = f(F(t), I_F(t)) \tag{8}$$

where F stands for Fear, I_F for fear-related social influence, and f for a nonlinear function of these two arguments. In Euler numerical method this leads to

$$F(t + \Delta t) \approx F(t) + \Delta t \,.\, f(F(t), I_F(t)) \tag{9}$$

where Δt is the simulation time step. $F(t + \Delta t)$ stands for the new "continuous" value of Fear, to which the discrete part of the dynamics (E_F) is yet to be added:

$$F_T(t + \Delta t) = F(t + \Delta t) + \Delta E_F \tag{10}$$

where F_T stands for the new total value of Fear and ΔE_F for the cumulative fear-related impact of the external events perceived by the agent during the time interval $(t, t + \Delta t>$. This means we model the external events as taking the effect at the end of the time interval during which they occur.

Causal partitioning starts by linearizing the function f through its partial derivatives with respect to its two parameters F and I_F:

$$f_j \approx f_{j-1} + \partial f/\partial F \,.\, \Delta F + \partial f/\partial I_F \,.\, \Delta I_F \tag{11}$$

where ΔF and ΔI_F stand for the differences in the values of F and I_F, respectively, between the start and the end of the time interval $(t - \Delta t, t>$. For brevity we have switched to indexing, where f_j represents the current value $f(t)$ and f_{j-1} the previous one, $f(t - \Delta t)$. Next, we exploit the fact that ΔF over the time interval $(t - \Delta t, t>$ equals the sum of the discrete and the continuous changes during that period, i.e. $\Delta F = \Delta E_F + f_{j-1} \,.\, \Delta t$. Substituting this into (11) yields

$$f_j \approx f_{j-1} + \partial f/\partial F \,.\, (\Delta E_F + f_{j-1} \,.\, \Delta t) + \partial f/\partial I_F \,.\, \Delta I_F \tag{12}$$

which can be rewritten as

$$f_j \approx C_1 \,.\, f_{j-1} + C_2 \,.\, \Delta E_F + C_3 \,.\, \Delta I_F \tag{13}$$

with C_1, C_2 and C_3 representing the weighting factors that equal, respectively, $1+\Delta t.\partial f/\partial F$, $\partial f/\partial F$, and $\partial f/\partial I_F$. These factors can be evaluated numerically. As we explained in [4], this formula is the basis for our algorithm for causal partitioning of *fear* into causal partition vectors, where each vector component represents the quantitative contribution of one "causing" factor. The first derivative of fear f at any moment is then represented by the causal partition vector (f_E, f_I), whose components sum up to f. The first component f_E stands for the cumulative contribution of the external events E_F, the second f_I for the cumulative contribution of fear-related social influence I_F. Analogously, the value of fear F can be represented by the partition vector (F_E, F_I) whose components sum up to F. The causal partitioning algorithm proceeds roughly as follows:

To get the current partition of the first time derivative of fear (f_j), take its previous partition $f_{j-1} = (f_{E,\,j-1}, f_{I,\,j-1})$, multiply its members by C_1, then add the contributions of the external events and social influence over the interval $(t - \Delta t,\ t\rangle$ as per (13) to their respective partition components f_E and f_I.

Next, to get the new partition for Fear (F_{j+1}), take its current partition (F_j) and add to it, component by component, the increment as per equation (9) using the current partition of its first time derivative f_j. The increment is a vector $(\Delta t \,.\, f_{E,\,j}, \Delta t \,.\, f_{I,\,j})$.

Last, add the cumulative value of the external events perceived during the new step (ΔE_F for time interval $(t,\ t + \Delta t\rangle$) directly to the F_E component.

In this simplified account we have assumed the zero initial value of Fear (F_0). If it is non-zero, it qualifies as a separate causal factor and requires a dedicated component in the causal partition vector (F_{F0}). Thus, the value of Fear is in fact partitioned into a casual partition vector (F_{F0}, F_E, F_I).

The analysis of Anger proceeds analogously. The continuous part of its dynamics is driven by the equation

$$dA/dt = g(A(t), L(t), I_A(t)) \tag{14}$$

where A stands for Anger, L for Arousal, I_A for anger-related social influence, and g for a nonlinear function of these arguments. The Euler method then leads to

$$A(t + \Delta t) \approx A(t) + g(A(t), L(t), I_A(t)) \,.\, \Delta t \tag{15}$$

Again, to this new "continuous" value of Anger, the discrete anger-related impacts of the events perceived during the time interval $(t,\ t + \Delta t\rangle$ have to be added:

$$A_T(t + \Delta t) = A(t + \Delta t) + \Delta E_A \tag{16}$$

A process of causal partitioning analogous to that for Fear then partitions A_T, the new total value of Anger, into a casual partition vector (A_{A0}, A_E, A_I, A_L)

In general, a causal partition of a model variable X is a vector-like structure (X_1, X_2 ... X_n) whose components sum up to X and where each component represents the portion of the value of X attributed to one specific factor. This makes it possible to quantify the extent to which various factors can be considered "responsible" for the value of X at any given moment in a given simulation scenario.

Concerning the simulation experiments in this paper, by a causal summary of a simulation run we mean the causal partition vectors representing the final values of *fear* and *anger* averaged over all the civilian agents in the scenario. This data, supplemented with a few other attributes, is then passed on to the machine learning algorithms for further analysis.

3 Simulation Experiment Scenario

As mentioned, we revisit the scenario from [4], in which a crowd of civilians is looting a shop, and the approaching soldier patrol is supposed to stop the looting and disperse the crowd. The scene is shown in Fig. 4. Black areas represent buildings and barriers unreachable to agents. The rectangle with gray interior near the top is the shop being looted. It is surrounded by dots, each representing one agent. The dark ones are the looters; the light-colored ones are the violence-prone individuals, whose intention is to attack the soldiers. The soldiers are represented by the three medium gray dots in the bottom part of the figure.

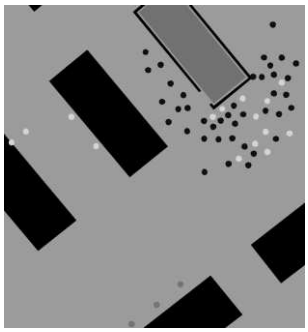

Figure 4
Initial stage of the simulation scenario

Civilian agents are endowed with one "default" motive and a matching behavior by which they try to satisfy it. For looters this leads to "looting" and for the violence-prone individuals to stone-pelting the soldiers. Additionally, the agents monitor what happens around them, which may excite fear or anger, in which case they start behaving fearfully (i.e. run away) or aggressively. As the patrol nears, this may induce fear in some looters who then start leaving the scene. The violence-prone individuals, however, do not get afraid but attack the patrol. The violence may impact the remaining looters in two possible ways – they may either get afraid and leave, or get angry and join the attack. How many get afraid and how many get angry depends on various parameter settings. The key ones are the initial values of *fear* and *anger* (which were set to $F_0 = 0.3$ and $A_0 = 0.2$) along with the main event impacts summarized in Table 1.

Table 1
Main event impacts on *fear* and *anger*

Impacts:	Impact on Fear		Impact on Anger	
Events:	Direct	Indirect	Direct	Indirect
Effective shot	0.4	0.35	0.1	0.25
Warning shot	0.3	0.3	0.1	0.1
Stone thrown	0.002	0.002	0.18	0.15

The values of *fear* and *anger* are incremented by the event impacts shown in Table 1 every time the corresponding event is perceived by the agent. The "direct" values from Table 1 are used when the perceiving agent is the target of the event; otherwise the "indirect" values are used. What may seem counterintuitive at first, is that each event affects both *fear* and *anger*, but in different proportions. All the agent motives, including *fear* and *anger*, are real-valued and restricted to the closed interval <0, 1>. *Looting* motive is set to a constant value of *0.7*, so *fear* or *anger* must cross this level in order to affect the agent behavior. Sensory perception of the agents is limited both spatially (by a radius of 50 m for throwing stones and 150 m for gun shots) and emotionally (if the average of *fear* and *anger* crosses the level of 0.5, further sensory perception of events is blocked).

Unlike our civilians, our soldier agents are much simpler: they are just passing by and act in self-defense. Their rule of self-defense says that when a given civilian first throws a stone at a soldier, that soldier responds by a warning shot in the air. If the same civilian throws a stone at the same soldier a second time, the soldier is permitted to use an effective shot aimed at the legs of the attacker in order to immobilize him. That is, of course, an extreme simplification, but it proved useful in the early phases of project EUSAS for calibrating the civilian agents.

As part of the present case study, we ran this simulation scenario 300 times with the simulation time step of 300 milliseconds, and then again 300 times with the time step of 100 ms. This enabled us to gauge the effect of the time step size (and of the resulting discretization errors) on the observed emerging behavior of the agents. Since the time-evolution of our scenario is rather fast, it was sufficient for each simulation to cover just 90 seconds of simulated time. At the end of this period, the average values of *fear* and *anger* were recorded and their causal partition vectors (along with other relevant data) were passed on to machine learning algorithms for further analysis.

4 Machine Learning

Regarding data structure and pre-processing, our data consisted of two data sets, one for 100 ms and another for 300 ms time step. Each set contained 300 records with 12 numerical attributes: 7 components of causal partitions of average final values of *anger* (A_{A0}, A_E, A_I, A_L) and *fear* (F_{F0}, F_E, F_I), followed by 3 measures of effectiveness (MoE) used to evaluate scenarios in project EUSAS: N_E (total number of effective shots), N_W (total number of warning shots), and N_S (total number of thrown stones). The last two attributes, *A-count* and *F-count*, stand for the cumulative numbers of times that *anger* and *fear*, respectively, became the strongest motives in some civilian agent. For scenarios that turn aggressive we expect a high *A-count* as well as high MoE values and a low *F-count*, while for the "timid" scenarios we expect a high *F-count* and a low *A-count* as well as low MoE

values. We have included MoE as a sort of "competition" to our causal summaries: it is evident that MoE can classify the scenarios well, since aggressive developments imply high numbers of thrown stones as well as gunshots. MoE, however, lack the explanatory power: they do not tell us anything about why a particular scenario took an aggressive or a timid turn. We have verified our expectations by the clustering exercise shown in Fig. 5.

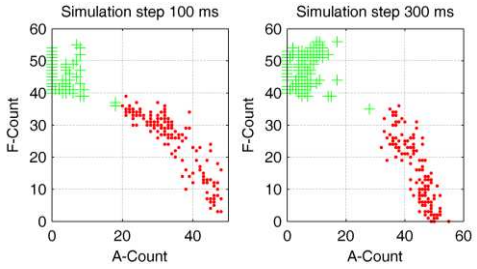

Figure 5
Data clustering into two clusters for 100 ms and 300 ms data sets

The charts have *A-count* on the x-axis, *F-count* on the y-axis and represent each simulation run as one data point. In order to improve readability, we have used the jitter method (adding noise with small amplitude). The left chart represents the 100 ms data set, the right one the 300 ms data set. As expected, in both data sets there seem to be two distinct clusters: the compact one in the top left corner ("timid" scenarios), and the elongated one in the bottom right part ("aggressive" scenarios). The elongated shape of the "aggressive" cluster is due to the varying levels of fearful behaviors that appeared alongside aggression. The elongation points towards the "timid" cluster because an increase in fearful behaviors goes hand in hand with a reduction in the aggressive ones. In other words, although our agents can switch between *fear* and *anger* several times during one scenario, this is rare and most of them switch just once from their "standard" motive to either *fear* or *anger*. This explains why simulations tend to cluster near the diagonal.

Both the clustering exercise and the classification experiments described below were executed in Weka [15], ver. 3.7.9, which uses expectation maximization algorithm. Clustering added a new attribute (cluster ID) to our data. On the scaled data thus pre-processed, we then trained several classification models, choosing the "cluster ID" as the target. Our classifiers were based on SVM (Support Vector Machine) with SMO algorithm (Sequential Minimal Optimization algorithm) [12]. Compared to other techniques, SVM is known to be more intuitively interpretable. For two clusters, an SVM model consists of a function describing the boundary hyperplane separating the clusters in the feature space. If the boundary function gives a positive value for some data point, then it belongs to one cluster, and if the value is negative, then it belongs to the other cluster. Zero value means the point lies on the boundary. In the exercise, we used the number of correctly classified instances as a quality measure in 10-Fold Cross Validation.

We start our classification along the lines of forward parameter selection in order to find out which of the causal attributes is the best standalone predictor of "cluster ID". For each attribute X, SVM produces a classification model of the form $aX + b$. The value of X for which $aX + b = 0$ is the *cut-off value* defining the boundary: $X = -b/a$ (for $a \neq 0$). Models with $a = 0$ are trivial as they assign all the simulations to one cluster. The results of this exercise are shown in Table 2 (mark "--" in the place of a cut-off value means the model was trivial, having $a = 0$). Since all the attributes were normalized, all the cut-off values (so long as they exist) fall within the closed interval <0, 1>. For comparison, we have also included the "competing" SVM models based on MoE (N_E, N_W, N_S).

Table 2
Forward selection of the most important attributes on the basis of SVM models

Attribute: / Measure:	A_{A0}	A_E	A_I	A_L	F_{F0}	F_E	F_I	N_E	N_W	N_S
Cut-off value 100 ms	0.45	0.24	0.48	--	0.52	0.39	0.47	0.22	0.37	0.12
Accuracy [%] 100 ms	88.7	61.0	93.0	51.7	99.0	97.7	80.3	97.0	95.3	88.7
Cut-off value 300 ms	0.70	0.78	0.01	0.44	0.59	0.40	0.39	0.31	0.35	0.20
Accuracy [%] 300 ms	80.0	67.7	48.7	60.3	97.0	93.0	91.0	98.0	93.0	92.0

The big surprise for us was the high prediction accuracy of the causal partition component corresponding to the initial value of fear (F_{F0}): 99 % for 100ms dataset and 97 % for the 300ms dataset. If we were just looking for a high-quality classifier, we could have proclaimed our task finished at this point. For us, however, these classifiers are simply a source of hints about the underlying mechanism responsible for the observed divergence of the simulation trajectories (timid versus aggressive). And in this respect, as it turned out, things were much more complicated. In a straightforward interpretation the attribute F_{F0} being the best predictor indicates that the initial setting of the value of fear (F_0) might be the underlying cause of the observed divergence of simulation trajectories. But we know this cannot be, since in all the 600 simulation runs this initial setting was kept the same ($F_0 = 0.3$). Thus, the fact that F_{F0} does not remain constant must be due to other factors, most likely the other components of the causal partition of fear, to which it is tied by the partition definition constraint $F = F_{F0} + F_E + F_I$.

This brings us to the question of mutual correlations among the attributes, which we show in Table 3. Its lower triangular portion shows them for the 100 ms data set, the upper triangular one for the 300 ms data set. We see that F_{F0} is indeed highly correlated with F_E and F_I in both data sets. We also note another redundant attribute A_{A0} (highly correlated with F_E), which again cannot lead us towards the cause of the divergence, since the initial value of anger A_0 was the same ($A_0 = 0.2$) in all the simulations. Overall, this points towards F_E as the primary factor, since it is also the second best standalone causal predictor of "cluster ID", with 97.7% accuracy for the 100 ms dataset and 93% for the 300 ms one. Before delving into possible explanations, however, we shall first try to confirm this finding by a process similar in spirit to backward parameter selection.

Table 3
Mutual correlations of attributes (lower-triangular section: 100 ms, upper triangular: 300 ms)

	A_{A0}	A_E	A_I	A_L	F_{F0}	F_E	F_I
A_{A0}	1	0.46	-0.34	0.22	0.49	-0.55	-0.32
A_E	0.54	1	-0.50	-0.28	0.44	-0.40	-0.41
A_I	0.44	0.13	1	0.19	0.31	-0.23	-0.28
A_L	-0.17	-0.67	-0.14	1	0.44	-0.47	-0.41
F_{F0}	0.72	0.36	0.76	0.11	1	-0.89	-0.88
F_E	-0.73	-0.32	-0.68	-0.14	-0.93	1	0.75
F_I	-0.35	-0.33	-0.53	-0.12	-0.71	0.52	1

The initial steps of backward parameter selection are shown in Table 4. We start with "complete" models with 7 causal attributes (top two lines) which reach 99% accuracy for both data sets. For comparison, we include the SVM models based on MoE in the next two lines. These perform slightly better for the 300 ms data set and slightly worse for the 100 ms one, thus confirming the quality of our causal models. We now remove the two "redundant" causal attributes F_{F0} and A_{A0}, expecting that this should not impair the accuracy of our models, which is borne out by the last two lines in the table. Having got rid of high correlations, we can gauge the key factors among the remaining variables. In SVM models, these tend to be the ones whose coefficients in the boundary plane function have the highest absolute value. On this criterion, F_E comes out as the most important attribute for both data sets – in total agreement with the first step of forward parameter selection in Table 2. In the 100 ms data set, the second and the third place belong to A_I and F_I, respectively; while for the 300 ms data set their ranking is reversed. Although these additional attributes only add a few percent to the accuracy (since F_E alone reaches 97.7% accuracy), we decided to explore in more detail the pair-wise combinations for additional clues they might offer.

Table 4
Trained SVM models with causal attributes and MoE

Time Step	Function of the boundary plane	Correctly Classified
100 ms	$-0.10 * A_L + 0.23 * A_E + 1.44 * A_{A0} + 2.39 * A_I - 2.10 * F_E + 3.21 * F_{F0} - 0.79 * F_I - 2.22$	99.0%
300 ms	$-0.77 * A_L + 0.24 * A_E - 0.69 * A_{A0} + 2.04 * A_I - 1.65 * F_E + 4.51 * F_{F0} - 1.92 * F_I - 0.78$	99.0%
100 ms	$4.53 * N_E + 3.41 * N_W + 1.98 * N_S - 2.36$	97.3%
300 ms	$3.23 * N_E + 3.05 * N_W + 1.49 * N_S - 2.46$	99.3%
100 ms	$0.47 * A_L + 1.03 * A_E + 3.16 * A_I - 5.16 * F_E - 1.61 * F_I + 0.77$	99.3%
300 ms	$-0.43 * A_L + 0.85 * A_E + 2.96 * A_I - 4.49 * F_E - 4.16 * F_I + 2.74$	98.3%

Considering the five causal attributes A_E, A_I, A_L, F_E and F_I, there are ten possible pairs. In the 100 ms data set only one of them (F_E x A_I) was found to outperform F_E on its own. At the same time, this pair reached the same 99% accuracy as the full SVM model with seven causal attributes in Table 4. Thus, we can conclude that for the 100 ms dataset A_I and F_E together contain all the information present in the causal partitions regarding the aggressive versus the timid turn of our simulations. In the 300 ms dataset, the best pair is F_I and F_E reaching 97% accuracy, which comes close to the 99% accuracy of the full causal model. We discuss the implications of these results in the next section.

5 Discussion

Some of our causal SVM models reached very high quality, correctly classifying 99% of simulations, which means the causal partitions are good predictors of their "aggressive" or "timid" turn. On this basis, we feel justified in affirming the *relevance* of causal partitions for human behavior model exploration. As for their *practical utility*, this is more challenging, because by *practical utility* we mean their ability to guide us toward the aspect of the model which, if modified, would bring about the disappearance of the diverging trajectories – "aggressive" versus "timid" – for one input parameter setting. We do not expect our method to directly "compute" the answer, but rather assist us in the process of formulating and testing hypotheses. Toward this end, we first need to identify and interpret the key factors behind the good performance of our "causal" classifiers. Exploration along the lines of forward and backward parameter selection pinpointed F_E as the primary candidate for explanation. Additionally, the interpretation of the reduced models in Table 4 supplied the second and third most important factors: A_I and F_I. In general, we can therefore conclude that the most important factors influencing the trajectory of the simulations seem to be, first, external events acting through fear (F_E), followed by social influence acting through both anger (A_I) and fear (F_I). This is the kind of hint that machine learning techniques could extract from our causal partitions. In order to proceed further, we needed to incorporate deeper technical knowledge of our simulation model in our hypotheses.

Our initial hypothesis was that early in the scenario – as a result of some unknown process or a random fluctuation – there forms a nucleus of agents that are either angry or afraid (while the other agents are still under the influence of their standard motives) and this nucleus then "converts" the rest of the agents by their social influence. If this were the case, we would expect the social influence components A_I and F_I to be negatively correlated (i.e. working against each other) and at the same time to be the best predictors for classification. However, Table 3 shows only a small (albeit negative) correlation and, moreover, they are not the best predictors, since their combined accuracy was only about 95%. At this point

of time our method was not yet so mature as to enable us to reject this hypothesis outright, but its likelihood certainly decreased. The main weakness of our approach was that we causally partitioned only the final values of fear and anger, while the really "decisive" period seemed to be the early part of the scenario. We needed to dynamically identify the moment in which the scenario divergence began and then apply the causal partition process at that point.

Our second hypothesis dealt with F_E and the early attack by the violence-prone individuals. There was an element of uncertainty as to how many stones they would be able to throw. They select the closest soldier as their target, and if they hit him twice, they are immobilized by an effective shot. Thus, in the worst case, they only throw two stones, while in the best case, four (with three soldiers, the fourth stone throw always results in immobilization). Given that stone throws incite more anger, while the effective shots more fear, the proportion of the stone throws versus effective shots in the early part of the scenario might be the tipping factor determining its subsequent aggressive or timid turn. If this hypothesis were true, then by adjusting the soldiers to use only warning shots we should force all the scenarios to take the aggressive turn. We tested this experimentally, permitting soldiers only to use warning shots, but the two divergent trajectories still persisted. Thus the second hypothesis had to be discarded as well.

The above experiment also rendered unlikely our third hypothesis – that our agent-based system was simply displaying chaotic behavior. The first counter-argument had already been furnished by the clustering exercise in Fig. 5, where the system behavior was shown to be robust, without undue sensitivity to the change in the simulation time step. We would expect high sensitivity if the observed divergence was primarily due to random fluctuations. Forcing soldiers to use only warning shots was a significant change and yet the divergence persisted. We can therefore quite safely conjecture that the divergence is caused by some stable and robust mechanism. This does not mean that the element of randomness plays no role – in fact it has to because without it the simulations would be completely deterministic – but that there are likely to be other, deterministic factors amplifying and stabilizing the divergence.

Our fourth hypothesis was that the external events and social influence acted together, perhaps as part of a two-stage or even a multi-stage process. However, in order to verify this we needed to improve our method first.

5.1 Method Improvements and New Preliminary Results

As mentioned above, the first improvement aimed at identifying decisive moments early in the simulations. This we have solved by logging causal partitions every 2 seconds during the simulation. Later, off-line, we could then identify the moment at which the causal partitions started exhibiting increased predictive power, and which partition components were responsible.

The second improvement reflected our need for more detailed information: instead of considering the combined effect of all the external events lumped together, we recorded the effect of soldier actions separately from that of civilian actions. This meant a split of each "external event" component of our causal partitions into two. Thus, F_E was split into F_{EC} (civilian actions) and F_{ES} (soldier actions), and A_E into A_{EC} (civilians) and A_{ES} (soldiers). The causal partitions of anger and fear thus became $A = (A_{A0}, A_{EC}, A_{ES}, A_I, A_L)$ and $F = (F_{F0}, F_{EC}, F_{ES}, F_I)$.

At present, our exploratory analysis with the improved method proceeds along two dimensions. The first (and currently the more advanced) relates to data mining, namely to alternative ways of determining the relative importance of causal attributes for prediction, e.g. through decision trees. We have published a preliminary study [6], where we have shown that the 10th second of the simulated time was the earliest moment in which the outcome could be predicted with an increased accuracy (72%), mainly thanks to the component F_{EC} (the effect of civilian actions on fear). In the 12th second, the prediction accuracy jumped to 87.6%, but here the importance of F_{EC} faded, having been replaced by F_I (the effect of social influence on fear), followed by F_{ES} (the effect of soldier actions on fear). In the 14th and 16th seconds the prediction accuracy reached 98.6% and 99.1%, respectively, and here F_I strengthened its lead, followed by F_{EC} and F_{ES} (in that order). Thus we indeed saw the expected staged process: the external events (civilian actions) starting it, and social influence taking over. Actions of soldiers seemed to play a temporary and intermediary role. We consider the fact that so early in the scenario we could predict so precisely its subsequent aggressive or timid turn (covering 90 seconds of simulated time) as very significant and promising. Yet, this result is not exactly what we had hoped for, because we still do not know which feature of our model is causing it. In order to answer that question, we need to devise new hypotheses and new experiments, which we envisage as the second, and more challenging, dimension of our future work.

Conclusions

In this paper we have shown how the principles of structural causal analysis can be adapted for exploratory analysis of a hybrid dynamical system whose continuous dynamics is described by ordinary nonlinear differential equations. The key step in the process is the introduction of "causal partitions" of model variables – vector-like structures whose components quantify the influence of various causal factors on a given variable. Causal partitions can be processed by machine learning techniques and assist in the process of meaningful interpretation of the emergent behavior of the simulated system.

In our practical experiments we have demonstrated the *relevance* of causal partitions, that is, their ability to classify the simulations accurately into two classes – timid and aggressive. Regarding the *practical utility* of our method, we formulated several hypotheses and tried to qualitatively assess their likelihood based on the results of our clustering and classification experiments. We have also

implemented the improvements proposed in [3] and presented the first tentative results reached with the improved method. The successful resolution of our task requires further work along two dimensions:

- To develop reliable methods of determining the relative importance of causal attributes for prediction
- To formulate new hypotheses regarding the underlying causes of the observed behavior, and design new experiments to verify them

In spite of the work that is yet to be done, we feel justified in concluding that structural causal analysis and causal partitions represent potentially valuable tools not only for hybrid dynamical systems, but also for simulation studies in general.

Acknowledgement

This work was supported by the European Defence Agency project A-0938-RT-GC EUSAS, by the Slovak Research and Development Agency under the contract No. APVV-0233-10, and by projects KC-INTELINSYS ITMS 26240220072 and VEGA No. 2/0054/12.

References

[1] J. Y. Halpern and J. Pearl, "Causes and Explanations: a Structural-Model Approach. Part I: Causes," *Brit. J. Phil. Sci.*, 56, pp. 843-887, 2005

[2] J. Y. Halpern and J. Pearl, "Causes and Explanations: a Structural-Model Approach. Part II: Explanations," *Brit. J. Phil. Sci.*, 56, pp. 889-911, 2005

[3] M. Kvassay, L. Hluchý, P. Krammer and B. Schneider, "Exploring Human Behaviour Models through Causal Summaries and Machine Learning," in *Proceedings of INES 2013*. Budapest: IEEE Industrial Electronic Society, 2013, pp. 231-236

[4] M. Kvassay, L. Hluchý and B. Schneider, "Summarizing the Behaviour of Complex Dynamic Systems," in *Proceedings of SAMI 2013*. Piscataway: IEEE, 2013, pp. 15-20

[5] M. Kvassay, L. Hluchý, B. Schneider and H. Bracker, "Towards Causal Analysis of Data from Human Behaviour Simulations," in *Proceedings of LINDI 2012*. Piscataway: IEEE, 2012, pp. 41-46

[6] M. Kvassay, P. Krammer and L. Hluchý, "Validation of Parameter Importance in Data Mining: a Case Study," in *Proceedings of WIKT 2013*, Eds. F. Babič and J. Paralič. Košice: Centre for Information Technologies, Technical University in Košice, 2013, pp. 115-120

[7] B. Latané, "Dynamic Social Impact," in *Philosophy and Methodology of the Social Sciences*, Vol. 23, R. Hegselmann, U. Mueller and K. G. Troitsch, Eds. Dordrecht: Kluwer Academic Publishers, 1996

[8] J. Pearl, “The Art and Science of Cause and Effect” 1996 Faculty Research Lecture, http://singapore.cs.ucla.edu/LECTURE/lecture_sec1.htm

[9] J. Pearl, *Causality: Models, Reasoning, and Inference.* New York: Cambridge University Press, 2000

[10] J. Pearl, "An Introduction to Causal Inference," *The International Journal of Biostatistics* Vol. 6 (2010), Issue 2, Article 7. Available at: http://ftp.cs.ucla.edu/pub/stat_ser/r354-corrected-reprint.pdf

[11] J. Pearl, “Reasoning with Cause and Effect,” 1999 IJCAI Award Lecture, URL: http://singapore.cs.ucla.edu/IJCAI99/index.html

[12] J. Platt, “Fast Training of Support Vector Machines using Sequential Minimal Optimization,” in B. Schoelkopf and C. Burges and A. Smola, editors, *Advances in Kernel Methods - Support Vector Learning*, 1998

[13] B. Schmidt, “Modelling of Human Behaviour: The PECS Reference Model,” in *Proc. 14th European Simulation Symposium*, A. Verbraeck, W. Krug, Eds. SCS Europe BVBA, 2002

[14] C. Urban, “PECS A Reference Model for the Simulation of Multiagent Systems,” in *Tools and Techniques for Social Science Simulation,* R. Suleiman; K. G. Troitzsch and N. Gilbert, Eds. Heidelberg; New York: Physica-Verlag, 2000, pp. 83-114

[15] Weka 3: Data Mining Software in Java, 2013, URL: http://www.cs.waikato.ac.nz/ml/weka

Graphs with Equal Irregularity Indices

Darko Dimitrov[1], **Tamás Réti**[2]

[1]Institute of Computer Science, Freie Universität Berlin
Takustraße 9, D–14195 Berlin, Germany
E-mail: dimdar@zedat.fu-berlin.de

[2]Óbuda University
Bécsi út 96/B, H-1034 Budapest, Hungary
E-mail: reti.tamas@bgk.uni-obuda.hu

Abstract: The *irregularity* of a graph can be defined by different so-called *graph topological indices*. In this paper, we consider the irregularities of graphs with respect to the *Collatz-Sinogowitz index* [8], the *variance of the vertex degrees* [6], the *irregularity of a graph* [4], and the *total irregularity of a graph* [1]. It is known that these irregularity measures are not always compatible. Here, we investigate the problem of determining pairs or classes of graphs for which two or more of the above mentioned irregularity measures are equal. While in [17] this problem was tackled in the case of bidegreed graphs, here we go a step further by considering tridegreed graphs and graphs with arbitrarily large degree sets. In addition we pressent the smallest graphs for which all above irregularity indices are equal.

Keywords: irregularity measures of graph; topological graph indices

1 Introduction

Let G be a simple undirected graph of order $n = |V(G)|$ and size $m = |E(G)|$. The *degree* of a vertex v in G is the number of edges incident with v and it is denoted by $d_G(v)$. A graph G is *regular* if all its vertices have the same degree, otherwise it is *irregular*. However, in many applications and problems it is of big importance to know how irregular a given graph is. The quantitative topological characterization of irregularity of graphs has a growing importance for analyzing the structure of deterministic and random networks and systems occurring in chemistry, biology and social networks [7, 12]. In this paper, we consider four graph topological indices that quantify the irregularity of a graph. Before we introduce those indices, we present some necessarily notions and definitions.
A *universal* vertex is the vertex adjacent to all other vertices. We denote by $m_{r,s}$ the number of edges in G with end-vertex degrees r and s, and by n_r the numbers of vertices n G with degree r. Numbers $m_{r,s}$ and n_r are referred as the *edge-parameters* and the *vertex-parameters* of G, respectively.

The *mean degree* of a graph G is defined as $\overline{d}(G) = 2m/n$. Graphs G_1 and G_2 are said to be *edge-equivalent* if for their corresponding edge-parameters sets $\{m_{r,s}(G_1) > 0\} = \{m_{r,s}(G_2) > 0\}$ holds. Analogously, they are called *vertex-equivalent* if for their vertex-parameters sets $\{n_r(G_1) > 0\} = \{n_r(G_2) > 0\}$ is fulfilled.

A sequence of non-negative integers $D = (d_1, d_2, \ldots, d_n)$ is said to be *graphical* if there is a graph with n vertices such that vertex i has degree d_i. If in addition $d_1 \geq d_2 \geq \cdots \geq d_n$ then D is a *degree sequence*. The *degree set*, denoted by $\mathcal{D}(G)$, of a simple graph G is the set consisting of the distinct degrees of vertices in G.

The *adjacency matrix* $A(G)$ of a simple undirected graph G is a matrix with rows and columns labeled by graph vertices, with a 1 or 0 in position (v_i, v_j) according to whether v_i and v_j are adjacent or not. The *characteristic polynomial* $\phi(G, t)$ of G is defined as characteristic polynomial of $A(G)$: $\phi(G, \lambda) = \det(\lambda \mathbf{I_n} - A(G))$, where $\mathbf{I_n}$ is $n \times n$ identity matrix. The set of eigenvalues of the adjacent matrix $A(G)$ is called the *graph spectrum* of G. The largest eigenvalue of $A(G)$, denoted by $\rho(G)$, is called the *spectral radius* of G. Graphs that have the same graph spectrum are called *cospectral* or *isospectral* graphs.

The four irregularity measures of interest in this study are presented next. The first one is based on the spectral radius of graph. If a graph G is regular, then it holds that the mean degree $\overline{d}(G)$ is equal to its spectral radius $\rho(G)$. Collatz and Sinogowitz [8] introduced the difference of these quantities as a measure of irregularity of G:

$$\mathrm{CS}(G) = \rho(G) - \overline{d}(G).$$

The first investigated irregularity measure that depends solely on the vertex degrees of a graph G is the *variance of the vertex degrees*, defined as

$$\mathrm{Var}(G) = \frac{1}{n} \sum_{i=1}^{n} d_G^2(v_i) - \frac{1}{n^2} \left(\sum_{i=1}^{n} d_G(v_i) \right)^2.$$

Bell [6] has compared CS(G) and Var(G) and showed that they are not always compatible. Albertson [4] defines the *irregularity* of G as

$$\mathrm{irr}(G) = \sum_{uv \in E} |d_G(u) - d_G(v)|.$$

In [1] a new irregularity measure, related to the irregularity measure by Albertson was introduced. This measure also captures the irregularity only by the difference of vertex degrees. For a graph G, it is defined as

$$\mathrm{irr}_t(G) = \frac{1}{2} \sum_{u,v \in V(G)} |d_G(u) - d_G(v)|.$$

Very recently, irr and irr_t were compared in [9].
These irregularity measures as well as other attempts to measure the irregularity of a graph were studied in several works [2,3,5,13–15]. It is interesting that the above four irregularity measures are not always compatible for some pairs of graphs. The main purpose of this paper is to determine classes of graphs for which two or more of the above mentioned irregularity measures are equal.
The rest of the paper is organized as follows: In Section 2 we investigate tridegreed graphs that have equal two or more of the above presented regularity measures. In Section 3 we consider the same problem but for graphs with arbitrary large degree sets. The smallest graphs with equal irregularity measures are investigated in Section 4. Final remarks and open problems are presented in Section 5.

2 Tridegreed graphs

Most of the results presented in this section are generalized in Section 3. However, due to the uniqueness of the related proofs and used constructions, we present the results of tridegreed graphs separately.

2.1 An infinite sequence of tridegreed graphs with same irr and irr_t indices

Proposition 1. *Let n be an arbitrary positive integer larger than 7. Then there exists a tridegreed graph with n vertices $J(n)$ for which* $\mathrm{irr}(J(n)) = \mathrm{irr}_t(J(n))$ *holds.*

Proof. The graph $J(n)$ can be constructed as $J(n) = C_{n-3} + P_3$, where C_{n-3} is a cycle on $n-3$ vertices and P_3 is a path on 3 vertices. It is easy to see that the graph obtained is tridegreed if n is larger than 7, and it contains one universal vertex, exactly. The vertex degree distribution of $J(n)$ is $n_5 = n-3$, $n_{n-2} = 2$ and $n_{n-1} = 1$. It can be shown that for $J(n)$ the equality $\mathrm{irr}(G) = \mathrm{irr}_t(G)$ holds. As an example graph $J(9)$ is depicted in Figure 1.
It is easy to show that for graph $J(9)$ the corresponding edge parameters are: $m_{5,5} = 6, m_{5,7} = 12, m_{5,8} = 6, m_{7,8} = 2$. Moreover, the equality $\mathrm{irr}(J(9)) = \mathrm{irr}_t(J(9)) = 44$ holds. □

2.2 Pairs of tridegreed graphs with same irr, irr_t and Var indices

Theorem 1. *Let G_a and G_b be connected edge-equivalent graphs. Then the equalities* $\mathrm{irr}(G_a) = \mathrm{irr}(G_b), \mathrm{irr}_t(G_a) = \mathrm{irr}_t(G_b)$ *and* $\mathrm{Var}(G_a) = \mathrm{Var}(G_b)$ *hold.*

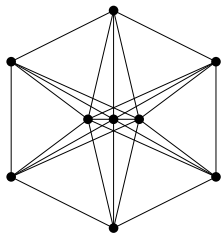

Fig. 1. The tridegreed graph $J(9)$

Proof. By definition, $\mathrm{irr}(G)$ depends solely on the edge parameters of G. Since graphs G_a and G_b have same edge parameters, it follows that $\mathrm{irr}(G_a) = \mathrm{irr}(G_b)$. From the definitions of $\mathrm{irr}_t(G)$ and $\mathrm{Var}(G)$ indices, we have

$$\mathrm{irr}_t(G) = \frac{1}{2} \sum_{u,v \in V(G)} |d(u) - d(v)| = \sum_r \sum_{s<r} n_r n_s (r-s),$$

$$\mathrm{Var}(G) = \frac{1}{n} \sum_{u \in V(G)} d^2(u) - \left(\frac{2m}{n}\right)^2 = \frac{1}{n} \sum_r n_r \left(r - \frac{2m}{n}\right)^2.$$

So, $\mathrm{irr}_t(G)$ and $\mathrm{Var}(G)$ depend only on the vertex parameters of G. Since

$$r \cdot n_r(G) = \sum_{s \neq r} m_{r,s} + 2m_{r,r},$$

it follows that if graphs G_a and G_b are edge-equivalent, then G_a and G_b are necessarily vertex-equivalent as well, that is they have identical vertex-parameter set. Then, it also holds that $\mathrm{irr}_t(G_a) = \mathrm{irr}_t(G_b)$ and $\mathrm{Var}(G_a) = \mathrm{Var}(G_b)$. □

In Figure 2, two infinite sequences of pairs of tridegreed planar graphs that satisfied Theorem 1 are depicted. For a fixed integer $k \geq 1$, the graph $G_a(k)$ contains k hexagons, while the graph $G_b(k)$ contains k quadrangles. Graphs $G_a(k)$ and $G_b(k)$ have identical edge-parameters: $m_{3,1} = 4$, $m_{3,2} = 4k$, $m_{3,3} = k+1$, and $n = 4k+6$, $m = 5k+5$. This implies that $G_a(k)$ and $G_b(k)$ have identical irregularity indices irr, irr_t and Var.
In what follows, we will verify that the converse of Theorem 1 is not true.

Proposition 2. *There exist tridegreed connected graphs with different edge-parameter distributions but identical* $\mathrm{irr}, \mathrm{irr}_t, \mathrm{Var}$ *and* CS *irregularity indices.*

Proof. An example is given in Figure 3. It is easy to see that polyhedral graphs (nanohedra graphs) depicted in Figure 3 are characterized by the following fundamental properties:

i) Polyhedral graphs G_c and G_d have $n = 8$ vertices and $m = 15$ edges.

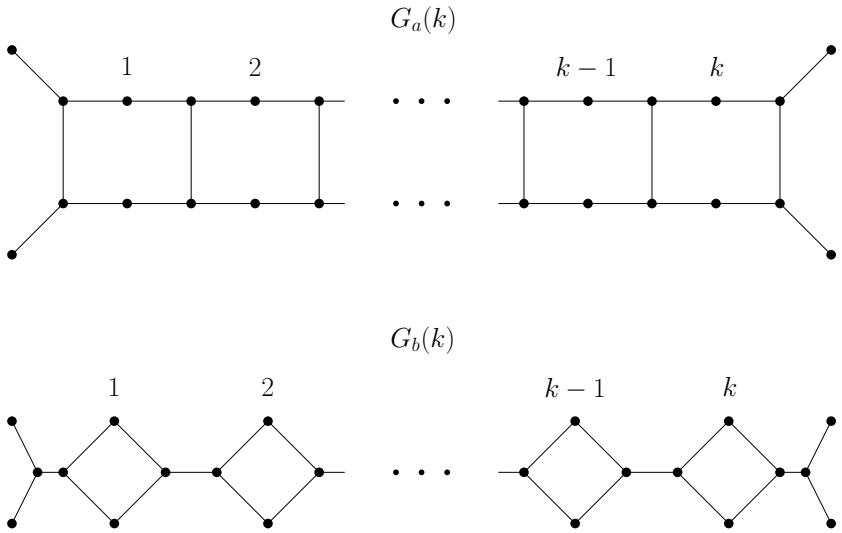

Fig. 2. Edge-equivalent graphs $G_a(k)$ and $G_a(k)$

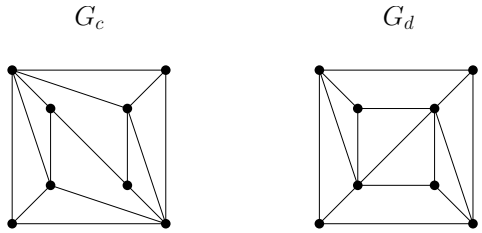

Fig. 3. Tridegreed polyhedral cospectral graphs [16] having identical degree sequence and different edge-parameter distribution, but identical $\mathrm{irr}, \mathrm{irr}_t, \mathrm{Var}$ and CS irregularity indices

ii) They have the same degree distribution: $n_3 = 4$, $n_4 = 2$ and $n_5 = 2$. This implies that $\mathrm{Var}(G_c) = \mathrm{Var}(G_d)$, and their total irregularity indices are equal, $\mathrm{irr}_t(G_c) = \mathrm{irr}_t(G_d)$.

iii) Their edge-parameter distributions are different, namely for graph $G_c(m_{33} = 1, m_{34} = 4, m_{35} = 6, m_{45} = 4)$ and for graph $G_d(m_{34} = 6, m_{35} = 6, m_{45} = 2, m_{55} = 1)$.

iv) Their Albertson indices are equal, $\mathrm{irr}(G_c) = \mathrm{irr}(G_d) = 20$. (This is an interesting fact, because the edge-parameter distributions of graphs G_c and G_d are different).

v) G_c and G_d are isospectral graphs (polyhedral twin graphs) [16] . This implies that their Collatz-Sinogowitz indices are equal, as well. □

2.3 Pairs of tridegreed graphs with same $\mathbf{irr}, \mathbf{irr}_t, \mathbf{Var}$ and CS indices

First, we state some necessary definitions and results needed for the derivation of the main results of this section. A bipartite graph G is *semiregular* if every edge of G joins a vertex of degree δ to a vertex of degree Δ. The 2-*degree* of a vertex u, denoted by $d_2(u)$ is the sum of degrees of the vertices adjacent to u [20]. The average-degree of u is $d_2(u)/d(u)$ and it is denoted by $p(u)$. A graph G is called *pseudo-regular* (or *harmonic*) if every vertex of G has equal average-degree. A bipartite graph is called *pseudo-semiregular* if each vertex in the same part of a bipartition has the same average-degree [20]. It follows that semiregular graphs form a subset of pseudo-semiregular graphs.

Theorem 2 ([20]). *Let G be a connected graph with degree sequence $(d_1, d_2, \ldots, d_n)$. Then*

$$\rho(G) \geq \sqrt{\frac{d_2(v_1)^2 + d_2(v_2)^2 + \cdots + d_2(v_n)^2}{d_1^2 + d_2^2 + \cdots + d_n^2}},$$

with equality if and only if G is a pseudo-regular graph or a pseudo-semiregular graph.

The following result is a consequence of Theorem 2.

Corollary 1 ([20]). *Let G be a pseudo-regular graph with $d_2(v) = p \cdot d(v)$ for each $v \in V(G)$, then $\rho(G) = p$.*

Theorem 3. *There are infinitely many pairs of tridegreed pseudo-regular graphs (G_1, G_2) for which* $\mathrm{irr}(G_1) = \mathrm{irr}(G_2)$, $\mathrm{irr}_t(G_1) = \mathrm{irr}_t(G_2)$, $\mathrm{Var}(G_1) = \mathrm{Var}(G_2)$, *and* $\mathrm{CS}(G_1) = \mathrm{CS}(G_2)$.

Proof. We prove the theorem by a construction. Let $G(2, x, y)$ be a graph with vertex set $V(G(2, x, y)) = U \cup W \cup \{z\}$ with connectivity determined as follows: vertex set $U = \{u_1, u_2, \ldots, u_x\}$ induces connected 2-regular subgraph (cycle $c_1 c_2 \cdot c_x$); W is comprised of $y \cdot x$ pendant vertices such that each vertex from U is adjacent to y vertices from W; and the 'central vertex' z is adjacent to each vertex from U. Two instances of such graphs, $G_1 = G(2, 7, 1)$ and $G_3 = G(2, 13, 2)$, are depicted in Figure 4. The parameter 2 in the graph's representation indicates that the vertex set U induces connected 2-regular subgraph. The average degree of a vertex from U is $(2(3+y)+x+y)/(3+y)$. The average degree of a vertex from W is $3+y$, which is also the average degree of z. Thus, $G(2, x, y)$ is pseudo-regular graph if $(2(3 + y) + x + y)/(3 + y) = (3 + y)$, or if

$$x = y^2 + 3y + 3. \tag{1}$$

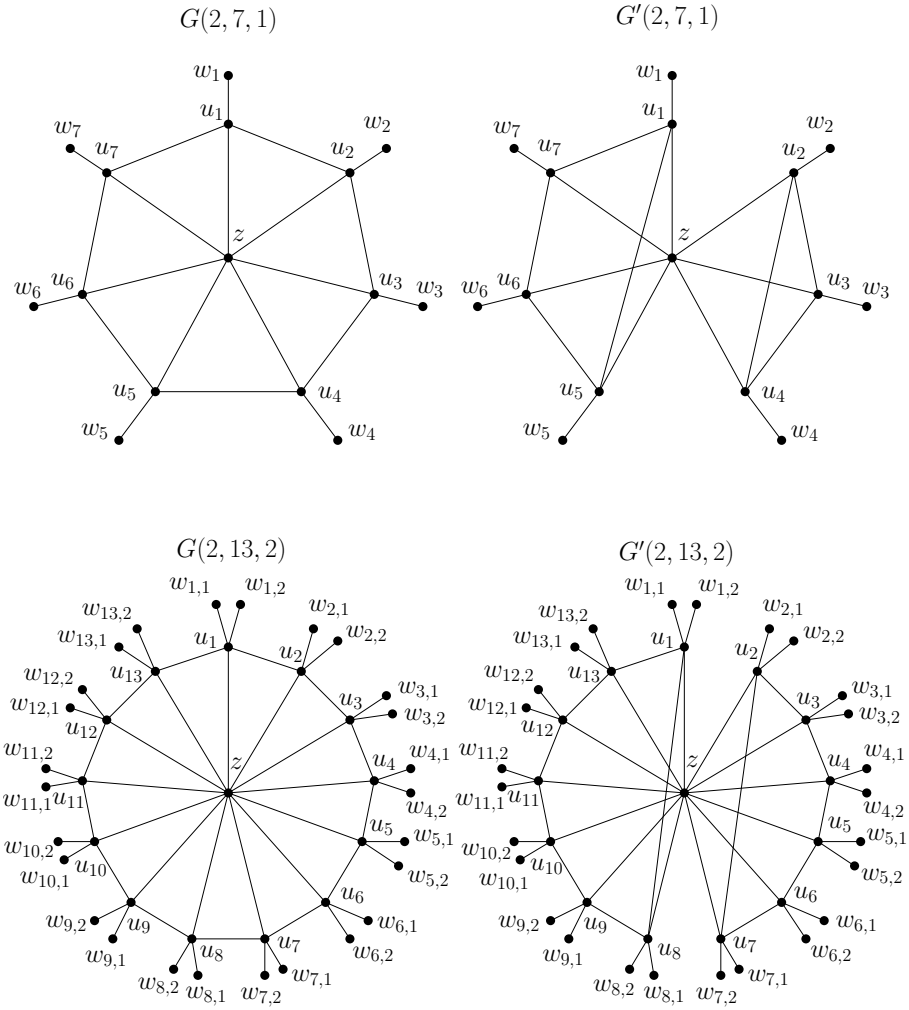

Fig. 4. Pseudo-regular graphs $G(2,7,1)$, $G'(2,7,1)$, $G(2,13,2)$, $G'(2,13,2)$, with $\rho(G(2,7,1)) = \rho(G'(2,7,1)) = 4$ and $\rho(G(2,13,2)) = \rho(G'(2,13,2)) = 5$

Next, consider a pair of edges (u_iu_{i+1}, u_ju_{j+1}) such that $(i \bmod x) + 2 < j$. We delete edges u_iu_{i+1} and u_ju_{j+1} and add edges u_iu_{j+1} and $u_{i+1}u_j$ to G_1, obtaining a graph $G'(2,x,y)$, which is edge equivalent (and therefore vertex equivalent) to $G(2,x,y)$. Also, the average degrees of the vertices of $G'(2,x,y)$ are equal to the average degrees of the vertices of $G(2,x,y)$. By Corollary 1, $\rho(G(2,x,y)) = \rho(G'(2,x,y)) = 3+y$, for infinitely many integer solutions (x,y) of (1). This together with the fact that $G(2,x,y)$ and $G'(2,x,y)$ are

edge equivalent, gives that $G(2,x,y)$ and $G'(2,x,y)$ have equal irr, irr_t, Var and CS indices. □

Two pairs of pseudo-regular graphs $G(2,7,1)$ and $G'(2,7,1)$, and pair $G(2,13,2)$ and $G'(2,13,2)$, for which Theorem 3 holds, are depicted in Figure 4. These graphs corresponds to the first two smallest pairs of integers that solve the equation (1).
Observe that the class of pair of graphs that satisfies Theorem 3 can be extended by considering graphs $G(k,x,y)$, $k \geq 2$. These graphs are generalization of $G(2,x,y)$ graphs, in such a way that the vertex set U induces a k-regular subgraph.

An alternative construction. Next, we will present a new construction, that asserts the claim of Theorem 3. This construction is based on so-called *Seidel switching* [19], which for a vertex v flips all the adjacency relationships with other vertices, i.e, all of the edges adjacent to v are removed and the edges that were not adjacent to v are added. In general, for a subset S of $V(G)$, the graph H is obtain from the graph G by *switching about* S if $V(H) = V(G)$ and $E(H) = \{uv \in E(G) | u,v \in S \text{ or } u,v \notin S\} \cup \{uv \notin E(G) | u \in S \text{ and } v \notin S\}$.

Construction by local switching.[[11]] Let G be a graph and let $\pi = (C_1, C_2, \ldots, C_k, D)$ be a partition of $V(G)$. Suppose that, whenever $1 \leq i,j \leq k$ and $v \in D$, we have

(a) any two vertices of C_i have same number of neighbors in C_j, and
(b) v has either 0, $n_i/2$ or n_i neighbors in C_i, where $n_i = |C_i|$.

The graph $G^{(\pi)}$ formed by *local switching in G with respect to π* is obtained from G as follows. For each $v \in D$ and $1 \leq i \leq k$ such that v has $n_i/2$ neighbors in C_i, delete these $n_i/2$ and join v instead to the other $n_i/2$ vertices in C_i.

The property of the above construction that will be used here is the following one.

Theorem 4 ([11]). *Let G be a graph and let π be a partition of $V(G)$ which satisfies properties (a) and (b) above. Then $G^{(\pi)}$ and G are cospectral, with cospectral compilements.*

The following construction is a special case of the construction by local switching, and will be used to construct infinite series of pairs of graph with the property stated in Theorem 3.

An example of the construction by local switching. A graph G is comprised of k-regular graph H on even number of vertices and one additional vertex v

adjacent to exactly half of the vertices of H. For $\pi(V(H), \{v\})$, we have that $G^{(\pi)}$ is obtained by joining v instead to the other vertices of H.

In the above example, as it was mentioned in [11], if H has $2m$ vertices and a trivial automorphism group, than all $\binom{2m}{m}$ possible realisations of H are non-isomorphic. By Theorem 4 the graphs G and $G^{(\pi)}$ are cospectral. G and $G^{(\pi)}$ have also same degree set $\mathcal{D}(G) = \mathcal{D}(G^{(\pi)}) = \{k, k+1, m\}$. The number of edges with endvertices with degrees m and k in G is the same as in $G^{(\pi)}$. The same holds for edges with endvertices with degrees m and $k+1$, and m and $m+1$. Thus, G and $G^{(\pi)}$ are edge equivalent, and $\mathrm{irr}(G) = \mathrm{irr}(G^{(\pi)})$, $\mathrm{irr}_t(G) = \mathrm{irr}_t(G^{(\pi)})$,$\mathrm{Var}(G) = \mathrm{Var}(G^{(\pi)})$ and $\mathrm{CS}(G) = \mathrm{CS}(G^{(\pi)})$. Note that if H has less than 8 vertices, then G and $G^{(\pi)}$ are isomorphic. In Figure 5 an example of Seidel switching for $H = C_8$ (cycle with 8 vertices) is depicted.

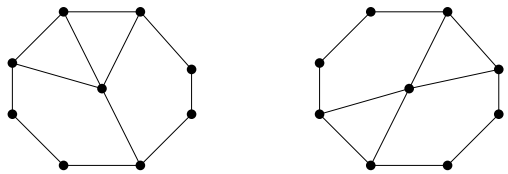

Fig. 5. Seidel switching when H is a cycle with 8 vertices

3 Graphs with arbitrary large degree set and same irregularity indices

3.1 An infinite sequence of graphs with same irr and irr_t indices

A graph G is a *complete k-partite* graph if there is a partiton $V_1 \cup \cdots \cup V_k = V(G)$ of the vertex set, such that $uv \in E(G)$ if and only if u and v are in different parts of the partition.

Proposition 3. *There is an infinite sequences of graphs $\mathcal{G}$, such that for a graph $G \in \mathcal{G}$ $\mathrm{irr}(G) = \mathrm{irr}_t(G)$ holds.*

Proof. If every two vertices of G with different degrees are adjacent, then $\mathrm{irr}(G) = \mathrm{irr}_t(G)$. Graphs that satisfy this condition are the complete k-partite graphs. □

3.2 Pairs of graphs with arbitrary large degree set and same $\mathrm{irr}, \mathrm{irr}_t$, and Var indices

Proposition 4. *There are infinitely many graphs G_1 and G_2 with same arbitrary cardinality of their degree sets satisfying $\mathrm{irr}(G_1) = \mathrm{irr}(G_2)$, $\mathrm{irr}_t(G_1) = \mathrm{irr}_t(G_2)$, and $\mathrm{Var}(G_1) = \mathrm{Var}(G_2)$.*

Proof. Consider the graphs $G^1_{csl}(14,2,4)$ and $G^2_{csl}(14,2,4)$ depicted in Figure 6. The graphs are bidegreed edge-equivalent, belong to the so-called *complete split-like* graphs, and were introduced and studied in [17]. Choose ver-

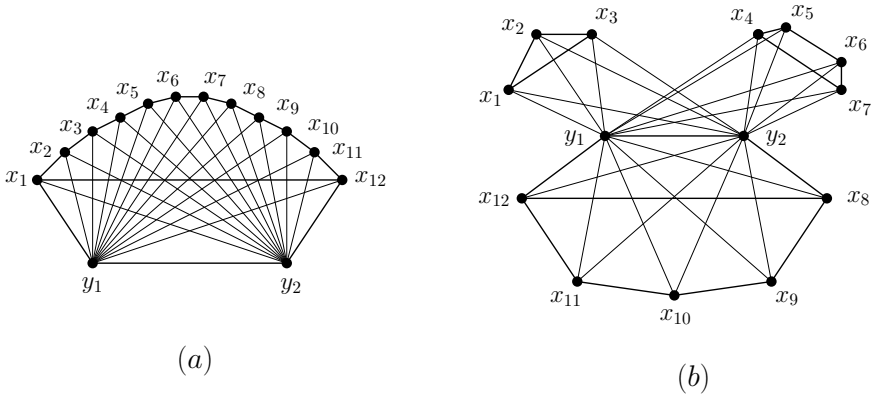

Fig. 6. Bidegreed edge-equivalent complete split-like graphs, (a) $G^1_{csl}(14,2,4)$ and (b) $G^2_{csl}(14,2,4)$

tices $u \in V(G^1_{csl}(14,2,4))$ and $u \in V(G^2_{csl}(14,2,4))$ such that $d(u) = d(v)$. Attach to u an arbitrary graph H obtaining a graph G_1. Attach to v a copy of H obtaining a graph G_2. The graphs G_1 and G_2 are also edge-equivalent and therefore, $\mathrm{irr}(G_1) = \mathrm{irr}(G_2)$, $\mathrm{irr}_t(G_1) = \mathrm{irr}_t(G_2)$, $\mathrm{Var}(G_1) = \mathrm{Var}(G_2)$. □

Observe that in the construction, presented in the above proof, one instead of $G^1_{csl}(14,2,4)$ and $G^2_{csl}(14,2,4)$ can use any edge-equivalent graphs, for example graphs $G_a(k)$ and $G_b(k)$ in Figure 2.

3.3 Pairs of graphs with arbitrary large degree set and same $\mathbf{irr}, \mathbf{irr_t}, \mathbf{Var}$ and CS indices

The 0-*sum* of two graphs G and H is got by identifying a vertex in G with a vertex in H. To obtain the result of this section, we will use the following theorem and a corollary of it.

Theorem 5 ([10]). *Let F be a 0-sum obtained by merging v in G with v in H, then the characteristic polynomial of F is*

$$\phi(F,\lambda) = \phi(G,\lambda)\phi(H \setminus v,\lambda) + \phi(G \setminus v,\lambda)\phi(H,\lambda) - \lambda\phi(G \setminus v,\lambda)\phi(H \setminus v,\lambda).$$

Corollary 2 ([10]). *If we hold G and its vertex v fixed, then the characteristic polynomial of the 0-sum of G and H is determined by the characteristic polynomials of H and $H \setminus v$.*

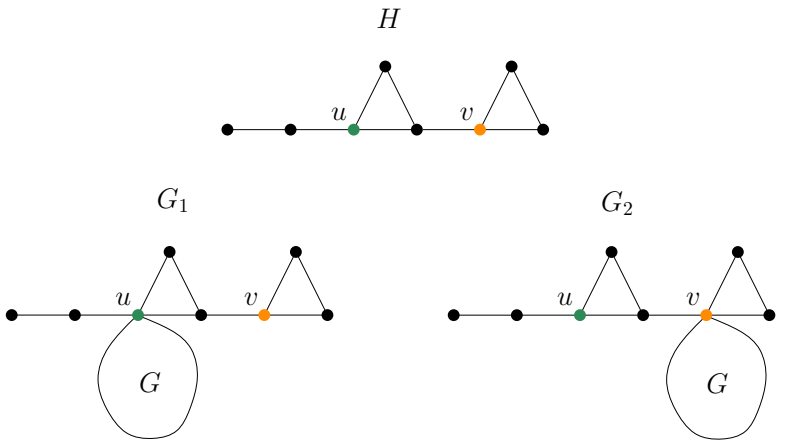

Fig. 7. Two cospectral and edge-equvivalent graphs G_1 and G_2 obtained as 0-sums of H and arbitrary graph G

Theorem 6. *There are infinitely many graphs G_1 and G_2 with same arbitrary cardinality of their degree sets satisfying* $\mathrm{irr}(G_1) = \mathrm{irr}(G_2)$, $\mathrm{irr}_t(G_1) = \mathrm{irr}_t(G_2)$, $\mathrm{Var}(G_1) = \mathrm{Var}(G_2)$, *and* $\mathrm{CS}(G_1) = \mathrm{CS}(G_2)$.

Proof. Let G be an arbitrary graph. Consider the graph H in Figure 7. Let G_1 be a 0-sum of H and G, obtained by merging v in G with v in H, and G_2 be a 0-sum obtained by merging u in G with u in H. Note that $H \setminus v$ and $H \setminus u$ are isomorphic, so $\phi(H \setminus v, \lambda) = \phi(H \setminus u, \lambda)$. Together with Corollary 2, we have that $\phi(G_1, \lambda) = \phi(G_1, \lambda)$, or that G_1 and G_2 are cospectral. Also, it is easy to see that G_1 and G_2 are edge-equivalent. Thus, G_1 and G_2 have same irr, irr_t, Var and CS indices. □

A generalization of the example from Figure 7 is given in Figure 8. The graph H is comprised of three isomorphic subgraphs Q_l, Q_m, Q_r, each of order at least 3, and two vertices u and v. Between the vertex v and the subgraph Q_r, there are same number of edges as between the vertex u and the subgraph Q_m. Also, between the vertex u and the subgraph Q_l, there are same number of edges as between the vertex v and the subgraph Q_m. The number of the edges between v and subgraph Q_m differs than the number of the edges between v and subgraph Q_r. We require these conditions to avoid an isomorphism of graphs G_1 and G_2, obtained as 0-sums of H and arbitrary graph G. The graphs G_1 and G_2 are constructed in the same manner as above: G_1 is a 0-sum obtained by merging v in G with v in H, and G_2 be a 0-sum obtained by merging u in G with u in H. From the construction it follows that G_1 and G_2 are edge-equivalent. In this case also $H \setminus v$ and $H \setminus u$ are isomorphic, so $\phi(H \setminus v, \lambda) = \phi(H \setminus u, \lambda)$. Together with Corollary 2, we have that $\phi(G_1, \lambda) = \phi(G_1, \lambda)$, or that G_1 and G_2 are cospectral. Thus, it

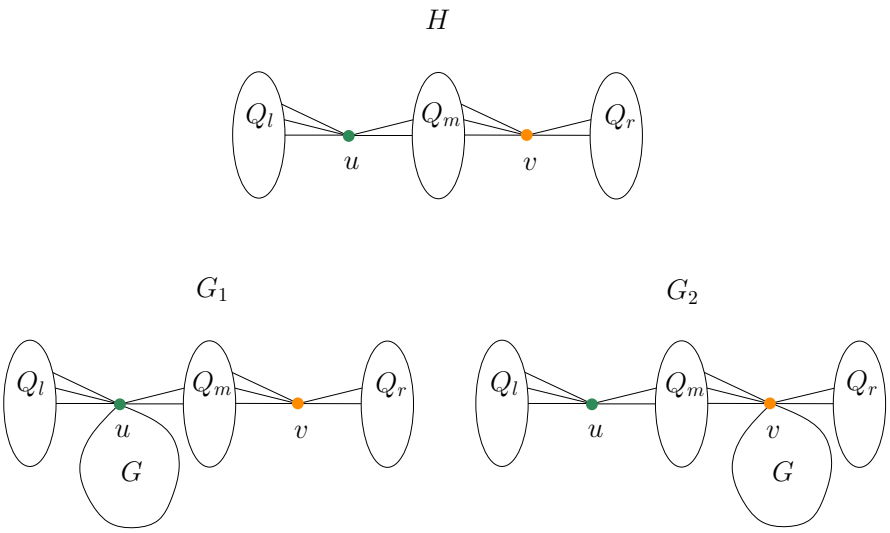

Fig. 8. A generalization of the example from Figure 7

holds that $\mathrm{irr}(G_1) = \mathrm{irr}(G_2)$, $\mathrm{irr}_t(G_1) = \mathrm{irr}_t(G_2)$, $\mathrm{Var}(G_1) = \mathrm{Var}(G_2)$, and $\mathrm{CS}(G_1) = \mathrm{CS}(G_2)$.

4 Small graphs with identical irregularities

Let $G_1 = (V_1, E_1)$ and $G_2 = (V_2, E_2)$ be two graphs. We said that G_1 *is smaller than* G_2 if and only if $|V_1| + |E_1| < |V_2| + |E_2|$. Consequently, for two pairs of graphs $P_1 = (G_1, G_2)$ and $P_2 = (G_3, G_4)$, we said that P_1 *is smaller than* P_2 if and only if $|V_1| + |E_1| + |V_2| + |E_2| < |V_3| + |E_3| + |V_4| + |E_4|$. The results in this section are obtained by computer search using mathematical software package Sage [18].

Proposition 5. *There are no two graphs, both of same order $n \leq 5$, that have identical irregularity indices* $\mathrm{CS}, \mathrm{Var}, \mathrm{irr}$ *and* irr_t.

Next the smallest example of pair of graphs will be given with equal $\mathrm{CS}, \mathrm{Var}, \mathrm{irr}$ and irr_t indices.

4.1 Graphs of order 6

The smallest pair of graphs with identical irregularity indices $\mathrm{CS}, \mathrm{Var}, \mathrm{irr}$ and irr_t is depicted in Figure 9. Both graphs are of order 6, but one is of size 6 and the other of size 9. Their $\mathrm{CS}, \mathrm{Var}, \mathrm{irr}$ and irr_t indices are 0.236068, 0.800000, 8, and 16, respectively. They have different spectral radii, namely

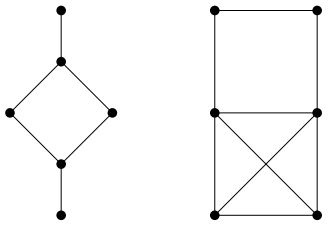

Fig. 9. The smallest pair of (tridegreed) connected graphs with identical irregularity indices $\mathrm{CS}, \mathrm{Var}, \mathrm{irr}$ and irr_t

the smaller one has spectral radius 2.236068 and bigger one 3.236068. The rest of the graphs of order 6, with identical irregularity indices $\mathrm{CS}, \mathrm{Var}, \mathrm{irr}$ and irr_t are given in Figure 10. The parameters of the graphs of order 6 with

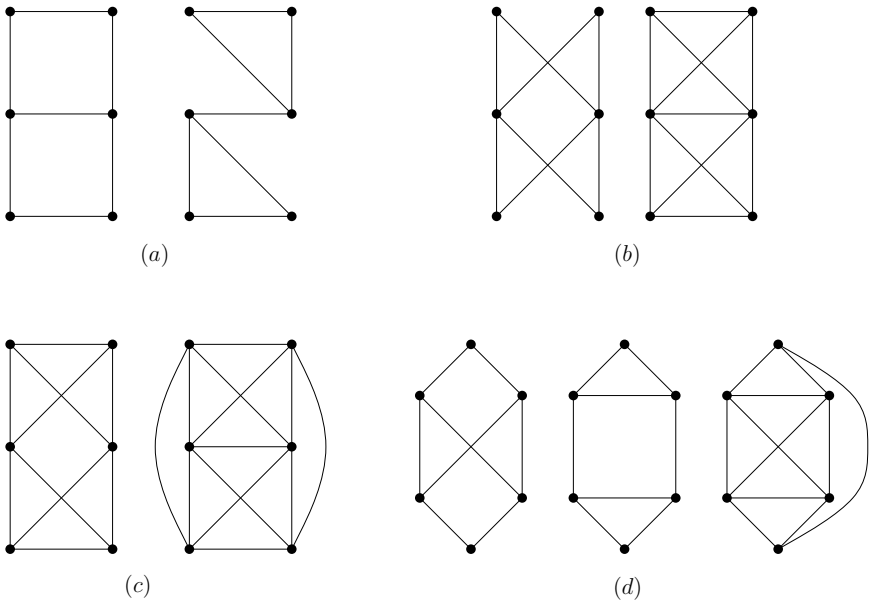

Fig. 10. Besides the pair in Figure 9, there are three other pairs of connected graphs of order 6 (a), (b), (c), and only one triple of graphs of order 6 (d) with identical irregularity indices $\mathrm{CS}, \mathrm{Var}, \mathrm{irr}$ and irr_t

identical irregularity indices $\mathrm{CS}, \mathrm{Var}, \mathrm{irr}$ and irr_t are summarized in Table 1. The graphs are enumerated with respect to their sizes, a smaller graph has smaller associated number (G_no). For a given graph, beside the values of the

indices CS, Var, irr and irr_t, its spectral radius ρ, degree sequence and graph6 code are given. There are 112 non-isomorphic connected graphs of order 6.

Table 1: All four pairs and the only triple of graphs of order 6 with identical irregularity indices CS, Var, irr and irr_t

tuple_no	G_no	graph6	degree sequence	irr	irr_t	CS	Var	ρ
1	10	E?]o	[3, 3, 2, 2, 1, 1]	8	16	0.236068	0.800000	2.236068
	77	E\`]w	[4, 4, 3, 3, 2, 2]	8	16	0.236068	0.800000	3.236068
2	36	EKNG	[3, 3, 2, 2, 2, 2]	4	8	0.080880	0.266667	2.414214
	37	E\`NG	[3, 3, 2, 2, 2, 2]	4	8	0.080880	0.266667	2.414214
3	40	E?∼o	[4, 4, 2, 2, 2, 2]	16	16	0.161760	1.066667	2.828427
	100	EK∼w	[5, 5, 3, 3, 3, 3]	16	16	0.161760	1.066667	3.828427
4	90	EK∼o	[4, 4, 3, 3, 3, 3]	8	8	0.038948	0.266667	3.372281
	110	E]∼w	[5, 5, 4, 4, 4, 4]	8	8	0.038948	0.266667	4.372281
5	54	EImo	[3, 3, 3, 3, 2, 2]	4	8	0.065384	0.266667	2.732051
	55	EJeg	[3, 3, 3, 3, 2, 2]	4	8	0.065384	0.266667	2.732051
	103	Ejmw	[4, 4, 4, 4, 3, 3]	4	8	0.065384	0.266667	3.732051

4.2 Graphs of order 7

There are 853 non-isomorphic connected graphs of order 7. The pairs of graphs of order 7 with identical irregularity indices CS, Var, irr and irr_t are given in Table 2. The smallest pair of connected graphs of order 7 with identical irregularity indices is depicted in Figure 11.

Table 2: All pairs of graphs of order 7 with identical irregularity indices CS, Var, irr and irr_t.

pair_no	G_no	graph6	degree sequence	irr	irr_t	CS	Var	ρ
1	104	FK?}O	[3, 3, 2, 2, 2, 2, 2]	6	10	0.057209	0.238095	2.342923
	105	F\`?}O	[3, 3, 2, 2, 2, 2, 2]	6	10	0.057209	0.238095	2.342923
2	177	FAerO	[3, 3, 3, 3, 2, 2, 2]	6	12	0.069758	0.285714	2.641186
	178	FAdtO	[3, 3, 3, 3, 2, 2, 2]	6	12	0.069758	0.285714	2.641186
3	213	FK?}W	[4, 4, 2, 2, 2, 2, 2]	12	20	0.242178	0.952381	2.813607
	214	F\`?}W	[4, 4, 2, 2, 2, 2, 2]	12	20	0.242178	0.952381	2.813607
4	244	F?v\`w	[4, 4, 4, 2, 2, 2, 2]	16	24	0.217713	1.14285	3.074856
	269	FA_∼o	[5, 3, 3, 3, 2, 2, 2]	16	24	0.217713	1.142857	3.074856
5	274	F@VTW	[4, 4, 3, 3, 2, 2, 2]	12	22	0.173179	0.809524	3.030322
	275	F@UuW	[4, 4, 3, 3, 2, 2, 2]	12	22	0.173179	0.809524	3.030322

6	321	FIe`w	[4, 3, 3, 3, 3, 2, 2]	8	16	0.142857	0.476190	3.000000
	322	FJaHw	[4, 3, 3, 3, 3, 2, 2]	8	16	0.142857	0.476190	3.000000
7	348	FBY^?	[3, 3, 3, 3, 3, 3, 2]	2	6	0.046069	0.142857	2.903212
	349	FHU^?	[3, 3, 3, 3, 3, 3, 2]	2	6	0.046069	0.142857	2.903212
8	471	Fie`w	[4, 3, 3, 3, 3, 3, 3]	4	6	0.034553	0.142857	3.177410
	472	FjaHw	[4, 3, 3, 3, 3, 3, 3]	4	6	0.034553	0.142857	3.177410
9	438	FBY^G	[4, 4, 3, 3, 3, 3, 2]	8	16	0.093211	0.476190	3.236068
	439	FHU^G	[4, 4, 3, 3, 3, 3, 2]	8	16	0.093211	0.476190	3.236068
10	450	FKMiw	[4, 4, 4, 3, 3, 2, 2]	10	22	0.210999	0.809524	3.353856
	451	FKLkw	[4, 4, 4, 3, 3, 2, 2]	10	22	0.210999	0.809524	3.353856
11	444	FHU[w	[4, 4, 4, 4, 2, 2, 2]	8	24	0.346431	1.142857	3.489289
	469	FKWyw	[4, 4, 4, 3, 3, 3, 1]	8	24	0.346431	1.142857	3.489289
12	500	F?]}w	[5, 5, 5, 3, 2, 2, 2]	24	36	0.399856	2.285714	3.828427
	536	F@U^w	[6, 4, 4, 4, 2, 2, 2]	24	36	0.399856	2.285714	3.828427
13	543	FBY|o	[4, 4, 4, 4, 4, 2, 2]	8	20	0.217180	0.952381	3.645751
	544	FB]lg	[4, 4, 4, 4, 4, 2, 2]	8	20	0.217180	0.952381	3.645751
14	604	FIefw	[6, 3, 3, 3, 3, 3, 3]	18	18	0.217180	1.285714	3.645751
	613	FJaNw	[6, 3, 3, 3, 3, 3, 3]	18	18	0.217180	1.285714	3.645751
15	609	FkUhw	[4, 4, 4, 3, 3, 3, 3]	6	12	0.074653	0.285714	3.503224
	610	FkYXw	[4, 4, 4, 3, 3, 3, 3]	6	12	0.074653	0.285714	3.503224
16	656	FG]}w	[5, 5, 5, 3, 3, 3, 2]	20	30	0.268873	1.571429	3.983159
	665	FHU^w	[6, 4, 4, 4, 3, 3, 2]	20	30	0.268873	1.571429	3.983159
17	695	FKNNw	[6, 4, 4, 3, 3, 3, 3]	20	24	0.203000	1.238095	3.917286
	697	F`NNw	[6, 4, 4, 3, 3, 3, 3]	20	24	0.203000	1.238095	3.917286
18	701	FbY|o	[4, 4, 4, 4, 4, 3, 3]	4	10	0.064171	0.238095	3.778457
	702	Fb]lg	[4, 4, 4, 4, 4, 3, 3]	4	10	0.064171	0.238095	3.778457
19	748	FImvw	[6, 4, 4, 4, 4, 3, 3]	18	22	0.156325	1.000000	4.156325
	750	FJenw	[6, 4, 4, 4, 4, 3, 3]	18	22	0.156325	1.000000	4.156325
20	501	F?∼v_	[4, 4, 4, 3, 3, 3, 3]	12	12	0.035530	0.285714	3.464102
	851	F]∼∼w	[6, 6, 6, 5, 5, 5, 5]	12	12	0.035530	0.285714	5.464102
21	810	FFzfw	[6, 4, 4, 4, 4, 4, 4]	12	12	0.086567	0.571429	4.372281
	812	FLvfw	[6, 4, 4, 4, 4, 4, 4]	12	12	0.086567	0.571429	4.372281

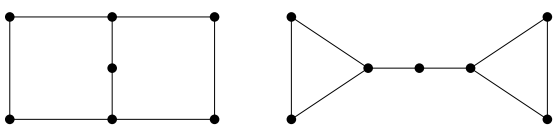

Fig. 11. The smallest pair of connected graphs of order 7 with identical irregularity indices CS, Var, irr and irr_t (the pair 1 in Table 2)

We would like to note that there is no triple of graphs of order 7 with identical irregularity indices $\mathrm{CS}, \mathrm{Var}, \mathrm{irr}$ and irr_t.

5 Conclusion and open problems

We have studied four established measures of irregularity of a graph. In particular, we have considered the problem of determining pairs or classes of graphs for which two or more of the purposed measures are equal. Some related results in the case of bidegreed graphs were presented in [17]. Here we have extended that work for tridegreed graphs and graphs with arbitrarily large degree set.

In the investigations here, it was assumed that considered graphs are of the same order, or they even have same degree sets. With respect to that, there are several interesting extension of the work done here.

It would be of interest to determine graphs of same order which have different degree sets, but their corresponding irr_t and irr indices are identical. A graph pair of such type with 5 vertices is illustrated in Figure 12. Also, it would be

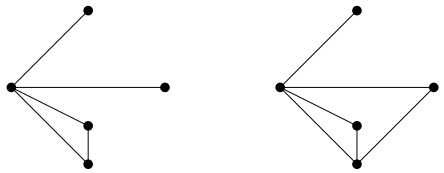

Fig. 12. A tridegreed and a four degreed planar graphs with identical $\mathrm{irr}_t = 14$ and $\mathrm{irr} = 10$ irregularity indices

of interested to find classes of graphs of different order with equal irregularity measures. Most of the result presented have involved only pairs of graphs. Extending those results to larger classes of graphs seems to be demanding but interesting problem. Finally, considering other irregularity measures could offer new insights in the topic.

References

[1] H. Abdo, S. Brandt, D. Dimitrov, *The total irregularity of a graph*, Discrete Math. Theor. Comput. Sci. **16** (2014) 201–206.

[2] H. Abdo, N. Cohen, D. Dimitrov, *Graphs with maximal irregularity*, Filomat (2014), to appear.

[3] Y. Alavi, J. Liu, J. Wang, *Highly irregular digraphs*, Discrete Math. **111** (1993) 3–10.

[4] M. O. Albertson, *The irregularity of a graph*, Ars Comb. **46** (1997) 219–225.

[5] F. K. Bell, *On the maximal index of connected graphs*, Linear Algebra Appl. **144** (1991) 135–151.

[6] F. K. Bell, *A Note on the irregularity of graphs*, Linear Algebra Appl. **161** (1992) 45–54.

[7] R. Criado, J. Flores, A. García del Amo, M. Romance, *Centralities of a network and its line graph: an analytical comparison by means of their irregularity*, Int. J. Comput. Math., to appear.

[8] L. Collatz, U. Sinogowitz, *Spektren endlicher Graphen*, Abh. Math. Sem. Univ. Hamburg **21** (1957) 63–77.

[9] D. Dimitrov, R. Škrekovski, *Comparing the irregularity and the total irregularity of graphs*, Ars Math. Contemp., to appear.

[10] C. D. Godsil, *Are almost all graphs cospectral?,* slides from a 2007 talk.

[11] C. D. Godsil, B. D. McKay, *Constructing cospectral graphs,* Aequationes Math. **25** (1982) 257–268.

[12] E. Estrada, *Randić index, irregularity and complex biomolecular networks,* Acta Chim. Slov. **57** (2010) 597–603.

[13] I. Gutman, P. Hansen, H. Mélot, *Variable neighborhood search for extremal graphs.* 10. *Comparison of irregularity indices for chemical trees*, J. Chem. Inf. Model. **45** (2005) 222–230.

[14] P. Hansen, H. Mélot, *Variable neighborhood search for extremal graphs.* 9. *bounding the irregularity of a graph*, in Graphs and Discovery, DIMACS Ser. Discrete Math. Theoret. Comput. Sci **69** (2005) 253–264.

[15] M. A. Henning, D. Rautenbach, *On the irregularity of bipartite graphs*, Discrete Math. **307** (2007) 1467–1472.

[16] H. Hosoya, U. Nagashima, S. Hyugaji, *Topological Twin Graphs. Smallest Pair of Isospectral Polyhedral Graphs with Eight Vertices,* J. Chem. Inf. Comput. Sci. **34** (1994) 428–431.

[17] T. Réti, D. Dimitrov, *On irregularities of bidegreed graphs*, Acta Polytech. Hung. **10** (2013) 117–134.

[18] Sage Mathematics Software (Version 5.11), (2013), `www.sagemath.org/`.

[19] J. J. Seidel, *Graphs and two-graphs,* Proc. Fifth Southeastern Conf. on Combinatorics, Graph Theory and Computing, Congr. Num. X, Utilitas Math., Winnipeg Man. (1974) pp. 125–143.

[20] A. Yu, M. Lu, F. Tian, *On the spectral radius of graphs,* Linear Algebra Appl. **387** (2004) 41–49.

A Novel-weighted Rough Set-based Meta Learning for Ozone Day Prediction

Hala S. Own[1], Ajith Abraham[2]

[1]Department of Solar and Space Research, National Research Institute of Astronomy and Geophysics, El-Marsad Street, P. O. Box 11421 Helwan, Egypt. hala@cs.ku.edu.kw

[2]Machine Intelligence Research Labs (MIR Labs), Scientific Network for Innovation and Research Excellence, WA, USA, ajith.abraham@ieee.org

Abstract: Nowadays, classifier combination methodsreceives great attention from machine learning researchers. It is a powerful tool to improve the accuracy of classifiers. This approach has become increasingly interesting, especially for real-world problems, which are often characterized by their imbalanced nature. The unbalanced distribution of data leads to poor performance of most of the conventional machine learning techniques. In this paper, we propose a novel weighted rough set as a Meta classifier framework for 14 classifiers to find the smallest and optimal ensemble, which maximize the overall ensemble accuracy. We propose a new entropy-based method to compute the weight of each classifier. Each classifier assigns a weight based on its contribution to classification accuracy. Thanks to the powerful reduct technique in rough set, this guarantees high diversity of the produced reduct ensembles. The higher diversity between the core classifiers has a positive impact on the performance of minority class as well as on the overall system performance. Experimental results with ozone dataset demonstrate the advantages of weighted rough set Meta classifier framework over the well-known Meta classifiers like Bagging, boosting and random forest as well as any individual classifiers.

Keywords: Weighted Rough Set; real world web service; class imbalance learning; entropy

1 Introduction

Practical experience has indicated that hybrid intelligence techniques might be helpful to solve some of the challenging real-world problems. In an hybrid intelligence system, a synergistic combination of multiple techniques is used to build an efficient solution to deal with a particular problem. One field of the hybrid intelligent approaches that has recently become a topic for researchers is Meta learning.

Meta learning refers to employing a set of base predictors for a given classification task and then fuse the output information using a fusion technique. Meta learning approach can be found under different names in literature such as decision combination [9], mixture of experts [10], classifier ensembles [5], classifier fusion [16] consensus aggregation [7], hybrid methods [8] and more.

The main purpose of Meta learning techniques is to improve the performance of a single classifier. Different classifiers usually make different predictions on the same sample of data. This is due to their diversity and many research works illustrated that the sets of misclassified samples from different classifiers would not necessary overlap [28]. This observation motivated the idea of using multiple sets of classifiers.

The techniques used to develop Meta learning (multi classifiers) can be divided into two categories: classifiers disturbance and sample disturbance. The first approach utilizes the instability of the base classifiers. This is applied to classifiers which are very sensitive to the initialization parameters like neural networks, random forests, and decision trees. The second approach even trains the classifier with different sample subsets or to train classifiers in different feature subspaces. Bagging works by resampling the original training data set of size M to produce N bootstrap training data sets of size M. Each of the bootstrapped training data sets are then used to train the classifier. Boosting on the other hand generates a series of base models. Each model is learned from a weighted training set whose weights are determined but the classification error of the preceding model [28]. The Adaboost was introduced by Freund et al. [14] and is based on weighting the data instead of randomly sampling it by putting more weight on the misclassified examples and smaller weights on the correctly classified examples.

Staking [21] is concerned with combining multiple classifiers generated from using different learning algorithms on a single dataset. This task is performed through different phases. In the first phase, the learning is performed individually for each classifier to output a new data set. In the second phase, a meta-level classifier is learned that combines the outputs of each individual classifier.

ECOC is a technique thatmanipulates output labels of the classes [12]. In the ECOC method, a discrete decomposition matrix (code matrix) is first defined for the problem at hand. Then this problem is decomposed into a number of binary sub-problems according to the content of the code matrix. After training binary classifiers on these sub-problems and testing them on any incoming test sample, a binary output vector is created. The final label is assigned to the class with the shortest distance between this vector and the code words.

Jin and Liu proposed a novel method for heterogeneous data [17]. The classifier system divided heterogeneous data into homogeneous subsets of similar sizes in order to generate reliable and accurate classification models. They proposed a novel algorithm, HISS, which allows for data overlapping between different

clusters (strata) and promises size-balanced clusters. The partitioning method was shown to perform well with heterogeneous data classification.

Akdemir [23] proposed the logic rule ensembles approach for unsupervised and semi-supervised cluster learning. They constructed the target variables by mapping the input variables. Each of these target variables can be used to extract several rules, and overall cluster rules are obtained from combining the rules for many target variables into an ensemble distance matrix, D(x). The clustering of the observations is accomplished by applying a distance-based hierarchical clustering algorithm to the rule-based distance matrix D(x). They use the cluster-based similarity partitioning method to combine the clusters from many rules.

Therest of the paper is organized as follows: motivation and review about imbalanced data learning are presented in section 2. Section 3 gives a brief introduction to the rough sets. Section 4 discusses the proposed weighted function. The proposed weighting rough set based meta learning is discussed in section 5 in detail. The characteristics of the Ozone data set as well as the chosen meta base classifiers are presented in Section 6. In Section 7 the proposed performance evaluation measures used in the paper are introduced. Experimental analysis and discussion of the results are described in Section 8. Finally, conclusions are presented in Section 9.

2 Imbalanced data Problem

Meta learning is one of the suggested techniques to deal with the class imbalance problem, a currently popular research area..Imbalanced data means that one of the classes has more samples than the other classes. The class with more samples is called the majority class while the other is the minority class. In many applications the minority class holds the most important information, such as in disease prediction, fraud detection, risk management, natural and physical phenomena, etc. Most classification techniques perform poorly with the minority class. There are three suggested techniques to overcome imbalanced data problems. The first is to create or modify the existing classification algorithms to deal with class imbalance problems. Data resampling is the second technique which includes over sampling or under sampling the data set to adjust the size of data set. The last approach is the feature selection, which was recently used to select a subset of features that allow the classifier to reach optimal performance [29].

The aim of modifying the algorithm is to provide adjustments on the learning algorithm (decision tree, regression, factor analysis, etc.) so it is more relevant and appropriate to imbalanced data situations. This approach is used mainly with decision tree and support vector machines (SVM); however few studies were done through this approach, since and opportunities within it are limited [27].

The main drawback of data resampling approach is that it may exclude useful information or increase the data size with artificial samples without having a real impact in the classification process, which will probably lead to the over-fitting problem [15]. The feature selection approach is applicable only for high dimension data, it selects data features that have great impact in classification of different classes, however, its performance in solving imbalanced data problems depends on the nature of the application domain.

Therefore, in imbalanced data learning, the unique optimal solution does not exist [27]. The different approaches were recently combined andapplied to SVM [26], and it had a better performance than applying separate techniques. However it is known that the SVM learning algorithm is sensitive to outliers and noise present in datasets, and it needs more work to reduce the effect of these problems.

Rough set theory [3, 6, 11] is a fairly new intelligent technique that has been applied to different domains and is used for the discovery of data dependencies, evaluates the importance of attributes, discovers the patterns of data, reduces all redundant objects and attributes, and seeks the minimum subset of attributes. Moreover, it is being used for the extraction of rules from databases.

Recently, there has been a few papers introducing rough set into imbalance learning techniques. Hu et al. [20] used rough set as an ensemble model generation. They proposed attribute reduction algorithms to find a set of reduct and trained a base classifier with each reduct. Then they presented an accuracy-guided forward search and post-pruning strategy (FS-PP) to select parts of base classifiers for ensemble systems. As ensemble system is to ensemble multiple rough subspace, they called it FS-PP-EROS. On the other hand, Saha et al. [21] used rough set as ensemble combination. They combined the results of a number of individually trained classifiers to construct a decision table. Then rough set attribute reduction and rule generation processes were used to construct Meta classifiers. However, the main disadvantage of the previous algorithm is that they consider all classifiers to act on the classification performance equally likely. Moreover, it is known that the performance of the ensemble members is not uniform. Therefore when we considered an equal weight for each one this negatively affected the performance [22].

In this paper we propose a hybrid approach combining algorithm modification and feature selections to solve the class imbalance problem. A modification of classical rough set theory is proposed by introducing a new weighting function. We apply a weighted entropy-based function to build a weighted Meta information table. By using this method, samples (classifiers) are weighted by its local contrast entropy of the training set. After building our weighted Meta information table, a weighted rough set reduction technique, which was proposed in our previous work [22], is applied to find the core base classifiers. This step will guarantee high diversity between ensembles. The higher diversity between the core classifiers has a positive impact on the performance of minority class as well as in overall system

performance [28]. Finally, a set of classifications rules are extracted based on a modified version of MLEM2 called a weighted MLEM2 algorithm [22]. We apply our scheme to an ozone data set, a highly imbalanced dataset.

The generated rules will be able to classify the minority class (ozone day) with high accuracy.

3 Rough Sets: Basic Notation

3.1 Information System and Approximation

Definition 1 (Information System) An information system is a tuple (U, A), where U consists of objects and A consists of features. Every a $\in$ A corresponds to the function $a : U \to V_a$, where Va is the value set of a. In the applications, we often distinguish between conditional features, C, and decision features, D, where C ∩ D = ϕ . In such cases, we define decision systems (U, C, D).

Definition 2 (Indiscernibility Relation) Every subset of features $B \subseteq A$ induces indiscernibility relation:

$$Ind_B = \{(x, y) \in UXU : \forall_{a \in B} a(x) = a(y)\} \tag{1}$$

for every x $\in$ U, $[x]_B$ is an equivalence class in the partitioning of U defined by Ind_B .

Definition 3 (Lower and Upper Approximation) In the rough sets theory, the approximation of sets is introduced to deal with inconsistency. A rough set approximates traditional sets using a pair of sets named the lower and upper approximation of the set. Given a set $B \subseteq A$, the lower and upper approximations of a set $Y \subseteq U$ are defined by, respectively,

$$\underline{B}Y = \{x \mid [x]_B \subseteq X\}$$
$$\overline{B}Y = \{x \mid [x]_B \cap X \neq \phi\} \tag{2}$$

Definition 4 (Lower Approximation and Positive Region) The positive region $POS_C(D)$ is defined by

$$POS_C(D) = \bigcup_{X : X \in U / \overline{Ind}_D} \underline{C}X \quad ; \tag{3}$$

$POS_C(D)$ is the set of all objects in U that can be uniquely classified by elementary sets in the partition U/IndD by means of C [15].

Definition 5 (Upper Approximation and Negative Region) The negative region NEGC(D) is defined by

$$NEG_C(D) = U - \bigcup_{X:X \in U/Indo} \overline{C}X \tag{4}$$

that is the set of all objects that can be definitely ruled out as a member of X.

Definition 6 (Boundary Region) The boundary region is the difference between upper and lower approximations of a set X that consists of equivalence classes having one or more elements in common with X; it is given by the following formula:

$$BND_B(X) = \overline{B}X - \underline{B}X \tag{5}$$

A rough set can be characterized using the accuracy of approximation as defined below

$$\alpha_B(X) = \frac{\left|\underline{B}X\right|}{\left|\overline{B}X\right|}, \tag{6}$$

where $|\bullet|$ denotes the cardinality of a set. X is definable with respect to B if $\alpha_B(X) = 1,$ otherwise X is rough with respect to B.

3.2 Reduct and Core

Definition 7 (Degree Of Dependency) Given a decision system, the degree of dependency of D on C can be defined as

$$\gamma(C, D) = \frac{\left|POS_C(D)\right|}{\left|U\right|}, \tag{7}$$

Definition 8 (Reduct) Given a classification task related to the mapping $C \vec{\square} D$, A reduct is a subset $R \subseteq C$ such that

$$\gamma(C, D) = \gamma(R, D) \tag{8}$$

and none of the proper subsets of R satisfies analogous equality.

Definition 9 (Reduct set) Given a classification task mapping a set of variables C to a set of labeling D, a reduct set is defined with respect to the power set P(C) as the set $R \subseteq P(C)$ such that

$\Re = \{A \subseteq P(C) : (A, D) = (C, D)\}$. That is, the reduct set is the set of all possible reducts of the equivalence relation denoted by C and D.

The reduct set is a minimal subset of attributes that preserves the degree of dependency of decision attributes on full condition attributes. The intersection of all the relative reduct sets is called the core.

3.3 Significance of the Attribute

Significance of features enables us to evaluate features by assigning a real number from the closed interval [0, 1], expressing how important a feature is.

Definition 10 (Significance) For any feature $a \in C$, we define its significance ξ with respect to D as follows:

$$\xi(a, C, D) = \frac{\left|POS_{C\setminus\{a\}}(D)\right|}{\left|POS_C(D)\right|}. \tag{9}$$

Based on the significance of an attribute, a heuristic attribute reduction algorithm can be designed to find a reduct by selecting an attribute with maximum significance interactively [11].

4 The Proposed Weighting Function

Several weighting functions have been introduced in ensemble learning. The most primitive one is simple voting. In the simple voting, the final decision is taken according to the number of votes given by the individual classifiers. Unfortunately, Matan [13] verified that in some cases, simple voting might perform worse than any of the members of combined classifiers. Therefore, several weighting voting methods were proposed to tackle this problem [2, 3, 5]. In this approach the decision of each classifier is multiplied by a weight to reflect its individual confidence in the decision.

In this paper, we introduce an entropy-based method to compute the weight of each classifier. We define the Local Contrast Entropy (LCE) function which is based on the relationship between each classifier and the overall entropy. We were motivated by the fact that if the classifier has a higher local contrast entropy it means that it makes a significant contribution to the classification accuracy. The

fundamental concept of the proposed technique is to reward the individual classifier a weight according to its local contrast entropy.

Entropy is widely used for the measuring of local information content or uncertainty and the information content in a probability distribution [1]. The entropy function is calculated by the following formula:

$$H = -\sum_{i=1}^{N} P_i \log P_i \tag{10}$$

To take into account the classification accuracy of each classifier in classifying a minority class,let D= {D1, D2, ….., DN} be the set of N classifiers,where D is considered to be a set of individual variables.

Each classifier Di assigns an input feature vector x to one of the possible classes C.

We can define the local contrast entropyas follows:

$$L(¿¿i) = \frac{D}{\sum_{j=1}^{N} D_j(x)} \tag{11}$$

¿.

where , Di(x) is the classification accuracy of the classifier Di in classifying the minority class.

Therefore our idea is to assign for each classifier a weight equal to its local contrast entropy:

$$w(D_i) = \frac{D_i}{\sum_{j=1}^{N} D_j} \tag{12}$$

This weight represents its ability to correctly predict the minority class.

5 Weighted Rough Set Based Meta Classifier

In this paper, we train a set of different classifiers D= {D1, D2, ….., DN} on an ozone dataset. We will divide the data into three sets, atraining, testing and validation set. The training set used to train each classifier to build the classification model for each classifier. Then, the generated model is then tested using the testing set. The output of each classifier Dj on sample xi is di(xi).

Now we will define the new weighted meta decision table:

Definition (Weighted Meta Decision Table) The weighted meta decision table is a tuple (U, D, Dec), where U consists of objects and D consists of features. Every d $\in$ D corresponds to the function $d : U \to V_d$ where Vd is the value set of d. Dec is the decision feature, where Dec ∩ D =φ.

In our proposed approach the objects are a set of trained classifiers. Each classifier generates an instance in the meta decision table containing the prediction made by the classifier, as conditional feature D, and the class label as decision feature Dec.

Informally speaking, in the meta decision table the columns represents the classifier name and the rows represents the Ozone instance data in the validation set. The values represents the prediction of the corresponding classifier which reflects its correctness in the classification process. The next step in the proposed approach is to form a weighted meta decision table. As shown in Table 1. The entry in information table U is defined as:

$Ui_{,}j= w(Dj)$ if training sample xi is classified correctly by base classifier Dj.

$Ui_{,}j= 0$ otherwise.

Where w (Dj) calculated by equation 12. The decision class in this table represents the actual class for the Ozone day data.

Table 1
Weighted meta Decision table

ID	BFTREE	J48	RD	RPTREE	DT	PART	MLP	RBFN	SMO	BAYES	NAIV	IBK	LWL	LAZYSTAR	OZONE
x1	0.909	0.895	0.934	0.920	0.929	0.890	0.891	0.937	0.937	0.692	0.621	0.883	0.937	0.891	NOT OZONE
x2	0.909	0.895	0.934	0.920	0.929	0.890	0.891	0.937	0.937	0.692	0.000	0.883	0.937	0.891	NOT OZONE
x3	0.909	0.895	0.934	0.920	0.929	0.890	0.891	0.937	0.937	0.692	0.621	0.883	0.937	0.891	NOT OZONE
x4	0.000	0.000	0.000	0.000	0.000	0.890	0.000	0.000	0.000	0.692	0.621	0.000	0.000	0.000	OZONE
x5	0.909	0.895	0.934	0.920	0.929	0.890	0.891	0.937	0.937	0.692	0.621	0.883	0.937	0.891	NOT OZONE
x6	0.909	0.895	0.934	0.000	0.929	0.890	0.891	0.000	0.000	0.692	0.621	0.883	0.000	0.000	OZONE
x7	0.909	0.000	0.000	0.000	0.000	0.000	0.000	0.000	0.000	0.692	0.621	0.000	0.000	0.000	OZONE
x8	0.909	0.895	0.934	0.920	0.929	0.890	0.891	0.937	0.937	0.692	0.621	0.883	0.937	0.891	NOT OZONE
x9	0.909	0.895	0.934	0.920	0.929	0.890	0.891	0.937	0.937	0.692	0.621	0.883	0.937	0.891	NOT OZONE
x10	0.000	0.000	0.934	0.920	0.929	0.000	0.891	0.937	0.937	0.692	0.621	0.000	0.937	0.000	NOT OZONE

Once we build the decision table; the next step is to reduce the attributes in the data set based on the information content of each attribute or collection of attributes. Generally in information tables, there often exist conditional attributes that do not provide significant information for identifying the decision class. So we should remove those attributes, since it reduces complexity and cost of the decision process [11].

Our aim in this step is to find a subset of base classifiers that maximize the overall accuracy for each decision class. Our motivations in this step are the following:

Some of the base classifiers produce good classification results for one of the decision classes but not all. Producing a reduct set for each class will decrease the overall complexity since we will use only a subset of the base classifiers.

The important effect of reduct set extraction is that we will know which base classifiers are more significant for each decision class.

By extracting the reduct set, we exclude all redundant classifiers. As a consequence, we guarantee diversity. Diversity among the base classifiers is considered important when constructing a classifier ensemble.

For the new weighted meta decision table, the weights generated do not change the equivalence relation and do not change the upper and lower approximation of arbitrary subset [22].

Finally, a set of classification rules are extracted based on a modified version of MLEM2, called the weighted MLEM2 algorithm [22]. This process leads to the final goal of generating classification rules from the information or decision system of the Ozone day database. Figure 1 shows the overall steps in the proposed Weighted Rough Set based Meta Classifier.

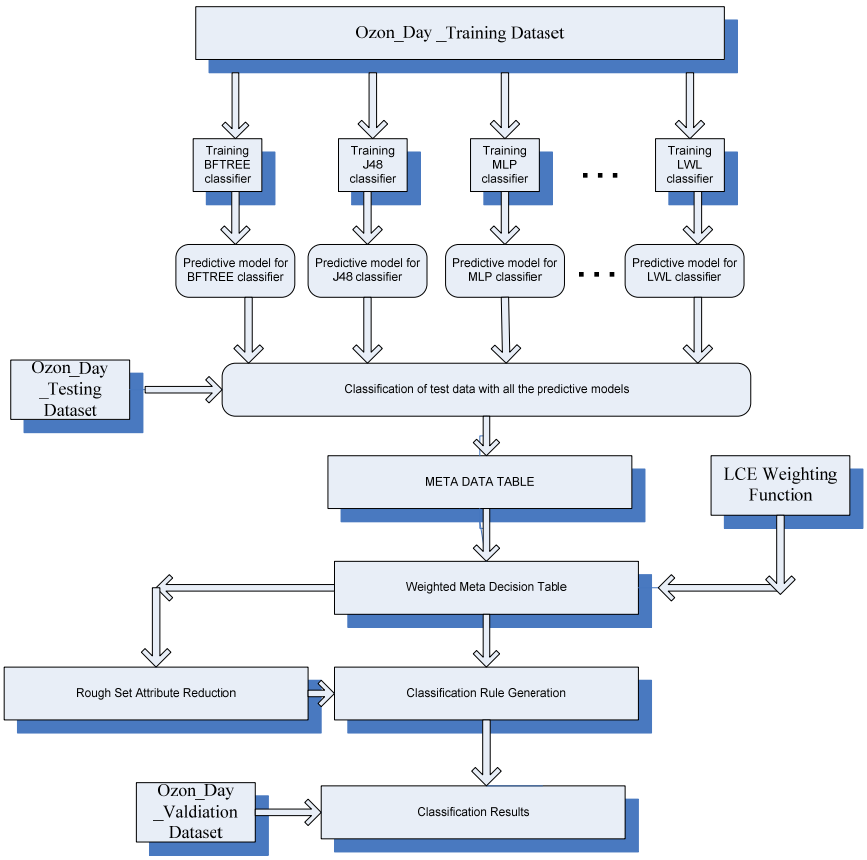

Figure 1
A Weighted Rough Set based Meta Classifier Scheme

6 Case Study: Ozone Day Prediction

6.1 Dataset

In this work, we use the dataset in the UCI machine learning repository [30] called "ozone". The number of objects is 2534 with 71 conditional attributes and a decision attribute. More information about the dataset can be found in [18]. The data set possesses very important properties that makes it a good example for imbalanced data learning:it contains high dimension of features, andit is very biased towards one of its decision classes. Table 2 describes the class distribution within the data set. As shown in Table 2, the NOZON class is small 6.3% compared with the NONOZON classes 93.7%.

Table 2
Class distribution on ozone data set

Class name	class size	class distribution
NONOZONE	2374	93.7%
OZONE	160	6.3%

With most well-known classifiers, when the class distribution of a data set is skewed, the classification method will be biased to the majority classes, and therefore will perform poorly in recognition of the minority classes because the prior knowledge of class distribution is not taken into account. Other classifiers will ignore the minority classes and will treat them as noise [26]. In this paper, we apply our proposed approach to try to overcome these well-known problems of inbalanced data.

6.2 Base Classifiers Proposed

We use 14 known classifiers:

RFTree: for building a best- first decision tree classifier.

J48: generating a pruned or unpruned C4.5 Decision Tree.

DT: DecisionTable: using simple decision table majority classifier.

MLP: Multilayer perceptron with number of different hidden layers chosen as (attribs + classes) / 2.

RD: RandomForest: generating a forest of random trees.

REPTree : Fast Decision tree learner.

PART: using divide and conquer to generate a PART decision list.

RBFN: RBFNetwork: implementation of normalized Gaussian radial basis function network.

SMO: implementation of Sequential minimal optimization algorithm for training a support vector classifier.

BNet: BayesNet, Bayes network learner using various search algorithms and quality measures.

NV: NaiveBayes, using naïve base classifier with estimator class.

IBk: K- nearest neighbors classifier.

LWL: Locally weighted learning.

lazy.KStar: instance based classifier; it uses an entropy-based distance function.

7 Performance Evaluation Measure

The evaluation criterion is a key factor both in the assessment of the classification performance and guidance of the classifier modelling. Traditionally, the accuracy rate has been the most commonly used empirical measure. The validation is done on a validation data set to guarantee the split fairness; we use 10 fold cross-validations in all of our measures. The confusion matrix is a matrix of size CxC, and each entry in the matrix Ai,j represents the number of instances observed in class Ci, and classified in class Cj. The rows of the matrix represent the set of classes and the column represents the classification result for each class. When working with skewed data, accuracy doesn't adequately serve as a measure for the success of ensembles as it is strongly biased with the majority class. What we need is another measure to correctly distinguish between the numbers of correctly classified examples of different classes. In this study, we used the following performance measures [19]:

Recall: Theratio of the number of correctly classified instances to the number of total instances of that class.

Precision: The ratio of number of correctly classified instance of the class to the number of predicted instance to that class.

F-measure: The weighted average of the precision and recall.

The most important property of these metrics is that they can be distinguished between positive and negative classes independently. Therefore it gives us a clear view inside the classification method especially when dealing with imbalanced data as we search for a good performance in the minority class.

8 Empirical Analysis

By applying the rough set reduct generation; we computed the weighted dependency degree and the classification performance for each classifier. We reached the minimal number of reducts that contains a combination of classifiers that have the same discrimination factor. The final generated reduct sets, which are used to generate the list of rules for the classification, are {LWL, RBFN, SMO, RPFTree, NV}. This reduct set represents the best classifiers for ozone day. After producing the reduct set; a set of rules will be generated. Table 3 introduces the best rules of the 34 generated decision rules.

The overall accuracy of the proposed technique is represented in Table 4. The table shows that the proposed system achieving high accuracy rate in predicting majority and minority class.

Table 3
The most significant rule generated

Rule #	Rule
1	RBFN==(0.467048-inf)& SMO ==(0.460142-inf)& RPFTree ==(0.464681-inf)& NV =(-inf-0.610093]=>OZON==NOTOZON
2	SMO==(-inf-0.46843]&LWL==(-inf-0.46843]&RBFNETWORK==(-inf-0.46843]=>(OZON==OZON)
3	(RONDOMF==(0.467048-inf)& RPFTREE==(0.460142-inf)& DECISIONTABLE==(0.464681-inf)& NV=(-inf- 0.702379]=> OZON=NOTOZON
4	RPFTree ==(0.447711-inf)&lwl==(0.460142-inf)& NV =(0.464681-inf)& SMO ==(0.610093-inf)=> OZON==NOTOZON

Table 4
The overall accuracy

	Non-Ozone	Ozone	No. of tested objects	Accuracy
Non-Ozone	955	2	957	0.998
Ozone	0	57	57	1
True Positive Rate	1	0.97		

8.1 Comparison with Other Meta Classifier Techniques

We compare the performance of the proposed technique with well-known meta classifiers such as Adaboost, bagging, and stacking. The compression done in terms of recall, precision and accuracy. Table 5 summarizes the performance of different meta classifiers when applied to the ozone data set.

Table 5
Comparing the proposed technique with other meta classifiers techniques

Method	Recall	Precision	Accuracy
Adaboost	98%	97%	96%
Stacking	96%	95%	92%
Bagging	95%	85%	89%
Our Method	100%	99%	99%

In the next experiments, we want to investigate the performance of our technique in predicting each class. The classification performance of each classifier in terms of recall, precision, accuracy and f measure for non ozone class is presented in Table 6.

In Table 7, the classification performance of each classifier in terms of recall precision, accuracy and f measure for ozone class is summarized.

Table 6
Classification performance for non ozone day

Measure	Classifier	RFTree	J48	DT	MLP	RD	REPTree	PART	RBFN	SMO	BNet	NV	IBk	LWL	lazy.KStar
PRECISION		0.95	0.95	0.94	0.95	0.94	0.94	0.95	0.93	0.93	0.98	0.98	0.95	0.93	0.95
RECALL		0.98	0.95	0.99	0.96	0.99	0.98	0.96	1	1	0.75	0.66	0.95	1	0.96
F-MEASURE		0.96	0.95	0.96	0.96	0.96	0.96	0.95	0.96	0.96	0.85	0.79	0.95	0.96	0.95
ACCURACY		0.98	0.96	0.99	0.96	0.99	0.98	0.96	1	1	0.75	0.66	0.95	1	0.96

Table 7
Classification performance for ozone day

Measure	Classifier	RFTree	J48	DT	MLP	RD	REPTree	PART	RBFN	SMO	BNet	NV	IBk	LWL	lazy.KStar
PRECISION		0.47	0.34	0.38	0.45	0.72	0.34	0.36	0	0	0.17	0.14	0.36	0	0.37
RECALL		0.24	0.26	0.05	0.38	0.05	0.1	0.32	0	0	0.78	0.85	0.35	0	0.31
F-MEASURE		0.32	0.29	0.08	0.42	0.09	0.15	0.34	0	0	0.29	0.25	0.35	0	0.34
ACCURACY		0.24	0.26	0.05	0.38	0.05	0.1	0.32	0	0	0.78	0.85	0.35	0	0.31

As evident from Tables 6 and 7, although the performance measures of the proposed classifiers in identifying a nonozone day are high its performance is very low with the ozone day. This is because of the imbalanceof the data, as we mentioned before. From table 8, we see that the overall accuracy of each classifier may give us a false indication about the ability of classifier to correctly identify the correct class of the instances.

Table 8
Performance of the14 individual classifiers

Measure	Classifier	RFTree	J48	DT	MLP	RD	REPTree	PART	RBFN	SMO	BNet	NV	IBk	LWL	lazy.KStar
Accuracy		93.5 %	92.1%	93. 4%	93.2 %	93.8 %	93.1 %	92.1 %	93.6%	93.6 %	75 %	67.8 %	92 %	93.6%	90.2%

8.2 Meta Learning Performance Measures

The studies have shown that the accuracy of prediction model in meta learning depend highly on the degree of diversity (difference) of the base classifiers. It has been proved to be one of the main reasons for the success of ensembles from both theoretical and empirical perspectives [28]. The larger the diversity value, the more evenly distributed the predictions are for the base classifiers, while a smaller

diversity value represents base classifiers that have more biased predictions.[25]. Therefore it is important to measure the diversity of our chosen classifiers.

8.2.1 Diversity Test

Meta learning techniques are expected to increase the prediction performance by considering the opinions from multiple classifiers. Therefore, diversity becomes an important factor. If every classifier gives the same opinion, constructing multiple classifiers becomes meaningless. Generally, larger diversity causes better recall for minority. To prove that the generation of reduct set guarantee high diversity between the different classifiers. We introduce two measures: a correlation measure between the different classifiers and a pair-wise Q-statistic.

8.2.2 Correlation Measure

We adopt the method used in [24] to calculate the correlation between two classifiers i and j. They calculated the total correlation between two classifiers as the sum of correlations of individual instances.

$$Total\ correlation(i, j) = \sum_{a} correlation(d_i, d_j) \tag{13}$$

Where di denotes the output of classifier i for the correct class on instance a , the results are shown in Table 9. We consider a correlation under 0.5 as a weak correlation (denoted as bold in the tables). As we see from the Table 9 The lowest correlated classifiers are LWL, RBFN, SMO, NV, and RPFTree. When the correlation becomes low the similarity between the classifiers is also low. In Meta learning we aim to group high diversity classifiers together to guarantee high performance predication. The results in Table 9 shows that lowest correlated classifiers, which constitute the reduct set generated by applying our method. This proves that the set of minimal classifiers satisfy the diversity required.

Table 9

Correlation between different classifiers for ozon day dataset

	RFTree	J48	DT	MLP	RD	REPTree	PART	RBFN	SMO	BNet	NV	IBk	LWL	lazyKStar
RFTree	1	0.8	0.88	0.74	0.79	0.75	0.81	0.87	0.68	0.56	0.56	0.58	0.76	0.54
J48	0.8	1	0.86	0.78	0.76	0.87	0.86	0.85	0.69	0.58	0.51	0.58	0.75	0.65
DT	0.88	0.86	1	0.81	0.82	0.52	0.79	0.79	0.78	0.64	0.61	0.64	0.66	0.69
MLP	0.74	0.78	0.81	1	0.9	0.89	0.85	0.86	0.84	0.74	0.74	0.65	0.85	0.66
RD	0.79	0.76	0.82	0.9	1	0.91	0.78	0.91	0.86	0.79	0.79	0.79	0.81	0.68
REPTree	0.75	0.87	0.52	0.89	0.91	1	0.91	0.94	0.51	0.36	0.26	0.76	0.45	0.69

PART	0.81	0.86	0.79	0.85	0.78	0.91	1	0.91	0.84	0.68	0.68	0.68	0.86	0.66
RBFN	0.87	0.85	0.79	0.86	0.91	0.94	0.91	1	0.86	0.69	0.69	0.69	0.86	0.68
SMO	0.68	0.69	0.78	0.84	0.86	0.51	0.84	0.86	1	0.33	0.22	0.82	0.39	0.84
BNet	0.56	0.58	0.64	0.74	0.79	0.36	0.68	0.69	0.33	1	0.38	0.95	0.42	0.75
NV	0.56	0.51	0.61	0.74	0.79	0.26	0.68	0.69	0.22	0.38	1	0.96	0.46	0.79
IBk	0.58	0.58	0.64	0.65	0.79	0.76	0.68	0.69	0.82	0.95	0.96	1	0.82	0.75
LWL	0.76	0.75	0.66	0.85	0.81	0.45	0.86	0.86	0.39	0.42	0.46	0.82	1	0.76
lazy.KStar	0.54	0.65	0.69	0.66	0.68	0.69	0.66	0.68	0.84	0.75	0.79	0.75	0.76	1

8.2.3 Q-Statistic

Between the different measures proposed to evaluate the diversity, the simplest pair Q-Statistic is widely used. In [28] authors mathematically and empirically prove that there is strong correlation between the Q-Statistic and the imbalance performance measurements we choose (Recall, Precision, F-measure).

Given two classifiers Di and, Dj the pair-wise Q-statistics measure are defined as the following:

$$Q_{i,j} = \frac{(TP \cdot FN - TN \cdot FP)}{(TP \cdot FN + TN \cdot FP)} \tag{14}$$

where

TP: the number of instances that are correctly classified by Di and Dj.

TN: the number of instances that are correctly classified by Di but incorrectly classified by Dj.

FP: the number of instances that are correctly classified by Dj but incorrectly classified by Di.

FN: the number of instances that are incorrectly classified by Di and Dj.

In this experiment the pair-wise Q-statistics between the 14 classifiers were calculated. The high value of pair-wise Q-statistics measure indicates that the diversity between them is low and vice versa. It means that ensemble learning using these two classifiers will not lead to good performance measures.

From Table 10, the low Q-statistics combination between classifiers (denoted as bold in the tables) matches the same result that the reduct set generated. For example the Q-statistics between NV and DT is high also between RD and PART. It indicates that the diversity between them is also high as well. On the other hand we found that the Q-statistics between NV and SMO is low (0.45) which indicates the diversity between them is very low; this emphasizes the output of the reduct that NV and SMO are in the reduct set.

Table 10
Pair-wise Q-statistics measure between 14 classifiers

	RFTree	J48	DT	MLP	RD	REPTree	PART	RBFN	SMO	BNet	NV	IBk	LWL	lazy.KStar
RFTree	1	0.9	0.86	0.5	0.65	0.68	0.55	0.68	0.85	0.91	0.94	0.89	0.65	0.67
J48	0.9	1	0.79	0.58	0.59	0.72	0.61	0.67	0.86	0.88	0.79	0.84	0.75	0.73
DT	0.86	0.79	1	0.54	0.61	0.65	0.54	0.64	0.88	0.79	0.91	0.86	0.84	0.68
MLP	0.58	0.58	0.54	1	0.89	0.96	0.94	0.94	0.72	0.69	0.78	0.74	0.63	0.63
RD	0.65	0.59	0.61	0.89	1	0.95	0.93	0.93	0.84	0.68	0.75	0.79	0.88	0.67
REPTree	0.68	0.72	0.65	0.96	0.95	1	0.86	0.94	0.37	0.44	0.29	0.81	0.44	0.8
PART	0.55	0.61	0.54	0.94	0.93	0.86	1	0.96	0.91	0.88	0.87	0.82	0.65	0.66
RBFN	0.68	0.67	0.64	0.94	0.93	0.94	0.96	1	0.68	0.69	0.69	0.72	0.84	0.78
SMO	0.85	0.86	0.88	0.72	0.84	0.37	0.91	0.68	1	0.31	0.45	0.55	0.41	0.49
BNet	0.91	0.88	0.79	0.69	0.68	0.44	0.88	0.69	0.31	1	0.35	0.89	0.51	0.58
NV	0.94	0.79	0.91	0.78	0.75	0.29	0.87	0.69	0.45	0.35	1	0.98	0.48	0.65
IBk	0.89	0.84	0.86	0.74	0.79	0.81	0.82	0.72	0.55	0.89	0.98	1	0.54	0.65
LWL	0.65	0.75	0.84	0.63	0.88	0.39	0.65	0.84	0.41	0.51	0.48	0.54	1	0.61
lazy.KStar	0.67	0.73	0.68	0.63	0.67	0.8	0.66	0.78	0.49	0.58	0.65	0.65	0.61	1

Conclusion

A variety ofMeta learning techniques have emerged recently. The ozone day prediction is an important issue due to its harmful effect onall creatures. The imbalance nature of the Ozone data set as well as the large number of features makes the prediction of the ozone day a challenging problem. In this paper we introduce a rough set as a Meta classifier technique with new entropy-based method to compute the weight of each classifier to improve the performance of ozone day prediction. The experiments show it to perform better over the well-known meta classifier techniques.

References

[1] Shannon, C.: The Mathematical Theory of Communication. Bell System Technical Journal, Vol. 27, 379-423, 1948

[2] S. A. Dudani: The Distance-weighted k-nearest Neighbor Rule. IEEE Trans. on Systems, Man and Cybernetics, Vol. 6:325-327, 1976

[3] Pawlak, Z.: Rough Sets, Journal of Computer and Information Science, Vol. 11, 341-356 (1982)

[4] B. V. Dasarathy: Nearest Neighbor Norms. NN Pattern Classification Techniques, IEEE ComputerSociety Press, Los Alamos, CA, 1991

[5] L. Hansen, P. Salamon: Neural Networks Ensembles. IEEE Transactions on Pattern Analysis and Machine Intelligence, Vol. 12(10), 993-1001, 1990

[6] Pawlak, Z.: Rough Sets. Theoretical Aspect of Reasoning about Data. Springer Verlag, 1991

[7] J. Benediktsson, P. Swain.: Consensus Theoretic Classification Methods. IEEE Transactions on System and Man Cybernetic, Vol. 22 (4), 688-704, 1992

[8] B. Dasarathy: Decision Fusion. IEEE Computer Society Press, Silver Spring, MD, 1994

[9] T. Ho, J. Hull, S. Srihari: Decision Combination In Multiple Classifier Systems. IEEE Transactions on Pattern Analysis and Machine Intelligence, Vol. 16 (1), 66-75, 1994

[10] M. Jordon, R. Jacobs: Hierarchical Mixtures of Expert and the EM Algorithm. Neural Computing, 181-214, 1994

[11] Pawlak, Z., Grzymala-Busse J., Slowinski R., Ziarko, W.: Rough Sets. Communications of the ACM, Vol. 38, No. 11, 89-95, 1995

[12] T. G. Dietterich and G. Bakiri: Solving Multiclass Learning Problems via Error-Correcting Output Codes, Vol. 2, 263-286, 1995

[13] O. Matan: On Voting Ensembles of Classifiers. Proceeding of the 13th International Conference on Artificial Intelligence, 84-88, 1996

[14] Y. Freund and R. E. Schapire: A Decision-Theoretic Generalization of On-Line Learning and an Application to Boosting. Journal of Computer And System Sciences, Vol. 55, 119-139, 1997

[15] Kittler, J., Hatef, M., Duin, R. P. W., Matas, J: On Combining Classifiers. Pattern Analysis and Machine Intelligence, IEEE Transactions, Vol. 20, 226-239, 1998

[16] L. Kuncheva: Switching Between Selection and Fusion in Combining Classifiers: An Experiment. IEEE Transactions on System and Man Cybernetic Part B, Vol. 32 (2), 146-156, 2002

[17] Rong Ji, Huan Liu: A Novel Approach to Model Generation for Heterogeneous Data Classification. Proceedings of the 19th international joint conference on Artificial intelligence, IJCAI'05, Edinburgh, Scotland, UK.30 July-5 August, 746-751, 2005

[18] Kun Zhang, Wei Fan, XiaoJing Yuan, Ian Davidson, Xiangshang Li: Forecasting Skewed Biased Stochastic Ozone Days: Analyses and Solutions. Proceedings of the Sixth International Conference on Data Mining, Hong Kong, China 18-22 December,753-764, 2006

[19] Costa, E., Lorena, A., Carvalho, A., Freitas: A., A Review of Performance Evaluation Measures for Hierarchical Classifiers. Association for the Advancement of Artificial Intelligence AAAI, 1-6, 2007

[20] Hu Q, Yu D, Xie Z, Li X: EROS: Ensemble Rough Subspaces. Pattern Recognition, Vol. 40(12), 3728-3739, 2007

[21] Suman SahA C. A. Murthy, Sankar K. Pal: Rough Set Based Ensemble Classifier. Lecture Notes in Computer Science, Vol. 6743, 27-33, 2011

[22] Hala S. Own, Ajith Abraham: A New Weighted Rough Set Framework Based Classification for Egyptian Neonatal Jaundice. Applied Soft Computing. Elsevier Vol. 12(3), 999-1005, 2012

[23] Deniz Akdemir: Ensemble Clustering with Logic Rules. eprint arXiv:1207.396, http://arxiv.org/abs/1207.3961, 2012

[24] Aydın Ulaş, Olcay Taner Yıldız, Ethem Alpaydın: Eigenclassifiers For Combining Correlated Classifiers. Vol. 187, 109-120, 2012

[25] Joseph Pun Yuri Lawryshyn: Improving Credit Card Fraud Detection using a Meta-Classification Strategy. International Journal of Computer Applications, Vol. 56(10), 41-46, 2012

[26] Mikel G., Alberto F., Edurne B., Humberto B., Francisco H.: A Review on Ensembles for the Class Imbalance Problem: Bagging-, Boosting-, and Hybrid-Based Approaches. IEEE Transactions on Systems, Man, and Cybernetics, Vol. 42, 463-484, 2012

[27] Mohamed B., Taklit A. A: Imbalanced Data Learning Approaches Review. International Journal of Data Mining & Knowledge Management Process (IJDKP) Vol. 3, 15-33, 2013

[28] Shuo Wang, Xin Yao: Relationships between Diversity of Classification Ensembles and Single-Class Performance Measures. IEEE Transactions on Knowledge and Data Engineering, Vol. 25, 206-219, 2013

[29] Rushi L., Snehlata S. D., Latesh M.: Class Imbalance Problem in Data Mining: Review. International Journal of Computer Science and Network (IJCSN), Vol. 2, 226-230, 2013

[30] UC Irvine Machine Learning Repository. http://archive.ics.uci.edu/ml/ last acesses 2014

Fuzzy Membership, Possibility, Probability and Negation in Biometrics

Nicolaie Popescu-Bodorin[†], Valentina E. Balas[‡]

[†] University of S-E Europe Lumina, Colentina 64B, 021187, Bucharest, Romania.
[‡] 'Aurel Vlaicu' University, Bd. Revolutiei 77, 310130, Arad, Romania.
[†] popescu.bodorin@lumina.org, [‡] valentina.balas@uav.ro

Abstract: This paper proposes a new formalization of the classical probability-possibility relation, which is further confirmed as a much complex, but natural provability – reachability - possibility - probability - fuzzy membership – integrability interconnection. Searching for the right context in which this relation can be consistently expressed for the particular case of experimentally obtained iris recognition results brought us to a natural (canonic) and universal fuzzification procedure available for an entire class of continuous distributions, to a confluence point of statistics, classical logic, modal logic, fuzzy logic, system theory, measure theory and topology. The applications - initially intended for iris recognition scenarios - can be easily extrapolated anywhere else where there is a need of expressing the relation possibility - probability - fuzzy membership without weakening the σ-additivity condition within the definition of probability, condition that is considered here as the actual principle of possibility-probability consistency.

Keywords: σ-additivity, principle of possibility-probability consistency, provability, reachability, possibility, probability, fuzzy membership, Riemann integrability, negation, consistent experimental frameworks, Turing test, iris recognition, biometrics.

1 Introduction

Implementing biometric identification systems means advancing from human intuition to artificial but formally correctly biometric decisions. To be specific, when a human agent analyzes a pair of two good quality iris biometric samples (two iris images) – for example, it is easy for him to decide if the pair is a genuine or an imposter one, hence it is simple for him to have the intuition that designing a reliable artificial agent able to recognize genuine against imposter pairs should be possible. A first guess is that, as a decision system, the biometric system should be a binary one. Theoretically, in ideal conditions, it should be able to map all its legal inputs (pairs of iris templates) onto a set of two concepts and linguistic labels '*imposter'* and '*genuine'* whose extensions should be disjoint, since in a logically consistent iris recognition system and also in our reasoning, no imposter

pair is a genuine one and vice versa. Unfortunately, the field of iris recognition is full of counter-examples to this ideal situation, some of them as old as the domain of iris recognition itself [3], [4] and others, very recent indeed [6]-[10], [24], [25], some of them in more direct connection with what follows to be presented in this paper [2], [12]-[17], [19]-[23]. In all of these counter-examples it happens that the linguistic labels '*imposter'* and '*genuine'* are, in fact, represented as two overlapping fuzzy sets of recognition scores, the overlapping being itself a fuzzy boundary in between the first two mentioned fuzzy sets. Therefore, a second guess is that, as a decision system, the biometric system outputs three possible values: '*imposter'*, '*uncertain'* and '*genuine'*. A step further is analyzing the causes for which some imposter similarity scores are too big and some genuine similarity scores are too small, in an attempt to better isolate from each other the extreme values *imposter* and *genuine*. The result is a 5-valued recognition function that splits the input space (of iris template pairs) in five fuzzy preimages of five labels *imposter*, *hyena* (degraded imposter), *uncertain*, *goat* (degraded genuine) and *genuine*, all of them represented as fuzzy sets of recognition scores. All in all, the non-ideal conditions occurred from the stage of image acquisition up to the stages of image processing and matching fuzzify the prototype binary crisp recognition function that all biometric systems are normally expected to have (in ideal conditions) up to a binary, ternary, quaternary or even quinary fuzzy recognition function. Therefore, the initial intention of designing an identification system must be weakened when necessary to designing verification systems. However, when the aim is to design a logically consistent recognition system within the limits of consistent biometry [22], the difference between verification and identification vanishes.

This framework of iris recognition (and biometric recognition at large) is the context in which we talk here about fuzzy membership, probability and negation while searching for appropriate ways of expressing (precisiating, [31]) facts, rules and phenomena of iris recognition in a computational manner such that to maximize the cointension [31] between the real world of iris recognition and its computational model. By adopting a Turing perspective [27], we classify such a task as a process of human intelligence and its computational model as an artificial agent whose degree of intelligence can be determined through the test that today bears his name (Turing test, [27]). In other words, ideally, artificial intelligence is a way of representing processes of human intelligence as computational (artificial) software agents with as much cointension as possible, the degree of cointension being verifiable in principle [1] through a Turing test [27]. The results of all major iris recognition experiments (such as [4], [8], [10], [13], [19], [20], [22], [24]) are in fact partial Turing tests of iris recognition in which only the software agent is interrogated. Completing these partial tests can be done easily by attaching to them the corresponding iris recognition results obtained while interrogating qualified human agents using the same iris image databases. Surprisingly, especially when using iris image databases containing good quality images, the histogram of biometric decisions given by the human agents are indeed very

different by those summarizing the biometric decisions given by the artificial agents (the iris recognition systems). The huge discrepancy between the two types of iris recognition results was for the first time observed and understood in [21] and further commented and used in [22] as an argument for searching a better methodology for non-stationary machine-precisiation of iris recognition. Here we will insist now on the lack of cointension between the human-precisiated and machine-precisiated iris recognition and on the lack of instruments for quantifying it. Let us start with a tentative of quantifying the degree of separation between the distributions of imposter and genuine similarity scores. In the classical statistical approach of iris recognition proposed by Daugman, the decidability index,

$$d' = \frac{|\mu_I - \mu_G|\sqrt{2}}{\sqrt{\sigma_I^2 + \sigma_G^2}}, \tag{1}$$

is such a measure of separation (where μ_I, μ_G, σ_I^2 and σ_G^2 are the means and the variances of imposter and genuine score distributions respectivelly), values of 4, 8, and 14 being already reported in the literature [3], [4]. Hence, the separation between the distribution of imposter and genuine similarity scores is in this case precisiated numerically in such numeric values exemplified above. However, the histograms summarizing the biometric decisions given by qualified human agents are crisp 0-1 (binary) histograms for which the same decidability index takes the value of positive infinity. How relevant are 4, 8, or 14 against the infinity? How much cointension is in this case in between the human-precisiated and machine-precisiated iris recognition? We could not say otherwise than not too much at all, and this is what motivates our paper, which is further organized as follows:

1.1 Outline

Section 2 presents a newly proposed formalization of the classical probability-possibility relation, whereas the sections 2.1 and 2.2 introduce the notions of consistent experimental setups and frameworks exemplified in section 2.3. Section 3 presents and analyzes some cases of imperfect experimental frameworks (especially cases of iris recognition, see section 3.1) study that leads to the finding of a new possibility – probability – fuzzy membership relation for Gaussian distributed random numbers and also for other continuously distributed random numbers, finding that points out that weakening the σ –additivity condition is not necessarily required for establishing a consistent possibility-probability-fuzzy membership relation. On the contrary, the σ –additivity condition is the bridge that ensures this relation and therefore statistics and fuzzy logic could share a common side-by-side evolution – fact that is commented in section 3.4. The sections 3.5 and 3.6 are dedicated to exemplifying some issues that negation has when it comes to deal with fuzzy membership assignments. At last, the 4th section deals with two types of negation in the context of implemented biometric systems and is followed by conclusions.

2 A new formalization of the classical probability-possibility relation.

Let us consider a data spring, i.e. an input-output relation R of a theoretical system S_T actually implemented as S_P, a data spring that throws an uniformly distributed number y in the discrete set of fuzzy values $Y=[0:1:255]/255=\{y_k=k/255 \mid k \in Z_{256}\}$ as a response to the excitation $x \in X$. By intentionally confounding the output y with the state of system S, X is the input space and Y is the state-output space. Given the fact that the data spring is a uniformly distributed number in Y, all $y \in Y$ are observable outputs/states and the event $y \in Y$ is not just possible, but certain. The possibility that $y \in Y$ originates in the nature of data spring R, whereas for any R taken such that R(X)=Y, the probability of $y \in Y$ is unitary. In such cases, while the system S_P is functioning, the actual outcome y=R(x) cannot enter in the output/state space through its empty subset, i.e. the event $R(x) \notin Y$ is impossible, whereas its probability is zero. In such cases, even if we consider the possibility is a matter of degree, the (maximally) impossible event is not *improbable* (as Zadeh said in [30]), but actually it is *not probable at all* (i.e. it is 0–probable). On the other hand, the maximally possible event is the certain event whose probability is unitary. In what follows here, all 0-probable events are impossible, all p-probable events with $1 \geq p > 0$ are possible and all 1-probable events are not just possible, but certain. The possibility of an event is not fuzzy, but binary: all possible or impossible events have their possibility coefficients equal to 1 or 0, respectively. Hence probability follows, originates in and expresses possibility (probable events are not impossible) and possibility is causal to probability. This state of facts is already expressed in probability theory as a precise law, namely the σ–additivity axiom within the definition of probability, which can be also viewed as a principle of consistent possibility-to-probability translation, i.e. as an instance of the so called *possibility/probability consistency principle* introduced by Zadeh in [30],

$$\gamma = \sum_{k=1}^{n} p_k \pi_k \text{ , with } p \text{ and } \pi \text{ denoting probability and possibility values,} \qquad (2)$$

where all possibility values are taken unitary. In our modeling, a state or an output is observable if and only if it is possible, i.e. the possibility and observability are interchangeable (synonyms). In terms of formal languages, there is a formal grammar that describes the systems S_T and S_P able of producing that specific state/output also. In a consistent experimental setup, all possible events should be observed and, as a consequence, their statistics can be made, probability being a nuance, a refinement of possibility (among all possible events, some are more probable than others), a finer precisiation / quantization of possibility in a numeric space after the knowledge resulting from a certain experiment is gathered as statistics data. Hence, the main differences between the classical possibility-probability relation that we are bounded to here and the model proposed by Zadeh in [30] are the following:

Possibility is encoded binary.	Possibility is a matter of degree.
Possibility and probability values satisfy the σ –additivity condition, and therefore, they are cointensive and fully consistent to each other – i.e. in formula (2), γ and possibility values are all unitary.	Possibility and probability values are not necessarily cointensive, nor fully consistent to each other, since their degree of consistency (2) marks a weakening of the σ –additivity condition.
For any consistent experimental setup 'E', any event 'e' and any $p \in (0,1]$:	
impossible(e) $\leftrightarrow$ 0-probable(e, E)	impossible(e) $\rightarrow$ improbable(e)
possible(e) $\leftrightarrow$ p-probable(e, E)	probable(e) $\rightarrow$ possible(e) (if contrapositive principle still stands)
certain(e) $\leftrightarrow$ 1-probable(e, E)	formula (2)

Let us comment now on these matters. First of all, the relation between impossibility and 0-probability,

$$\text{impossible(e)} \leftrightarrow \text{0-probable(e, E)}, \tag{3}$$

tells that in any consistent experimental setup 'E' (situation further denoted as $E \in \xi$, where the space of consistent experimental setups ξ follows to be defined on the run, by natural restrictions that appear during formalization), an impossible event cannot be observed as an outcome, or otherwise, the experimental setup is not consistent (situation further denoted as $E \notin \xi$). This mechanism can be used to endow any computational artificial agent with the capacity of predicting (having an expectation and a prior knowledge on) the future outcomes of an experiment that it follows to witness, observe and understand, and also with the capacity of knowing who is responsible when these outcomes do not meet its expectation. However, formula (3) is a simplified instance of a more complex one that belongs in a second-order formal language describing the systems S_T and S_P (in what follows, t and f are used as true and false):

$$\text{impossible(e)} \leftrightarrow \{(\forall E \in \xi)[\, t \rightarrow \text{0-probable(e, E)}\,]\} \tag{4}$$

telling that an event 'e' is impossible if and only if, in any consistent experimental setup 'E', its probability is null. Its dual by contraposition principle is:

$$\text{possible(e)} \leftrightarrow \{\ (\exists E \in \xi)[\ \text{0-probable(e, E)} \rightarrow f]\ \} \tag{5}$$

telling that an event 'e' is possible if and only if there is a consistent experimental setup in which the assertion that 'e' is 0-probable in 'E' is false. Formula (5) is further equivalent to:

$$\text{possible(e)} \leftrightarrow \{\ (\exists E \in \xi)(\exists p \in (0,1])[\, t \rightarrow \text{p-probable(e, E)}]\ \} \tag{6}$$

telling us that an event 'e' is possible if and only if there is a consistent experimental setup in which the assertion that the probability of 'e' is not null in 'E' is true.

Secondly, the relation between possibility and p-probability (when $p \in (0,1]$),

$$\text{possible(e)} \leftrightarrow \text{p-probable(e, E)}, \tag{7}$$

is also a simplified instance of a more complex formula:

$$\text{possible(e)} \leftrightarrow \{\ (\forall E \in \xi)(\exists p \in (0,1])[\ t \rightarrow \text{p-probable(e, E)}\ ]\ \}, \tag{8}$$

that tells that an event 'e' is possible if and only if, in any consistent experimental setup 'E', (is true that) its probability is not null. Formula (8) is actually a strengthening of (6) by universal quantification of E in ξ, and therefore, a strengthening of (4). Besides, the relations (8) and (5) could not be simultaneously true outside ξ, hence ξ is necessarily defined as follows:

2.1 Consistent experimental setups

Definition 1 The space of consistent experimental setups ξ for the system S_T whose observable state/output space Y is entirely covered by its input-output (X-R-Y) relation (i.e. R(X)=Y) is a space of experiments (on implemented systems S_P) in which:

(i) any two members are interchangeable, i.e.:

$$t \rightarrow \{[(\exists E \in \xi)(P(e, E))] \rightarrow [(\forall E \in \xi)(P(e, E))]\}, \tag{9}$$

where P(e, E) is a property of 'E' relative to a given event 'e'.

(ii) the following rewriting rule holds true:

$$\{(\exists p \in (0,1])[\ t \rightarrow \text{p-probable(e, E)}\ ]\} \leftrightarrow [\text{0-probable(e, E)} \rightarrow f] \tag{10}$$

(iii) there is a negation operator 'n' defined such that $n^2=1$ (in terms of string functions) and:

$$n\{(\forall E \in \xi)[t \rightarrow \text{0-probable(e,E)}]\} \leftrightarrow \{(\exists E \in \xi)[\text{0-probable(e, E)} \rightarrow f]\}, \tag{11}$$

(iv) the following rewriting rule for complementary events e and $\bar{e}$ holds true:

$$(\forall E \in \xi)(\forall p \in [0,1])\{[\text{p-probable(e,E)}] \leftrightarrow [\text{(1-p)-probable}(\bar{e}, E)]\} \tag{12}$$

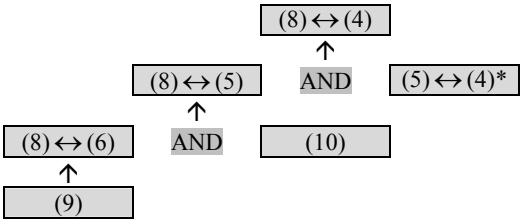

(13)

(where * is provable by (11) and contraposition principle)

In these conditions, a formal proof that (8) ↔ (4) is presented here as formula (13), where the equivalence relation * within the formula (13) is provable by (11)

and contraposition principle. The condition (iv) within Definition 1 establishes the natural meaning of both labels *impossible* and *certain* by correspondence with the trivial two-elements Boolean algebra defined by the empty set and Y, on the one hand, and with the two extreme values (0 and 1) that the cumulative of probability takes for the empty (impossible) and total (certain) events, respectively, on the other.

In the third place, the relation between certain and 1-probable events:

$$\text{certain(e)} \leftrightarrow \text{1-probable(e, E)}, \tag{14}$$

is also a simplified instance of a more complex formula:

$$\text{certain(e)} \leftrightarrow \{(\forall E \in \xi)[\, t \rightarrow \text{1-probable(e, E)}\,]\}, \tag{15}$$

affirming that the event 'e' is certain, if and only if, it is 1-probable in any consistent experimental setup 'E'. Given the rewriting rule (iv) stated in Definition 1, formula (15) is further equivalent to:

$$\text{impossible}(\bar{e}) \leftrightarrow \{(\forall E \in \xi)[\, t \rightarrow \text{0-probable}(\bar{e}, E)\,]\}, \tag{16}$$

that further is an instance of formula (4). By summarizing this section up to this point, an important remark is that the three ways of describing the classical possibility-probability relation for the impossible, possible and certain events, namely the formulae (4), (8) and (15), or their simplified forms (3), (7) and (14) and also the axioms within the definition of probability are not independent, but intimately interconnected as three images of the same thing, namely the concept denoted above as ξ - the space of all consistent experimental setups ξ for the system S_T whose observable state/output space Y is entirely covered by its input-output relation. ξ is a formal, logical, computational and physical concept, a coherent non-contradictory framework of expressing the natural relation between possibility, probability and negation for all observable states/outputs of a physical system S_P given as an implementation of S_T. By contrast, now the reader knows what could mean to weaken any of the three axioms within the probability definition while attempting to define a possibility-probability relation different from the canonic natural one that exists by default in ξ.

A second remark is that investigating the possibility-probability relation in ξ shows how many things confirm each other and group together coherently in a consistent and computational knowledge ensemble.

A third remark is that all formulae from above that contain the symbols t and f - i.e. (4)-(6), (8)-(12), (15) and (16) - are written in a formal logical dialect that extends the cognitive dialect introduced in [17], which on its turn is derived from the sound and complete formal theory of Computational Cognitive Binary Logic (CCBL) introduced in [15] and implemented online in [18]. However, the marker (!:) signalizing an assertion in cognitive dialect is omitted in the above formulae, because here in this article there is no chance of confusing queries and assertions. Hence, our discourse presented here on the possibility-probability relation is strictly a logical and computational one.

2.2 Consistent experimental frameworks

An artificial computational agent produces its states/outputs accordingly to a sound formal theory in which the states/outputs are formally and logically provable in terms of a generative grammar. Hence, in ξ, a more complex relation holds between possibility, probability, observability and provability: observable events (states/outputs) of S_T and S_P are possible, probable and provable, any time when the input-state/output relation is theoretically known as a provable formula of a sound theory describing S_T and practically implemented in S_P without errors. This motivates the following definition:

Definition 2 A Consistent Experimental Framework (CEF) is a formal ensemble (X,R,Y,S_T,T_S,ξ) in which:

(i) ξ is the space of consistent experimental setups for the system S_T;

(ii) the observable state/output space Y of the system S_T is entirely covered by the input-output (X-R-Y) relation (i.e. R(X)=Y);

(iii) input-state/output relation (X-R-Y) is know explicitly as a provable formula of a sound formal theory T_S describing S_T, on the one hand, and implemented without errors on S_P, on the other.

In this context, since T_S is a sound formal theory, it cannot prove contradictions. Therefore, contradictions are impossible / unreachable / unprovable events in T_S. Since the formal theory of T_S actually describes the functioning of S_T and S_P, the practice on S_P is not able to deliver events that are theoretically impossible / unreachable / unprovable (in S_T), and therefore, the practice on S_P (further denoted P_S) cannot deliver counter-examples for S_T and T_S. In other words, there is a unitary cointension between S_T and S_P, between the theory T_S and the practice P_S on the theoretical and actual systems S_T and S_P. In general, the lack of cointension between practice (experiments) and theory could be expressed in experimental results that contradict the theoretical model of the system in some aspects. On the contrary, a unitary cointension between practice and theory ensures that in any consistent experimental setup it is impossible to obtain experimental results that contradict the expectations motivated by the sound theory T_S. There are only two possible gates that could allow inconsistency (contradiction) within an experimental framework, namely T_S is not sound or P_S is outside ξ. In addition, there are three ways in which contradiction could be expressed in an experimental framework: inside T_S, inside P_S, and between theoretically predicted events in T_S and the actual events taking place in P_S, i.e. between expectations and the actual experimental outcomes.

2.3 Examples of consistent experimental frameworks

The extension of the concept introduced in Definition 2 from above is not the empty set: propositional logic is the formal theory that describes any logical circuit both as theoretical design S_T and as implemented system S_P. Given a

sequence of excitations in the input space, the corresponding outputs are formally provable in propositional logic (hence, accordingly to the formal theory of the system they are expected values) and practically observable. For a given input-output relation, any two consistent experimental frameworks differ only by equivalent (interchangeable) logical circuits that support that input-output relation. Given an input-output relation and a trajectory $(x,y)_t$ in $X \times Y$, output statistics is invariant along all consistent experimental frameworks that support that input-output relation, and therefore, the possibility-probability relation is invariant.

This example is also important for establishing two things, once for good: logical circuits are the most basic intelligent agents (where intelligence means Turing defined intelligence, i.e. the artificial intelligence provable by Turing tests) and secondly, in a Turing test, it is mandatory that the human agent to be qualified (besides being informed). Obviously, there is only one chance for the human agent to predict correctly all outputs of a logical circuit, namely to know propositional logic (besides knowing the circuit design). Otherwise, the results of a Turing test on a logical circuit are not relevant at all. On the other hand, the human or artificial agent that organizes the Turing test must be able to recognize intelligence regardless if is human intelligence or artificial intelligence. The true output is either certain and 1-probable or possible and p-probable (with $p \in (0,1)$) or impossible and 0-probable for any logical circuit implementing a tautology / a contextual truth / a contradiction, respectively.

A second example of consistent experimental frameworks can be built for any digital circuit in general, by analogy with the first example from above. We make this remark because, ultimately, a biometric system can be viewed today as a complex digital circuit.

3 Imperfect experimental frameworks

ξ and CEF are introduced exactly for ensuring that what is theoretically possible / probable / certain is also practically possible / probable / certain, respectively. On the other hand, ξ and CEF allow us to study weakened models, when the weakening is made otherwise than changing the axioms within the definition of probability, for example. We do not have any clue that weakening probability axioms could prove to be maximally productive, because even in imperfect experimental frameworks the probability theory continues to function despite the adequacy of our beliefs and intentions. In other words, when a system evolves on and within measurable sets/spaces, we can ignore the probability theory if we prefer, but we cannot abolish it, simply because it is engraved/embedded within the structure of the space itself. Besides, we will illustrate further, how probability distribution functions (PDFs) and cumulative distribution functions (CDFs) appearing in biometrics (or anywhere else) can generate fuzzy membership functions easily, in more than a single way. Hence, adopting a fuzzy approach in a

given matter is not necessary equivalent with contradicting probability theory (by weakening some of its axioms). The major difference between our approach and [30] is that in ours, the classical possibility-probability relation (described above in terms of ξ and CEF) stays unchanged while the experimental frameworks that we work with - despite being allowed to be imperfect - are not allowed to decay up to the abolition of probability theory.

A first degree of imperfection illustrated here is when accurately implementing S_T is practically impossible or technically and economically unfeasible. For example, when N is big enough, a preferable alternative for implementing N-dimensional dynamical systems with predefined input-output behavior is designing a simpler n-dimensional system (n<<N) that supports *almost* the same input-output behavior - a technique known as order reduction. However, in such case, the practical n–dimensional implementation S_{Pn} and the theoretical N-dimensional model S_{TN} are still highly cointensive, whereas the practical n-dimensional implementation S_{Pn} and the theoretical n-dimensional reduced model S_{Tn} are still totally cointensive, and therefore, the classical possibility-probability relations (3), (4), (7), (8), (14) and (15) still hold true in the consistent experimental framework (X,R,Y,S_{Tn}, ξ) when ξ is S_{Pn} based.

3.1 Imperfect experimental frameworks in iris recognition

One of the worst but still manageable (hence acceptable) degree of imperfection is when the required (target) input-output (i-o) behavior is known as being possible, but all practical implementations S_P attempted up to some point for mimicking the target i-o behavior are almost failed resulting in practical i-o behaviors that are very different from the target i-o behavior. This is currently the case of all iris recognition results and biometric systems belonging to the statistical paradigm pioneered by Daugman [3], [4]. The target i-o behavior assigned to an a priori unknown target system S_T that the user intends to design (proved possible by interrogating a qualified human agent during a Turing test while using good quality eye images) can be statistically illustrated as a 0-1 histogram of correct biometric decisions (0 - for identifying a pair of iris images taken for different eyes, 1 - for identifying a pair of iris images taken for the same eye), as in Figure 1, whereas the i-o behavior of implemented system is statistically illustrated in Figure 2. As exemplified in Figure 1 and Figure 2, plotting the statistics of the results recorded in a Turing test is a way of visually quantifying the loss in precision occurred for the implemented system in comparison with the target i-o behavior. The lack of cointension between target i-o behavior and implemented i-o behavior is obvious. Figure 1 illustrates a logically consistent, crisp, artificial and binary understanding (logical, crisp, binary and lossless human-precisiation of meaning) for two concepts whose extension are not just disjoint but complementary in the input space of the recognition system: 'imposter pairs' (IP) and 'genuine pairs' (GP). Figure 2 illustrates a lossy compression of the original meaning of the two concepts, a fuzzy artificial perception and a fuzzy

machine-precisiation of meaning for the two original human-precisiated concepts. The artificially perceived fuzzy concepts (further denoted as f-IP and f-GP or as f-imposter and f-genuine) are no longer disjoint. There are pairs of irides qualifying simultaneously and equally as f-genuine and f-imposter pairs, while others qualify ambiguously but with different probabilities. A better situation in terms of cointension can be observed by comparing Figure 1 from here to Figure 2 from [19], Figure 4 from [20] and Figure 5 from [22].

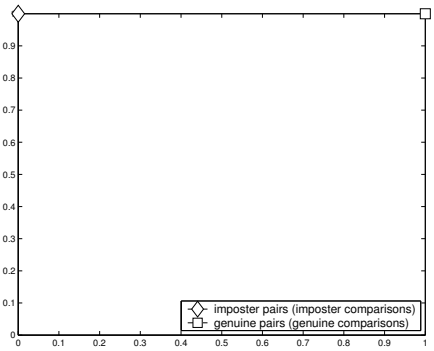

Figure 1
Human-precisiation of iris recognition: PDFs corresponding to the correct biometric decisions given by a qualified human agent during a Turing test of iris recognition (diamond for imposter pairs, square for genuine pairs)

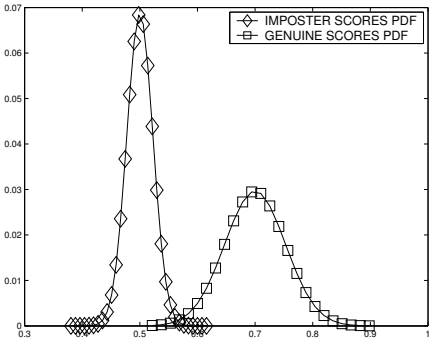

Figure 2
Machine-precisiation of iris recognition: PDFs of the imposter scores (diamond) and genuine scores (square) collected during a Turing test of iris recognition while interrogating an artificial agent implementig statistical iris recognition.

The imperfection of such an experimental framework illustrated in Figure 1 and Figure 2 is further commented in terms of possibility-probability relation: in theoretical target system corresponding to Figure 1 the confusion between an imposter and a genuine pair is impossible, whereas in the implemented system it is possible, indeed. Forcing the correct recognition of all imposter pairs within the implemented system comes at the price of not recognizing correctly all genuine pairs. This trade-off is inherent in classical statistical iris recognition. Therefore, despite the original concepts consistently support negation, the fuzzy concepts f-IP and f-GP cannot be consistently negated.

The consistent experimental frameworks are contexts in which the cointension between a target formal theory and the actual implemented system transports probability-possibility relation between theory and practice in the same manner in which continuity transports convergence from the argument space to the image space in the framework of topology. On the contrary, in the imperfect experimental frameworks the cointension between theory and practice (or between target and implemented system) can be so weak that even theoretically but still logically impossible events could appear as practically probable (hence practically possible). However, the fact that cointension is weak enough and consequently unable to establish a consistent bridge between what is practically probable and theoretically possible does not mean that the possibility-probability relation is

broken inside the set of events concerning the implemented system alone: confusion between the two artificially perceived concepts (imposter and genuine pairs) is practically p-probable (1>p>0) and therefore practically possible. On the other hand, when logical inconsistency gets its place inside an imperfect experimental framework, the right contra-measure to take is attempting to recover logical consistency, not attempting to redefine possibility-probability relation, because otherwise, contradiction being explosive, sooner or later, anything can be proved and some logically impossible events could appear as proved/supported by "experimental evidence" to be probable (hence possible) events. In short, when it comes to test or to design systems in imperfect experimental frameworks, there is no sound argument to extrapolate experimental evidence to expectations for real life without precautions, regardless if the channel on which the extrapolation is made is possibility-to-probability or possibility-to-fuzzy membership relation.

3.2 A possibility – probability – fuzzy membership relation for Gaussian events

The most important aspect revealed by the comparison between Figure 1 and Figure 2 is the lack of cointension between what is maximally achievable (Figure 1) and what is currently achieved in implementation (Figure 2). The relation between what is theoretically possible and practically probable is broken, whereas the relation between what is practically possible and practically probable still stays consistent. Translating probability to fuzzy membership is possible in many ways. However, this operation is closed in the semantics of implemented system, is an operation whose result is at most an equivalent of some facts already known, i.e. it is at most a rule for rewriting known facts, not an attempt to improve the actual implemented system. Regardless the way chosen to express fuzzy membership based on statistics of experimental data, in the absence of cointension, there is no instrument to carry this information back and forth between theory and practice. Besides, as the following example illustrates, forcing the meaning of the data to conform to a pattern that it is not really exhibited as an observable behavior, inevitably brings more inconsistency to an already imperfect experimental framework. In short, interpreting the experimental data does not solve the problems, but only point out to them.

Since in the case investigated here, the errors are inherent to the implemented system (Figure 2), computing right-to-left CDF under the imposter distribution (FAR - False Accept Rate, diamond markers in Figure 3 and Figure 4) and left-to-right CDF under the genuine distribution (FRR - False Reject Rate, square markers in Figure 3 and Figure 4) define a way of interpreting fuzzy membership of the recognition scores obtained by the input iris pairs to two fuzzy sets corresponding to the two artificially perceived concepts f-imposter and f-genuine scores (see Figure 3 and Figure 4). However, according to this interpretation, 0 is an imposter score (a convenable interpretation, given the target behavior in Figure 1), fact that is neither confirmed experimentally (Figure 2) nor confirmed

theoretically in statistical iris recognition. Moreover, the means of the two Gaussian variables in Figure 2 have the degrees of membership to the fuzzy sets f-imposter and f-genuine scores expressed as 0.5, which is clearly counter-intuitive, the mean being the most representative sample of a Gaussian signal.

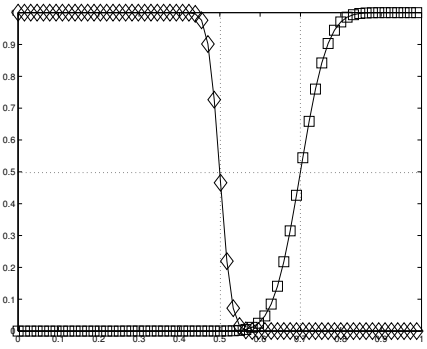

Figure 3
Machine-precisiation of statistical iris recognition: False Accept Rate (FAR, diamond markers) and False Reject Rate (square markers) represented with liniear y coordinate; zoom to membership degrees that the means of the two Gaussians (Figure 2) have in f-imposter and f-genuine fuzzy sets.

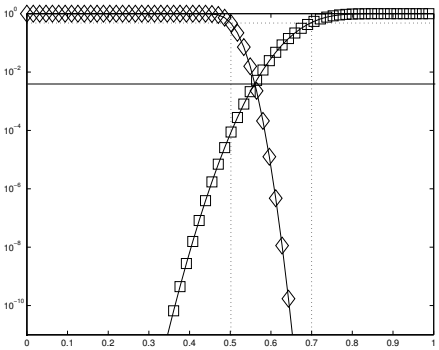

Figure 4
Machine-precisiation of statistical iris recognition: False Accept Rate (FAR, diamond markers) and False Reject Rate (square markers) represented with logarithmic y coordinate - zoom to the Equal Error Point (indicated above by the continuous horizontal line situated slightly under 1E-2).

Experimental data can be interpreted using fuzzy if-then rules. For example, the ensemble of fuzzy if-then rules producing the fuzzy-membership assignments represented in Figure 3 as FAR and FRR curves is the following:

- fewer successors a score has within the imposter distribution, weaker its degree of membership to f-imposter fuzzy set is;
- fewer predecessors a score has within the genuine distribution, weaker its degree of membership to f-genuine fuzzy set is;

However, the same interpretation can easily fail in contradiction or in counter-intuitive facts, as illustrated above.

A different interpretation of experimental data can be made accordingly to the following ensemble of fuzzy if-then rules, which is better suited for describing Figure 2 (probability) in terms of fuzzy membership as in Figure 5:

- for scores situated on the right/left side of the mean, fewer successors / predecessors a score has within the (imposter or genuine) distribution, weaker its degree of membership to the corresponding fuzzy set (f-imposter or f-genuine) is;
- recognition score equals to the mean of (imposter or genuine) distribution has unitary membership degree with respect to the corresponding fuzzy set (f-imposter or f-genuine);

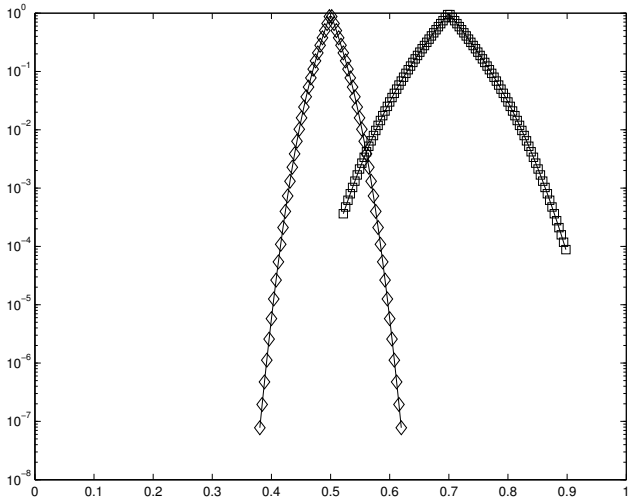

Figure 5

Machine-precisiation of statistical iris recognition: fuzzy membership assignment of the recognition scores obtained experimentally and represented in Figure 2 as the two fuzzy sets f-imposter (diamond markers) and to f-genuine (square markers).

Given the symmetry of Gaussian variables, the fuzzy membership function should also be symmetric. For any given distribution and any given score from Figure 2 there is a pair of left- and right-side cumulatives under that distribution and the sub-unitary ratio of these two cumulatives is a plausible fuzzy membership assignment of the given score to the corresponding fuzzy set (f-imposter or f-genuine) that satisfies the two fuzzy if-then rules from above. Fuzzy membership functions constructed this way are illustrated in Figure 5, which represents a fuzzy decisional model associated to the statistics of experimental data within Figure 2. This second interpretation of the experimental data within Figure 2 is better that the previous one (illustrated in Figure 3 and Figure 4) at least for three reasons: the means are scored with a unitary degree of membership, membership is not arbitrarily extended to scores that are not obtained experimentally, and at last, but not the least, the abscise of the Equal Error Point is preserved from Figure 4 to Figure 5 (i.e. the point of equal error expressed in Figure 5 in terms of fuzzy memberships corresponds exactly to the point of equal error expressed in Figure 4 in statistical terms of FAR and FRR).

Summarizing, even in imperfect experimental frameworks, iris recognition experimental results can be expressed in terms of practical possibility - probability - fuzzy membership on the experimental side of the framework, because a recognition event 'e_s' with a given score 's' recorded experimentally (in Figure 2) is practically possible, practically probable and maps the input pair into the two fuzzy sets f-imposter through the fuzzy membership assignment illustrated in Figure 5. However, in an imperfect experimental framework there are at least two unsolved problems:

- the formal logic involving experimentally recorded recognition events is contextual and temporal because all true sentences that can be derived on the experimental side of the framework are true *at some specific time*, *in some specific case*, *accordingly to a specific experiment*, *accordingly to specific experimental data*. This situation emphasizes the importance of condition (9) within the Definition 1.
- the huge difference between what is achievable (in human-precisiated iris recognition Figure 1) and what is achieved (in machine-precisiated statistical iris recognition, Figure 2, Figure 5), a gap that can be filled through creativity only, not through interpretation.

On the other hand, Gaussian events that vanish at some left- and right-side points (for example, the recognition of imposter pairs in statistical iris recognition and the corresponding Gaussian distributed numbers) define specific fuzzy sets as follows: if s_g / e_g is a Gaussian distributed number / event vanishing at some left and right points, its membership to any continuous or (discretized) interval considered within the vanishing left and right limits can be expressed as a fuzzy degree of membership (Figure 2, Figure 5):

$$FM(s_g) = \min(L_C(s_g)/R_C(s_g), R_C(s_g)/L_C(s_g)), \quad (17)$$

where $L_C(s_g)$ and $R_C(s_g)$ are the left- and right-side cumulatives under the given Gaussian distribution to the left and right vanishing points, respectively.

3.3 Natural fuzzification of a continuous distribution

Theorem 1: For any 1-dimensional, real-valued random variable s that is continuously distributed on a real interval and vanishes at some left and right points, the fuzzy membership FM defined in formula (17) is bounded in [0,1] and has a single global maximum point s_M for which $FM(s_M)=1$;

Proof: When thinking at the upper bound of FM, the most favorable situation is for that point s_M where the right-side cumulative equals the left-side cumulative. Indeed, if such point s_M exists, $FM(s_M)=1$. Since the left-side cumulative on the given continuous distribution computed in the current point s with respect to the left vanishing point increases with s and since the value of the left-side cumulative evolves continuously between 0 and 1, the point s_M exists and it is defined by the abscise where the left-side and right-side cumulatives are equal to 0.5. Hence, FM has upper bound that is also its maximum value 1. Given the definition (17), FM strictly increases with s - when s is between left-side vanishing point and s_M, and strictly decreases with s - when s is between s_M and the right-side vanishing point of the given distribution, hence, (s_M, 1) is the only local and global maximum point of FM, whereas its lower bound is given by the values of FM in the left and right vanishing points of the distribution, namely zero.

Formula (17) establishes the degree of fuzzy membership (FM) as being the most pessimistic degree of interiority that s_g has with respect to the left and right

vanishing points of the distribution. FM is bounded between 0 and 1, and has always a single maximum point. In the case of Gaussian events, this maximum point corresponds to the mean and is the first point around which long enough experiments throws enough neighboring values such that to emulate topological density in a given precision (a property that does not hold true for bimodal Gaussian distributed numbers – for example).

Searching for the right context in which the relation between possibility, probability and fuzzy membership can be consistently expressed for the particular case of experimentally obtained iris recognition results brought us inevitably to a natural (canonic) and universal fuzzification procedure available for an entire class of continuous distributions, for which the formula (17) is formally correct (is actually making sense) due to Riemann integrability of all continuous distributions. Formula (17) is a meeting point where classical logic, modal logic, fuzzy logic, probability theory, measure theory, system theory and topology shake their hands explaining consistently the complex but natural provability – observability / reachability - possibility - probability - fuzzy membership - integrability relation *without pointing out to a need for weakening the* σ *–additivity condition* within the definition of probability up to the formula (2). The σ –additivity condition is actually *the true principle of possibility-probability consistency*. Conversely, not any fuzzy membership assignment that we would wish to operate with can be consistently mapped onto a continuous distribution, especially when it is not compatible with the σ –additivity condition and consequently, the interpretation given by such fuzzy membership assignments can be neither confirmed nor infirmed by measurable experiments (organized in consistent experimental frameworks). Therefore, the reader should figure out if using such fuzzy membership assignments in connection with measurable things and spaces is a matter of excessive oratorical talent or a matter of logic and sound science.

3.4 The future of statistics and fuzzy logic

In the context of measurable spaces and consistent experimental frameworks, the σ –additivity condition ensures that the answer to the question "*is there a need of fuzzy logic?*" (Zadeh, [31]) is "*yes, in the same degree in which there is a need for statistics, classical logic, modal logic, system theory, measure theory and topology*". Otherwise, operating fuzzy logic while weakening σ –additivity condition results in a contradiction, namely the finding of a hypothetically consistent way (science/theory) of quantifying things that by their nature are not theoretically (mathematically) measurable and practically (physically / experimentally) measurable, a theory that unfortunately, cannot be confirmed with instruments of statistics, classical logic, modal logic, system theory, measure theory and topology. On the contrary, formula (17) shows there is at least one way of consistently expressing an agreement point for all these sciences/theories

(including fuzzy logic) while maintaining σ –additivity condition. The lack of interconnection between probability theory and fuzzy logic evidenced here when fuzzy logic accepts the weakening of the σ –additivity condition is just the small empty part of a bottle of very old wine: given the huge diversity of fuzzy membership assignments and the natural parity that exists between at least a part of them and the continuous distributions, a real explosion of new probability distribution models is expected to happen in the years to come, marking a point from where fuzzy logic and statistics will further develop side-by-side exactly because of the bridge established in between them by the σ –additivity condition.

3.5 Negation of fuzzy membership

As far as we know, expressing probable events (like those represented in Figure 2) as fuzzy membership (Figure 5) is a matter of *interpretation*, a matter of rewriting some facts from a dialect of statistics to a dialect of fuzzy logic using a rewriting rule, for example formula (17) – in our specific case considered here. Therefore, in this context, the negation operates at a semantic level: for example, if 0.5 *is interpreted* as a certain imposter score - and this interpretation is allowed by formula (17) because FM(0.5)=1 (despite the fact that the statistics of experimental data says nothing more than 0.5 score is the most probable imposter score), then logically, should be impossible for the same 0.5 score to be interpreted as a genuine score, fact that is indeed true, despite some false appearances in Figure 2 and Figure 5. Indeed, the index of genuine pairs can be intoxicated accidentally by wrong segmentation results or by the impossibility that the implemented recognition system to deal successfully with the variability of acquired iris instances. This is also another facet of the imperfect experimental frameworks where the job of solving apparently conflicting information obtained through interpretation of experimental data must be done carefully by a qualified human operator / system administrator.

3.6 Blind negation of fuzzy membership

If no attention is given to the semantic of actually implemented system and to the actual input-output relation, negation can be made by applying fuzzy complement [29]. For example, if FM is defined by (17) as the fuzzy membership of all scores within [0,1] interval with respect to the imposter distribution, 1-FM is a complementary fuzzy membership assignment defining a sort of negation in which a single element within [0,1] interval is certainly a non-imposter score, namely 0.5 – the mean of the imposter distribution. This fact is, of course, counter-intuitive with respect to the practical problem. Besides, we are talking again about many values situated outside the set of experimentally observed imposter scores. This operation is meaningless with respect to the actual implemented system. This is why we called this sort of negation, blind negation.

On the contrary, if we remember that negation by complement should have a meaning with respect to the practical problem (implemented system) and should make a real sense inside the set of reachable scores, the situation changes completely: since f-imposter and f-genuine are two fuzzy granules covering the set of reachable scores, the assertion '*s is an f-imposter score*' means accordingly to the actual experimental data that s is the Gaussian distributed number as illustrated in Figure 2 (i.e. is 0.5 with maximal probability, 0.51 with other probability and so on) whereas its negation should be '*s is an f-genuine score*' whose interpretation should be derived by analogy from the previous one.

4 Negation in biometrics

The important remark to make here is that since the fuzzy membership assignment is an interpretation of data, there is not a unique way of negating it, as already exemplified above. Even at this stage it is not capitally important to find a negation operator meaningful with respect to the practical problem, we will try this in a future paper, eventually. Bell that saved us this time is the fact that the final stage in obtaining a practicable crisp decisional model from the fuzzy model within Figure 5 is defuzzification of f-imposter and f-genuine fuzzy sets to classical disjoint intervals labeled 'imposter' and 'genuine' and partitioning [0,1] interval.

4.1 Negation as a Boolean algebraic operator

After defuzzification, the Boolean logic of recognition can be expressed through isomorphism with the Boolean algebra generated by the empty set, [0,1] interval and the two intervals 'imposter' and 'genuine', whereas negation is simply a transcript of complement operation within this Boolean algebra. This is a way of implementing a binary recognition function and a binary decisional model for biometrics, a model in which the recognition error rates are hopefully stationary (there is no proof for that, whereas increased recognition errors over time is already documented under the wrong name of "template ageing" (critical analyses of this concept can be found also in [6] and [9]). A ternary recognition function and a ternary decisional model for biometrics is obtained if the two intervals 'imposter' and 'genuine' are separated by a third one labeled 'uncertain' and covering ambiguous score values.

By investigating the consistency of the concepts of "template ageing" and "biometric menagerie" [12], [23] we found an improved quinary recognition function and a quinary decisional model for iris biometrics, which is obtained while practicing iris recognition on intelligent iris verifier systems with stored digital identities [22]. In such systems, it is possible that the lowest scores are

imposter scores, followed by a class of degraded imposter scores obtained by dishonest users when claiming (actively hunting) different identities than they actually have (*hyena*), followed by a class of *uncertain* scores centered in 0.5, and further to the right by a class of degraded genuine scores (*goats*). The rightmost class is that of *genuine* scores. All of these models are illustrated in Figure 6, whereas the binary and the ternary models are applicable also for classical statistical iris recognition (Figure 2, Figure 5).

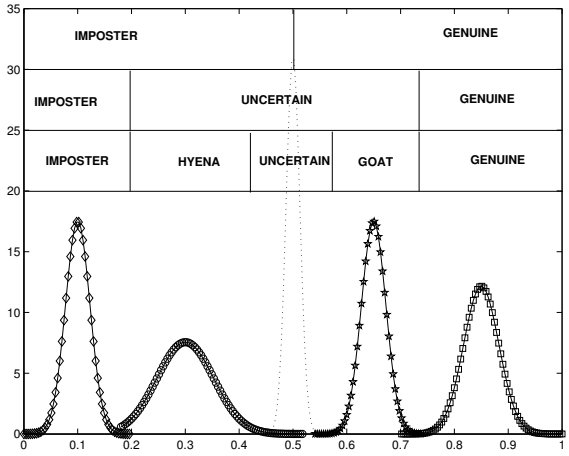

Figure 6

A better machine-precisiation of statistical iris recognition with distant imposter and genuine score classes; From top to bottom: binary, ternary, respectively quinary decisional models.

For all decisional models within Figure 6, negation is expressed within a Boolean logic induced by a partial power set Boolean algebra (in a similar manner as that described in [21]): the negation of the assertion '*s is an impostor score*' is intuitively and naturally expressed as '*s is either hyena, or uncertain, or goat, or genuine score*', for example. This is why we did not insist on finding the negation operator in the previous step (prior to defuzzification). Besides, between an interpretation and a Boolean logic, the latter is clearly the appropriate context of negation.

4.2 Strong negation in biometrics

Blind negation of fuzzy membership by fuzzy complement (see section 3.6) is a negation practiced in the codomain of the fuzzy membership function. On the contrary, the negation by complement applied to individual recognition scores s,

$$N(s) = 1-s, \tag{18}$$

acts in the domain of that fuzzy membership function. The negation N in (18) satisfies boundary condition N(0)=1, is continuous, involutive and decreasing with

respect to the score s, hence it is a strong negation [7], as all instances of Sugeno λ- complement [26], [32]. The effect of this negation is a rewriting of all recognition results from terms of similarity (proximity) in terms of non-similarity (distance). For example, applying the strong negation (18) for all available Hamming distance scores, expresses the same experimental results in terms of Hamming similarity (the complement of Hamming distance) and vice versa.

Graphically, the effect of this negation is that the score distributions are all symmetrized against the vertical pointing in 0.5, regardless how many they are (2, 3 or 5). Hence, strong negation on all recognition scores has a meaningful effect with respect to the practical problem of recognition. However, the appropriate context of applying it is prior to defuzzification. After defuzzification, depending on the number of values chosen for the recognition function, the decisional model is still binary, ternary or quinary, but the order of the intervals reverses: genuine, imposter – for the binary case, genuine, uncertain, imposter – for the ternary case, and finally, genuine, goat, uncertain, hyena, imposter – for the quinary case.

Conclusions

This paper proposed a new formalization of the classical probability-possibility relation, which was further confirmed as a much complex, but natural relation between provability, observability, reachability, possibility, probability, fuzzy membership and Riemann integrability. Searching for the right context in which this relation can be consistently expressed for the particular case of experimentally obtained iris recognition results brought us inevitably to a natural (canonic) and universal fuzzification procedure - formula (17) - available for an entire class of continuously distributed random numbers, as a confluence point of statistics, classical logic, modal logic, system theory, measure theory and topology. The applications were initially intended for iris recognition scenarios and can be easily extrapolated anywhere else where there is a need of expressing the relation possibility - probability - fuzzy membership without weakening the σ-additivity condition within the definition of probability, which as this paper suggested is actually the true principle of consistent possibility-probability translation. .

Acknowledgement

This work was supported by the University of South-East Europe Lumina (Bucharest, Romania) and the Lumina Foundation (Bucharest, Romania).

References

[1] A.J. Ayer, *Language, Truth, and Logic*, Victor Gollancz Ltd., London, 1936.

[2] V.E. Balas, I.M. Motoc, A. Barbulescu, *Combined Haar-Hilbert and Log-Gabor Based Iris Encoders*, New Concepts and Applications in Soft Computing, Series: Studies in Computational Intelligence, vol. 417, pp. 1-26, Springer, 2013.

[3] J.G. Daugman, *Biometric Personal Identification System Based on Iris Analysis*, U.S. Pattent 5291560 / 1991 / 1994.

[4] J.G. Daugman, *How Iris Recognition Works*, in Proc. 2002 IEEE Conf. on Image Processing, vol 1, pp.33-36, Rochester, New York, USA.

[5] G. Doddington, W. Liggett, A. Martin, M. Przybocki, D. Reynolds, *Sheep, Goats, Lambs and Wolves: A Statistical Analysis of Speaker Performance in the NIST 1998 Speaker Recognition Evaluation*, Int'l Conf. Spoken Language Processing (ICSLP), Sydney, vol. 4., pp. 1351-1354, 1998.

[6] M. Fairhurst and M. Erbilek, *Analysis of physical ageing effects in iris biometrics*, IET Computer Vision, 5(6):358–366, 2011.

[7] J. Fodor, *Preferences and Decisions without Numbers*, Online Proceedings of Budapest Tech International Jubilee Conference, 2004.

[8] P. Grother, E. Tabassi, G.W. Quinn, W. Salamon, *IREX 1 Report - Performance of Iris Recognition Algorithms on Standard Images*, NIST, USA, 2009.

[9] P. Grother, J.R. Matey, E. Tabassi, G.W. Quinn, M. Chumakov, *IREX VI: Temporal Stability of Iris Recognition Accuracy (Iris Ageing)*, Information Access Division, NIST, USA, July 24, 2013.

[10] L. Ma, T.N. Tan, Y.H. Wang, D.X. Zhang, *Efficient iris recognition by characterizing key local variations*, IEEE Transactions on Image Processing, 13(6), 739–750, 2004.

[11] S.H. Moi, H. Asmuni, R. Hassan, R.M. Othman, *Multimodal biometrics: Weighted score level fusion based on non-ideal iris and face images*, Expert Systems with Applications, 2014, In Press, Elsevier.

[12] I.M. Motoc, C.M. Noaica, R. Badea, C.G. Ghica, *Noise Influence on the Fuzzy-Linguistic Partitioning of Iris Code Space*, Soft Computing Applications, Advances in Intelligent Systems and Computing, vol. 195, pp. 71-82, Springer, 2013.

[13] N. Popescu-Bodorin, *Exploring New Directions in Iris Recognition*, in proc. 11th Intl. Sym. on Symbolic and Numeric Algorithms for Scientific Computing, Conference Publishing Services - IEEE Computer Society, pp. 384-391, September 2009.

[14] N. Popescu-Bodorin, *A Fuzzy View on k-Means Based Signal Quantization with Application in Iris Segmentation*, 17th Telecommunications Forum, University of Belgrade, November 2009.

[15] N. Popescu-Bodorin, L. State, *Cognitive Binary Logic - The Natural Unified Formal Theory of Propositional Binary Logic*, CoRR abs/1106.2352, 2010.

[16] N. Popescu-Bodorin, V.E. Balas, *Comparing Haar-Hilbert and Log-Gabor based iris encoders on Bath Iris Image Database*, 4th Intl. Workshop on Soft Computing Applications, pp. 191-196, IEEE Press, July 2010.

[17] N. Popescu-Bodorin, V.E. Balas, *From Cognitive Binary Logic to Cognitive Intelligent Agents*, Intelligent Engineering Systems (INES), 2010 14th International Conference on, pp.337-340, 5-7 May 2010.

[18] N. Popescu-Bodorin, *Online CCBL Demonstrator*, Applied Computer Science Testing Lab, http://lmrec.org/bodorin/ccbl/ , 2011.

[19] N. Popescu-Bodorin, V.E. Balas, *Exploratory Simulation of an Intelligent Iris Verifier Distributed System*, Proc. 6th IEEE Intl. Symposium on Applied Computational Intelligence and Informatics, pp. 259 - 262, IEEE Press, June 2011.

[20] N. Popescu-Bodorin, V.E. Balas, I.M. Motoc, *Iris Codes Classification Using Discriminant and Witness Directions*, Proc. 5th IEEE Intl. Symp. on Computational Intelligence and Intelligent Informatics, pp. 143-148, IEEE Press, 2011.

[21] N. Popescu-Bodorin, V.E. Balas, I.M. Motoc, *8-Valent Fuzzy Logic for Iris Recognition and Biometry*, Proc. 5th IEEE Intl. Symp. on Computational Intelligence and Intelligent Informatics, (Floriana, Malta, September 15-17), pp. 149-154, IEEE Press, 2011.

[22] N. Popescu-Bodorin, V.E. Balas, *Learning Iris Biometric Digital Identities for Secure Authentication. A Neural-Evolutionary Perspective Pioneering Intelligent Iris Identification*, Recent Advances in Intelligent Engineering Systems, pp. 409–434, vol. 378, Series: Studies in Computational Intelligence, Springer, 2012.

[23] N. Popescu-Bodorin, V.E. Balas, I.M. Motoc, *The Biometric Menagerie - A Fuzzy and Inconsistent Concept*, Soft Computing Applications, Advances in Intelligent Systems and Computing, vol. 195, pp. 27-43, Springer, 2013.

[24] H. Proenca, L.A. Alexandre, *Toward Covert Iris Biometric Recognition: Experimental Results From the NICE Contests*, IEEE Transactions on Information Forensics and Security 7(2), 798–808, 2012.

[25] P. Radu, K. Sirlantzis, G. Howells, S. Hoque, F. Deravi, *A Multi-algorithmic Colour Iris Recognition System*, Advances in Intelligent Systems and Computing Volume 195, 2013, pp 45-56.

[26] M. Sugeno, *Fuzzy measures and fuzzy integrals: A survey*, in Gupta *et al.*, Fuzzy Automata and Decision Processes, North-Holland Publisher, Amsterdam, 1977, pp. 89–102.

[27] A.M. Turing, *Computing machinery and intelligence*, Mind, 59, 433-460, 1950.

[28] N. Yager, T. Dunstone, *The Biometric Menagerie*, IEEE Transactions on Pattern Analysis and Machine Intelligence, vol. 32, no. 2, February 2010, pp. 220 - 230, ISSN 0162-8828, doi 10.1109/TPAMI.2008.291.

[29] L.A. Zadeh, *Fuzzy Sets*, Information and Control, 8, 338-353, 1965.

[30] L.A. Zadeh, *Fuzzy sets as a basis for, a theory of possibility*, Fuzzy Sets and Systems, nr. 1 /1978, pp. 3-28, North-Holland Publishing Company.

[31] L.A. Zadeh, *Is there a need for fuzzy logic?*, Information Sciences, nr. 178/2008, pp. 2751–2779, Elsevier, 2008.

[32] D. Dubois, H. Prade, *Fuzzy sets and systems: theory and applications*, volume 144, Mathematics in Science and Engineering Series, Academic Press Inc., 1980, London, UK.

Collective Behavior in Wireless Sensor Networks

Ryszard Klempous

Wroclaw University of Technology
27 Wybrzeze Wyspianskiego street, 50 – 370 Wroclaw, Poland
e-mail: ryszard.klempous@pwr.wroc.pl

Abstract: The system of homogeneous nodes, cooperating with each other, pursuing strictly defined goals for the exchange of information… this is a Wireless Sensor Network (WSN). WSN's are network radio equipment (transmitters, sensors and microcontrollers), that are geographically distributed in a defined area. These autonomous nodes communicate with each other and jointly submit their data through the network to the Base Station (BS). The basic objective of such activity is to monitor environmental conditions, such as: light, pressure, temperature, motion and/or chemical pollution. This paper describes a relational shape adaptive collective behavior. On the basis of formal set theory, as shown from the perspective of global managed adaptive WSN actions, and how local activity adaptation is guaranteed.

Keywords: adaptive systems; collective behavior; Wireless Sensors Network; WSN

1 Introduction

Wireless Sensors Networks (WSN's) are important for the following reasons:

- Limited range radio communications nodes naturally breakdown to local and global. This is all that is heard in the environment is for the local node, the rest of the network from the perspective of node WSN is global
- Radio frequency communications nodes, in the common band, provide an effective exchange of information between neighbors. A node, while monitoring communication in the environment continues to monitor the needs and situations of neighbors and can interact with them in the attainment of common objectives.
- Radio communications in a limited range, stimulates group activities. A node, as an entity, performs simple activities and I limited to neighbor

relationships (and therefore local) jobs. In order to achieve the objective, joint actions for the entire network (global) cooperation is essential in many nodes. Without interaction and group activities the WSN is not justified.

Normally, distributed WSN's integrate and manage a wide range of systems that use low power microcontrollers (or smart sensors), and in addition, are equipped with sensors, radio transmitters and power sources [6, 12]. The sensors perform regular measurements that monitor, for example, vibration, temperature, humidity and light. Then, the results of the measurements are forwarded to the base station (BS), which is connected to the computer network in which aggregation/synthesis are performed and the final analysis of the data. In isolation, the individual nodes are limited, but become powerful, when numbers integrate into a larger network and collaboration environment. The WSN's are a usual asset of two subsystems; the collection of data and the network broadcast information system [12]. Also, in this case, we will use a layered model network as applied to the ZigBee protocol (IEEE 802.15.4).

1.1 Network Layer Communication and Routing in WSN

Usually in hierarchical design communication in a WSN network, a layer is located between the application layer (APS) and MAC [9, 20]. It provides the MAC layer data services and traffic management services. The transmission of data, in order to determine flow of packets in a network, uses the higher layer mechanisms. It consists of packet header information, including the address, and if this requires the implementation, as well as, authentication and confidentiality codes. The traffic management provides several control functions; it may start setting up new network routing, set up a new device, determine the level of performance/failure of adjacent nodes, and thus decide whether and which of the nodes are adjacent to the shortest path (routing), change diagrams (e.g., unicast to broadcast) and monitor the WSN nodes to determine their usefulness in creating the communication network structure. The higher Layer (application) is helpful when configuring the network layer.

1.2 A Self Organization and WSN Protocols

The WSN can often be used in difficult conditions, which results in a high rate of electrical energy consumption within the nodes. In order to ensure, that the WSN will be still effective, certain mechanisms that compensate for energy degradation should be an integral part of design of the WSN [16].

In order to achieve this, the core of the WSN must have very robust routing protocol algorithms that are needed to ensure that the network will be able to refocus itself to make ad hoc or self repairs. When is such a property desirable? Most often this will be in the event of changes in the environment, which will

reduce performance of the communication networks [15]. Hence an important component design of WSN's is the choice of network protocol, which is matched to the tasks for which the network is intended. There is no single or universal solution. There are different size memory resources for nodes for communication node strategies and that is their complexity. As an example here, we can give ZigBee [20], Wi-Fi, Bluetooth, enOcean, Z-wave and Insteon [25].

1.3 Capabilities and WSN Limitations

In order to determine a paths packet flow, most routing protocols in a WSN terminate at the network layer, using exploring/discovering attempts. On the basis those control packets, routing tables are dynamically refreshed. If a known node is not responding, the item is removed from the routing table and node propagates the modified information, in order to reflect observed changes in the network configuration [22].

An intelligent collaboration environment results from the use in each of the component WSN chipset drivers. This approach is crucial for the use of sensors that incorporate microprocessors, after their integration, with a certain form of intelligence [1] or the microprocessor signal alignment systems, which enhance the capabilities. Integration of devices with microcontrollers have brought significant benefits to the technology of sensors, so that now they match signal interfaces, hardware, multicast routes and the opportunities for cooperative networks are increasingly integrated within the sensor. Adding to the sensor microcontroller, in addition, makes it possible to use advanced algorithms, digital signal processing (DSP), leading to faster and more reliable data acquisition systems.

WSN networks cannot guarantee a direct connectivity communication type Line-Of-Sight (LOS), we need to try and eliminate any impact of terrain or weather effects on the RF transmission. Oxygen and water are two of the main atmospheric factors filtering in the frequency range 2 GHz to 40 GHz. It should therefore be expected to account for these factors on the communication capabilities and routing paths to the base station in the WSN. Signal loss in the atmosphere, and multi-displacement terrestrial communications also takes place, so to find the appropriate routing paths in the network topology is an important factor. Transmission between two nodes may not be maximal due to interference in the band RF and as practice shows, it is not a very important factor. The interference in the band RF very often eliminates a number of nodes shared in communication. For example, Bluetooth communication operates in the 2.4 GHz band. So, if a computer that communicates with peripheral devices wirelessly (e.g. keyboard, mouse, printer, etc.) using this Bluetooth standard and it operates in the same environment as the WSN, the risk of interference is very real. Other sources of interference are harmonics generated by monitors, fluorescent lights or electric motors [20].

Density of sensors in the network must be designed with the optimal number of nodes, with the flexibility of accuracy spatial distribution of collected data, as well as to ensure flexible routing decision-making at the time, such as rebuilding route tracks. Comparison to the neighbor devices interval Signal to Noise Ratio (SNR) to make it easier to select your device with higher SNR and therefore find best (cooperating) nodes in the vicinity is the foundation for efficient routing. If the density increases, the sensor spatial distribution increases the level of flexibility of solutions, and to find the best path routing is more likely. In addition, additional nodes in the network reduce network congestion, which ensures the additional benefit of high Quality of Service (QoS).

Usually, sensors need to work in an environment where energy is retrieved from a battery, which is an important constraint on the design and implementation WSN. Because of the spatial distribution and the limited resources available, the activity sensor is reset to the local activities and mutual communication between neighbors. The network communications (local) coordination of activities for the WSN implementation tasks, which one node cannot achieve, is one of the key actions in the network.

Information that is collected by the sensors in a specific area must be forwarded to the BS, however, because of the reduction in power and limited range radio transmission at each node, communication is carried out with the multi-hop. As a result, information may be transmitted by a large area, which significantly exceeds radio coverage one single node. Indiscriminate broadcasting of information does not guarantee success in a WSN, since it takes up bandwidth. Reducing the transmission bandwidth channel, thereby increasing the usable collisions probability in a communications channel, ensures an increase in energy consumption. Individual nodes have limited resources and the flow of information which is required for nodes to the BS must be implemented in a manner that minimizes energy consumption.

2 Multi-Hop Routing

There are a considerable number of investigations for routing WSN algorithms, which allow you to transfer information between nodes and a BS [2, 3, 19]. The flat algorithm (e.g. flooding) ensures that information ends at the BS, unless there is no node that can communicate with it directly. Such protocols use broadcast to most techniques and practically entail flooding the WSN data packets. This results in collisions in the communication channel and repeated retransmissions. Approach flooding is not only fully ineffective, but also deteriorates usable bandwidth and restricts communication speed, resulting in poor quality communications, leading in extreme cases, to a cut off in areas of the WSN. These disadvantages are minimized in the GLIDER protocols [7], where communication

is limited only to broadcast neighborhood nodes. Routing Protocols, such as data Centric Routing for Sensor Protocol for information via Negotiation (SPIN) in implementing communication is geared to minimize the duration of transmissions, the number of additional queries and response times to events recorded by the sensor is at the end of other information requirements.

Rumor routing protocol [2, 23] attempts to take advantage of software agents and directed communication mechanisms. In this case, positive results are achieved on a relatively small number of scenarios, in situations where the cost/energy resources are small compared to the costs of communications. Hierarchical protocols, such as LEACH, PEGASIS or TEEN [17, 20, 24, 27] use a directed communication implemented mechanism by creating a hierarchical topology with clusters or divisions by zone. In this paper we to go further, using a routing protocol based on a tree structure so that the chains use a novel energy efficient tracking algorithm called Predict-and-Mesh (PaM) [28, 29, 30], which is suitable for energy sensitive distributed wireless tracking systems. Making use of the PaM algorithm, it is possible to adaptively adjust the sensing frequency for pervasively monitoring various kinds of targets with random movement patterns.

All the above mentioned protocols make use of a single multi-hop communication path, between a node and a BS. The resulting communication path is used as long as it is energy efficient justified [8, 9, 10, 13]. If the level of a node, which is one of the tracks, drops below a certain minimum level, path determination algorithms are activated. The newly created track is in operation after the energy resource exhaustion of its elements. This is repeated as long as the algorithm is not able to set a new path. Then we recognize that the WSN ceases to operate.

2.1 Routing Systems with Retransmission

Construction track routing protocols in multi-hop neighborhood nodes requires cooperation in order to establish communication routes. Regardless of whether one or multiple paths are designated, routing protocols attempt to construct them so that they lead to the BS. The operation of a single node when routing, although carried out locally in the neighborhood, needs to be underpinned by an objective, that is, to provide global data packet to the base station (BS). Additional criteria, such as cost minimization of energy consumed, to minimize the number of retransmissions, minimize delays, expressed as functions, to help you to choose the appropriate data transfer direction collected in the WSN. For a spatial communication approach, it is slightly different than those described above. Instead of making use of the features, we use relationships. There is no need to (although it is possible for them to do so) make accurate decisions, which node is to be the next in the path to the BS. Instead, what we need is only to create a communication pathway to meet a specific relationship between the successive nodes forming it. Such an approach requires that already in the path are required data packets, nodes cooperate different locally in the neighborhood, based on

local/current criteria and making decisions locally. However, all of these local measures must be correlated in such a way that the resulting spatial communication meet the criteria set out on a global scale. Developing cooperation within network nodes uses topological properties, but it is not centered on a specific direction - nodes simply cooperate with each other in the vicinity [10, 11]. However, the entire WSN focuses on the collection of information from the sensors and sends it to BS. Thus, the nodes, which operate in the vicinity, must ensure that the deposit local actions will establish a path through the nodes in the BS.

3 A Description of the Actions Using Relations

The proposed method for *Multi-hop routing* uses three, two-fold, relations defined in activities set (Act) that describe communication activity in the WSN. These three relations are: subordination (π), tolerance (ϑ) and collision (χ), proposed by Jaron [8]. They are particularly useful in modeling and visualization quality interactions, especially within the WSN [5, 17, 18]. In order to present our solutions, we will utilize the following relationships:

$$\pi := \{< x, y >; x, y \in Act \,|\, x \pi y\} \tag{3.1}$$

An expression $x \ \boldsymbol{\pi} \ y$ - defines operation *x,* which is subordinated to *y,* otherwise saying the *y* dominates the *x*,

$$\vartheta := \{< x, y >; x, y \in Act \,|\, x \vartheta y\} \tag{3.2}$$

The ϑ means that the x and y are very sensitive to each other,

$$\chi := \{< x, y >; x, y \in Act \,|\, x \chi y\} \tag{3.3}$$

It should be noted that each two-fold relation *R* defined on a set *A*, can be represented as a set of ordered pairs < x, y >. In set theory, basic properties of our three relationships mentioned above we define [10] as follows:

$$\pi \cup \vartheta \cup \chi \subset Act \times Act \neq \emptyset, \tag{3.4}$$

$$\iota \cup (\pi \cdot \pi) \subset \pi \tag{3.5}$$

Where $\iota \subset Act \times Act$ is identity on the *Action* set. Next

$$\pi \cup \vartheta^{-1} \cup (\vartheta \cdot \pi) \subset \vartheta \tag{3.6}$$

Where ϑ^{-1} means an inverse relationship to ϑ.

Thus,

$$\vartheta^{-1} := \{< x, y > \in X \times Y \,|\, y \,\vartheta\, x\} \tag{3.7}$$

For the relation of collision taking place:

$$\chi^{-1} \cup (\pi \cdot \chi) \subset \chi \subset \vartheta^{,} \tag{3.8}$$

Where $\vartheta^{,}$ is the relationship ϑ, which is expressed as:

$$\vartheta^{,} := \{< x, y > \in X \times Y \,|\, < x, y > \notin \vartheta\} \tag{3.9}$$

Axiom (3.8) in relation to collision was separable in relation to tolerance, symmetrical and that the actions were subordinated in collision with all the activities, which is dominant in the collision. In [14, 15, 18] shown as using these two-fold relations for model spatial communication. The subordination relation can be applied for multi-hop routing path determination; the tolerance allows multiple paths to exist simultaneously while the relation of collision represents some form of conflicts and restrictions in communications space. The relation of subordination allows you to specify the routing path retransmission, while the tolerance permits the existence of many such paths, and relationship conflict creates a limitation required communication space.

4 Chaining in WSN

Using the appropriate relationship for chains is, in most cases, describing synergisms between adjacent nodes and adjusting them to the general conditions prevailing in the area. Let's look at the relationship of subordination (π). Among all three relationships, only that the only is transitive, this allows us to track modeling retransmission. Relation (π) is a transitive and reflexive one and is therefore preorder in the set of *Actions*.

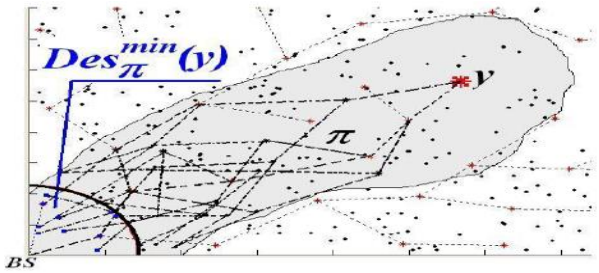

Figure 1
Creating $Des_{\pi}(y)$ in the WSN [17]

Further studies, however, require more powerful order in the A*ctions* set. Entering a partial order, which is a particular instance of preorder, does not seem to be difficult. In real-time applications, nodes are distributed more or less randomly in the area. In the case where the two nodes of the network are located very close to each other, one of them is mute remaining in the stand by. This creates a "single" node communication with much greater energy resources. Such a combination of two components can be expressed by applying the anti-symmetric condition on the relationship of subordination. So we have in the set of activities *Action* defined partial order (weak). Let us go a step further, set *Action* is partially ordered (weak), but strong and weak relations are closely related in the sense that it's easy to convert one type of relationship to another one. So let's do this, the relationship of subordination is asymmetrical in nature, which is related to its axiomatic anti-reflexivity. So let's assume that our relationship of subordination will be additionally anti-reflexive. Is this assumption is consistent with the status of the actual WSN network? This seems to be the case. The situation, when a node transmits a packet to itself seems not to be in the category of reasonable behavior. Therefore, eliminating such situations is most appropriate. Reached in this way the relationship of anti-reflexivity is strong partial order in the *Actions* set. Further, a detailed description of the chain of relationships can be found in [18] and as the final result

Figure 2
Examples of chains of the $Chn_{\pi}(y)$ set

One obtains four partially ordered sets:

$$Des_{\pi}^{min}(\mathrm{y}) = \{\mathrm{x} \in Des_{\pi}(\mathrm{y}) |\, BS\pi\, x)\} \tag{4.1}$$

$$Des_{\pi}^{max}(\mathrm{y}) = \{\mathrm{x} \in Des_{\pi}(\mathrm{y}) |\, x\, \pi\, BS\} \tag{4.2}$$

$$Des_{\pi}^{mis}(\mathrm{y}) = \{\mathrm{x} \in Des_{\pi}(\mathrm{y}) |\, \neg(\exists n \in N)(BS\pi^{n}\, x)\} \tag{4.3}$$

$$Des_{\pi}^{pfex}(\mathrm{y}) = \{\mathrm{x} \in Des_{\pi}(\mathrm{y}) |\, Card(Asc_{\pi}(x)) > 1\} \tag{4.4}$$

And family $Chn_{\pi}(y) = \left\{ Chn_{\pi}^{i}(y) \middle| i \in I \right\}$ linear ordered chains directed to the base station:

$$(Chn_{\pi}^{i}(y) \subset Des_{\pi}(y) | \, i \in I)(\mathrm{BS} = \bot \wedge \mathrm{y} = \top) \tag{4.5}$$

Where the symbol $\bot$ indicates the minimum in the set (i.e. base station), a symbol $\top$ indicates the maximum in the set (the node *y*) (Fig. 1 and Fig. 2).

5 Modeling Adaptive Behavior in WSN

5.1 Actions and in WSN

For modeling the activity adaptive WSN, we approach relational and define such basic concepts as well as action and behavior. The activity will be considered as network nodes activity, while preserving the activity from the perspective of external node. In addition, behavior is the result of activities of the group nodes on the network.

Network communication activities are described using three, dyadic relationships defined by the activities set *Act*. Activities are activities that have each of the nodes performing individually, however, depending on any other nodes, which are located in its vicinity. Ability to perform an action depends on the state, in a node (other actions will be carried out at the time of creating, other during normal network operation) and its end causes a change in the node status. Therefore, all actions which may take network nodes are described as a transformation of a Cartesian product of the WSN nodes set (*Nodes*) and a set of nodes state (*States*) The result is a new node, therefore, the *Act* is defined as ternary relation:

$$\mathrm{Act} : \mathrm{Nodes} \times \mathrm{States} \rightarrow \mathrm{States} \tag{5.1}$$

Examples of actions may be: measuring environmental parameters, data aggregation, sending data to a selected/all nodes or the reception of the data. Since the nodes are autonomous, each of them may act independently of the other nodes. This has an unquestionable advantage, because in this way, the WSN may also carry out a number of different operations. On the other hand, a number of actions makes perfect sense only when two or more nodes cooperate with each other in carrying out the activities related to each other (cooperate with each other). The node activity makes a lot of sense, if in its vicinity there is at least one node that performs an action - *receiving*. In this case, cooperation between the nodes is required to perform such that each of the nodes of remains with each other in defined relationships. We propose to do this with the relations of subordination -π, tolerance; -ϑ and collisions -χ. Behavior of a collection of relations with each

other, in certain cause-and-effect relations, (here we are using the relation π, ϑ and χ), are temporary as well as spatial (neighbor relation).

On this basis we can build the product set *Behavior* (*Beh*), whose elements are equivalence classes of the relation *R*:

$$Beh : Act / R = \{act_{[x]} \in Act \mid act_{[x]}\ R\ x\} \tag{5.2}$$

The theoretical basis for the research activity (WSN) is the relational model [12] of cooperation between individual nodes on the network. This model describes the relations between the nodes and determining what action these nodes may take. Most of the advantages are in describing actions of individual nodes, which are autonomous components compatible, in order to achieve the objective defined globally for the entire network. Thus, the relational, not only contains in itself the existing solutions for communication routing, but you can also achieve global objectives through local action by individual network nodes in the WSN. Ultimately, it is a bridge between a locality and global behavior in the network, and thus between the actions of a group of behaviors of these elements.

5.2 Design with Adaptive Behavior in the Neighborhood Node

Routing multi-hop node cooperation is a key form of activity in the WSN [4, 21, 22]. Most nodes cannot communicate directly with the BS, because their range of radio communications is not sufficient. The WSN is a fully distributed system in which nodes with resources necessary for the implementation of calculations need to communicate with neighbors in order to maintain a compact state across network infrastructure. There are many WSN algorithms, which use some of the neighborhood concepts (e.g. neighborhood algorithms; multi-hop, reliable, bidirectional or geographic). We also we will use this concept, starting from its definition. Let *Map(X,Y)* is a mapping from X to *Y* (*surjection*), where *Sub(X)* is defined as family all subsets of *X*. In the presented model the *neighborhood N* can be expressed as follows:

$$N \in Map\big(Nodes,\ Sub(nodes)\big) \tag{5.3}$$

Let *N(k)* will be neighbor of node *k* and *N(S)* will be neighbor of set nodes *S* be defined as follows:

$$N(k)_{|k \in Nodes} = \{y \in Nodes\ |yR_N k)\} \tag{5.4}$$

$$N(S)_{|S \in Nodes} = \{y \in Nodes\ |(\exists x \in S) yR_N k)\} \tag{5.5}$$

In the WSN there is present a natural localism, associated with the concept of a natural neighborhood. Both of these concepts are the result of radio coverage restrictions (mainly technical) or anisotropic propagation radio waves. Thus, the term, *the natural locality occurs*. Another locality type is introduced by

clusterization. In this case, their locality is limited to the cluster and is type of simplification. It makes it easy to calculate, but at the same time, the potential solutions became narrowed. As a result, *the natural locality* is seen as the most appropriate approach, particularly from the perspective of a node. Formally, the natural neighborhood in the WSN is family indexed sets $N = \{N_i | i \in I\}$ and is globally characterized as follows:

$$(\forall i \in I)(N_i \neq \emptyset) \cup N_i = Nodes \tag{5.6}$$

$$(\exists\, i,j \in I | i \neq j)\left(N_i \cap N_j \neq \emptyset\right) \tag{5.7}$$

From a local node point of view we obtain:

$$(\forall y \in Nodes)(\exists^{!} i \in I | y \in \bigcap N_i \neq \emptyset) \tag{5.8}$$

Where the symbol $\exists^{!}$ means "there are many". So, based on a relation (5.8) we can say that the defined neighbor relationship is not a partition of a set *Node*.

With a well defined neighborhood (5.6) - (5.8) we will try to make decomposition chains (4.5) for the various neighborhood nodes. The decomposition must be simple and identical for each of the nodes. After this, as nodes are scattered in the area, self organization of WSN nodes takes place. A set of nodes is not an ordered set and the main task is to establish a certain order. It supports the network communications further activity. The considerations made in the previous sections result that in the relationship of subordination π, which is transitive and reflexive one, define preorder. Unfortunately, this does not exclude loops in the process of building routing paths (Fig. 3, left). The possibility of loop occurrence is excluded due to presence of weak partial order through requirement that the relation π was an anti-symmetric one (Fig. 3, right)**.** Such an outcome is already a considerable success of self-organization. However, average energy expenditures in designing routing paths, are very high. A packet, not spread in the network indefinitely, but very often long circulates in the WSN before it reaches the BS|. Only linear ordered chains (4.5) are the expected final result (Fig. 4).

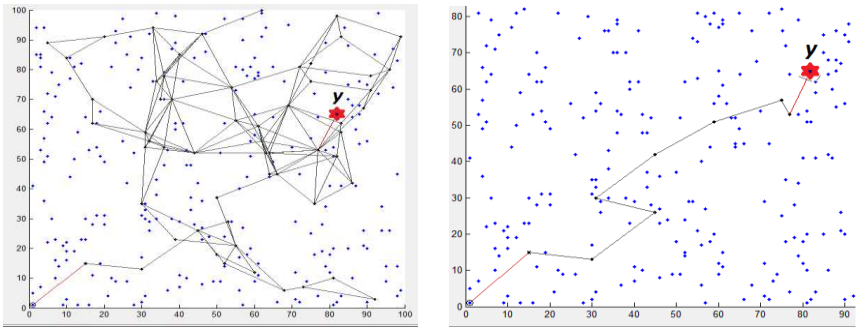

Figure 3

Sample tracks/chains of N(*y)* with preordered graph (left) and weak ordered partial graph (right)

Before introducing a proper order let's look now at its familiar algorithm for determining distance from the base station [26]. This algorithm does not determine the Euclidean distance, but it specifies a minimum number of retransmissions, which must be carried out to ensure a packet submission to the BS. Procedure to be followed in *broadcast mode i*s started by the BS sending the message *"my distance from BS is 0 "*. Each node that receives a message *"my distance from BS 0" defines* its status as *"my distance from BS is 1"* and the message is disseminated within the neighborhood. In general, a node that receives a message *"my distance from BS is x",* determines their status as *"my distance from BS is x+1 ",* then if it has received the message for the first time, broadcasts this message in its vicinity. The initial status of each node is 0, allowed status operations are: an increase in status, when it is zero and a reduction in status, when it is non-zero. When this procedure is completed, each node with non-zero status *X+1* can communicate with at least one node with status *X*. If a node has a status 0, this means that it does not have any neighbors and may not participate in the WSN network activity. As a result, each *k* node knows its distance to the base station, *dish(k) defined* as the minimum number of retransmissions. More importantly, knows the distance all neighbors *dish(x)*, where $x \in N(k)$ (Fig. 5).

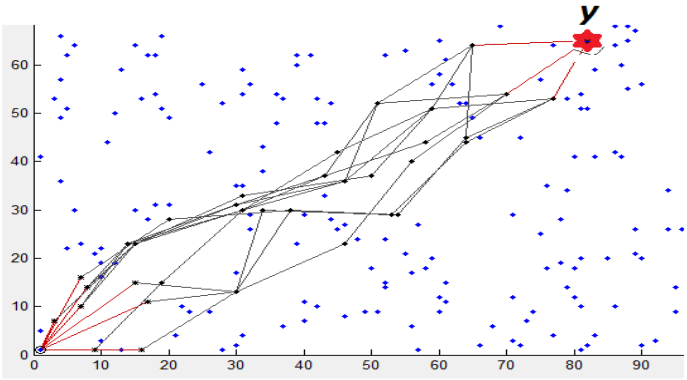

Figure 4
Sample tracks/chains of N(*y*) with the order line

On the basis of this information is possible to split neighborhood *N(k) into three* subsets:

$$N_{<}(k) = \{y \in N(k) | \, dis^h(y) < dis^h(k)\}$$
$$N_{\leq}(k) = \{y \in N(k), y = k \mid dis^h(y) \leq dis^h(k)\} \quad (5.9)$$
$$N_{>}(k) = \{y \in N(k) | dis^h(y) > dis^h(k)\}$$

In considering the relationship of *Subordination* (π) for any node $k \in Des_{\pi}(y)$ its communication activity is limited only to its neighbors, i.e.:

$$N_\pi(k) = \{x \in N(k) | x\pi k\} \tag{5.10}$$

Knowing $N_<(k)$, which was set in the WSN, we intend to identify the components of the node set (5.8). Accept that $N_\pi(k) \subseteq N_<(k)$

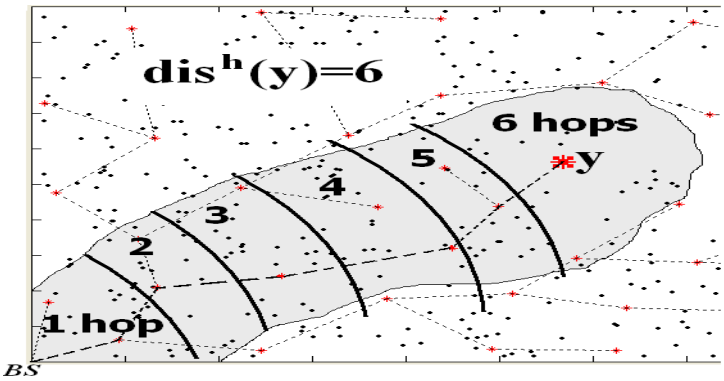

Figure 5
Determination of distance *dish(s)* from the base station (*BS*) [17]

and it is sufficient that designated paths shall drift to the BS. Cardinality of the set $N_<(k)$ shall determine the maximum number of such possible paths. Moreover, each of these paths will be optimal in the Pareto sense. For instance in Figure 5: retransmission to the base station - there are seven relays, regardless of which path is selected. It is likewise with a tolerance relation ϑ. For any node $k \in Des_\vartheta(y)$ its communication activity is limited only to its neighbors, i.e.

$$N_\vartheta(k) = \{x \in N(k) | x\vartheta k\} \tag{5.11}$$

Knowing $N_\leq(k)$, which was set created in the WSN self organization process, identify the components of the set (5.11) for the node *k*. Accept that $N_\vartheta(k) \subseteq N_\leq(k)$, But it does not guarantee that every simple path will strive to the BS. Tolerance is symmetrical and reflexive, and it is not enough to have a relation of the ordering. However, the tolerance and the subordination results on *fuzzy effect* of subordination, which is very important in situations of routing paths in areas of excessive noise. Of course, the sole relation tolerance is insufficient to guarantee the network cooperation sensors will ensure that messages are sent to the BS. Tolerance, however, has properties that make it very useful as secondary/complementary relation to the relation of Subordination. Especially when due to their locality effects, the packet becomes stuck in the blind localization (*dead end*). The relation of Subordination will not address this situation. The Tolerance relation is perfect and can handle it because of the symmetry (returning a packet to the last source) by proposing an alternative path. The relations of Subordination and Tolerance ensure that the message always reaches the BS, but at the same time allowing transmission to nodes tolerated to increase the number of available communication paths.

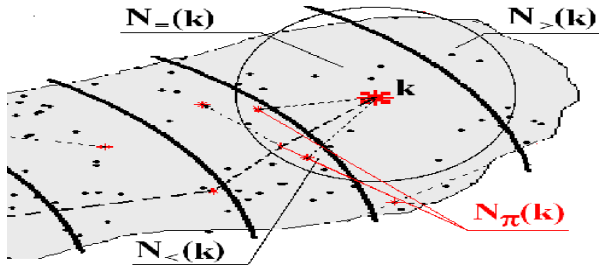

Figure 6
Building chains *Chn(k)* in the neighborhood node *k* [17]

As before, the maximum number of possible paths is equal to the cardinality of the set $N_{\leq}(k)$ (Fig. 6).

Third relation, the Collision χ, which for any node $k \in Des_{\chi}(y)$, limited communication activity to neighbors:

$$N_{\chi}(k) = \{x \in N(k) | x \chi k\} \tag{5.12}$$

Knowing the $N_{>}(k)$, which was set in the WSN self organization process, we intend to identify the node components of the set (5.12). Let's us assume $N_{\chi}(k) \subseteq N_{>}(k)$, but because of Collision the package in all the paths will be directed away from the BS. A Collision is symmetrical and anti-reflexive, hence, may not be an ordering relationship. However, for nodes it is useful, because it allows for definition of a neighbors set, with which cooperation is undesirable. As in the previous two cases, the maximum number of possible paths is the cardinality of the set $N_{>}(k)$ (Fig. 7).

5.3 Management of Adaptive Behaviors

In the process, preceding the appropriate operation of the network, nodes of the network will learn about their neighborhood. Then, by using the globally defined metric *dish(s),* as described in previous sections, each node orders its neighborhood, creating sets (5.9). Node remains only to realize the following assignments:

$$N_{\pi}(k) \subseteq N_{<}(k) \quad ; \quad N_{\vartheta}(k) \subseteq N_{\leq(k)} \quad ; \quad N_{\chi}(k) \subseteq N_{>}(k) \tag{5.13}$$

Sets $N_{\pi}(k)$, $N_{\vartheta}(k)$, $N_{\chi}(k)$ are respectively, subsets of sets $N_{<}(k)$, $N_{\leq}(k)$, $N_{>}(k)$. The following questions appear: which node should determine all of them? Which and how many nodes adjacent to them belong to them? The first question answer is determined by node on the basis of globally defined objective (e.g. from the neighborhood are selected these nodes, which have the highest energy). The number of nodes that belong to the specific sets is determined globally and is being implemented by the base station *BS*.

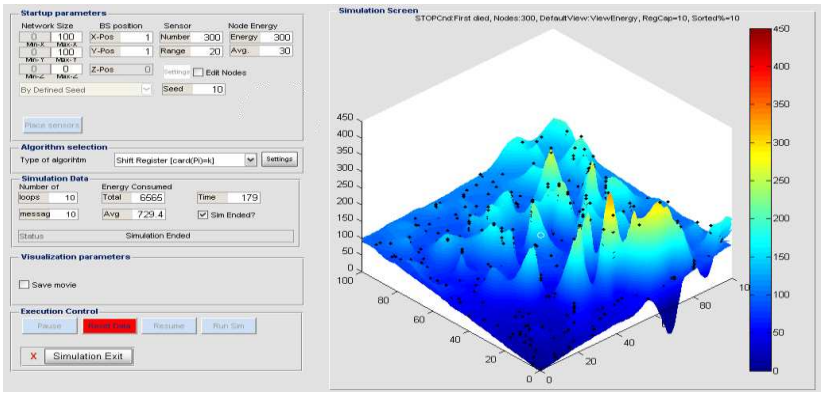

Figure 7

View simulator adaptive behavior with a locator, required globally by coefficients of relationship π, ϑ, χ

Globally, therefore, the main task of adaptive behavior management is to determine by the BS and send in the packet broadcast, required the number of sets $N_{\pi}(k)$, $N_{\vartheta}(k)$, $N_{\chi}(k)$. These are the cardinality of the set for individual subsets or percentage of cardinality of the set related to the cardinality of the number of neighborhoods (Fig. 7). Locally, on the basis of known resources neighbors, each node selects neighbors who will belong to specific subsets.

Summary

A relational approach provides a good presentation for adaptive collective behavior in a WSN. Quality of this tool is mainly due to the fact that it allows a consistent modeling of global and local phenomena. Locally means, in this approach, in the neighborhood. We also have neighborhood node (5.4), as is the other approaches, but we extend the concept of neighborhood to neighborhood nodes (set (5.5)). Assuming this set is a single set, these concepts are equivalent. Another extreme case is that, when a node for which neighborhood is the entire WSN. Then neighbors are also the entire WSN named global, and this is the case. Transition between these two extremes; local and global is smooth, because the cardinality of nodes set, for which we set neighborhood (5.5), can vary from *1* to the cardinality of *Nodes* WSN *(*all nodes). Partition to the local/global ceases to be dichotomous, moving from the alternative "*or either' to 'this or that'*.

Adaptive behavior is characterized accordingly:

- Locally, by selecting retransmitter, suitable to the prevailing ambient conditions. As a node retransmitting short extracts is the one that best meets the criterion, adopted centrally routing quality.
- Globally, routing path is modified, according to transmission constraints arising in the WSN. So, conversion to bypass routing areas of high noise.

Group behavior is respectively:

- Locally, a relational approach gives the ability to use spatial routing. A node does not choose one retransmitter but indicates a recommended one to undertake these role nodes/neighbors. Groups indicated in this way, neighbors shall decide which of them receives a packet and forward it.
- Globally, the build routing path is the result of intentionally targeted individual nodes. None of the nodes (except last one) forming a routing path to the BS, is not able to send information to it. This is why group interaction between nodes, in the relational schema restrictions, gives a result achieved by nodes, which are not able to do it separately.

Bibliography

[1] Braginsky, D., Estrin, D, Rumor Routing Algorithm for Sensor Networks, Proc. of the 1st Workshop on Sensor Networks and Applications, Atlanta, GA, 2002

[2] Brooks, R. R., Pirretti, M. Zhu, M. Iyengar, S. S., Distributed Adaptation Methods for Wireless Sensor Networks, Global Telecommunications Conference, GLOBECOM '03, 2003, Vol. 5, pp 2967-2971, DOI10.1109/GLOCOM.2003.1258778

[3] Burmester, M., Le T. V., Yasinsac, A., (2007) Adaptive for Protocols: Managing Security and Redundancy in Dense Ad Hoc Networks, Ad Hoc Networks, Volume 5, Issue 3, pp. 313-32

[4] Cohn, A. G. , Bennett, B. , Gooday, J. M., Gotts, N. M. , Representing and Reasoning with Qalitative Spatial Relations about Regions, Cohn, A. G., Bennett B., Gooday J. M., Gotts N M, eds. Spatial and Temporal Reasoning, Dordrecht, Kulwer, 1997, 97-134

[5] G. Coulouris, J. Dollimore, T. Kindberg, Distributed Systems: Concepts and Design, Addison-Wesley, June 2005. ISBN13:9780321263544

[6] Descartes R., L. J. Lafleur, Discourse on Method and Meditations, 1960, New York, the Liberal Arts press, ISBN10:0-672 -60278-4

[7] Fang O., Gao J., Guibas L. J., de Silva V., Zhang L., Glider: Gradient Landmark-based Distributed Routing for Sensor Networks, 24th Annual Joint Conference of the IEEE Computer and Communications Societies. INFOCOM 2005, 13-17 March 2005, Vol. 1, pp. 339-350

[8] Jaroń, J., Systemic Prolegomena to Theoretical Cybernetics, Scient. Papers of Inst. of Techn. Cybernetics, Wroclaw Techn. Univ., No. 45, Wroclaw, 1978

[9] Manjeshwar, A., Agrawal, D. P., Teen: A Routing Protocol for Enhanced efficiency in Wireless Sensor Networks, 15th International Parallel and Distributed Processing Symposium (IPDPS' 01), Parallel and Distributed Processing Symposium, International, 2001, Vol. 3, pp 30189, Sun courseware

[10] Mills, Kevin L., A Brief Survey of Self-Organization in Wireless Sensor Networks, Wirel. Commun. Mob. comput., 2007, Vol. 7, pp. 1-12, Wiley InterScience, DOI: 10.1002/WCM.499

[11] Nikodem J., Autonomy and Cooperation as Factors of Dependability in Wireless Sensor Network, Proceedings of International Conference on Dependability of Computer Systems, Poland, June, 2008 / Eds Wojciech Zamojski, .Los Alamitos, IEEE Computer Society [Press], 2008, pp. 406-413, http://dx.doi.org/10.1109/DepCoS-RELCOMEX.2008.50

[12] Nikodem J., Klempous R., Chaczko Z., Modeling of Immune Functions in a Wireless Sensor Network, 20th European Model. and Simul. Symp.. EMSS 2008, Campora S. Giovanni, Italy, 2008. pp. 45-50

[13] Nikodem J.: Designing Communication Space in Wireless Sensor Network Based on Relational Attempt, LNCS, Roberto Moreno-Díaz, Franz Pichler, Alexis Quesada-Arencibia (Eds.). Berlin, Springer, 2009, Vol. 5717, pp. 83-90, http://dx.doi.org/10.1007/978-3-642-04772-5_12

[14] Nikodem J., Modelling of Collective Animal Behaviour Using Relations and Set Theory /. Lecture Notes in Computer Science, ISSN 0302-9743; Vol. 8111Pt. 1 / Roberto Moreno-Díaz, Franz Pichler, Alexis Quesada-Arencibia (eds.). Berlin; Heidelberg, Springer, 2013, pp. 110-117, http://link.springer.com/chapter/10.1007/978-3-642-53856-8_14

[15] Nikodem J., The Dilemma of Choice in Management of Communication Process in WSN / Lecture Notes in Computer Science, ISSN 0302-9743; Vol. 6927,Pt. 1 / Roberto Moreno-Díaz, Franz Pichler, Alexis Quesada-Arencibia (eds.). Berlin: Springer, 2012. pp. 48-55, http://dx.doi.org/10.1007/978-3-642-27549-4

[16] Nikodem J., Modelling and Activity in Wireless Sensors Network / Lecture Notes in Computer Science, Roberto Moreno-Díaz, Franz Pichler, Alexis Quesada-Arencibia (eds.). Berlin, Springer, 2007, Vol. 4739, pp. 18-25

[17] Nikodem J., Klempous, R., Nikodem M., Chaczko, Z., Woda M., Directed Communication in Wireless Sensor Network Based on Digital Terrain Model, 2nd Intern. Symp. on Logistics and Industr. Informatics, Sept. 2009, Linz, Austria. Piscataway, NJ: IEEE, 2009, s. 87-91

[18] Nikodem J., Klempous, R., Woda M., Chaczko Z.: Multihop Communication in Wireless Sensor Network Based on Directed Cooperation, Selected papers on Broadband Communication, Information Technology & Biomedical Application, BroadBandCom'09, Technical University of Wroclaw, 2009, s. 239-241

[19] Nikodem J., Woda M., Nikodem M., Spatial Communication Activity in Wireless Sensor Networks Based on Migrated Base Stations, Wireless Sensor Networks Technology and Protocols, ed. by Mohammad A. Matin. Rijeka: InTech, 2012, pp. 99-116, http://www.intechopen.com/books/wireless-sensor-networks-technology-and-protocols

[20] Sung-Min, J., Young-Ju, H., Tai-Myoung, C, 2007. The Concentric Clustering Scheme for Efficient Energy Consumption in the PEGASIS, 9th International Conference on Advanced communication Technology, Vol. 1, page(s): 260-265

[21] Vaidya, D., Peng, J., Yang, L. , Rozenblit, J. W. (2005) A Framework for Sensor Management in Wireless and Heterogeneous Sensor Network, 12th IEEE International Conference on the Engineering of Computer-Based Systems, pp. 155-162, April 2005, Greenbelt, MD, USA

[22] Vakil, S., Liang, B., Balancing Cooperation and interference in Wireless Sensor Networks, IEEE Comm. Society on Sensor and ad hoc Communications and Networks, Secon '06, Vol. 1, pp. 198-206

[23] Veyseh, M., Wei, B., Mi, N. F. (2005) An Information Management Protocol to Control Routing and Clustering in Sensor Networks, Journal of Computing and Information Technology - CIT 13 (1), pp. 53-68

[24] O. Younis, Fahmy S.: Heed: A Hybrid, Energy-Efficient, Distributed Clustering approach for ad hoc Sensor Networks, IEEE Transactions on Mobile Computing, October 2004 (Vol. 3, No. 4), pp. 366-379

[25] H. Kaur, S. Sharma; *A Comparative Study of Wireless Technologies: Zigbee, Bluetooth LE, Enocean, Wavenis, Insteon and UWB;* Proc. of the Intl. Conf. on Recent Trends In Computing and Communication Engineering, RTCCE 2013; Institute of Research Engineers and Doctors; ISBN: 978-981-07-6184-4; DOI:10.3850/ 978-981-07-6184-4_60

[26] Akyildiz F., W. Su, Sankarasubramaniam Y., and Cayirci E, Wireless Sensor Networks: a Survey, *Computer Networks*, March 2002, Vol. 38, No. 4, pp. 393-422

[27] Szymanski J., Chaczko, Z. C., Rodanski, B., Enabling Design and Development of Wireless BANs using 802.15.x Standards, in Moreno Diaz, Roberto; Pichler, Franz; Quesada Arencibia, Alexis (eds), LNCS, Eurocast 2013, Springer-Verlag, Las Palmas de Gran Canaria, Spain, 2013

[28] C. Feng, L. Yang and J. W. Rozenblit, Adaptive Tracking in Energy Sensitive Distributed Wireless Sensor Networks, Ad Hoc and Sensor Wireless Networks, 12(1-2), pp. 55-77, 2011

[29] Yang, C. Feng, J. Peng, and J. W. Rozenblit, "A Multi-modality Framework for Energy Efficient Tracking in Large Scale Wireless Sensor Networks," *Proc. of the 2nd IEEE International Conference on Networking, Sensing and Control*, pp. 916-921, Ft. Lauderdale, FL, USA, April 2006

[30] L. Yang, C. Feng, J. W. Rozenblit and H. Qiao, "Adaptive Tracking in Distributed Wireless Sensor Networks," *Proc. of the 13th IEEE Intl. Conference and Workshops on the Engineering of Computer Based Systems (ECBS' 06)*, pp. 103-111, Potsdam, Germany, March 2006

Control of Centerline Segregation in Slab Casting

Mihály Réger[1], Balázs Verő[2], Róbert Józsa[3]

[1]Óbuda University, Bánki Donát Faculty of Mechanical Engineering, Bécsi út 96/b, 1034 Budapest, Hungary, reger.mihaly@bgk.uni-obuda.hu

[2]Bay Zoltán Nonprofit Ltd. for Applied Research, Fehérvári út 130, 1116 Budapest, Hungary, vero@bzaka.hu

[3]ISD Dunaferr Co. Ltd., Vasmű tér 1-3, 2400 Dunaújváros, Hungary, jozsa.robert@isd-dunaferr.hu

Abstract: A complex mathematical model characterizing the centerline segregation level in the midregion of continuously cast slabs was developed. The basic heat transfer and solidification model connected to the semi-empirical liquid feeding model (LMI - Liquid Motion Intensity model) gives the possibility to estimate the centerline segregation parameters of slab cast under industrial circumstances. Solid shell deformation changes the volume of the space available for the liquid inside the slab and hereby also changes the conditions of liquid supply. In modelling slab casting in practical industrial cases the deformation of the solid shell cannot be ignored, especially from the point of view of centerline segregation formation. From this aspect, the most important effects resulting in deformation of the solid shell are as follows: shrinkage of the solid shell due to solidification and cooling; setting of the supporting rolls along the length of the casting machine i.e. decreasing the roll gaps as a function of cast length; bulging of the solid shell between successive supporting rolls; positioning errors and wear of rolls; eccentricity of individual rolls; etc. The critical parameter to describe the inhomogeneity in the center area of slabs is the porosity level in the mushy region. As a result of calculations performed by the model, ISD Dunaferr Co. Ltd. has changed the strategy of supporting roll settings in their continuous casting. After the modification had been implemented on casting machines, the quality problems due to centerline segregation of slabs decreased to a great extent.

Keywords: slab casting; centerline segregation; porosity; deformation of solid shell; mushy; permeability; pressure drop

1 Introduction

The continuous casting of slabs is aimed at producing a product with a proper chemical composition, geometry and surface quality, without any or a minimum acceptable level of external and internal defects. One of the most unpredictable defects of the slabs is centerline segregation, which has a negative effect on further processing of the slabs and hence on the possible uses of the final product.

The solidification of continuously cast products is accompanied by the volume changes of shrinkage and deformations. In order to compensate for the volume changes, the gaps between the supporting rolls decrease along the casting machine as a function of distance from the meniscus level. The proper compensation is important mainly in the last third of the solidification, where the center area of the strand has a two-phase mushy structure (mushy area of the slab). In case of improper correspondence between volume change and roll setting, the melt is forced to flow in the mushy area. If the liquid supply is insufficient to compensate volume changes, then discontinuities or inner porosity will develop, typically accompanied with macrosegregation. This phenomenon is the centerline segregation. The required liquid supply is provided by melt flow due to ferrostatic pressure. The liquid flow in the mushy area of the strand is impeded by the network of solid dendrites, and hence ferrostatic pressure decreases and liquid supply becomes uncertain. The reduction itself and the reduction rate of ferrostatic pressure play a key role in porosity formation. In order to investigate porosity formation, it is necessary to learn about the volume changes inside the strand. The Liquid Motion Intensity (LMI) model provides these kind of data[1,2)]. The suitability of the LMI model for the estimation of centerline segregation level has been demonstrated in previous research[3,4)].

2 Nature of the Centerline Segregation

Centerline segregation of slabs relates partly to macrosegregation and partly to the shrinkage of melt, the formation of small shrinkage holes and, occasionally, the formation of inclusions[5-8)]. In continuous casting centerline segregation develops in the middle part of the slab due to solidification and transformation processes, to fluid flow and also to constrained liquid supply, which is necessary for solidification shrinkage compensation. Only enriched melt is present between solid dendrite trunks. Any effect that enhances fluid flow (i.e. cooling conditions, setting of the supporting rolls, bulging between successive rolls, etc.) necessarily results in the flow of the enriched melt, i.e. macrosegregation will form. The possibility of sufficient liquid supply in the mushy area decreases depending on the ratio of solid phase. At the same time the permeability of zigzag channels between dendrite arms also decreases. Lessening the possibility of liquid supply

inevitably leads to the formation of shrinkage holes and porosity, which is also typical of centerline segregation formation. In Fig. 1, photographs taken by a scanning electron microscope, shows details of the rupture surface in the slabs mid-region. Relatively fine dendrites and highly fragmented channels of fluid flow can be identified in these pictures.

The macrosegregation part of centerline segregation can be characterized by the segregation ratio of individual elements[5]. Porosity can be measured by metallographic, ultrasound or density measurement methods[5-7]. In everyday industrial practice, steel producers prefer to apply cheap, fast and automated methods to characterize centerline segregation. The two most common methods are: comparison with standard images and measurement of the amount of shrinkage holes by image analysis. The latter one produces a relatively well quantifiable result. Because of the connection between the amount of shrinkage holes and the level of macrosegregation[7], the application of image analysis method and characterization of centerline segregation of the slabs by the porosity level is widely accepted by industry.

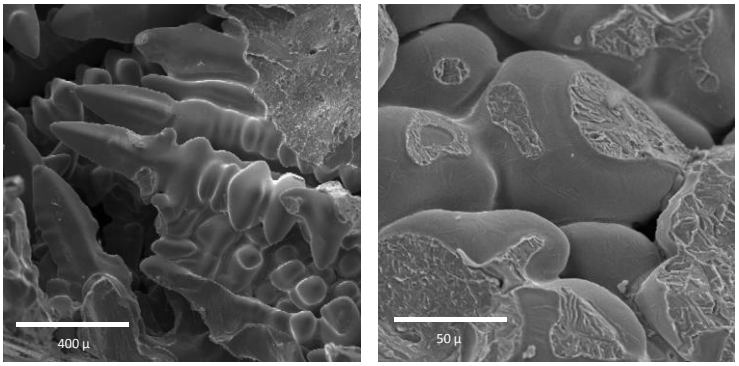

Figure 1
Shrinkage holes in the mid part of continuously cast slab

Despite the high ratio of plastic deformation, strips hot rolled from slabs with centerline segregation contain, in a modified form, the consequences of this type of inner defect[9]. As a result of inheritance, the middle part of the strip has a chemical composition (and structure) different from the average, which results in differing properties in the mid section of strip. The thickness of the defected part in the strip depends on the extent of plastic deformation. In general, the lower the thickness of the strip (i.e. the higher the amount of plastic deformation), the thinner the defect is in the strip. Accordingly, centerline segregation can cause problems in particular in the further processing of heavy plates (during cutting, drilling, welding, etc.).

Experience shows that the unfavorable properties of strips due to centerline segregation cannot be improved at a later stage and the level of macrosegragation

cannot be reduced significantly[10,11]. This is explained, initially, by the cross effects of diffusion processes of individual enriched elements (e.g. the local manganese content affects the diffusion of carbon).

It follows that the centerline segregation level can only be controlled during the solidification process. The resultant acceptable centerline segregation level for the users must hence be ensured by the application of a proper continuous casting technology.

3 Characteristics of the Mushy Area of the Slab

A sketch of the structure of a cast slab is shown in Fig. 2. If a vertical type casting machine is used, during casting the slab is in a vertical position. In curved casting machines, on the other hand, solidification starts in a vertical position but is completed in a horizontal position. In the first stage of solidification the dendrites growing from both sides do not reach each other and the center part of the strand contains pure liquid steel. The fluid flow in the upper part of the strand is mainly controlled by the inlet of steel from a submerged entry nozzle, by differences in density (thermal or solutal) and also by the deformation of the solid. Deformations of the solid shell originate from shrinkage (solidification, cooling and re-heating of the shell, allotropic transformations), from bending of the strand, from setting of the roll gaps and from bulging between successive rolls. The liquid flow and liquid supply (in the casting direction and perpendicular to the casting direction between dendrites) are supposed to be unlimited because only liquid can be found in the center part of the strand.

Depending on the casting parameters and on the composition of steel at a given distance from the meniscus level, the solidification fronts (liquidus fronts) growing from both sides touch each other. Therefore, (for the sake of simplicity, columnar solidification of the dendrites is supposed) the tips of the dendrites reach each other. In the case of slab casting in a curved caster, this occurs at about 12-15 m from the meniscus level in the unbent zone or after it. In a vertical casting machine the beginning of the mushy area is about 5-7 m from meniscus because of the constrained metallurgical length.

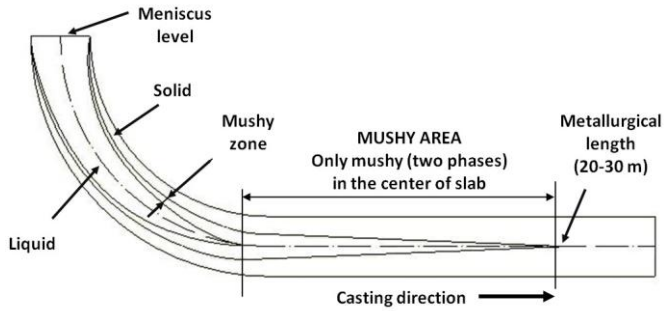

Figure 2
Sketch of inner structure of cast slab

At the beginning of the mushy area, the temperature of dendrite tips that meet each other is approximately equal to liquidus. From the point of view of liquid flow, a fundamentally different situation starts here because liquid supply in the casting direction must be realized through the zigzag and highly fragmented channels of the solid dendrite structure. The amount of liquid necessary in the mushy area is determined by the deformations in the mushy area and of the solid shell (mainly the shrinkage of the solid shell, setting of the supporting roll gaps, bulging). The roll gap in this case includes the prescribed roll gap setting, the errors of this setting, the wear and eccentricity of individual rolls.

Realization of the necessary amount of liquid supply through the fragmented tunnel system of dendrite arms depends on the pressure conditions that have developed in the liquid of the mushy area. The ferrostatic pressure of the liquid is determined by the height of liquid steel and by the pressure drop due to the constrained melt flow through the porous medium. The pressure drop depends on the volumetric flow rate and on the permeability in the mushy area. The permeability is the function of liquid ratio and the characteristics of the primary dendrite structure.

In the last stage of solidification the liquid supply must be realized by liquid flow through the mushy area. The length of the mushy area is between 3-10 m, depending on the structure of the casting machine and the casting technology (see Fig. 2). Ferrostatic pressure within this distance can decrease, to such an extent, that it is no longer sufficient to produce the required melt supply.

According to preliminary calculations, pressure drop is very low above the mushy area. This has no effect on the liquid supply in the casting direction or perpendicular to the casting direction of the mushy zone. However, in the mushy area, in casting direction, the melt supply is likely to be hindered. It should be noted that in the last stage of solidification the pressure conditions and liquid supply also affected by the formation of porosity (melt sucking) and the pressure of gases released inside the pores.

4 Pressure Drop in the Mushy Area

Decrease in the ferrostatic pressure in the interdendrite channels within the mushy area, can be estimated by the Darcy law:

$$Q = \frac{-KA}{\mu} \frac{\Delta P}{L} \tag{1}$$

where Q the volumetric flow rate (m^3/s), A the cross sectional area (m^2), ΔP the pressure drop (Pa), μ viscosity of the melt (Pas), L length of the section under investigation (m), K permeability (m^2).

In order to estimate the pressure drop, the volumetric flow rate along the mushy area must be known. Volumetric flow rate in the mushy area of the strand depends on the space available for liquid inside the strand. In the calculation of this space, shrinkage during solidification and cooling (chemical composition of steel, cooling conditions, etc.), and deformations of the strand (settings of the supporting rolls, bulging) must be taken into account. The volumetric flow rate can be calculated by the Liquid Motion Intensity (LMI)[1-4] model, taking into consideration also all the above mentioned and important deformation effects.

5 Main Characteristics of the LMI Model

The Liquid Motion Intensity[1-4] (LMI) 2D model is used for the calculation of volume changes inside the strand under steady and non-steady casting conditions within the longitudinal cross section of the slab. The main task of the model is to define volumetric flow rate function (Q) inside the strand, taking into account the effect of chemical composition of the steel, the steel casting technology and the casting machine parameters as well. The main idea of the model is that the amount of liquid entering or exiting from a volume section (slice) of a strand at a given distance from meniscus can be calculated by taking into account the effect of composition, casting technology and casting machine. The amount of melt moving between the slices can be summarized along the whole strand or along the mushy area and from this the amount of melt flow and the rate of the flow can be defined. A detailed description of the model principles and of the simplifications applied can be found in earlier publications[1-4]. The following deformations of the strand can be taken into account in the model:

- Shrinkage of solidification
- Shrinkage of solid shell because of temperature changes
- Shrinkage of solid due to transformations

- Nominal roll gap settings along the casting machine
- Real roll gaps along the casting machine (roll checker data, if available)
- Eccentricities of supporting rolls (if data are available)
- Bulging of the solid shell between supporting rolls (calculated or measured data, if available).

In order to define the volume changes inside the slab, thermal and solidification modeling of slab casting is necessary. Thermal and solidification data are provided for the LMI model by the following software:

- IDS (Interdendritic solidification) – calculation of composition and temperature dependent material data
- TEMPSIMU (Temperature simulation of CC) – 3D temperature and solidification model of cast strand for steady and non-steady state casting conditions
- BOS (Bulging of slab) – determination of bulging between successive rolls

All the above software was developed and tested by the Laboratory of Metallurgy, Helsinki University of Technology (today: Aalto University).

6 Permeability of the Mushy Area

The permeability of isotropic porous medium is typically described by using the Kozeny-Carman equation[12]:

$$K = \frac{1}{k S_V} \frac{g_L^3}{(1-g_L)^2} \tag{2}$$

where k Kozeny constant (supposed to be 5[12]), S_V the solid/liquid surface in unity volume (m^2), g_L ratio of liquid. The equiaxed dendrite structure can be considered to be isotropic porous medium.

A number of experiments have been performed to define the permeability in case of non-isotropic interdendrite fluid flow (e.g. solidification with columnar structure). The authors published their results in the form of empirical equations[13-15]. In these calculations the primary and secondary dendrite arm spacing and the direction of flow compared to primary dendrite arm are also taken into consideration. The permeability parallel to primary arms and perpendicular to primary arms are different.

If liquid ratio is not too high, the results of the different models give similar results. In general, the liquid in the mushy area is typically between a 0 and 0.6

ratio. For the calculation of permeability in the mushy area the equation published by Bhat et. al.[13] was considered:

$$K_P = 3.75 \cdot 10^{-4} \, d_1^2 \, g_L^2 \quad (g_L <= 0{,}65) \tag{3}$$

$$K_N = 1.09 \cdot 10^{-3} \, d_1^2 \, g_L^{3{,}32} \quad (g_L <= 0{,}65) \tag{4}$$

where K_P permeability parallel to primary arms (m^2), K_N permeability perpendicular to the growth direction of primary arms (m^2), d_1 primary dendrite arm spacing (m). In this model the secondary spacing is taken into account through the correlation of primary and secondary spacing.

7 Application for Continuous Casting

The ferrostatic pressure drop in the mushy area and its consequences are presented in a practical example of casting on a curved machine. In order to demonstrate the practical applicability, the calculation was performed by supposing two different roll setting strategies. In the first case there is no change in roll gaps along the casting machine (constant setting). In the second case a roll setting applied in the industrial practice was used (prescribed setting used by the steel producer). Although the first case has no practical relevance, the difference between the two cases highlights the extremely important role of a precise roll setting from the viewpoint of centerline segregation. The roll gap data applied in the calculations are shown in Fig. 3a as a function of distance from the meniscus level.

7.1 Volumetric Liquid Flow Rate Function

Liquid flow conditions in the mushy area are presented in Fig. 3b for both roll setting strategies. In this casting case the pool lengths are: 15.7 m (for the liquidus temperature) and 23.8 m (for the solidus temperature). Hence the mushy area (see Fig. 2) starts at 15.7 m and ends at 23.8 m; its length is 8.1 m. Between meniscus and 15.7 m, the mid part of the strand contains homogeneous liquid and the liquid supply is not hindered (Q is not calculated for this part of the strand). After solidification has been completed (the distance from meniscus is over 23.8 m), there is no more liquid in the slab, hence $Q = 0$. In the mushy area, between 15.7 and 23.8 m for compensation of volume changes, liquid steel flows into the cross sections of the mushy area. By the application of the LMI model (summarizing the liquid necessary for each volumetric slice), the liquid flow rate function in Fig. 3b can be calculated. The function gives the amount of necessary flow rate of liquid for each cross section in the mushy area. At the beginning of the mushy area (at 15.7 m) the value of the function indicates the amount of necessary liquid that should enter the mushy area from the direction of meniscus in order to maintain

the solidification without formation of discontinuity. By definition, the positive value of the function indicates the flow in the casting direction. Fig. 3b shows the volumetric liquid flow rate function for both roll settings (Fig. 3a).

From the viewpoint of centerline segregation it is desirable that flow rate be close to zero. The flow rate function (Fig. 3b) is basically determined by the setting strategy of the supporting rolls. The figure also indicates that if the roll setting is fine tuned, the flow rate can be further reduced.

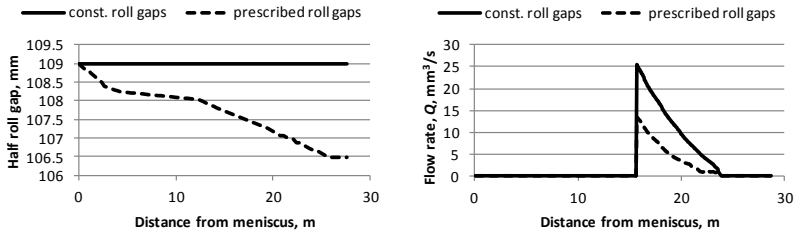

a/ b/

Figure 3
Flow rate necessary for solidification without discontinuities (b/)
for two different settings of the supporting rolls (a/)

The volumetric flow rate function indicates the harmony between the steel composition to be cast, the casting technology and the casting machine. The better the harmony, the closer the function approaches zero. The flow rate function is applicable for the complex evaluation of a casting case from the point of view of probability of centerline segregation formation.

7.2 Pressure Drop and Porosity Function

If the volumetric flow rate function, the permeability and the geometric and microstructure parameters of the dendrite structure are known, the ferrostatic pressure drop in the mushy area can be estimated. For the explanation of results let us consider the diagram in Fig. 4 showing the ferrostatic pressure drop in the mid part of the slab in the mushy area. The two vertical lines indicate the beginning and the end of the mushy area. The dotted line represents the ferrostatic pressure evolving as a result of difference in height between the actual position and the meniscus level (curved machine). The thin line describes the ferrostatic pressure drop caused by the liquid flow in a porous medium; it can be calculated by Eq. (1). The final ferrostatic pressure (sum of the original ferrostatic pressure and of the pressure drop) in the liquid is represented by the thick dashed line. As a result of pressure drop in the mushy area, the final pressure decreases drastically (depending on casting and structural parameters) and can even reach zero value.

The distance from the meniscus level at which zero pressure was reached is the Zero Liquid Supply (ZLS) value. The ZLS point divides the mushy area into two parts. From the ZLS to the direction of meniscus (on the left), sufficient liquid supply is provided by the ferrostatic pressure. When the ferrostatic pressure reaches zero, there is no more pressure that would force the melt to fill the volume changes developed by shrinkage and deformation. In this range, melt supply is not necessarily provided. Cavities formed during solidification can exert a sucking influence on the surrounding melt but its rate and efficiency are rather uncertain in the highly fragmented channel network between solid dendrites. Actual pressure is also affected by gases released inside the cavities. It is assumed in the calculations that after the ZLS point has been reached, there is no further possibility for melt flow, i.e. shrinkage and deformation between ZLS and the end of solidification results in porosity in the center area of slab.

The LMI model gives the opportunity to calculate that amount of volume which is not compensated by liquid filling between ZLS and the end of the mushy area, i.e. this will be the expected porosity level. The diagrams in Fig. 5 a/ show the pressure drop and the ZLS position for both roll settings in the casting case discussed above (see Fig. 3 a/). In this calculation 0.8 mm primary arm spacing and 5 mPas melt viscosity were supposed.

In the case of constant roll gaps, the ferrostatic pressure reaches zero at 21.6 m (ZLS1) whereas in case of a prescribed setting it is 23.1 m (ZLS2). In the first case, the amount of necessary liquid flow is much larger (see Fig. 3a), which results in a greater pressure drop according to the Darcy-law.

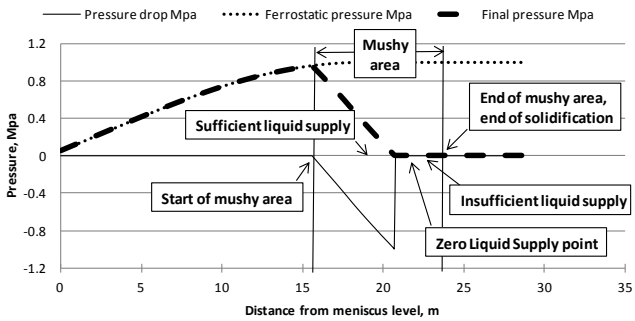

Figure 4
Pressure conditions in the mid part of slab

Between ZLS and the end of solidification zero ferrostatic pressure is assumed, which means that the cavities formed will not be filled by liquid melt. If the perfect and imperfect filling cases of these cavities are also calculated, the amount of cavities is characterized by the necessary liquid difference. These calculation results are displayed in Fig. 5b. Unit of porosity in the LMI model: mm^2.

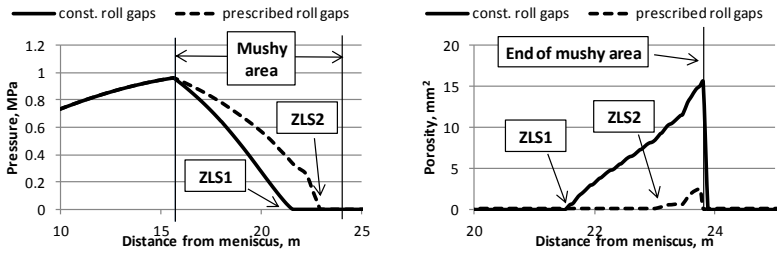

a/ b/

Figure 5
ZLS positions (a/) and expected porosity values (b/) in the same casting case with two different roll settings

In the case of constant roll gaps the distance from ZLS1 to the end of solidification is 23.8-21.6 = 2.2 m. If prescribed roll gaps are used, this value decreases to 23.8-23.1 (ZLS2) = 0.7 m. The possibility of liquid supply is maintained for a much longer distance from meniscus in the case of prescribed roll gaps, and therefore the sum of discontinuities without melt filling will be much lower.

The expected porosity and centerline segregation level can be predicted by using the pressure drop and porosity functions.

7.3 Effect of the Primary Structure on Pressure Drop and on Expected Porosity

The permeability of the mushy area (Eq. (2-4)) is very sensitive to the solid dendrite primary structure that has developed. The finer the primary and secondary dendrite arm spacing, the lower the permeability. The diagrams in Fig. 6 show the effect of the primary structure on pressure drop process and on expected porosity level (same casting case as in Fig. 5, with prescribed roll gaps).

In Fig. 6 the primary arm spacing changes from 0.4 to 1.2 mm. These values are realistic in the middle part of slabs cast under industrial casting conditions. The average value of primary spacing in the slab center is about 0.8-1.2 mm but a finer structure can be developed if tertiary arms are growing as primary arms or the composition changes because of enrichment. Improperly defined cooling rate and temperature gradient (distant from the surface of slab) can also result in structural parameters different from the average. Dendrites in Fig. 1 show a very fine structure despite the fact that they developed absolutely in the slab center, 120 mm away from the surface. Consequently, the primary structure has a great effect on the pressure drop process and on the possibilities of liquid feed. Dendrite arm spacing is also affected by several factors during casting.

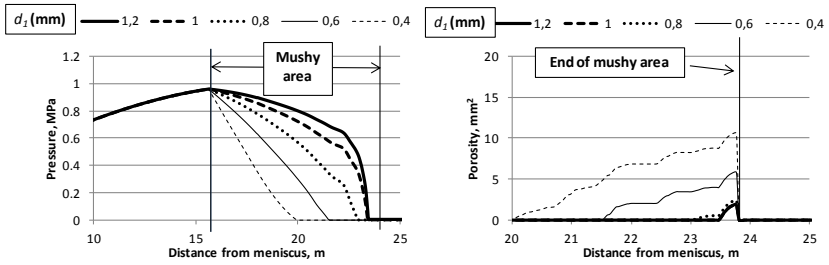

a/ b/

Figure 6

Effect of primary spacing on ferrostatic pressure drop in the mushy area (a/) and on expected centerline porosity (b/)

The local fluctuation of the primary dendrite structure around an average value can result in the variation of expected porosity and, accordingly, in the variation of macrosegregation and centerline segregation as well. We presume that this mechanism too plays a role in the variation of centerline segregation in the bridge formation mechanism and in the fluctuation of centerline segregation along the strand length. A detailed investigation of this problem including the effect of columnar to equiaxed transition is thus one of the directions of this research in the future.

At the end of solidification, the viscosity of the steel melt with a carbon content of 0.08-0.2% is around 5 mPas according to calculations performed by JMatPro and IDS software. Only small variations of viscosity can be expected as a function of steel composition and liquid ratio, i.e. the position of the ZLS point is not significantly affected by the variation in viscosity.

7.4 Estimation of the ZLS Position Based on a Statistical Analysis of Industrial Data

The theory of porosity development outlined above is proven indirectly by an extended statistical analysis of a set of industrial data[16]. The analysis aimed to find a possible correlation between the complete technological database of slab castings and the centerline segregation index of cast products. The determination of centerline segregation index was based on an image analysis of porosity in the slab center. The highest level of correlation coefficient (R) identified was very poor, only 0.469. After the LMI model results were added to the analysis (i.e. shrinkage, deformation and roll gaps were also taken into account), the correlation coefficient increased significantly. In this calculation the position of the ZLS point (i.e. the position of the liquid supply stop) was defined at a given mushy liquid ratio (mushy liquid/complete mushy). Depending on the mushy liquid ratio, the correlation coefficient between measured and calculated porosity changed as

shown in the diagram in Fig. 7. The maximum value of correlation coefficient was identified at a mushy liquid content of 30%. This means that in industrial circumstances the blockage of liquid supply can be taken into account between 30% and 0% of mushy liquid ratio.

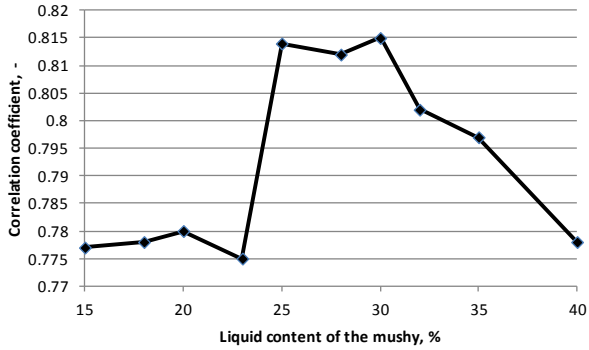

Figure 7
Change of correlation coefficient (R) between measured and calculated porosities as a function of mushy liquid ratio from which the stoppage of liquid supply is supposed

At the beginning of the mushy area an average value of mushy liquid content of 60% can be assumed. Along the mushy area in the casting direction the mushy liquid decreases nearly linearly; the 30% of mushy liquid content can be found in approximately half of the mushy area. In the industrial application of the LMI model (presented in the following chapter) the calculation was performed with this assumption, i.e. the ZLS position was supposed to be at 30% of the mushy liquid content.

8 Industrial Application

8.1 Introduction of the LMI Model

The development, verification and application of the LMI model was performed in cooperation with ISD Dunaferr Co. Ltd. The company has two vertical slab casters (two strands per caster). The main objective of this project was to ensure enhanced slab quality from the technological side, to increase casting capacity and to add new steel grades and slab sizes to production. From the viewpoint of slab quality the most important aspect was: reducing the centerline segregation of slabs.

ISD Dunaferr Co. Ltd. offers a wide range of products from the points of view of both steel grades and slab sizes. This is why, as a rule, the optimal setting of the supporting rolls is different in each case in order to ensure a centerline segregation level as low as possible. Due to the structural design of the casting machines, however, the roll gaps are fixed, and the same setting of supporting rolls is used in all casting cases. This fixed setting of rolls follows the shrinkage of the slab as a function of distance from the meniscus level.

A number of validation tests were performed in order to check the reliability of the model and of the calculated results. Numerous casting cases were modeled (thermal, solidification and LMI) and porosity results were evaluated on the basis of industrial experience. As a result, a proposal was made to modify the setting of the supporting rolls. According to preliminary calculations, the new setting was expected to produce a lower centerline segregation level for the complete diversified product structure (steel grades, slab sizes) of the steel plant.

8.2 Introducing the New Setting of the Supporting Rolls

On the basis of model calculation and validation tests, the management of ISD Dunaferr Co. Ltd. decided to modify the supporting roll setting according to the proposal.

The four strands were modified with utmost care, strand by strand. The process as a whole took about one year. During the conversion there were periods when the two strands of one casting machine were operated with different roll settings; in these periods we were able to evaluate the model amid particularly good conditions. In several casting cases the only difference between the two strands was the different setting of the roll gaps, thus the inner quality difference could directly be associated with the difference in roll gap setting.

The original and the modified roll settings are shown in Fig. 8 (the proposed change in the gap size affected the two last sections of rolls).

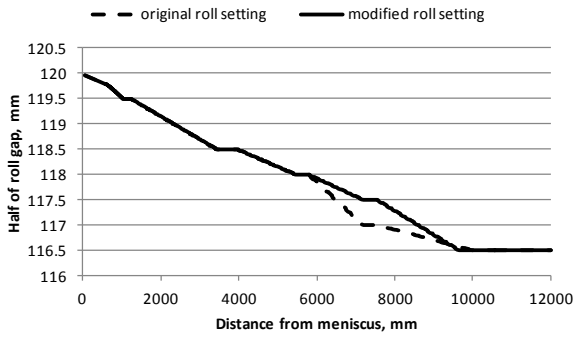

Figure 8
Original and modified settings of the supporting rolls

In the transition period altogether 21 casting cases were investigated in detail. The cases were modeled. In order to control the centerline segregation level, the complete cross sections of the slabs were macroetched. Test results proved that the modified roll setting produce lower centerline segregation levels.

9 Effect of the Modification of the Roll Gap

9.1 Investigation of a Particular Casting Case

The effect of roll gap modification can be clearly identified in those casting cases where the two strands were operated with different roll gap settings (original and modified). In these cases steel composition, superheating, casting rates and cooling intensities are the same and the difference in inner qualities can be explained by the differing roll gaps. From the castings case No. 136 is discussed here. Steel composition and main casting parameters are shown in Table 1.

Table 1
Steel composition and main technological parameters of the cast slab

Chemical composition		Slab geometry (both strands)	
C	0.175 wt%	Thickness	240 mm
Si	0.36 wt%	Width	1360 mm
Mn	1.47 wt%		
S	0.011 wt%	Supporting roll setting	
P	0.012 wt%	Strand No.1	modified
Cr	0.078 wt%	Strand No.2	original
Ni	0.036 wt%		
		Casting rate	
Superheating	35 ^{o}C	Strand No.1	0.53 m/min
		Strand No.2	0.53 m/min

Calculated porosity functions for the original and modified supporting roll settings can be seen in Fig. 9. The porosity developed in the last part of solidification was favorably affected by the modification of the roll gaps. On the basis of calculation results it was expected that the inner quality of the slab would improve.

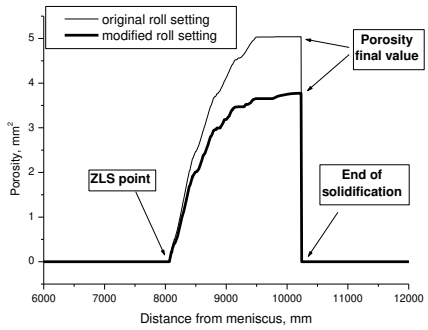

Figure 9
Expected porosity in casting case No. 136

In order to check the inner quality and the calculation results, samples were cut from both strands after casting. The samples (containing the whole cross sectional area) were ground and macroetched by ammonium-persulfate reagent. Pictures of macroetched samples can be seen in Fig. 10.

Before modification

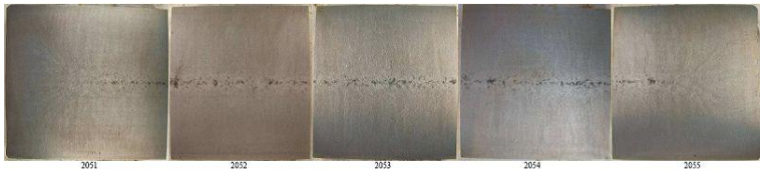

After modification

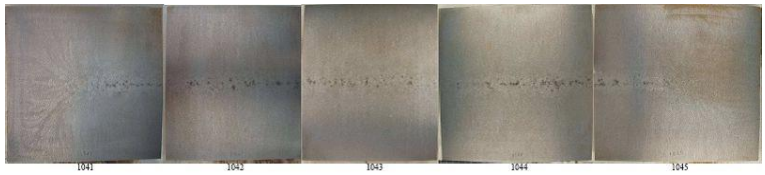

Figure 10
Macroetched cross sections of slabs cast with the original (above) and modified (bottom) roll setting (thickness of slab: 240 mm)

Describing the difference between the slabs in a numerical way is rather difficult. Yet, if the above pictures are compared, it can be clearly seen that the centerline segregation level is lower in the slab cast with the modified setting than in the slab cast with the original roll setting. After the modification, the segregated areas are smaller and the enriched parts are less coherent and more diffuse. At the same time, it can also be observed that the slab cast with the modified roll gaps contains several segregated areas. This means that the gap setting (in this particular case, at

least) can be further refined. The diagram in Fig. 9 shows about 3.6 mm^2 porosity in this case and, according to experience, centerline segregation cannot be identified in the cross section of slabs at a porosity of about 2.5 mm^2.

9.2 Overall Effect on Quality

In order to get reliable feedback of the effects of the modified roll settings on the quality of cast products, ISD Dunaferr Co. Ltd. - Quality Department, conducted a detailed survey into customer evaluations (claims and rejections). Three periods were examined in the survey: one year before the modification of the roll setting (when all the slabs were cast with the original setting), one year during the modification of the gaps (when part of the slabs were cast with the original setting, part of them with the modified setting), and one year after modification (when all the slabs were cast with the modified roll gap setting). All customer claims and all rejects related to centerline segregation were analyzed, the sum of problematic shipments was calculated. The period before roll gap modification (one year) was chosen as reference (at 100%). The results of survey can be seen in Fig. 11.

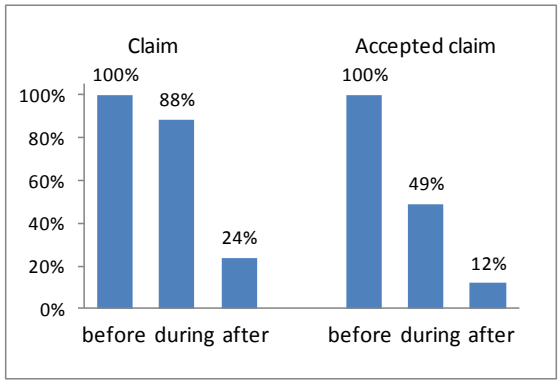

Figure 11
Customer claims and rejects related to centerline segregation before / during / after roll setting modification (each period of time represents one year)

The data above show a drastic decrease in quality problems related to centerline segregation. The number of claims decreased to 24%. Regarding the number of investigated and accepted claims, there was almost a tenfold decrease.

Summary

Any decrease in the centerline segregation of continuously cast slabs requires a full harmony between steel composition, casting technology and casting machine settings, in particular in the last third of solidification. Centerline segregation can be avoided if the liquid, in equilibrium with the solid, does not move away from the vicinity of solid. Hence, in order to reach zero centerline segregation, the

volumetric liquid flow rate function should be zero over the mushy area of slab. In practice, liquid moves in the slab because of volume changes. This flow is mainly generated by ferrostatic pressure developing within the strand.

The pressure drop calculation method and the LMI model can help answer the following important questions:

- How much liquid should move in the center of the slab in the mushy area, at a given steel composition, casting technology and casting machine settings?
- What level of porosity formation is likely to occur if flow and pressure drop occur?

If this model is applied, steel composition, casting technology and casting machine settings can be assessed in a complex way, especially from the point of view of centerline segregation formation.

If the LMI model is applied in practice, the position of the LMI point can be defined, on the basis of pressure drop calculations as well as of the statistical analysis of industrial data, at 30% mushy liquid content. Below 30% of mushy liquid, the dominant process is porosity formation, which can be affected by the sucking effect of cavities and by the pressure of released gases.

Based on the results of calculations aimed at defining the harmony between steel composition, casting technology and casting machine settings, ISD Dunaferr Co. Ltd. has changed the setting of supporting rolls on all its strands. Official data of the company's Quality Department, shows that the number of quality problems related to centerline segregation has decreased drastically due to the work presented in this paper.

Acknowledgement

We are very grateful for the financial contribution of EU Research Fund for Coal and Steel in the frame of Defect Free Casting (Deffree) project (RFSR-CT-2008-00007). The project was also supported by the assistance of the European Union, by the co-financing of the European Social Fund (TÁMOP-4.2.1.B-11/2/KMR-2011-0001). The financial and technical support provided by ISD Dunaferr Co. Ltd. is especially highly appreciated.

References

[1] M. Réger M, B. Verő, Zs. Csepeli, Z. Szabó, R. Józsa and T. Kelemen: Mater Sci Forum, 729(2013) 175

[2] M. Réger, H. Kytönen, B. Verő and A. Szelig: Mater Sci Forum, 649(2010) 461

[3] DEFFREE - Integrated Models for Defect Free Casting, Final Report, RFSR-CT-2008-00007, 2012

[4] M. Réger, H. Kytönen, B. Verő and A. Szelig: Mater Sci Forum, 589(2008) 43

[5] Y. Tsuchida, Y., Nakada, M., Sugawara, I., Miyahara, S., Murakami. and K. Tokushige: Transactions ISIJ, 24(1984) 899

[6] H. Jacobi: Steel Research, 74(2003) 667

[7] H. Presslinger, S. Ilie, P. Reisinger, A Schiefermüller, A. Pissenberger, E. Parteder and C. Bernhard.: ISIJ Int., 46(2006) 1845

[8] G. Lesoult: Mat. Sci. Eng. A, 413-414(2005) 19

[9] G. Krauss: Steels: Heat Treatment and Processing Principles, ASM Int. Metals Park Ohio, USA (1990) 6

[10] M. Réger, B.Verő, I. Kardos and P. Varga: Defect Diffus Forum, 297-301(2010) 148

[11[M. Réger, B. Verő, I. Kardos, E. R. Fábián and Gy. Kaptay: Mater Sci Forum, 659(2010) 441

[12] G. H. Geiger and D. R. Poirier: Transport Phenomena in Metallurgy, Addision-Wesley Publishing Company, Reading, MA (1973) 92

[13] M. S. Bhat, D. R. Poirier, and J. C. Heinrich: Metall. Mater. Trans. B, 26B(1995) 1049

[14] J. R. P. Rodrigues, M. M Mello, and R. G. Santos: Journal of Achievements in Materials and Manufacturing Engineering, 31(2008) 47

[15] Y. Natsume, D. Takahashi, K. Kawashima, E. Tanigawa and K. Ohsasa: ISIJ Int., 53(2013) 838

[16[M. Réger, B. Verő, Zs. Csepeli and Á. Szélig: Mater Sci Forum, 508(2006) 233

Design and Implementation of Differential Evolution Algorithm on FPGA for Double-Precision Floating-Point Representation

Prometeo Cortés-Antonio[1], Josue Rangel-González[1], Luis A. Villa-Vargas[1], Marco Antonio Ramírez-Salinas[1], Herón Molina-Lozano[1], Ildar Batyrshin[2]

[1]National Polytechnic Institute, Center for Computing Research, México City, México; acorteoa09@sagitario.cic.ipn.mx, joshuab09@sagitario.cic.ipn.mx, lvilla@cic.ipn.mx, mars@cic.ipn.mx, hmolina@cic.ipn.mx

[2]Mexican Petroleum Institute, Eje Central Lázaro Cárdenas Norte 152, Col. San Bartolo Atepehuacan, Mexico, D.F., C.P. 07730, Mexico; batyr@imp.mx

Abstract: The paper presents the results of implementation of differential evolution algorithm on FPGA using floating point representation with double precision useful in real numeric problems. Verilog Hardware Description Language (HDL) was used for Altera hardware design. Schematics of the modules of differential evolution algorithm are presented. The performance of the design is evaluated through six different functions problems implemented in hardware.

Keywords: FPGA; Differential Evolution Algorithm; floating point

1 Introduction

Metaheuristic optimization algorithms such as Genetic Algorithms, Estimation of Distribution Algorithms, Differential Evolution Algorithms, Particle Swarm Optimization, Ant Colony Optimization etc. have been widely accepted in engineering, economics and biotechnology optimization problems because they are derivative free optimization methods that can be used for optimization of complex functions [1, 2].

Implementation of the Differential Evolution Algorithm (DEA) on software has been used in applications such as [3-10], where an optimization of parametric model is carried out in conventional computer equipment. However the applications where optimization is necessary in runtime, for example in online learning [11-13] and remote access [14, 15], require that DEA to be implemented

in embedded systems such as FPGA device using evolvable hardware approach [16-18].

Several proposals for hardware implementation of evolutionary algorithms have been realized, such as Micro Algorithm [19-23] and Compact Genetic Algorithm (cGA) [24-28] with the aim of low resource consumption and minimal response time implementation. These algorithms lose the generality of solving problems of any kind, however such deployments have had success in combinatorial problems. However as it is shown in [29], cGA not always show good performance in solving nonlinear problems, and also complex linear problems. Furthermore if one considers the implementation of cGA presented in [30], where the probability vector is implemented using 8-bit integers, it is also clear that this implementation is limited by solution of only trivial problems.

It was shown in the seminal paper on Differential Evolution Algorithm [31] that this algorithm is very simple using only three evolutionary parameters and basic operations such as addition, subtraction, comparison, and its performance is comparable or even surpasses other evolutionary or heuristic algorithms. However, due to DEA used real value representation of variables and its operations are performed in floating point its hardware (FPGA) implementation in the time when this algorithm was published was not possible because FPGA in that time did not have the necessary resources for such implementations. Nowadays FPGA families have amazing abilities that make the implementation of such algorithms not only feasible, but also an excellent choice for designing evolutionary algorithms.

There are several design proposals for implementing evolutionary algorithms ranging from a dedicated system on only one chip until a cluster of FPGAs [32, 33] to perform concurrent computation, that can be useful for different applications.

The paper presents the design on EP4CE115F29C7 Altera FPGA device [34] for a Differential Evolution Algorithm with a number of function variables from 4 until 32 and population size from 16 to 128 using double-precision floating point representation. This work is divided into six sections. The next section gives theoretical bases of Differential Evolution Algorithms. A brief introduction to the Altera FPGA logic design is presented in Section 3. Section 4 presents the proposed design of the DEA showing schematics of each block that makes up the system. The results of resource consumption and latency time of the implementation are given in Section 5. Section 6 presents the conclusions and directions of future work.

2 Differential Evolution Algorithm

Differential Evolution Algorithm (DEA) belongs to the family of evolutionary algorithms, which has as aim to find the global optimum of a function over continuous space. In particular, and without loss of generality, this problem can be reduced to finding the minimum of a function:

$$minimize\ f(x) = f(x_1, x_1, \dots, x_n) \tag{1}$$

Where x is a n-dimensional vector and f is a real function of real valued arguments. DEA, proposed in [31], is an evolutionary algorithm that requires only three parameters CR (defining crossover and mutation operations that are mutually exclusive), F (scaling factor of the difference of two individuals) and NP (population size) to generate the evolutionary process for *n*-dimensional problem.

Differential Evolution Algorithm can be represented by a four-step process as shown in Fig. 1. Only the first step is performed once, the other steps are performed while an iterative process does not terminated by stop criteria.

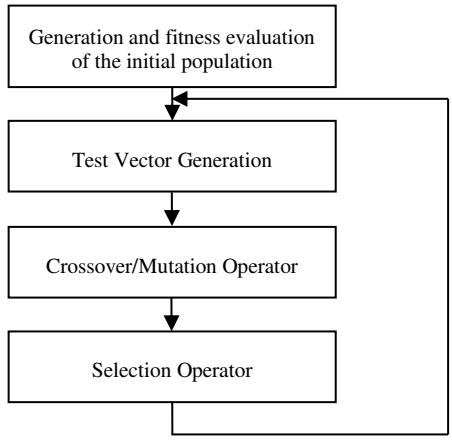

Figure 1
Bock diagram of Differential Evolution Algorithm

Complete pseudo-code is presented in Fig. 2, where the first 12 lines perform the block of generation and fitness evaluation of the initial population shown in Fig. 1, for dimensionality *D* and population size *NP*.

The algorithm contains three nested loops, where the outer loop is used to specify the stop condition, in this particular case it is determined by the parameter G_{max}(number of generations) but one can set other stop conditions such as minimum error or difference between sequential errors, etc.

The inner cycle indicates that for each individual in a generation with the probability defined by the parameter CR it is generated a new individual from three individuals chosen randomly, with indexes r_1, r_2 and r_3, using scale factor F, as described in line 21 of the algorithm. This cycle can be considered as a combination of crossover and mutation operations [31].

1 Begin
2 $G = 0$
3 $Create\ a\ random\ initial\ population$
4 $\boldsymbol{for}\ i = 1\ \boldsymbol{to}\ NP\ \boldsymbol{do}$
5 $\boldsymbol{for} j = 1\ \boldsymbol{to}\ \boldsymbol{D}$do
6 $x_{j,i}^{(G=0)} = x_j^{min} + rand_j[0,1].\left(x_j^{max} - x_j^{min}\right)$
7 $\boldsymbol{end\ for}$
8 $\boldsymbol{end\ for}$
9 $Evaluate\ Fitness\ Function\ for\ each\ individual\ of\ population$
10 $\boldsymbol{for} i = 1\ \boldsymbol{to}\ NP\ \boldsymbol{do}$
11 $f\left(x_i^{(G=0)}\right)$
12 $\boldsymbol{end\ for}$
13 $Test\ vector\ generation$
14 $\boldsymbol{for}\ G = 1\ \boldsymbol{to}\ MaxGen\ \boldsymbol{do}$
15 $\boldsymbol{for} i = 1\ \boldsymbol{to}\ NP\ \boldsymbol{do}$
16 $Select\ Randomly\ r1\ , r2, r3 \in [1, NP], r1 \neq r2 \neq r3 \neq i$
17 $Mutation\ and\ Crossover\ Process$
18 $jrand = randInt[1: D]$
19 $\boldsymbol{for} j = 1\ \boldsymbol{to} D\ \boldsymbol{do}$
20 $\boldsymbol{if}(rand[0,1] < CR\ \boldsymbol{or} j == jrand)\boldsymbol{then}$
21 $v_{i,j}^{(G+1)} = x_{i,r1}^{(G)} + F * \left(x_{i,r2}^{(G)} - x_{i,r3}^{(G)}\right)$
22 $\boldsymbol{else}$
23 $v_{i,j}^{(G+1)} = x_{i,j}^{(G)}$
24 $\boldsymbol{endif}$
25 $\boldsymbol{endfor}$
26 $\boldsymbol{endfor}$
27 $Seleccion$
28 $\boldsymbol{if}\left(f\left(v^{(G+1)}\right) \leq f\left(x_i^{(G)}\right)\right)\boldsymbol{then}$
29 $x_i^{(G+1)} = v_{i,j}^{(G+1)}$
30 $\boldsymbol{else}$
31 $x_i^{(G+1)} = x_i^{(G)}$
32 $\boldsymbol{endif}$
33 $\boldsymbol{endfor}$
34 $\boldsymbol{endFor}$
35 End

Figure 2
Pseudocode of Differential Evolution Algorithm

3 FPGA Device

The FPGA (Field-Programable Gate Array) is a device that is used to design a dedicated digital system or embedded platforms that perform specific tasks in a system. Its main characteristic is that it can be programmed several times, even after the system has been installed or finished to update its functionality. For this reason this device is very useful in evolved applications with dynamic environments.

Currently, FPGA has been used widely in several real applications of evolvable hardware, an emerging research area where intelligent computation techniques are implemented in digital system design that can be adaptive to environment changes, manage big data and process the information using intelligent techniques.

Altera FPGA [35] is a device consisted of programmable logic blocks (Logic Elements), and memory elements (Dedicated Logic Registers), which are interconnected to perform complex combinational and sequential functions. In addition it can contain specific resources such as embedded multipliers, SRAM, transceiver, or even hard intellectual propriety (IP) block and embedded processors for implementing SoC design. FPGA based system is implemented through modules describing basic digital logic circuits such as multiplexers, comparators, adders, registers, memory, and finite state machines use hardware description languages to perform specific and complex system tasks.

Altera provides a free library of parameterized intellectual property (IP) blocks called Megafunctions [36, 37]. The floating point Megafuctions implement hardware modules for performing customized floating point operations. Table 1 shows the resources used to perform the floating point arithmetic operations in Differential Evolution Algorithm implementation on EP4CE115F29C7 device for double precision floating point representation.

Table 1
Characteristics of tree floating point Altera Megafunction

MegafunctionName	Output Latency	Logic Elements	Logic Registers	Embedded multiplier	F_{MAX} (MHz)
FPMULT	5	552	530	18	102
FPCOMP	1	176	2	-	-
FPAddSub	7	1534	584	-	105

Differential evolution algorithm performs floating point operations only for generating the offspring individuals in mutation and crossover process; hence it needs only one module for floating point. Moreover, it is important to see that FPCOMP is a combinatorial module; because of the floating point comparator is the same that integer comparator. The complete hardware implementation of DEA is described in the next section.

4 Hardware Implementation of Differential Evolution Algorithm

The schematic hardware implementation of DEA consists of the following modules: i) PMem module to store individuals, ii) FXMem to store fitness function values, iii) fitness function module, iv) CrossOvermodule, v) four Random Number Generators and vi) Finite State Machine module to control the execution sequence of DEA. Fig. 3 presents all modules except of Finite State Machine module that controls all modules of the system. Fig. 3 depicts also the following registers: *i,j,*for addressing PMem and FXMem, three registers for storing indexes, three 64-bits registers for storing the values of X_{r1}, X_{r2} and X_{r3}attributes and a file register with D64-bits register for storing each attribute of offspring individual. Also some multiplexors and comparators are used that are not presented due to simplicity of the scheme. In the following the more detailed description of the modules will be given.

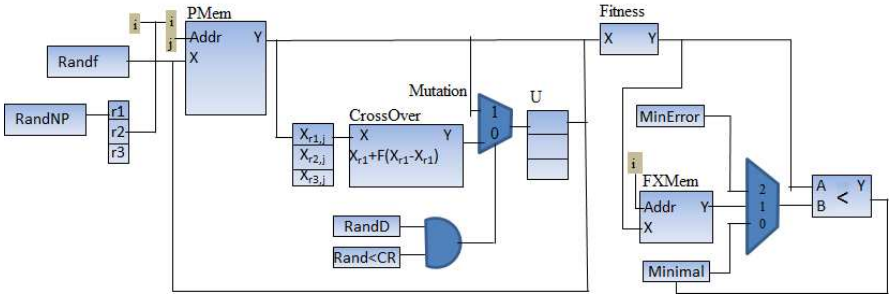

Figure 3
Complete hardware implementation of Differential Evolution Algorithm

4.1 Memories Modules

4.1.1 PMem Module

This module is implemented by using a RAM circuit for storing the population of current generation. Memory size is determined by population size parameter *NP,* and dimensionality *D*, the RAM size can be expressed as follows:

$$PMem[TAM] = NP * D \; words \tag{2}$$

If each word is specified by 8 bytes (64 bits), then the PMem size expressed in bytes is specified as follows:

$$PMem[TAM] = NP * D * 8 \;\; bytes \tag{3}$$

4.1.2 FXMem Module

This module is implemented similarly to PMem with the difference that FXMem size is determined only by *NP* parameter, due to only one value is stored by individual. The expressions for FXMem[TAM] are:

$$FXMem[TAM] = NP\ words \quad (4)$$

$$FXMem[TAM] = NP * 8\ \ bytes \quad (5)$$

Fig. 4a shows the block diagram of RAM specifying all control pin.

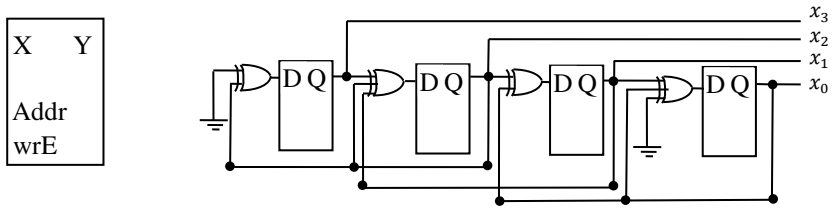

a) Memory b) Random Number generator

Figure 4
Schemes of general memory modules and Random Number Generator of 4 cells

4.2 Random Number Generator (RNG)

Cellular Automata(CA) circuits have been used to create random numbers. The corresponding module works with two rules[38] where the first one is defined by: $a_i(t+1) = a_{i-1}(t) \oplus a_{i+1}(t)$ and the second one is defined by: $a_i(t+1) = a_{i-1}(t) \oplus a_i(t) \oplus a_{i+1}(t)$, where $a_i(t+1)$represents the next state of the *i*-cell, $a_{i-1}(t)$ represents the current state of the (*i*-1)-cell (left neighbor), $a_i(t)$ represents the current state of the *i*-cell, and $a_{i+1}(t)$ is the current state of the (*i*+1)-cell (right neighbor). An *n*-CA can generate 2^m-1 different pseudo random numbers where *m* is a number of the cells. The scheme for *m* = 4 is presented in Fig. 4b.

Implementation of DEA contains 3 different modules for generating integer values in intervals [0-NP], [0-D], [0-127] and one module for generating floating point values.

For design of a comparator with parameter CR taking values in interval [0,1] instead of floating point representation of parameter values it is used a digital representation in interval [0-127] by means of 7 cells of CA.

For floating point number generator used for generation of values of individuals.

4.3 Crossover Module

To implement the pseudo code shown in Fig. 2, line 21:

$$v_{i,j}^{(G+1)} = x_{i,r1}^{(G)} + F * \left(x_{i,r2}^{(G)} - x_{i,r3}^{(G)}\right)$$

where $x_{i,r1}^{(G)}$, $x_{i,r2}^{(G)}$, $x_{i,r3}^{(G)}$and F are floating point values,the following three binary floating point operations have been used:

$$R1 = \left(x_{i,r2}^{(G)} - x_{i,r3}^{(G)}\right)$$

$$R2 = F * R1$$

$$v_{i,j}^{(G+1)} = x_{i,r1}^{(G)} + R2$$

This sequence of operations is implemented using FPMult and FPAddSub Megafuntions shown in Table 1. Therefore for a complete crossover operation be performed, it should run 22 clock cycles. Fig. 5 shows scheme of Crossover module.

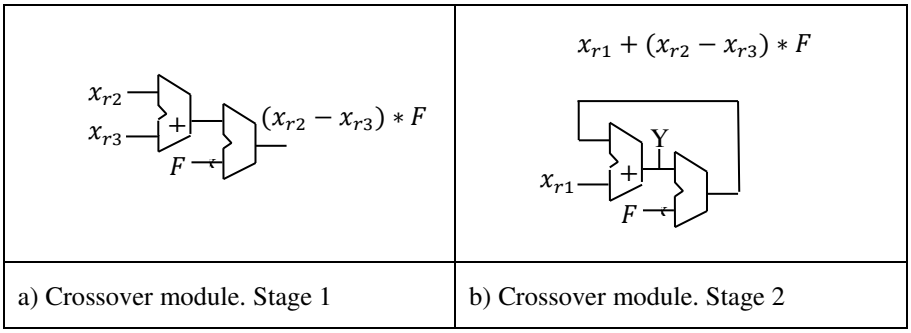

a) Crossover module. Stage 1 | b) Crossover module. Stage 2

Figure 5
CrossOver module implementations

4.4 Fitness Module

Fitness evaluation modules are dependent from specific applications therefore this modules are the only components that change from one application to another. In this paper we implement a set of six different benchmark mathematical functions traditionally used for evaluation of performance of metaheuristic algorithms (Table 2). The block diagram implementations of these functions are shown in Fig. 6.

Table 2
Benchmark mathematical functions

	Function	Ecuation
1	Sphere Mode	$f_1(x) = \sum_{i=1}^{D} x_i^2$
2	Schwefel's Problem 2.22	$f_2(x) = \sum_{i=1}^{D} \lvert x_i \rvert + \prod_{i=1}^{D} \lvert x_i \rvert$
3	Schwefel's Problem 1.2	$f_3(x) = \sum_{i=1}^{D} \left(\sum_{j=1}^{i} x_j \right)^2$
4	Schwefel's Problem 2.21	$f_4(x) = \max\{\lvert x_i \rvert, 1 \le i \le D\}$
5	Generalized Rosenbrock's Function	$f_5(x) = \sum_{i=1}^{D} \lvert 100(x_{i+1} - x_i^2)^2 + (x_i - 1)^2 \rvert$
6	Step Function	$f_6(x) = \sum_{i=1}^{D} \lvert (x_i + 0.5) \rvert^2$

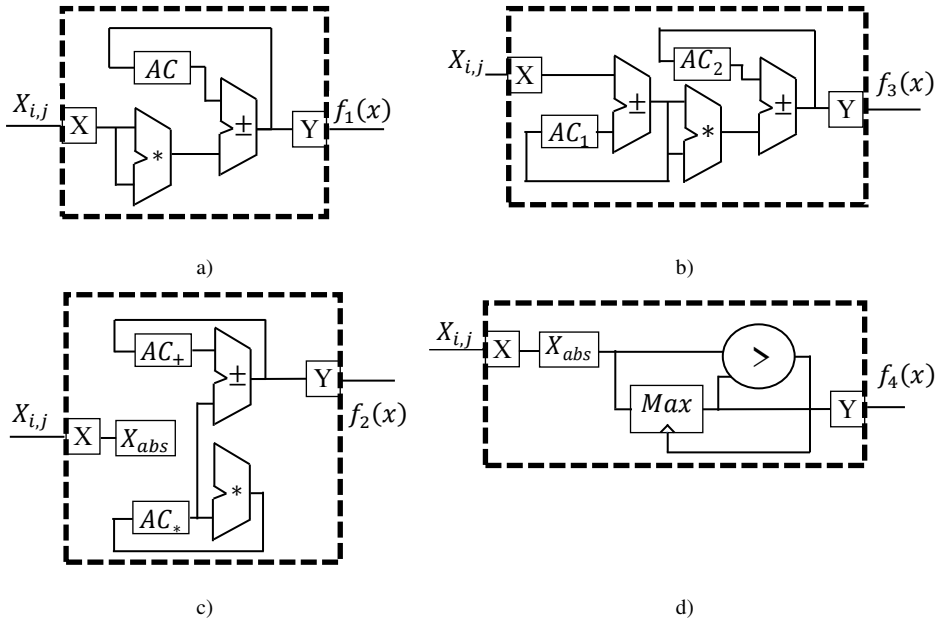

Figure 6.1
Fitness Functions Implementations

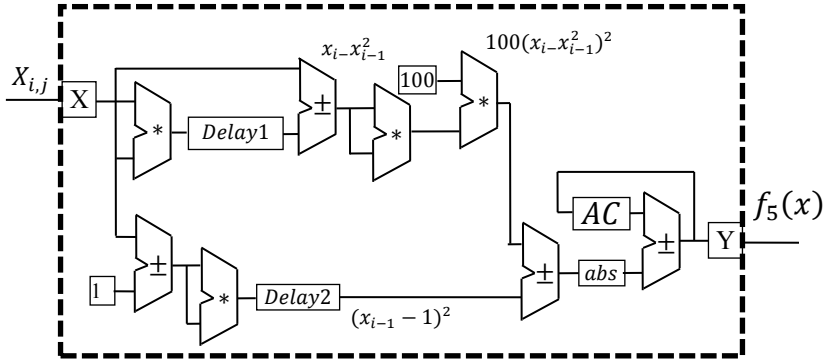

e)

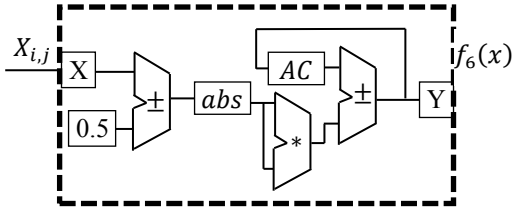

f)

Figure 6.2
Fitness Functions Implementations

4.5 Control Module

Each one of the considered modules contains a control inputs for deciding when to write or to read values on the register and which elements should be selected for a specific input. Control signals are managed by a control unit that performs the correct functionality of algorithm.

5 Results

Results presented in Table 3 show the resources consumed in the implementation of DEA with spherical objective function (f1) with *NP*=128 and *W*= 32 parameter values on EP4CE115F29C7 device of Cyclone IV E Altera Family. The Results column presents both the resources used in the implementation vs. the total available resources used by the device for different categories of resources. The column f1 of Table 4 shows what part of resources of Table 3 consumed by function f1. Total resources consumed in implementation of other benchmark functions used for evaluation of DEA performance also can be found in Table 4.

For evaluating the time performance of DEA implementation two tests over benchmark mathematical functions f_1-f_6 have been applied for two different *NP* and *W* parameter values. Table 5a shows results for parameter values *NP*= 128 and *W*= 32; Table 5b shows the results for *NP*= 16 and *W*= 4. The parameter values for CR and F used in simulations are taken from analysis presented in [39] where it was argued that these values are the best values for obtaining optimum with small number of generations. The parameter values presented for average number of generations (AveGen), average time (AveTime) and Error were obtained after the 20 running of the algorithm using an error $1e^{-12}$ or 20,000 generations as stop conditions.

Table 3
Resources consumed in DEA implementation

Category	Results
Total Combinational Functions (TCF)	10,330/114,480 (9%)
Dedicated Logic Registers (DLR)	5,366 /114,480 (5%)
Total Memory bits (TMb)	8480/3,981,312 (<1%)
Embedded Multiplier 9-bit elements (EM9)	72/512 (14%)
Fmax (MHz)	95 MHz

Table 4
Resources usedin implementation of objective functions

Category	f_1	f_2	f_3	f_4	f_5	f_6
TCF	2405	2915	4397	213	8501	4281
DLR	1182	1494	1929	74	4551	1880
TMb	71	54	140	0	293	113
EM9	18	18	18	0	72	18
F_{max}(MHz)	95	95	70	122	71	80
Latency	8clk*W	11clk* W+10clk	12clk* W	3clk* W	17clk* W	12clk* W

Table 5
Consuming time for different objective functions
a) *NP*=128,*W*=32

f(x)	CR	F	AveGen	AveTime(s)	Error
$f_1(x)$	0.9	0.7	11571	26.67	$1.00E^{-12}$
$f_2(x)$	0.2	0.7	2802	7.7484	$1.00E^{-12}$
$f_3(x)$	0.9	0.7	20000	442.0546	0.0911
$f_4(x)$	0.8	0.7	20000	91.8609	0.089
$f_5(x)$	0.9	0.7	20000	119.9898	$1.45E^{-06}$
$f_6(x)$	0	0.7	1521	7.4476	$2.57E^{-13}$

b) NP=16, W=4

f(x)	CR	F	AveGen	AveTime	Error
$f_1(x)$	0.9	0.7	121	6 ms	1.00E-12
$f_2(x)$	0.2	0.7	250	16 ms	1.00E-12
$f_3(x)$	0.9	0.7	144	75 ms	1.00E-12
$f_4(x)$	0.8	0.7	501	53 ms	1.00E-12
$f_5(x)$	0.9	0.7	1683	.24 s	1.00E-12
$f_6(x)$	0	0.7	101	12 ms	1.00E-12

Conclusions

The paper presented the design of Differential Evolution Algorithm on Altera FPGA following a sequential flow and using three parameter values defining crossover and mutation operations, scaling factor and population size.

The design does not exploit parallelism approach because we think that this technique depends of specific application. However we can mention that parallelism is more adequate in fitness functions module because it is a temporal bottleneck of many applications and its implementation is straightforward.

The paper describes an implementation of the basic version of EDA considered in [31].There exist several modifications of Differential Evolution Algorithm, with the following principal variations: a) the change of the number of individuals that participate in the crossover process, which are incrementing in even numbers for better exploring of the space; b) the use of the best individual of the population as a principal ancestor for better exploiting his local neighborhood into search space; c) the way in which the crossover-mutation operator is implemented. For more details about modified DEA see [39, 40]. The FPGA implementation of these variations of DEA are straightforward.

The paper contains the original results of research that were not submitted to other journals or conferences.

References

[1] H. Nejat Pishkenari, S. H. Mahboobib, A. Alasty, "Optimum Synthesis of Fuzzy Logic Controller for Trajectory Tracking by Differential Evolution", Scientia Iranica, Iran, pp. 261-267, April, 2011

[2] Shing-Tai Pan, "Evolutionary Computation on Programmable Robust IIR Filter Pole-Placement Design", Instrumentation and Measurement, Vol. 60 , pp. 1469-1479, April 2011

[3] A. Chandra, S. Chattopadhyay, "Novel Approach of Designing Multiplier-less Finite Impulse Response Filter using Differential Evolution Algorithm", Intelligent Systems and Applications, Vol. 4, pp. 54-62, June 2012

[4] A. Chandra, S. Chattopadhyay, "Role of Mutation Strategies of Differential Evolution Algorithm in Designing Hardware Efficient Multiplier-less Low-pass FIR Filter", Journal of Multimedia, Vol. 7, No. 5, pp. 353-363, October 2012

[5] A. Hiendro, "Multiple Switching Patterns for SHEPWM Inverters Using Differential Evolution Algorithms", International Journal of Power Electronics and Drive System, Vol. 1, pp. 94-103, December 2011

[6] C. Cheng-Hung, L. Cheng-Jian, Member, L. Chin-Teng, "Nonlinear System Control Using Adaptive Neural Fuzzy Networks Based on a Modified Differential Evolution", Systems, Man, and Cybernetics, IEEE, Vol. 39, pp. 459-473 , July, 2009

[7] C. J. François, et al, "FPGA Implementation of Genetic Algorithm for UAV Real-Time Path Planning", Intelligent and Robotic Systems, Vol. 54, pp. 495-510, March 2009

[8] D. Zaharie, D. Petcu, "Parallel Implementation of Multi-Population Differential Evolution", Concurrent Information Processing and Computing, IOS, Press, pp. 223-232, 2005

[9] V. Tirronen, et al., "An Enhanced Memetic Differential Evolution in Filter Design for Defect Detection in Paper Production", Evolutionary Computation, Vol. 16, No. 4, pp. 529-555, 2008

[10] W. Kwedlo, K. Bandurski, "A Parallel Differential Evolution Algorithm for Neural Network Training", Parallel Computing in Electrical Engineering, pp. 319-324, Sept. 2006

[11] H. Shayani, P. J. Bentley, A. M. Tyrrell, "Hardware Implementation of a Bio-plausible Neuron Model for Evolution and Growth of Spiking Neural Networks on FPGA", Adaptive Hardware and Systems, NASA/ESA, pp. 236-243, 2008

[12] J. M. Sánchez-Pérez, et, "Genetic Algorithms Using Parallelism and FPGAs: The TSP as Case Study", Parallel Processing, Portland, Oregon, USA, pp. 573-579, June, 2005

[13] R. Lovassy, L. T. Kóczy, L. G, "Function Approximation Performance of Fuzzy Neural Networks", Acta Polytechnica Hungarica, Vol. 7, No. 4, pp. 25-38, 2010

[14] E. Magdaleno, M. Rodríguez, F. Pérez, D. Hernández and E. García, "A FPGA Embedded Web Server for Remote Monitoring and Control of Smart Sensors Networks", sensors, Vol. 14, pp. 416-430, 2014

[15] R. Patel, A. Rajawat, R. N. Yadav, "Remote Access of Peripherals using Web Server on FPGA Platform", International Conference on Recent Trends in Information, Telecommunication and Computing, India, pp. 274-276, 2010

[16] E. Sanchez, M. Tomassini, "Towards Evolvable Hardware", Lecture Notes in Computer Science, Springer, Vol. 1062, 1995

[17] K. Hwang, S. Cho, "Improving Evolvable Hardware by Applying the Speciation Technique", Applied Soft Computing, Vol. 9, pp. 254-263, 2009

[18] Y. Thoma and E. Sanchez, "A Reconfigurable Chip for Evolvable Hardware", GECCO, Springer-Verlag Berlin Heidelberg, Vol. 3102, pp. 816-827, 2004

[19] K. Krishnakumar, "Micro-Genetic Algorithms for Stationary and non-Stationary Function Optimization", Intelligent Control and Adaptive Systems, Vol. 1196, pp. 289-296, 1989

[20] F. Viveros-Jiménez, E. Mezura-Montes, A. Gelbukh, "Elitistic Evolution: a Novel Micro-Population Approach for global optimization problems", Eighth Mexican International Conference on Artificial Intelligence, IEEE, México, pp. 15-20, 2009

[21] C. A. Coello-Coello, G. Tosano-Pulido, "A Miro-Geneti Algorithm for Multiobjetive Optimization", Evolutionary Multi-Criterion Optimization, Switzerland, pp. 126-140, 2001

[22] Wu, D., Gan, D. and Jiang, J. N, "An Improved Micro-Particle Swarm Optimization Algorithm and Its Application in Transient Stability Constrained Optimal Power Flow", International Transactions on Electrical Energy Systems, Vol. 24, pp. 395-411, 2012

[23] Huang T, Mohan AS, "Micro-Particle Swarm Optimizer for Solving High Dimensional Optimization Problems", Applied Mathematics and Computation, Vol. 181, pp. 1148-1154, 2006

[24] C. Ying-ping, C. Chao-Hong, "Enabling the Extended Compact Genetic Algorithm for Real-Parameter Optimization by Using Adaptive Discretization", Evolutionary Computation, Vol. 18, No. 2, pp. 199-228, 2010

[25] E. Mininno at al, "Compact Differential Evolution", IEEE Transactions on Evolutionary Computation, Vol. 15, pp. 32-54, February 2011

[26] J. I. Hidalgo, et al., "A Parallel Compact Genetic Algorithm for Multi-FPGA Partitioning", Parallel and Distributed Processing, Mantova, Italy, pp. 113-120, February, 2001

[27] K. H. Tsoi, K. H. Leung, P. H. W. Leong, "Compact FPGA-based True and Pseudo Random Number Generators", 11th Field-Programmable Custom Computing Machines, Napa, California, USA, pp. 51-61 , April, 2003

[28] Y. Jewajinda, P. Chongstitvatana, "FPGA Implementation of a Cellular Compact Genetic Algorithm", Adaptive Hardware and Systems, NASA/ESA, pp. 385-390, 2008

[29] R. Rastegar, A. Hariri, "A Step Forward in Studying the Compact Genetic Algorithm", Evolutionary Computation, Vol. 14, No. 3, pp. 277-289, August, 2006

[30] C. Aporntewan, P. Chongstitvatana, "A Hardware Implementation of the Compact Genetic Algorithm", Evolutionary Computation, Seoul, Korea, Vol. 1, pp. 624-629, May, 2001

[31] R. Storn and K. Price, "Differential Evolution - A Simple and Efficient Adaptive Scheme for Global Optimization over Continuous Spaces", Journal of Global Optimization, Vol. 11, pp. 341-359, March, 1995

[32] A. León-Javier, M. A. Moreno-Armendáriz, N. Cruz-Cortés, "Designing a Compact Genetic Algorithm with Minimal FPGA Resources", Advances in Computational Intelligence, Springer, Vol. 116, pp. 349-357, 2009

[33] A. Swarnalatha, A. P. Shanthi, "Optimization of Single Variable Functions Using Complete Hardware Evolution", Applied Soft Computing, Vol. 12, pp. 1322-1329, 2012

[34] Altera Inc, ftp://ftp.altera.com/up/pub/Altera_Material/12.1/Boards/DE2-115/DE2_115_User_Manual.pdf

[35] Altera Inc, "http://www.altera.com/literature/hb/cyclone-iv/cyclone4-handbook.pdf"

[36] Altera Inc, "http://www.altera.com/literature/ug/ug_intro_to_megafunctions.pdf"

[37] Altera Inc, "http://www.altera.com/literature/ug/ug_altfp_mfug.pdf".

[38] P. D. Hortensius, R. D. McLeod and H. C. Card, "Parallel Random Number Generation for VLSI Systems Using Cellular Automata," IEEE Transactions on Computers, Vol. 38, No. 10, pp. 1466-1473, 1989

[39] E. Mezura, J. Velázquez y C. A. Coello, "A Comparative Study of Differential Evolution Variants for Global Optimization", 8th annual conference on GECCO, USA, pp. 485-492, 2006

[40] A. K. Qin, V. L. Huang, and P. N. Suganthan, "Differential Evolution Algorithm with Strategy Adaptation for Global Numerical Optimization", IEEE Transactions on Evolutionary Computation, Vol. 12, No. 2, pp. 398-417, April, 2009

Estimating Hungarian Household Energy Consumption Using Artificial Neural Networks

András Szűts

Doctoral School of Applied Informatics and Applied Mathematics
Óbuda University
Bécsi út 96/b, H-1034 Budapest, Hungary
szuts.andras@phd.uni-obuda.hu

István Krómer

Kandó Kálmán Faculty of Electrical Engineering, Óbuda University
Bécsi út 96/b, H-1034 Budapest, Hungary
kromer.istvan@kvk.uni-obuda.hu

Abstract: In the European Union and Hungary more than one-third of the total energy consumption comes from households. Therefore, during both the planning of energy efficient investments and the design of energy production and consumption, one of the most important factors is estimating the rate of consumption. The determination of the exact consumption of households has not been achieved because the rates of consumption are calculated solely on the basis of technical parameters, and the results of these calculations are not sufficiently accurate or reliable, especially considering the uncertainties arising from consumer habits. To resolve the issue, we have created a database structure and a calculation model that helps to estimate a household's annual energy consumption based on factors that we have defined. Obviously, this does not mean that calculation based on technical parameters is now unnecessary, but applying the two methods together can significantly increase the accuracy of the estimation of household energy consumption at the individual, regional or national level.

Keywords: households; energy consumption; neural networks

1 Introduction

A current issue in the estimation and calculation of household energy consumption, is the lack of correct data and unified databases. Information about consumers, as well as, the information and databases related to technical solutions are virtually absent, or unavailable in a standardized form and, therefore, useless

for comparative analysis. In the United States, under the management of the National Renewable Energy Laboratory (NREL), a unified database in both software and manual on-demand format was created that contains data of various building materials; it provides the necessary information for the proper functioning of the energy simulation programs. The purpose for creating such a database is for use as a unified national repository, during the energy efficient renovation of residential buildings. It provides an appropriate basis for the cost-benefit analysis of investments.

During the planning of such investments, knowledge of environmental factors and the technical parameters of building materials are not sufficient to determine the energy consumption of households. In our opinion, a knowledge of the consumer and their consumption behavior is at least as important, if not more important, than the technical parameters. Thus, in order to calculate the expected energy consumption, it is important to create a database based on real consumer data and an inference system built upon it. In this article we attempt to provide a solution to eliminate the above mentioned information deficit related to consumers and to utilize this information captured. It is important to clarify that in our research the energy consumption of a household is understood as the total energy consumed. Therefore, we do not make such exceptions in the calculation that exist in regulation 7/2006 TNM, commonly used in Hungary, according to which, in the case of residential buildings, the energy demands of lighting does not need to be included in the calculation of the energy performance of the building, even though it may also be a significant part of a household's energy demand.

It must be noted that to manage the problem outlined above, with a single model, applicable world-wide, is only possible in a theoretical sense, because the factors that significantly impact energy consumption will vary across different geographic and social regions. Therefore, this article looks for a solution considering only Hungarian conditions. As the method is elaborated, it will be clear that the algorithm can be used in other countries or regions by simply gathering the appropriate data concerning the characteristic features for that area and society.

2 The Structure of Household Energy Consumption

According to our research, in order to ensure the effectiveness of investments in energy efficiency it is essential to know the structure of household energy consumption, since this is the way to identify the areas of energy saving potential and to achieve the desired decrease in consumption. Most of the households in Hungary generally use primary (e.g. gas, wood) and secondary (e.g. electricity) energy sources. In extreme cases, the use of only one kind of energy source is possible; however, it is relatively rare in Hungary due to the widespread

distribution of the natural gas service. The energy of the primary and secondary energy sources can be divided into three categories according to their use [2]:

- Energy consumption for heating, cooling and ventilation systems which help to ensure adequate air comfort in living spaces;
- Energy required for the production of domestic hot water;
- Energy required to operate household electrical appliances (e.g. fridge, stove) and lighting.

The above listed factors are obviously not completely independent from each other, since the lighting or any household electrical appliance can certainly produce some degree of heat energy, which may thus influence the energy needs of heating and cooling systems [2]. Thus, the areas with potential for energy savings can be grouped according to the previous list, which can be even further detailed by breaking it down to the energy sources used.

According to G. Swan et al. [2], the energy demand for heating and cooling basically depends on climatic conditions and the technical characteristics of the building, while the second two groups of the list are linked to consumer behavior, the household appliances, the demographic conditions and the number of the household residents. Based on these considerations, he finds the methods for determining the energy needs for indoor comfort based on engineering calculations sufficient; but he recommends statistical methods to determine the energy needs for hot water, household appliances and lighting. However, in contrast with the positions of the studies of G. Swan et al. [2], we believe we can benefit from statistics when considering all three factors. Our reasons are detailed herein.

Looking at households and energy consumption, the uncertainties of consumer behavior are present at virtually all levels, since it does not matter how effective the heating system of a house is if the residents have unrealistic expectations about achievable air comfort in the interior space or they improperly use the systems that are designed for major energy savings. Thinking through the above-mentioned example and similar cases, it is easy to see the importance of the uncertainties that derive from consumer behavior regarding the heating and cooling energy demand and that, according to our knowledge, can be solved by using statistical methods.

In regard to domestic hot water, we agree with the author of the study [2]. As regards household appliances and lighting, it is important to mention that these are an extremely important part of this research, since according to current practice in Hungary, this factor is not taken into consideration at all during the examination of household energy consumption. This importance is confirmed by a 2012 European Union report [3] that established that the achievable saving in this area is 12% of the total achievable potential savings in the residential sector. Since in our study we consider the total energy consumed by households, this factor is also part of the calculation model established.

3 Selection of the Proper Method

It seems to be obvious that some sort of IT-based solution is necessary to address the problems of the information gap that emerged during our research. According to research from international sources, multiple models and multiple methods can be used to estimate the energy consumption of a consumer unit (in this case a household). The basic properties of the different models are summarized in the following table based on Zhao and Magoulès [4].

Table 1
Models to calculate the energy consumption of buildings, and their attributes [4]

Methods	Model complexity	Running speed	Inputs needed	Accuracy
Elaborate Engine	Fairly high	Low	Detailed	Fairly high
Simplified Engine	High	High	Simplified	High
ANN	High	High	Historical data	High
SVM	Fairly high	Low	Historical data	Fairly high

Currently the most common method in Hungary for determining the energy consumption of buildings is calculation according to regulation 7 / 2006th TNM, which, with a little exaggeration, corresponds to the simplified simulation method detailed in Table 1 above. The calculation can be done relatively quickly, even in the case of limited data availability. However, given the results and limited accuracy, we believe there is a need to develop other methods. The greatest drawback with the method required by Hungarian law is that the calculation only considers the technical parameters, and thus fully excludes the impact of consumer behavior on energy consumption. If we consider the findings of the above section, examining the structure of household energy consumption, the consumers have an impact at least as important as the technical factors.

The full and detailed simulation models are also widely used methods. However, due to the time and expense of their use, they are only utilized for research and projects with considerable financial support. Their computational demand is very high, and therefore the running speed is too slow, so their use is not practical in the case of a large information demand. Artificial neural network-based (ANN) techniques are widely used in various calculations of energy consumption and for the approximation of energy consumption functions. Despite the fact that we are talking about a relatively complex model, thanks to today's IT systems with high processing speeds, it is possible to use IT solutions for solving the problems we have highlighted after forming the appropriate database and modeling. The SVM (support vector machine) model, like the artificial neural network based models, relies on a statistical information-based database, but the computational complexity and speed are also a problem in the large-scale application of the system.

After considering the various computation methods, our choice for the estimation of household energy consumption based on non-technical factors is an artificial neural network based inference system, the support for which is confirmed by Aydinalp-Koksal and Ugursal [5], according to whom, such models are suitable for considering technical parameters, as well as, social and economic conditions.

4 Determination of Energy Consumption Affecting Factors

The first step in building the necessary database for operating an artificial neural network based inference system is to identify the non-technical factors that affect household consumption. Research was carried out on the relevant international and national literature, and it was determined that Aydinalp et al. [6] best outline the factors affecting a household's energy consumption, beyond the technical parameters. These factors are as follows:

- Size of the settlement
- Form of the housing (owner, renter)
- Number of children living in the housing
- Number of the adults living in the housing
- Income level of the household
- Type of the housing/flat
- Size of the housing
- Number of the people staying at home during day-time hours

Adapting their conclusions to local Hungarian conditions and taking into consideration the availability of the statistical information required for the database to operate the inference system, the factors listed above were modified as follows:

- Size of the settlement
- Form of the housing (owner, renter)
- Number of people living in the housing
- Number of children living in the housing
- Number of household members actively working/employed
- Highest education level of the head of the household
- Income group of the household,
- Size of the actual living space of the property
- Type of the housing/flat

The factors specified in the list above are the backbone of the database and the research, according to which data collection should be performed, either to the desired geographical area or even to the whole country. Of course it is also necessary to include in the model the total energy consumption of the household,

to which the items of the above list are contributing factors. In case we do not want to use our system to determine the overall energy consumption, it is possible, for example, to group by energy sources or even by energy consumption purposes, as needed to solve the given task. The resulting database, with the adequate amount of sample data, provides the basic data for the operation of the neural network based inference system.

5 Data Source

To develop the database needed for the proper operation of the neural network, we basically relied on two sources. The primary source was the 2011 census conducted by the Central Statistical Office (CSO), which needed to be supplemented by a secondary data source, data from a 2011 survey on household consumption, also prepared by the CSO. The census presumably shows a realistic picture of domestic real estate holdings, family statistics, demographic data and other conditions, as participation and response was mandatory for the entire Hungarian population. Consequently, the backbone of the database was created based on the processing of these data, which define seven out of the earlier established nine factors for our work.

The other household consumption survey was unfortunately done on a smaller sample, but since in Hungary no comprehensive and detailed survey on income and consumption data has been done, it is the only source of statistics that includes feasible data for this research. The simultaneous use of two sources of statistics might appear strange, but there are plenty of examples in the international literature, for similar reasons, as we have listed. Also, on the topic of energy consumption, Aydinalp Koksal and Ugursal [5] are developing their own database based on two sets of statistics in an examination of the energy consumption of Canadian households.

Returning to the already mentioned income and consumption statistics, the sometimes lack of detailed information causes some uncertainty in the data accuracy, but this has no effect on the model or on the operation of the developed system, since in the future, a new, accurate, private or institutional survey for data input is possible in order to enhance the size of the database and thus the computational precision of the model. However, regarding the income and consumption conditions, it should be noted that in Hungary the rate of hidden income is measurable, and the presence of a black or gray economy can distort the statistics, as can the illegal purchase of energy. The preparation of a comprehensive energy consumption and income survey that can be combined with a real estate portfolio would be useful but would certainly raise concerns about the preservation of anonymity and data protection.

6 The Structure and Use of the Database

The process of the development of the database structure can be tracked on the flowchart shown in Fig. 1. Here we can observe the details for defining the various factors and the relationship between them, which is only needed to prepare the starting, training database necessary for the artificial neural network based inference system. In the future, a representative survey could significantly help to populate the database with real data, and the database could later also be expanded with the results from investments in energy efficiency. Since the preparation of such a survey is beyond both the time frame and financial resources of this current research, at present we rely solely on statistics. The spread of smart metering could help create a useful database, as connecting the consumption data with the household characteristics would supply us with detailed energy consumption data. However, this also raises data protection and legal issues.

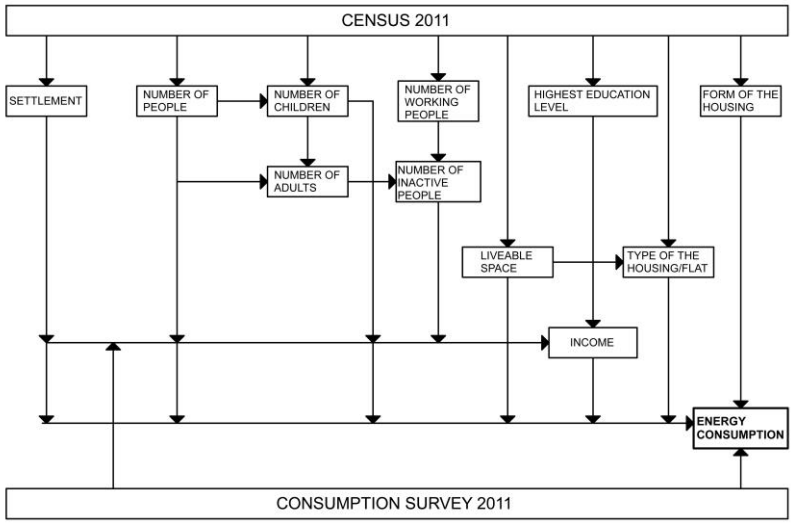

Figure 1
The block diagram of the database structure

On the basis of the above-described method, we have created a database of 1,000 samples, a sample size that in our experience satisfies the margin of error requirements in the training of artificial neural networks. In order to train and test the inference system, we need to divide the database into three parts. The largest part, 70%, is used to train the net, while 15% each is designated for checking and testing. Thus, from the database of 1,000 samples, we randomly assign the sample data in the given proportion to the defined groups. The greater the number of samples we have in our database for training, the greater will be the accuracy of the results and the fewer will be the number of errors that we can expect at the preparation of the model. Nevertheless, a database of 1,000 samples provides good accuracy, as we will demonstrate later.

7 The Neural Network Model

To create the artificial neural network based model, we used the Matlab software package, "Neural Network Toolbox", due to the availability of the devices. With the neural network module creator in the software package, we created a multilayer feed-forward network. The input layer consists of sensory units that are connected to a hidden layer of sigmoid transfer function neurons, which connects to an output layer consisting of linear transfer function neurons. [7] The sigmoid transfer function neurons are required because of the nonlinear nature of the problem; in the case of using linear transfer function neurons, we could also use a single-layer network, although only for linear approximation [7]. The sigmoid function used is defined in the software as follows:

$$tansig(x) = \frac{2}{1 + e^{-2x}} - 1$$

According to our research, this type of neural network model is capable of solving multi-dimensional problems if there are sufficient hidden neurons and a consistent data set. The scheme of the neural network used with 10 neurons in the hidden layer we can see in Fig. 2.

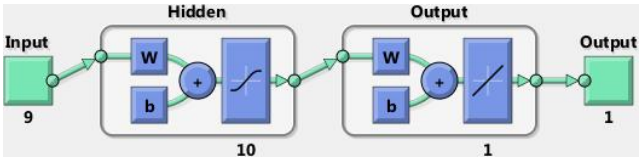

Figure 2

The scheme of the neural network used with 10 neurons in the hidden layer

The network is trained with the software according to the Levenberg-Marquardt backpropagation method that is based on the database discussed in the previous paragraph. The training mechanism is shown in Fig. 3. The number of iterations during the application of the algorithm depends on the degree of the gradient vector, the mean square error, or if these two values are not adequate, on the number of the pre-set maximum cycle number. The Levenberg-Marquardt algorithm can be called into the program with the "trainlm" command, which approximates the weight of the connections of neurons in the network as follows:

$$\mathbf{x}_{k+1} = \mathbf{x}_k - [\mathbf{J}^T \cdot \mathbf{J} + \mu \cdot \mathbf{I}]^{-1} \cdot \mathbf{J}^T \cdot \mathbf{e}$$

where J is the Jacobian matrix that contains the first derivatives of the network errors by weights, μ is the scalar, I is the identity matrix, and e is the vector of network errors.

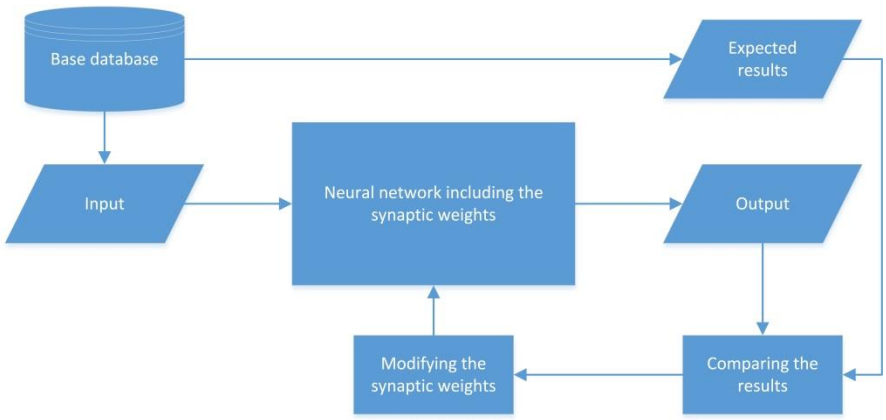

Figure 3
Neural network training with the Levenberg-Marquardt backpropagation method

The model was adjusted in a number of ways, in order to find the ideal number of neurons in the hidden layer. During modeling, this step is primarily required to maintain computational speed within reasonable limits. It should also be kept in mind that a "too complicated" model for a given problem not only decreases the running speed, but it can also significantly degenerate the accuracy of the estimations. Table 2 presents the results after the analysis of three significantly different models, thus supporting our assumptions as to the number of hidden neurons. During model testing the best results were obtained when using 10 hidden neurons, so the same structure is used hereafter.

Table 2
The performance of different models according to the number of hidden neurons

The number of hidden neurons	MSE - Training	MSE - Validation	MSE - Testing	Average difference
5				
Training cycle 1.	19,1280	17,1726	19,0161	
Training cycle 2.	19,5039	22,9476	18,0702	
Training cycle 3.	17,4450	29,9349	19,1352	
Training cycle 4.	16,7433	22,1691	23,4732	
Training cycle 5.	21,9828	19,6401	23,8509	
Mean	18,9606	22,3729	20,7091	**8,5085**
10				
Training cycle 1.	15,1974	20,9568	25,2963	
Training cycle 2.	18,1158	21,2136	16,7463	
Training cycle 3.	17,1003	22,0410	17,7402	
Training cycle 4.	17,3442	19,9203	17,8749	
Training cycle 5.	19,0449	18,7782	14,5440	
Mean	17,3605	20,5820	18,4403	**8,0301**

20					
	Training cycle 1.	17,0109	15,3666	22,7337	
	Training cycle 2.	16,2405	19,0206	24,9339	
	Training cycle 3.	14,0937	26,0877	25,3026	
	Training cycle 4.	17,4423	23,5560	18,0054	
	Training cycle 5.	16,7802	18,5667	22,2432	
	Mean	16,3135	20,5195	22,6438	**20,7830**

MSE - Mean Squaded Error

8 Results

We have created the artificial neural network-based model so that it can be embedded into the Matlab Simulink module. In our case, it is not necessary to create the Simulink model in order to estimate the household consumption because, as Fig. 4 illustrates, the operation requires only one input and one output variable. In further research, the option of embedding is an important aspect, since our neural network inference system can be part of a more comprehensive energy model.

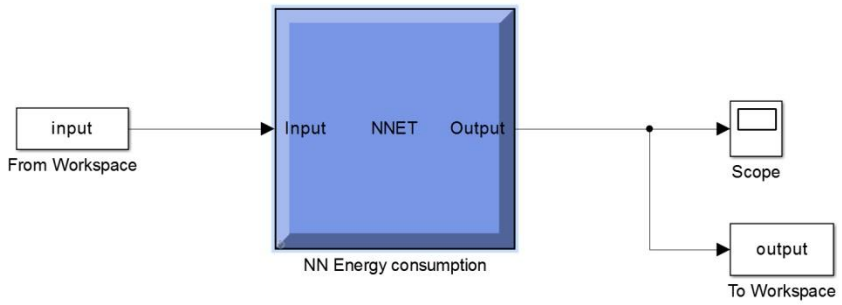

Figure 4
The embedded neural network model

Table 5 and Fig. 3 illustrate how the system works. We defined fictitious households in the sample database and then ran the inference system according to established criteria. We obtained the values presented in the last column of Table 3 and which we show as a bar chart in Fig. 5 for better visibility. We can see from the sample how the different types of settlements, the highest education level of the head of the household, the number of household members and other factors can influence changes in the annual energy consumption. Let us examine a random example: a household in Budapest in a 25 m^2 apartment, containing one working person with a university degree, and an energy consumption of 10,763 kWh of energy on an annual basis, which is considered realistic.

Table 3
The sample database to test the model and results

Number of sample	Settlement *1 = capital* *2 = county town* *3 = other towns* *4 = village*	Form of the housing *0 = renter* *1 = owner*	Number of people	Number of children	Number of working people
1	4	1	2	1	1
2	4	1	3	1	1
3	4	1	4	2	1
4	4	1	5	2	1
5	4	1	6	2	1
6	3	1	1	0	1
7	3	1	2	0	1
8	3	1	3	1	1
9	3	1	4	2	1
10	3	1	5	2	1
11	2	0	1	0	1
12	2	1	2	0	1
13	2	1	3	1	1
14	2	1	4	2	1
15	2	1	4	2	1
16	1	1	1	0	1
17	1	1	2	0	1
18	1	1	3	0	1
19	1	1	4	1	1
20	1	0	5	2	1

Number of sample	Highest education level *0 = nothing* *1 = primary school* *2 = secondary school* *3 = college graduate*	Income decile group	Liveable space *[m^2]*	Type of the housing *0 = house* *1 = flat*	Energy Consumption Results *[kWh/household* year]*
1	0	3	70	0	14831
2	0	4	70	0	24063
3	0	5	70	0	32188
4	0	6	90	0	33747
5	0	7	105	0	34447
6	1	3	45	1	8197
7	1	4	55	1	13876

8	1	5	55	1	19910
9	1	6	70	0	34026
10	1	7	70	0	39764
11	2	4	35	1	8988
12	2	5	35	1	14576
13	2	6	45	1	21842
14	2	7	45	1	28490
15	2	7	70	0	34716
16	3	6	25	1	10763
17	3	7	35	1	16442
18	3	8	45	1	24717
19	3	9	55	1	30343
20	3	10	70	1	39933

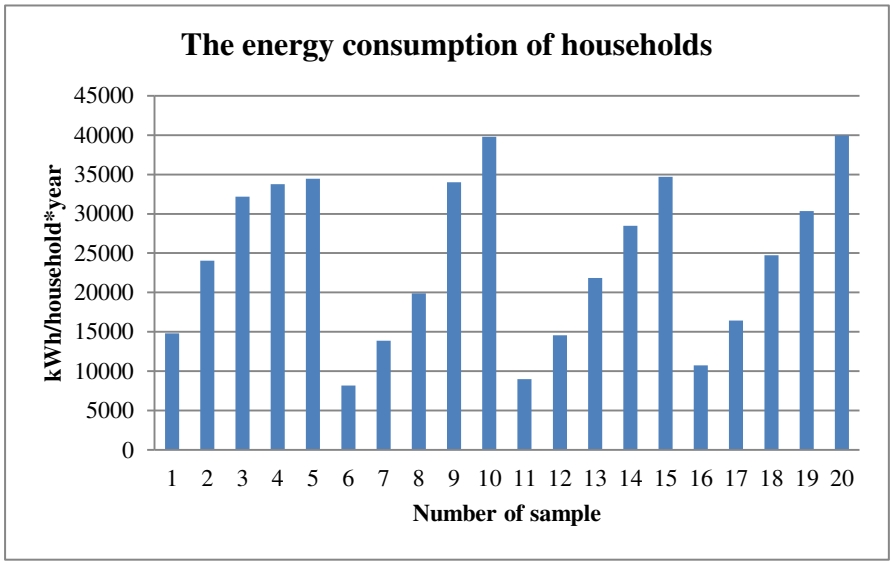

Figure 5
The results belong to the sample database

Conclusions

In summary, we can conclude that the method described in this work may be suitable for estimating the annual energy consumption of households based on statistical data, helping the goals of energy-efficiency and energy-saving programs. The developed model and the defined component factors or principals can be the basis for an accurate estimation of a household's energy consumption in other cases besides the one described; for example, the model can be used in the design phase for a new building to estimate the future energy consumption of the

households, though this is possible only if the prospective owners are known. Based on the obtained consumption results, we can produce a detailed energy cost analysis and identify the available savings potential for different parts of the household, though this would require taking into account technical characteristics as well. For practical application, further research is needed.

Acknowledgement

This work was supported by Doctoral School of Applied Informatics and Applied Mathematics of Óbuda University.

References

[1] National Renewable Energy Laboratory: National Residential Efficiency Measures Database, http://www.nrel.gov/ap/retrofits/about.cfm, download time: 2013.11.14.

[2] Lukas G. Swan, V. Ismet Ugursal, Ian Beausoleil-Morrison: Occupant-related Household Energy Consumption in Canada: Estimation Using a Bottom-Up Neural-Network Technique, Energy and Buildings, Vol. 43, pp. 326-337, 2011

[3] Federal Ministry for the Environment, Nature Conservation and Nuclear Safety, Fraunhofer Institute for Systems and Innovation Research ISI: Policy Report, Contribution of Energy Efficiency Measures to Climate Protection within the European Union until 2050, 2012

[4] Hai-xiang Zhao, Frédéric Magoulès: A Review on the Prediction of Building Energy Consumption, Renewable and Sustainable Energy Reviews, Vol. 16, pp. 3586-3592, 2012

[5] Merih Aydinalp-Koksal, V. Ismet Ugursal: Comparison of Neural Network, Conditional Demand Analysis, and Engineering Approaches for Modeling End-Use Energy Consumption in the Residential Sector, Applied Energy, Vol. 85, pp. 271-296, 2008

[6] Merih Aydinalp, V. Ismet Ugursal, Alan S. Fung: Modeling of the Space and Domestic Hot-Water Heating Energy-Consumption in the Residential Sector Using Neural Networks, Applied Energy, Vol. 79, pp. 159-178, 2004

[7] Arash Kialashaki, John R. Reisel: Modeling of the Energy Demand of the Residential Sectorin the United States Using Regression Models and Artificial Neural Networks, Applied Energy, Vol. 108, pp. 271-280, 2013

[8] D. Kolokotsa, C. Diakaki, E. Grigoroudis, G. Stavrakakis and K. Kalaitzakis: Decision Support Methodologies on the Energy Efficiency and Energy Management in Buildings, Advances in Building Energy Research, Vol. 3, pp. 121-146, 2009

[9] Kangji Li, Hongye Su, Jian Chu: Forecasting Building Energy Consumption Using Neural Networks and Hybrid Neuro-Fuzzy System: A Comparative Study, Energy and Buildings, Vol. 43, pp. 2893-2899, 2011

[10] Alberto Hernandez Neto, Flávio Augusto Sanzovo Fiorelli: Comparison between Detailed Model Simulation and Artificial Neural Network for Forecasting Building Energy Consumption, Energy and Buildings, Vol. 40, pp. 2169-2176, 2008

[11] Lukas G. Swan, V. Ismet Ugursala: Modeling of End-Use Energy Consumption in the Residential Sector: A Review of Modeling Techniques, Renewable and Sustainable Energy Reviews, Vol. 13, pp. 1819-1835, 2009

[12] Merih Aydinalp, V. Ismet Ugursal, Alan S. Fung: Modeling of the Appliance, Lighting, and Spacecooling Energy Consumptions in the Residential Sector Using Neural Networks, Applied Energy, Vol. 71, pp. 87-110, 2002

[13] Central Statistical Office (CSO) "Census 2011", http://www.ksh.hu/nepszamlalas/?langcode=hu, 2013 (in Hungarian: "Népszámlálás 2011")

[14] Central Statistical Office (CSO) "The Level and Structure of Household Consumption, 2011", Statistical Mirror, Vol. 108, 2012 (in Hungarian: "A háztartások fogyasztásának színvonala és szerkezete, 2011")

[15] Satute 7/2006. TMN (V.24): Regarding the Definition of Building Energy Characteristics, 2006 (in Hungarian: Az épületek energetikai jellemzőinek a meghatározásáról)

Heuristic Algorithms for the Robust PNS Problem

Dénes Almási, Csanád Imreh, Tamás Kovács

University of Szeged, Árpád tér 2, 6720 Szeged, Hungary
denes@rudanium.org, cimreh@inf.u-szeged.hu, tkovacs@inf.u-szeged.hu

József Tick

Óbuda University, Bécsi út 96/b, 1034 Budapest, Hungary, tick@uni-obuda.hu

Abstract: In this paper we study the robust PNS problem, which is the extension of the structural PNS problem used to model process network synthesis. This problem is NP-hard thus a heuristic algorithm can be very useful for large instances, where we do not have enough time for an exponential time algorithm, presenting a surely optimal solution, or they can be used to fasten branch and bound based algorithms. We present new heuristic algorithms for the solution of the problem which are extensions of the heuristic algorithms used to solve the classical structural PNS problem. The algorithms are analyzed empirically, where we compare the efficiency on randomly generated inputs.

Keywords: PNS problem; robust problems; heuristic algorithm, P-graphs; Business Process Modeling

1 Introduction

In the Process Network Synthesis (PNS for short) problem a set of materials is given and also operating units which are transforming some subset of materials into some other subset. The subsets assigned to the operating unit are called its input and output materials. In the problem two subsets of the materials are distinguished, one is the set of the raw materials and the other is the set of the desired products. Our goal is to find a minimal cost network of the operating units which can produce all desired products starting from the raw material. These systems can be modeled in the P-graph framework which is based on bipartite graphs. In these P-graphs we have two sets of vertices, one of them contains the possible materials, the other the operating units. The edges lead to an operating unit from its input materials and from an operating unit to its output materials.

Then the subgraphs satisfying some properties describe the feasible processes which produce the desired products from the raw materials. Thus our goal is to find the least expensive such subgraph. In the structural model the amounts of the material flows are not taken into account thus the cost of an operating unit is a constant, and the cost of a subgraph is the sum of the costs of the operating units contained in it. The foundations of PNS problem can be found in [9, 10], we will recall only the most important definitions in the next section.

The PNS problem and the P-graph technology to handle it were defined to model and solve problems in the chemical and allied industries. Later it was discovered that this terminology and the model itself can be very useful in other areas as well. The applications of P-graphs in workflow optimization are presented in [17, 18, 20]. It was also used in supply chain management; such results can be found at [1, 2, 8, 15, 22]. Moreover the P-graph framework was also used in planning building evaluation routes [11, 12].

In the structural PNS problem it is supposed that the exact cost of all operating unit is given in the input of the problem. Unfortunately in many applications this is not true. In these cases we do not have exact data there are some uncertainties in these values. There are several ways to solve this problem. In [16, 21] the fuzzy extension is presented of the PNS problem with applications on the area of workflow management. In [15] an application to supply chain management with uncertainty is presented where the P-graph is extended with the ROA (reliability of availability) value at the materials.

A further approach is the robust optimization where instead of the fixed values of the parameters we only know that they are in a given interval. Then we are minimizing the cost of the worst case of the possible values. Robust optimization is a widely studied area, one can find some overview in [3, 4]. The robust PNS problem was defined in [19]. In this model each operating unit has two different costs a nominal cost and an extended cost, and we know that at most b operating units have the extended cost; the others will have the nominal cost. The goal is to find the optimal solution for these assumptions. The definition of the model [19] presents a branch and bound based algorithm for the solution of the problem and also a polynomial solvable class of robust PNS problems.

In [6], it is proved that the structural PNS problem belongs to the complexity class of NP-hard problems, therefore it follows that the more difficult robust PNS problem is NP-hard as well. This means that we cannot expect a worst case polynomial time algorithm which surely finds the optimal solution unless P=NP. Therefore, some polynomial time heuristic algorithms which can find feasible solutions which are close to optimal can be very useful. They can be used if we have to solve large size problems in a short time. Moreover, such heuristic algorithms can be useful in accelerating Branch and Bound based algorithms. The application of a good starting solution can increase the efficiency of eliminating subsets not containing optimal solutions. In the case of the classical structural PNS

problem some heuristic algorithms are studied in [5] and [7]. In [5] a greedy type algorithm is presented for the solution of the general problem which is based on the ideas of algorithms from set covering. In [7] a special class of PNS problems is studied.

In this paper we extend and analyze the heuristic algorithms from [5] into the more general robust PNS problem. In the next section we recall the basic definitions in the area of robust PNS problem which will be used later in the paper. Then in Section 3, the heuristic algorithms which are studied in the paper are presented. Section 4 contains the analysis of the algorithms. We present the results of an experimental analysis, where the algorithms are compared to randomly generated inputs.

2 Notations and Basic Definitions

The structural PNS problem can be modeled in the P-graph framework. In the P-graph (Process Graph) we have the set of the materials denoted by M, which contain two special subsets, the set of raw materials and the set of desired products denoted by R and P respectively. The problem also contains a set of possible operating units which can transform some sets of materials. The set of operating units is denoted by O. An operating unit u is given by two sets, $in(u)$ denotes the set of the input materials $out(u)$ denotes the set of output materials of the operating unit. This means that the operating unit can work in a solution structure if all of its input materials are produced and in this case it produces all of its output materials. The P-graph (Process Graph) of the problem is defined by the sets M and O. It is a directed bipartite graph where the set of vertices is $M \cup O$, and have the following two sets of edges:

1) Edges which connect the input materials to their operating unit
2) Edges which connect the operating units to their output materials

Then some of the subgraphs of this P-graph describe the feasible solutions which produce the required materials from the raw materials. In [9] it is shown that a subgraph (m,o), where m and o are the subsets of M and O, represent a feasible solution if and only if the following properties called axioms are valid:

(A1) m contain all element of P

(A2) a material from m is a raw material if and only if no edge goes into it in the P-graph (m, o)

(A3) For each operating unit u from o there exists a path in the P-graph (m,o) which goes into a desired product from u

(A4) m is the union of the input and output material sets of the operating units contained in set o.

In the structural PNS problem we assign, to each operating unit u, a cost denoted by c(u) and the goal is to find a feasible solution, where the total cost of the contained operating units is minimal. In the robust version we assign two costs to the operating units: a nominal cost denoted by c(u) and an extra cost denoted by e(u). The sum c(u)+e(u) is called the extended cost of the operating unit. Furthermore, we have an a priori bound b, which means that in any solution, at most, b operating units can have the extended cost and the others have the nominal cost. We are interested in the worst case; therefore, if we consider a feasible solution of the problem then its cost will be the sum of the nominal costs of the operating units plus the sum of the b largest extra costs. We note that the set of feasible solutions, in the case of the robust problem, is the same as in the classical problem, the difference is that in the robust version we are considering a more difficult objective function.

3 The Heuristic Algorithms

First we present a framework heuristic which is the general version of the algorithms presented in [5]. Later we give several specialized version of the framework algorithm which can be used for the solution of the robust problem. The algorithm builds a solution step by step; it selects one operating unit in each iteration step. The algorithm uses three sets, the *set of the selected operating units,* the *set of the required materials* and the *set of the produced materials*. First the set of the selected operating units and the set of produced materials are empty and the set of the required materials is equal to the set of the desired products. Then, in each iteration step, we choose the operating unit minimizing some evaluation function and put it into the set of the selected operating units. We add its output materials to the set of produced materials, and delete them from the required materials set. Then each input material of the operating unit which is not raw material and not contained in the set of produced materials is put into the set of required materials. The procedure ends when the set of the required materials becomes empty. We obtain the feasible solution which contains the operating units from the set of selected operating units and the materials which are input or output materials of some of these operating units.

This algorithm, with some specialized evaluation functions, was defined for the solution of the structural PNS problem. In [5] it is proved that it always produces a feasible solution for the problem. Alternately, the proof does not use the definition of the evaluation function thus it works for arbitrary evaluation functions. Moreover, the set of feasible solutions is the same as in the classical and the robust PNS problem, thus we obtain the following statement.

Proposition 3.1 ([5]) The algorithm defined above results in a feasible solution of the robust PNS problem for any evaluation function on the operating units.

To specify the frame algorithm we have to define an evaluation function on the operating units. We will use a greedy type algorithm. On one hand we would like to choose an operating unit which produces the most elements from the set of the requested materials. On the other hand we would like to choose such operating units which have small cumulated costs, where in the cumulated costs not only the direct cost of the operating unit is estimated but also the cost of producing its input materials. Thus, we have to define a cumulated cost CU(o) for each operating unit, and then we choose the operating unit where the ratio of the cumulated cost and the number of the required material produced by the unit is minimal. The cumulated cost depends on the direct cost of the operating unit and also on the cost of its input materials. Since we consider the robust problem even the direct cost of the operating unit cannot be determined in advance, since we do not know whether a nominal or an extended cost will be calculated in the solution. We define, below, three possibilities for estimating the direct cost of the units and two possibilities for estimating the cost of the input materials, thus we will obtain six different estimations for the cumulative cost and this results in six heuristic algorithms.

In the case of the direct cost of the unit we can use the following estimations:

- Average cost: In this case, we use some weighted average of the two costs, thus $c_A(o)=\alpha c(o)+(1-\alpha)(c(o)+e(o))$ for some $0\leq\alpha\leq1$.
- Worst case cost: In this case we use the extended cost unless we already selected b operating units with at least as big extra cost as the actual unit has. In the latter case we use the nominal cost.
- Hybrid cost: This case is similar to the worst case cost but we use the average cost if we have not selected already b operating units with at least as big extra cost as in the actual unit.

We note that the average cost is a static one, in the sense that we can define it in advance and it is independent of the solution built by the heuristic algorithm. Contrarily, the worst case and hybrid costs are dynamic ones, they depend on the actual solution structure thus they cannot be calculated in advance.

To define the indirect cost resulting from the input materials, first we have to define a cost function MA on the materials. Here we use the same idea, which is used in the heuristic algorithms, of [5] and was defined in [13] for bounding function in a Branch and Bound algorithm. The only difference occurs when we use the costs of operating units in the calculation, then in the robust version we use the average cost of the operating units. We cannot use the other estimations here; since we have to calculate these costs in advance, thus we cannot apply the dynamic costs. We will use only cycle free P-graphs in our tests and the definition of the material costs are much easier in this case, therefore, we only recall the basic ideas of this simpler definition here. One can find the detailed general construction of the cost function on materials in [13].

We use two sets of materials: *I* denotes the materials with the given *MA* values and *J* denotes the complement set where we still have to calculate the value of *MA*. At the beginning, *I* contains the raw materials with *MA(m)=0*, and later in each step one element is moved from *J* to *I*.

We always choose such material *m* from *J,* which is only produced by operating units having all input materials in *I*. Using the cycle-free property, we also find such material. We give a production cost for each operating unit producing *m* as follows. We calculate the sum of the maximum of the *MA* values of the input materials and the c_A cost of the operating unit. (Note that by the definition of *m* we know that *MA* is known for all input materials.) Then *MA(m)* will be the minimum of the production costs calculated above for the operating units producing *m*. After defining *MA* on *m* we move it from *J* to *I*. The procedure ends when *J* becomes empty which means that *MA* has been calculated for all materials.

Based on this function *MA* we can use two methods to calculate the cumulative cost. In the first case the cumulative cost is the sum of the costs of the input materials plus the direct cost of the operating unit. Using the three direct costs this method yields three cumulative costs and this yields three algorithms. They are denoted by SA (Sum-average), SW (Sum-worst case), SH (Sum-hybrid). A further method to find cumulative costs is to take the sum of the maximal MA cost of the input materials and the direct cost of the operating unit. Again, we can use all of the direct costs thus we obtain three algorithms, which are denoted by MA (Max-average), MW (Max-worst case), MH (Max-hybrid).

We will compare these algorithms in the next section on randomly generated cycle-free inputs. Such cycle-free problems often appear in workflow management. First we describe the test environment and then we analyze the results.

4 Experimental Analysis of the Algorithms

4.1 Description of the Test Cases of the Experimental Analysis

To carry out tests of the algorithms, a problem generator was written. We use similar ideas to the problem generator used in [14] but we changed it to produce cycle free problems. A detailed description of the algorithm which generates the problems is not presented here; only the most important concepts are introduced.

Parameters: The generator has multiple input parameters. We can define the number of operating units to create (*n)*, the number of raw materials (*r)* and number of desired products (*p*) in the generated problem. There is an integral variable denoted by w_b that defines how many times it is more probable that an

operating unit will reproduce an intermediate material, instead of creating a new one. A further parameter is p_b, which is a probability, related to how likely it is that new operating unit will reproduce intermediate materials that were produced several iterations earlier by other machines. With a low p_b value (e.g. 0.2), newly created operating units will tend to reproduce intermediate materials that are closer to raw materials than to those materials created only some iterations ago. A high p_b value (e.g. 0.8) will introduce redundancy among the production of those intermediate materials that were produced only some iterations ago.

The generator: The generator creates the operating units in an iterative manner. In each iteration, at most one new operating unit and several new materials are created. After the generation of the n'th operating unit, there is a separate step in the algorithm which chooses p materials among those considered intermediate to become product materials. Having chosen the products, the last step is to assign nominal and extra costs to each machine.

The algorithm always keeps a set of materials that are available (W). Initially W only contains the raw materials indexed from 1 to r. An initially empty O set of operating units is maintained throughout the run of the algorithm and at any time it contains the units that are already constructed.

For each new operating unit, two random numbers are chosen in the range [1, 4] using a discrete distribution of (0.15, 0.35, 0.35, 0.15). These two numbers (a, d) represent the number of the inputs and outputs the new operating unit should have. In cases where choosing a number of inputs is impossible, a is truncated to the number of maximum possible inputs a machine might have at that moment.

The core concept of the algorithm is that in each iteration, where there is at most one intermediate material, we choose a limit u that is always greater than r. The operating unit being created, at that iteration, may have inputs only from the range $[1, u-1]$ and outputs from the range $[u, |W|]$. Decisions about whether to create a new material or reproduce an existing intermediate material are made using a dynamic discrete distribution that depends on how many times any intermediate material was chosen for reproduction during the creation of this operating unit, and how many times it was chosen that this operating will produce a new material and a factor that linearly weights these two numbers with a certain bias that is an input parameter of the generator (w_b). Whenever an existing material should be chosen, it is picked from $[u, |W|]$ with a uniform distribution. The u is chosen with binomial distribution over $[r+1, |W|]$ with p_b as its probability parameter.

The fact that any operating unit has a number u that partitions the W set into two parts while inputs can only be chosen from the lower and outputs can only be chosen from the upper partitions guarantees that no solution of the generated problem will contain a cycle.

In the first iteration there are no intermediate materials. This condition forces the algorithm to create an operating unit with all its outputs being new materials.

After a new operating unit is generated, it is inserted to O at the end of the iteration. We note that this set may already contain the same operating unit.

The algorithm first creates $m-1$ operating with the method given above. The method of generating the last operating unit differs from the above, only in that the number of outputs for the last operating unit must guarantee that there will be at least p intermediate materials. This ensures that it is possible to choose p products in the next step.

Having created all of the operating units, uniform integral distributions are used for picking nominal and extra costs for each machine. Random choices of costs are independent from each other.

After the operating units are generated, product materials are chosen from the intermediate ones: p materials are taken from W, whose indices must be in the range $[r+1,|W|]$. The initial probability of material i to be chosen is given by $p_i = (i-r)/S$ where $S = (|W|-r)(|W|-r+1)/2$.

The products are chosen in a non-independent way --- A new material is picked every time with the same distribution introduced above. Whenever such a material is picked that is already considered a product, a new one is picked using the same initial distribution. This method is repeated until p materials are picked. These materials will result in the set of the required products.

We implemented the six heuristic algorithms defined in previously. We used α=0.5 in the average cost in algorithms SA and MA, and also α=0.5 was used in the calculation of the MA function. We generated 1000 operating units and used the values $w_b = 4$ and $p_b = 0.2$. The number of raw materials was 5, and we generated test cases with the values $p=5, 20, 50$, $b=1, 5, 25$. We defined the costs of the operating units as the nominal costs picked from the interval [20, 100] uniformly and independently. For the extra cost we considered three different test cases: it was picked from the intervals [0, 50], [20, 100], [100, 500] uniformly and independently. Thus, we defined three possibilities for p, three possibilities for b, and three different distributions for the extra costs. We generated 100 problems from each of these 27 test cases and executed the 6 heuristic algorithms on each test. The results are summarized below.

4.2 The Results of the Experimental Analysis

First consider the test cases where the expected extended cost was smaller than the nominal costs, these cases happens if the uncertainties describe small problems which can be easily handled. The average costs are listed in Table 1. We denoted the best value in each column by bold text and the worst one by bold and italic.

We can see that the order of the efficiencies of the algorithms depends on the test cases. But we can obtain some conclusion.

Table 1
The average results for the extra cost from [0, 50]

	b=1, p=5	b=1 p=20	b=1 p=50	b=5 p=5	b=5 p=20	b=5 p=50	b=25 p=5	b=25 p=20	b=25 p=50
SA	1016	2430	***4167***	1198	2597	4255	1444	***3662***	***5430***
SW	1064	***2542***	**3996**	1341	2627	***4546***	1655	3347	5346
SH	1003	2487	4042	1186	***2781***	4449	**1438**	**3214**	5178
MA	1019	2283	4039	1177	2718	4253	1440	3498	5150
MW	***1074***	2264	4129	***1402***	**2537**	**4209**	***1706***	3220	5323
MH	**997**	**2180**	4150	**1175**	2638	4222	1466	3293	**5082**

Algorithm MH gave the best result 4 times in these test cases and it was never the worst thus we can say that it had the best performance. MW and SH both received the best results two times but MW was the worst 3 times, while SH resulted in the worst solution only in one case thus we can say that SH was better. We also checked the number of best solutions inside the test cases, and we obtained that MH was the best in 239 tests, MW was the best in 146 tests, MA was the best in 189 tests, SH was the best in 142 tests, SW was the best in 76 cases, and SA was the best in 145 cases among the 900 tests. (We note that the sum of the best performance of the algorithms is more than 900. This is not a mistake; if more algorithms achieved the same best result then all of them were considered best. It is likely that in these cases the heuristics found the optimal solution.) The order of the algorithms considering the best results is MH, MA, MW, SA, SH, SW. We also considered the worst cases. Then MH gave 79 times, MW gave 185 times, MA gave 95 times, SH gave 109 times, SW gave 238 times, SA gave 155 times the worst solution. (Here we can observe that the sum is smaller than 900. The reason is that we have not counted here the cases where all of the heuristic found solutions with the same objective value.) The order of the algorithms considering the worst results is MH, MA, SH, SA, MW, SW.

Therefore, our main conclusion that in the tests performed in this block of test cases algorithm MH gave the best results. We cannot clearly order the other heuristics since from different point of views we have different results. But we can observe in general, the maximum evaluation for the indirect costs of the operating units and the hybrid estimation for the direct costs seems to be a better strategy in these sets.

Now, consider the second block where the extra costs have the same distribution as the nominal cost. This block models the situation when the unexpected events are about replacing the operating unit, thus they approximately double the cost of the operating units. The average costs are collected in Table 2, again we denoted the best value in each column by bold, the worst one by bold and italic.

Table 2
The average results for the extra cost from [20, 100]

	b=1, p=5	b=1 p=20	b=1 p=50	b=5 p=5	b=5 p=20	b=5 p=50	b=25 p=5	b=25 p=20	b=25 p=50
SA	1123	2730	4595	1451	2867	4390	**2100**	4539	***6459***
SW	***1165***	***2808***	***4644***	1552	3014	4516	2200	***4823***	6297
SH	1098	2668	4561	1425	**2746**	**4301**	2146	4464	6431
MA	1121	2404	3965	1438	2948	4974	2157	4146	**5857**
MW	1157	2404	3942	***1583***	***3111***	***5042***	***2328***	4510	6524
MH	**1074**	**2308**	**3812**	**1417**	2844	4715	2171	**4133**	6430

Checking the average values we obtain that algorithm MH gave the best result 5 times in these test cases and it was never the worst thus we can again say that it had the best performance. SH received the best result two times and SA and MA both achieved the best average once. Most of the worst results were given by SW and MW both of them achieved a worst result 4 times.

We also checked the number of best solutions inside the test cases, and we obtained that MH was the best in 327 tests, MW was the best in 65 tests, MA was the best in 198 tests, SH was the best in 187 tests, SW was the best in 59 cases, and SA was the best in 86 cases among the 900 tests. The order of the algorithms considering the best results is MH, MA, SH, SA, MW, SW. We considered the worst cases as well. Then MH gave 69 times, MW gave 239 times, MA gave 63 times, SH gave 66 times, SW gave 332 times, SA gave 117 times the worst solution. The order of the algorithms considering the worst results is MA, SH, MH, SA, MW, SW.

Therefore our main conclusion is that in the tests performed in this block of test cases, again, algorithm MH gave the best result. It has slightly more worse cases than MA and SH, but it was much better in the other evaluations. We can also observe that the worst case estimation for the direct costs of the operating units had a very bad performance.

Now consider the last block of the tests, where the extra costs are larger than the nominal cost, this models the situation when the uncertain events cause serious problems which might have larger cost than just replacing the operating unit. The average costs are collected in Table 3, we denoted the best value in each column by bold, the worst one by bold and italic.

Checking the average values we obtain that algorithm MH gave the best result 7 times among the 9 these test cases. It gave the worst result in one case, still we think so that it has the best performance. MW gave the best average in two test cases and it was never the worst thus we can say that it also has a good performance on this block of tests. SW and SA had the worst average results in 5 and 3 cases thus we can say that these were the worse algorithms in this average case.

Table 3
The average results for the extra cost from [100, 500]

	b=1, p=5	b=1 p=20	b=1 p=50	b=5 p=5	b=5 p=20	b=5 p=50	b=25 p=5	b=25 p=20	b=25 p=50
SA	1609	3336	5263	***3086***	5162	6998	6208	***10702***	***14734***
SW	***1740***	***3467***	***5493***	2989	***5202***	***7310***	6113	10083	14050
SH	1596	3274	5235	3003	5038	7117	6198	10510	14333
MA	1715	3225	4951	3004	4953	6837	6220	10653	13542
MW	1746	3257	5137	3020	5066	7067	**6051**	**10024**	13312
MH	**1579**	**2984**	**4648**	**2887**	**4706**	**6785**	***6284***	10600	**13180**

We checked the number of best solutions inside the test cases, and we obtained that MH was the best in 424 tests, MW was the best in 144 tests, MA was the best in 107 tests, SH was the best in 103 tests, SW was the best in 63 cases, and SA was the best in 68 cases among the 900 tests. The order of the algorithms considering the best results is MH, MW, MA, SH, SA, SW. We also considered the worst cases as well. Then MH gave 47 times, MW gave 126 times, MA gave 106 times, SH gave 120 times, SW gave 256 times, SA gave 255 times the worst solution. The order of the algorithms considering the worst results is MH, MA, SH, MW, SA, SW.

Conclusions

Therefore, our main conclusion, that in the tests performed in this block of test cases, that the algorithm MH gave the best result. We can also observe that the sum estimations for the indirect costs of the operating units in general had worse performance.

Summarizing the experimental analysis we can observe that the performance of the algorithms strongly depends on the test cases, but we can draw some conclusion here. Algorithm MH had clearly the best result in each block of test cases, thus we can state that the experiments show that MH is the most efficient algorithm among the algorithms studied in this work. We could note that the difference between it and the other algorithms is the most significant when the extra costs are large. On the other hand SW was the worst in most cases. In general we can conclude that the maximum estimations perform in a better way for the indirect costs than the sum ones. And we can also conclude that the worst case estimation on the direct cost of the operating units has poorer performance than the other methods.

Acknowledgement

This work was partially supported by the European Union and the European Social Fund through project Telemedicina (Grant no.: TÁMOP-4.2.2.A-11/1/KONV-2012-0073).

References

[1] Bárány, M.; Bertók, B.; Kovács, Z.; Friedler, F.; Fan, L. T.: Solving Vehicle Assignment Problems by Process-Network Synthesis to Minimize Cost and Environmental Impact of Transportation, Clean Technologies and Environmental Policy, 13(4), 637-642, 2011

[2] Bertók, B.; Kalauz, K.; Süle, Z.; Friedler, F.: Combinatorial Algorithm for Synthesizing Redundant Structures to Increase Reliability of Supply Chains: Application to Biodisel Supply, Industrial & Engineering Chemistry Research, 52(1), 181-186, 2013

[3] Bertsimas, D.; Brown, D.; Caramanis, C.: Theory and Applications of Robust Optimization, SIAM Review, 53, 464-501, 2011

[4] Bertsimas, D.; Sim, M.: Robust Discrete Optimization and Network Flows, Mathematical Programming Series B, 98, 49-71, 2003

[5] Blázsik, Z.; Holló, Cs.; Imreh, Cs.; Kovács, Z.: Heuristics for the PNS problem, Optimization Theory, Mátraháza 1999, Applied Optimization 59 eds. F. Gianessi, P. Pardalos, T. Rapcsák, Kluwer Academic Publishers, Dordrecht, Boston, London, 1-18, 2001

[6] Blázsik, Z.; Imreh, B.: A Note on Connection between PNS and Set Covering Problems, Acta Cybernetica, 12, 309-312, 1996

[7] Blázsik, Z.; Keserű K.; Kovács, Z.: Heuristics for Simplified Process Network Synthesis Problems with a Blossom-Type Algorithm for the Edge Covering Problem, Optimization Theory, Mátraháza 1999, Applied Optimization 59 eds. F. Gianessi, P. Pardalos, T. Rapcsák, Kluwer Academic Publishers, Dordrecht, Boston, London, 19-31, 2001

[8] Fan, L.T.; Kim, Y.; Yun, C.; Park, S. B.; Park, S.; Bertok, B.; Friedler, F.: Design of Optimal and Near-Optimal Enterprise-Wide Supply Networks for Multiple Products in the Process Industry, Ind. Eng. Chem. Res., 48, 2003-2008, 2009

[9] Friedler, F.; Fan, L. T.; Imreh, B.: Process Network Synthesis: Problem Definition, Networks, 28, 119-124, 1998

[10] Friedler, F.; Tarján, K.; Huang, Y. W.; Fan, L.T.: Graph-Theoretic Approach to Process Synthesis: Axioms and Theorems, Chem. Eng. Sci., 47(8), 1973-1988, 1992

[11] Garcia-Ojeda, J. C.; Bertók, B.; Friedler, F.: Planning Evacuation Routes with the P-Graph Framework, Chemical Engineering Transactions, 29, 1531-1536, 2012

[12] Garcia-Ojeda, J. C.; Bertók, B.; Friedler, F.; Fan, L. T.: Building-Evacuation-Route Planning via Time-expanded Process-Network Synthesis, Fire Safety Journal, 61, 338-347, 2013

[13] Imreh, B.; Friedler, F.; Fan, L. T.: An Algorithm for Improving the Bounding Procedure in Solving Process Network Synthesis by a Branch-and-Bound Method Developments in Global Optimization, editors: I. M. Bonze, T. Csendes, R. Horst, P. M. Pardalos, Kluwer Academic Publisher, Dordrecht, Boston, London, 301-348, 1996

[14] Imreh, B.; Magyar, G.: Empirical Analysis of Some Procedures for Solving Process Network Synthesis Problem, Journal of Computing and Information Technology, 6, 372-382, 1998

[15] Süle, Z.; Bertók, B.; Friedler, F.; Fan, L. T.: Optimal Design of Supply Chains by P-Graph Framework Under Uncertainties, Chemical Engineering Transactions, 25, 453-458, 2011

[16] Tick, J.: Fuzzy Extension to P-Graph-based Workflow Models, Proceedings of the 7th IEEE International Conference on Computational Cybernetics, ICCC 2009, 109-112, 2009

[17] Tick, J.: P-Graph-based Workflow Modeling, Acta Polytechnica Hungarica (ISSN: 1785-8860) 4: (1), 75-88, 2007

[18] Tick, J.: Workflow Modeling Based on Process Graph, Proceedings of the 5th Slovakian-Hungarian Joint Symposium on Applied Machine Intelligence and Informatics (SAMI 2007) Poprad, Slovakia, 2007.01.25-26, 419-426, 2007

[19] Tick, J.; Imreh Cs.; Kovács Z.: Business Process Modeling and the robust PNS problem, Acta Polytechnica Hungarica (ISSN: 1785-8860) 10: (6) 193-204, 2013

[20] Tick, J.; Kovács, Z.: P-Graph-based Workflow Synthesis, Proceedings of the 12th International Conference on Intelligent Engineering Systems (INES 2008) Miami, USA, 2008.02.25-29, 249-253, 2008

[21] Tick, J.: Fuzzy Control Systems Based on Parametric T-Norm Function, Proceedings of the 4th International Symposium on Applied Computational Intelligence and Informatics (SACI 2007) Timisoara, Romania, 2007.05.17-18, 215-218, 2007

[22] Vance, L.; Cabezas, H.; Heckl, I.; Bertók, B.; Friedler, F.: Synthesis of Sustainable Energy Supply Chain by the P-Graph Framework, Industrial & Engineering Chemistry Research, 52(1), 266-274, 2013

The Role of Individual Differences in Learning

Péter Tóth

Trefort Ágoston Centre for Endineering Education, Óbuda University
Népszínház u. 8, H-1081 Budapest, Hungary
toth.peter@tmpk.uni-obuda.hu

Abstract: A precondition for the realization of the adaptive teaching process is a knowledge of the individual characteristics of learning, an understanding of the individual methods of learning and, through these, the selection and formation of a suitable teaching environment. Therefore the differences between students must be taken into consideration by the teacher. They are to be interpreted not only at the level of intellectual capacities but also with respect to the most different individual characteristics of sensation, perception, thought and learning. In the present empirical research the 12-item variant of Kolb's LSI questionnaire is applied for this purpose. First Kolb's learning model is briefly surveyed, then the objective of the research is stated, the results of the empirical research are shown and, finally, the most important statements of the research are presented.

Keywords: adaptive teching process; learning strategies; Kolb's learning styles

1 Preliminaries and Theoretical Background

In a former paper [1] the adaptive teaching process as well as the teaching strategies in this process were explained. Strategy was interpreted as such a complex system of procedures as organically combines method, work form and teaching aids. The preferred individual patterns of strategies characteristic of the individual were explained as style (of teaching and learning). Our former results [1] showed that certain learning strategies (e.g. the preferred way of information acquisition, perception modality [10]) reflect some kind of stability, whereas others (e.g. the preferred way of information processing and its application) show continuous variation.

A common feature of the many learning style theories is that students are classified according to their cognitive characteristics, based on single- or multi-dimensional bipolar (usually cognitive) scales. [2] Students' effective learning methods, forms and teaching aids are to be concluded from the preferred strategies that belong to learning style. The teaching strategies which elicit the most preferred learning strategies are also to be defined, based on which the learning environment or the learning process are to be designed.

Coffield formed five groups of the existing sixty to seventy theories. [2] Of these now the category is highlighted for the present research which interprets learning style as a flexibly stable learning preference. [3] [4] [5]

From the point of view of our research, the theory examining the learning preferences of the individual is to be highlighted. The most significant theory in this group is associated with the name of David Kolb, who has been studying learning style for more than 40 years. His Learning Style Inventory (LSI) is one of the most widespread measuring instruments in the examination of learning styles. His experimental theory of learning amalgamated the relevant and decisive movements of the 20th Century (John Dewey, Kurt Lewin, Jean Piaget, William James, Carl Jung, Paulo Freire, Carl Rogers, etc.) [6] [7]

His theory rests on six principles:

- Learning is interpreted as a relationship between the individual and the environment.
- Learning is interpreted as the holistic process of adaptation to the environment.
- Learning is to be regarded rather as a regulated process than an outcome condition.
- The student's existing knowledge and experience play a decisive role in processing new information.
- Piaget's adaptive theory is regarded as the basis of learning. Adaptation has two forms, namely assimilation and accommodation.
- Learning is a process of constructing knowledge, the result of which presents itself as a relationship between community knowledge and individual knowledge.

Kolb gives two important dimensions of learning: perception and processing. These dimensions are visualized as two intersecting axes, where each axis has two poles: perception (information acquisition) ranges from concrete experience (CE) to abstract conceptualization (AC), and information processing ranges from active experimentation (AE) to reflective observation (RO). The two axes form a four-quadrant field for mapping individual learning styles. On the basis of preferences along axes four kinds of learning style were differentiated: Converger, Diverger, Assimilator and Accommodator. [8] [9]

2 Aims and Means of Examination

David Kolb's LSI (Learning Style Inventory) underwent a lot of change and development during the years. [7] In our former examination [1] the 9-item questionnaire, whereas in the present research the 12-item one was used to decide the learning style of the age group 14 to 18 in basic professional education. The results were compared with those of the former longitudinal research.[1] However, it was not possible to draw real conclusions, because this survey – contrary to the previous one – was not representative (pilot test).

In adapting the questionnaire it was kept in mind that the participants were not students at higher or adult education (as most of them are in Kolb's tests), but at vocational secondary schools.

The questionnaire comprises 12 statements with 4 possible endings each. The student has to rank the following possibilities: 4= most like you, 3= second most like you, 2= third most like you, 1= least like you. They are worth 4, 3, 2 points or 1 point in that order. These points are added up as columns at the bottom of the table. The four columns show the above mentioned four kinds of learning variables and methods. [9]

The participants at the present pilot examination were grade 9, 10 and 11 classes of 29, 25 and 25 persons respectively at a vocational secondary school of informatics.

The basic purpose of the examination was, making use of the experience and results of the former research, to test in basic professional education the 12-item version of Kolb's questionnaire and thereby prepare a representative longitudinal examination.

Based on all these the hypotheses and a question of the empirical research focussing on vocational secondary school students who specialize in informatics are created according to the following.

H1. Learning variables in both dimensions are not normally distributed (students specializing in informatics have general preferences) and form a bipolar system.

H2. In the dimension of preferred information type and information acquisition, perception the learning variables act similarly to attitudes. In this dimension the preferred learning variable is experience acquisition based on concrete experiences.

H3. In the dimension of preferred information processing learning variables vary in a different way with a progress in studies. Productive application and experimentation is a preferred learning variable.

Q1. How does the ranking of learning style change with the progress in studies? Can any characteristic realignment or move be observed?

3 Results of Empirical Examination

3.1 Description of Learning Variables

First the descriptive statistical and normality examination of Kolb's learning variables (AC, RO, AC, CE) and difference variables (AE-RO, AC-CE) were performed. Both the analysis of descriptive statistical data (Skewness / Std. Error of Skewness, Kurtosis / Std. Error of Kurtosis; Table 1) and the Kolmogorov – Szmirnov as well as the Shapiro – Wilk tests (Table 2) unanimously justify that the less strict conditions of normality are fulfilled for all the variables while the stricter ones are fulfilled for the majority of them (CE, AC, AC-CE; AE-RO). The null hypothesis of the Kolmogorov – Szmirnov test is that the variable is not of normal distribution and the distribution of data based on significance level and marked by * does not differ from normal distribution.

Table 1

Descriptive statistical data of learning variables and difference variables

		AE	RO	AE-RO	AC	CE	AC-CE
Cases	Valid	77	77	77	77	77	77
	Missing	0	0	0	0	0	0
Mean		30.74	28.75	1.99	33.08	27.79	5.29
95% Confidence Interval for Mean	Lower Bound	29.66	27.77	0.32	31.87	26.61	3.27
	Upper Bound	31.82	29.74	3.66	34.29	28.97	7.30
Median		30	29	**1**	33	28	**6**
Modus		29	28*	0	32*	25	-4*
Std. Deviation		4.772	4.335	7.357	5.331	5.202	8.887
Skewness		0.259	-0.213	0.389	0.084	-0.164	-0.027
Std. Error of Skewness		0.274	0.274	0.274	0.274	0.274	0.274
Skewness / Std. Error of Skewness		0.945	-0.777	1.420	0.307	-0.598	-0.100
Kurtosis		-0.233	0.291	0.357	0.665	-0.442	0.720
Std. Error of Kurtosis		0.541	0.541	0.541	0.541	0.541	0.541
Kurtosis / Std. Error of Kurtosis		-0.431	0.538	0.660	1.229	-0.817	1.331
Percentiles	33.33	28.00	27.00	***-1.00***	31.00	25.00	***2.00***
	66.67	33.00	31.00	***5.00***	35.00	30.00	***9.00***

Note: Quotients of Skewness and Std. Error of Skewness as well as of Kurtosis and Std. Error of Kurtosis also fall within the strict limit value of ±1,96, therefore the more permissive conditions of normality are fulfilled.

* The smallest is given of the several modes.

As seen from the positive values of difference variables, students specialized in informatics have a stronger preference for the productive application of what they have acquired (AE), and even more so with respect to thought and concept formation (AC), which may also harmonize with the character of the profession. If these value pairs are compared with those gained at a former test [1], a more significant difference will appear with respect to AC-CE mostly. To value pairs (AE-RO;AC-CE) (+1;-2) were added at a former test, whereas (+1;+6) at the present one. (See Table 1 for median value.) In Kolb's 2005 examination the cut-points for learning style types were (+6;+7). [7]

Table 2
Test of Normality

	Kolmogorov – Smirnov[a]			Shapiro – Wilk		
	Statistic	df	Sig.	Statistic	df	Sig.
CE	0.081	77	0.200*	0.984	77	0.431
RO	0.093	77	0.094	0.982	77	0.364
AC	0.084	77	0.200*	0.982	77	0.342
AE	0.110	77	0.022	0.978	77	0.217
AE-RO	0.087	77	0.200*	0.979	77	0.220
AC-CE	0.059	77	0.200*	0.987	77	0.638

a. Lilliefors Significance Correction
* This is a lower bound of the true significance.

3.2 Learning Variables Through Time

The comparison of the statistical data of Kolb's learning variables was carried out according to the cross sectional model for each grade, too. The results partly coincide with and partly differ from the former ones. [1]

There is no difference from the former test results in the preferred mode of information processing. The mean values and standard deviation values of AE és RO variables are similar to the former ones. With the progress of studies a gap opens, that is the preference difference between the two variables increases. Standard deviation values are balanced with time (Fig. 1).

In the dimension of the preferred type of information acquisition, perception the change in the mean as well as the standard deviation values of the variables through time is also similar to the former change. However, the fact is not negligible that formerly it was the preference for syllabus acquisition based on concrete experience (CE) which was stronger than that for abstract conceptualization, but now the situation is quite the contrary (Fig. 2). This may be related to the syllabus specialities of the subject of informatics, which reinforces learning preferences of this type.

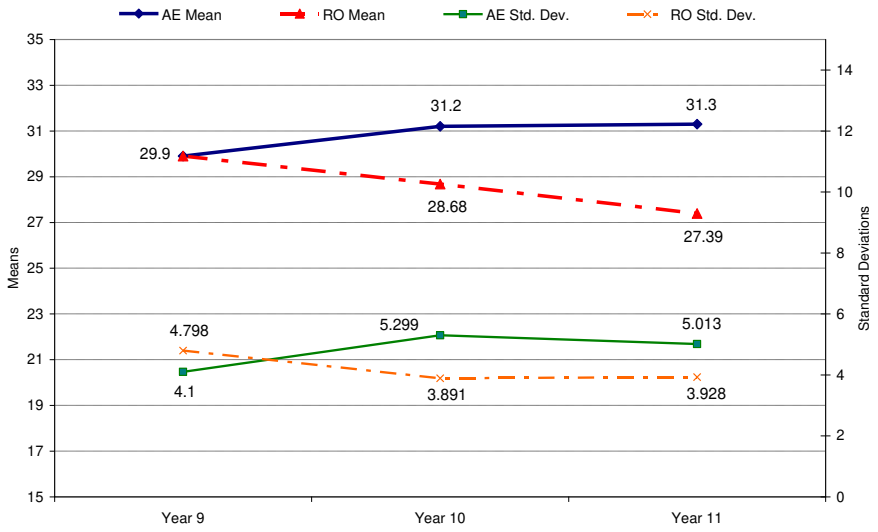

Figure 1
Means and standard deviations of learning variables I

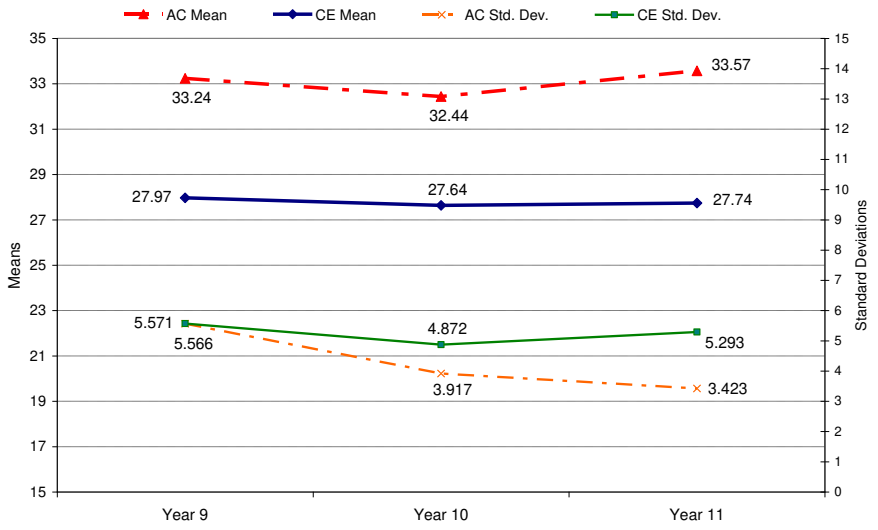

Figure 2
Means and standard deviations of learning variables II

AC and CE variables hardly change through time and may be considered attitudinal, whereas the same cannot be stated of AE and RO variables.

Tests of normality were performed for learning variables as well as difference variables in each grade, too.

The results show that in grade 9 conditions of normality are fulfilled for all variables while in grade 11 for almost none. From this the conclusion is to be drawn that balanced distributions still present in grade 9 tend to polarize in higher grades.

An analysis of variance was also carried out with the purpose of examining how learning preferences change with the progress of studies. As seen earlier, a precondition for variance analysis, the normal distribution of the learning variables, is fulfilled whereas the second condition, that is the homogeneity of variance, is justified by Levene-test, therefore there is no objection to performing an analysis of variance.

The results justify the former statements according to which the averages of variables AC and CE do not show a significant difference, while those of RO do, that is the role in the learning process of reflective observation and understanding (RO) changes (decreases) with the progress of studies, while that of active experimentation or productive application (AE) slightly increases.

Scheffe's a priori contrast test also throws some light on which grades' averages within a category have a significant or no deviation ($p<0.05$). The results prove that with respect to variable RO grades 9 and 11 show most deviations.

Finally the change through time of difference variables was examined with the progress of studies. Difference between these variables is seen to decrease significantly with students specializing in informatics in higher grades. It is all attributable to the increase in AE preference at the cost of RO, which means that practical application continuously gains dominance over reflective observation, the multi-aspectual examination of things and the search for their meaning. In its background it may be found that there is an increased number of practical courses such as for example computer programming or data base management in higher grades. Among the requirements for the development of the general education plan of the training is the improvement of students' skills at and familiarity with

- writing, running and testing the source code aiming at the solution of the algorithm designed by them,
- the conscious application of programming items,
- problem solving in the various programming environments,
- the creation of data tables, relation formation and normalization,
- the application of the basic elements of data base management systems,
- generating queries.

These syllabuses certainly offer a favourable opportunity for active experimentation, the application of skills in new situations which require different learning methods of students, in other words the preferred information processing methods alters.

3.3 The Problem of Defining Learning Style

The definition of learning styles was done on the basis of both Kolb's original values [8] and those of our own cut-points for learning style types. 72.73% of students (56 persons) did not change their learning style type. Of the remaining 21 students 12 shifted from the accommodator learning style to the diverger one, 4 from converger to assimilator, 3 from converger to accommodator and 2 from assimilator to diverger. In these cases the (AE-RO;AC-CE) value pairs apparently approximated an axis. Table 3 suggests that the converger style seems to be the most insensitive and the diverger style the most sensitive one to define the cut-points for learning style types. All the students classified as converger on the basis of our own results was ranked the same style according to Kolb's cut-points, too. The ranking of 41.18% of diverger students would change on the basis of the original Kolb's cut-points.

Table 3

Change in learning style classification

		Classification of learning styles (own, 2013)			
		Converger	Accommodator	Assimilator	Diverger
Learning style [7]	Converger	10	0	0	0
	Accommodator	3	8	0	0
	Assimilator	4	0	18	0
	Diverger	0	12	2	20

It was showed by Pearson Chi-square test ($p<0.05$) that the two types of learning styles classification significantly correlated with each other ($\chi^2=116.447$; df=9) and the Kolb's and my own classification coincide by the 63.2% of certainty ($\lambda=0.632$, $p<0.01$).

The classification of learning styles – based on our own value pair (+1;+6) – was compared according to grades as well (Figures 3-4). It is to be said that with the progress of studies the proportion of converger students significantly increases while that of assimilators, and even more of divergers, decreases.

The converger student is a real technical professional, who prefers logical thought of which he makes most in performing activities of a practical sort. He uses data founded on practical and tangible experience in order to construct his own system of skills and information. In his judgements he relies only on concrete facts and is not too keen on uncertain and inaccurate information. Being a „decision-maker", he enjoys problem situations. He is able to focus on the solution of problems by first thinking them over and then solving them. He is characterized by deductive thought, that is he readily applies the general skills, laws and rules to particular situations during problem solving. He is a pragmatist, with a narrow scope of interests and less flexible thought than that of his diverger companion. In case of the overwhelming dominance of this learning style (there were altogether 3

students of this kind) he often makes unfounded and hasty decisions and makes a mistake in the interpretation of the problem situation at hand. However, in a contrary situation, he is unable to concentrate on and solve a problem or adequately check his own ideas.

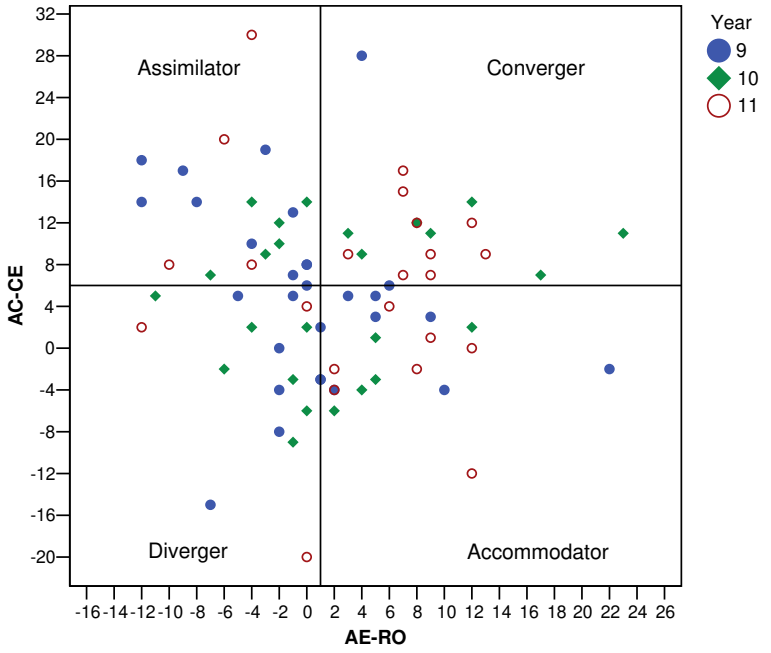

Figure 3
The classification of learning styles according to grades I

As seen from the above, students' learning style shifted in the direction mostly according to the specialities and requirements of subjects. Since learning style is an individual characteristic, a longitudinal examination would be even more precise in showing how this change took place from student to student. If this was reinforced, the stable and attitudinal personality indicator property of learning style could by all means be declared false.

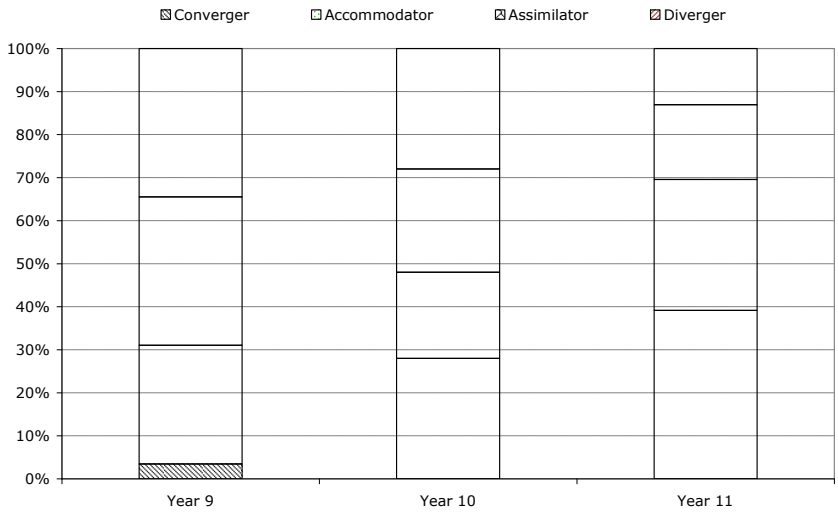

Figure 4
The classification of learning styles according to grades II

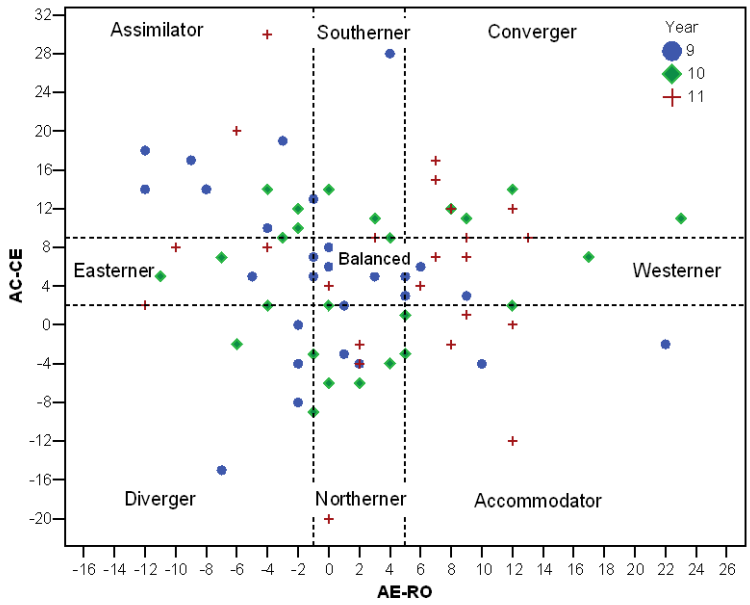

Figure 5
Learning styles in the nine-region model

Learning style classifications were analyzed by the nine-region Kolb model, too. As seen in the case of the four-region model and in our previous examination [1], many (AE-RO;AC-CE) value pairs fall in the proximity of one axis or both axes. In the nine-region model these were classified as Northerner, Southerner, Easterner, Westerner, or Balanced learning style. In this model the groups of those who have a definite or partly definite learning preference or who do not have one at all can be sharply distinguished (Fig. 5).

Following the statistical analysis of classifications it is to be observed that 53.25% of students have a strong preference in two directions, in other words they preserved their four-region preference, 40.26% have a one-direction strong preference, while 6.49% have no preference at all. The majority of students belong to Assimilator, Converger and Northerner (strong CE preference) learning style.

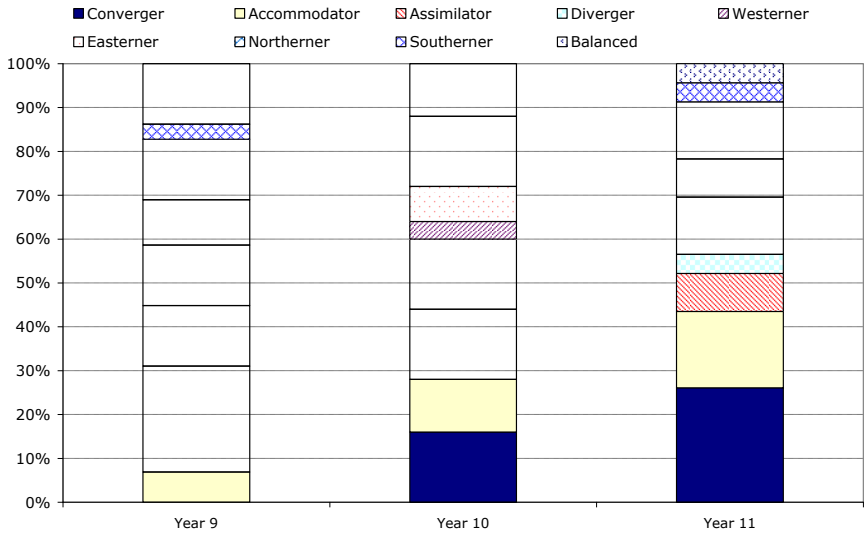

Figure 6

The distribution of learning styles according to classes in the nine-region model

The change of learning styles within the nine-region model through time was also tested (Fig. 6). The ratio of students with a two-direction strong preference rose from 44.83% measured in grade 9 to 56.53% by grade 11. It hardly altered in the case of those with a one-direction preference (from 41.38% to 39.13%), whereas the ratio of those of the balanced style without a preference significantly decreased (from 13.79% to 4.35%). Based on all that it is to be stated that the learning variables of students specializing in informatics polarize with the progress in studies by shifting from the balanced region first to the Northerner, Southerner, Easterner, Westerner and then to regions of a strong two-direction preference (χ^2=14.579; df=6; $p<0.05$). Again, only a longitudinal examination may provide absolute certainty.

In Fig. 7 the percentage distribution of our results in the nine-region model were compared with the results of the research Kolb did among 288 first-grade university students. [8] As can clearly be seen from the figure, with the exception of students of the Assimilator and Converger style, there are significant differences to be depicted. The results of 1286 MBA and 216 arts students in higher education were also published. [8] Our results tend to approximate those in the further regions.

Conclusions

In the course of our research among students specializing in informatics a latest version of Kolb's questionnaire for the empirical learning-model was tested (LSI 3.1). Making use of the results of our former longitudinal examination three hypotheses and one question were formed at the beginning of the research, the answers to which are given below.

H1. Learning variables in both dimensions are not normally distributed (students specializing in informatics have general preferences) and form a bipolar system.

Taking all students into consideration – in contrast to the results of the former longitudinal examination [1] – Kolb's learning variables follow a normal distribution, in other words, no speciality or preference generally typical of the group is to be observed. Normality is supported by Skewness, Kurtosis as well as the quotients of their faults together with the Kolmogorov – Szmirnov test.

The situation is, however, different if the various variables are compared in the individual grades. In grade 9 almost all variables follow a changeable normality distribution, while in year 11 almost none of them do. From this the conclusion is to be drawn that with the progress of studies polarization is more significant, that is the distinguished role of particular learning phases increases in number.

H2. In the dimension of preferred information type and information acquisition, perception the learning variables act similarly to attitudes. In this dimension the preferred learning variable is experience acquisition based on concrete experiences.

In the dimension of preferred information type and information acquisition, perception the mean values of the abstract conceptualization (AC) and concrete experience (CE) variables hardly change beside decreasing deviation values between grades 9 and 11, in other words, these two variables are to be regarded attitudinal. It is mainly the change in the mean values of CE that is minimal. The change through time of the results is greatly similar to that of former research.

However, there is considerable deviation in the (AC, CE) preference of these two variables. In this dimension students who participated in the earlier examination had a preference for experience acquisition, while those in the

present research preferred conceptualization and thought. If in both cases focus falls only on students of informatics, deviation will be similar. To explore the causes of this phenomenon it may be useful to have the same students fill in both questionnaires and then, following the evaluation of the results, the accuracy of either questionnaire is to be checked, too.

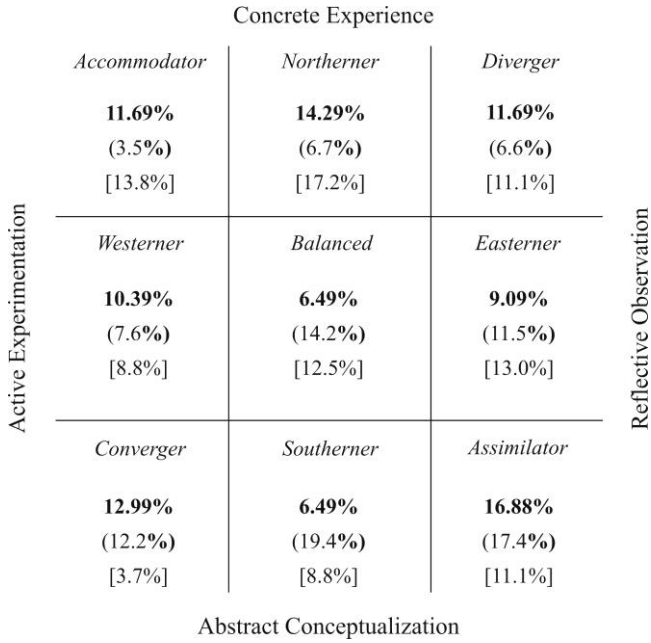

Note: Kolb and Kolb's results appear in brackets. First-grade students' in round brackets and arts students' in square ones. [8]

Figure 7
The comparison of learning styles in the nine-region model

H3. In the dimension of preferred information processing learning variables vary in a different way with a progress in studies. Productive application and experimentation is a preferred learning variable.

In the dimension of information processing the mean values of the reflective observation (RO) and active experimentation (AE) variables beside a slight change in distribution show variations with the progress of studies. RO values decrease, AE values increase, the mean values of the two variables deviate, the two lines produce a gap between them, that is the variables of this dimension do not show attitudinal tendencies.

Productive application and experimentation are increasingly becoming the decisive elements of the learning process with the progress in studies. The

behaviour of the variables of this dimension correspond to that seen in our former examination.

Q1. How does the ranking of learning style change with the progress in studies? Can any characteristic realignment or move be observed?

With the progress in studies the ratio of converger learning style students significantly increases whereas that of assimilator and diverger learning style students decreases. This is in agreement with Kolb's classification of the informatics profession, since the characteristics of converger students are the most suitable for studying this area.

Therefore the learning style of students moves in the direction most appropriate for subject specialities and requirements. Learning style is an individual characteristic, so it would take a longitudinal test to show how it varies from student to student. If this was reinforced, the stable and attitudinal personality indicator property of learning style could by all means be declared false.

Analyzing classifications in the nine-region model it is to be seen that more than 50% of students have a two-direction strong preference while almost 40% has a single-direction and approximately 10% has no preference at all.

In summary it is to be said that H1 is not at all, H2 is partly, while H3 is completely fulfilled, therefore the following theses are stated.

In the dimension of preferred information acquisition, perception learning variables are attitudinal.

In the dimension of preferred information processing learning variables (productive application, experimentation and reflective observation) vary with the progress in studies. Productive application and experimentation are a preferred learning variable.

References

[1] Tóth, P.: Learning Strategies and Styles in Vocational Education. Acta Polytechnica Hungarica, Vol. 9, No. 3, 2012, pp. 195-216

[2] Coffield, F. – Moseley, D. – Hall, E. – Ecclestone, K.: Learning Styles and Pedagogy in Post-16 Learning: A Systematic and Critical Review. Cromwell Press, Trowbridge, 2004, p. 165

[3] Kolb, D.A. – Fry, R.: Toward an Applied Theory of Experiential Learning. In: Cooper, C.L. (ed.) Theories of Group Processes. John Wiley, London, 1975, p. 277

[4] Honey, P. – Mumford, A.: The Learning Styles Helper's Guide. Peter Honey Publications, Maidenhead, 2000, p. 70

[5] McCarthy, B.: Using the 4MAT System to Bring Learning Styles to Schools. Educational Leadership, Vol. 48, No. 2, 1990, pp. 31-37

[6] Kolb, D. A.: The Process of Experimental Learning. In: Kolb, D. A. (ed.) The Experiential Learning: Experience as the Source of Learning and Development. Prentice-Hall, Englewood Cliffs, 1984, p. 288

[7] Kolb, D. A. – Kolb, A. Y.: The Kolb Learning Style Inventory – Version 3.1. 2005 Technical Specifications, HayGroup, Boston, 2005, p. 72

[8] Kolb, D. A. – Kolb, A. Y.: Learning Styles and Learning Spaces: Enhancing Experiential Learning in Higher Education. Academy of Management Learning and Education, Vol. 4, No. 2, 2005, pp. 193-212

[9] Kolb, D. A.: LSI Learning Style Inventory: Self Scoring Inventory and Interpretation Booklet. McBer and Company, Boston, 1985, p. 13

[10] Ősz, R. – Róbert, K.: The Use of Animations in Teaching Technical Drawing. In: Szakál, A. (Ed.): Proceedings of the 7th IEEE International Symposium on Applied Computational Intelligence and Informatics, Timisoara, 2012, pp. 311-314

Seven Passive Greenhouse Synergies

Marius M. Balas

Aurel Vlaicu University, 77 B-dul Revoluţiei, 310130 Arad, Romania
e-mail: marius.balas@uav.ro

Abstract: This paper describes the effects of applying at a large scale a new agricultural system, based on passive greenhouses, from a system engineering perspective. Passive greenhouses use only the renewable energy sources: geothermal, wind and sun, by means of cool water heat pumps, wind turbines and photovoltaic panels. Thereby they are fully free of any energetic infrastructure and can be installed in remote areas, even in deserts. They offer a fundamental sustainable agricultural resource and a global ecological reconstruction opportunity. The surface needed by a greenhouse is much smaller compared to an equivalent conventional agriculture exploitation. The huge unshackled surfaces that result if using passive greenhouses may be reconverted into forests, pastures, orchards or pounds, thereby decreasing the carbon footprint. The main obstacle is the high investment cost, which can be minimized by optimizing the size of each energy source according to the user's specifications, the local climate, and by intelligent control algorithms. The equipment prices are constantly decreasing and the newly created market will generate jobs and give a boost to related industries. A holistic view of a the passive greenhouse farming system reveals a set of synergies that increase chances for future implementation.

Keywords: sustainable energy; passive greenhouse; heat pump; wind generator; photovoltaic panel; Watergy; carbon footprint; environment reconstruction; intelligent control

1 Passive Greenhouses. The Renewable Energy Synergy

Passive Greenhouse PG is the agricultural equivalent of the Passive House. Instead of hosting people, PGs are hosting plants. A passive house reduces its ecological footprint by minimizing heating/cooling energy requirements, using special construction solutions. At the same time, they use only renewable energy sources [1]. The most effective renewable energy source that supports the Passive House is geo-thermal, by means of the heat pumps. Heat pumps may be found in two constructive versions: either with cool water (closed or open circuits) or simply with air [2]. Other common renewable energy solutions are wind turbines, solar panels (photovoltaic or thermal) and biomass [3].

The same ideas are animating the PG concept, which is even more radical: a PG uses *exclusively* renewable energy sources and is totally independent of any energetic infrastructure: gas, electricity, hot water, etc. We coined the term PG for the first time in 2004 [4]. We continued to develop this subject by some other papers and book chapters and in 2010 a more comprehensive chapter issued at an open publishing house [5]. The 2010 chapter is briefly exposing the essence of our approach. The present work is mainly synthesizing the argumentation that stands behind the PG concept and underlines numerous synergies that encourage a great number of potential users to invest into PGs.

We can now point to the first synergy that opens the way for the others:

1) **The renewable energy synergy:** *A PG can use in situ, with no grid conversion, all the significant renewable energy sources: geo-thermal, wind, solar and biomass*

The first three energy sources are found in any passive building, yet biomass is an unavoidable byproduct of greenhouse technology. The fact that this by-product can be turned into energy and fertilizer in situ is an asset of greenhouse technology, not fully exploited now, but tested at 1:1 scale with very positive results [6] (see next section).

All the components incorporated in PGs have been produced for decades and have created their own markets. The specific technical constraints are well known and no particular risks should be expected. On the other side, only one major obstacle stands to be removed: the initial investment price. The real contribution of the PG concept and its potential effects over our energetic, agricultural and food systems is to reveal hidden resources and their beneficial consequences, from the system engineering perspective, and to show ways to minimize the investment costs.

2 The Watergy Synergy

A particularly important new concept issued by the greenhouse scientific research is the *Watergy*, an integrated approach for water treatment, building climate control and food production [7]. The Watergy concept is materialized by a *closed greenhouse*, a well-insulated greenhouse, provided with devices able to condense the water vapors. A closed greenhouse can re-circulate the initial amount of water, and even produce fresh water out of salt or grey waters [8]. A related domain is the *Advanced Life Support*, bringing together research aimed at the habitation of remote areas (desert and polar regions) or for long-term space journeys. The Watergy is a key opportunity for arid regions with low water resources: the Gulf region, Sahara, Central Asia, Australia, south-western USA, Mexico and some Mediterranean countries. Temperate and cold climate countries could also use some of the Watergy principles.

Besides the specific water economy features of the closed greenhouse, any conventional greenhouse can be biased in accordance with the watergy principles, so we can point a second synergy:

2) **The water synergy:** *PGs need water at the same time, for the heat pumps and for the plants. Greenhouses are at the same time, water consumers and water recyclers*

A consequence of this fact is that one can install PGs anywhere one can find or build fresh water reserves (rivers, lakes, natural or artificial aquifers, glaciers, rain, even sea salt water) or where water can be transported and stocked.

The most audacious approach in this issue is represented by Fiwihex closed greenhouse, involving a great artificial aquifer that stores warm water and is synergistically used as a bioreactor, able to produce biogas [6]. Fiwihex of Netherlands is specialized in high efficiency fine-wire heat exchangers, which in this case, may replace heat pumps, thanks to the natural stratification of the different temperature water layers favored by the great volume of the aquifer. The high heat capacities of the water and of the aquifer rocks enable the storage of great amounts of energy. It is proved that during a year, the greenhouse effect can produce, in a non-ventilated closed greenhouse, more energy than is actually needed. The supplementary energy stored into the aquifer can sustainably support the Fiwihex closed greenhouse.

3 The Passive Greenhouse Construction Synergy

3.1 The Passive Greenhouse System

A standard PG aggregates three complementary energy sources:

A. ***A heat pump***, extracting energy from cold phreatic water or another type of aquifer

The heat pump is the main PG energy source, in an implicit open circuit configuration, with at least two water wells (cold and warm).

3) **The construction synergy:** *Drilling water wells for the heat pumps is synergetic with the watering of the plants*

Geo-thermal energy is reliable and stable, and the related heat pumps can be used for heating, as well as, for cooling. However, heat pumps cannot work totally independently; they need 15-20% of their nominal power for re-circulating the water of the exterior circuit. Instead of connecting to the electric energy distribution network, PGs are provided with two secondary renewable energy sources:

B. ***A wind generator***

C. ***A matrix of solar photovoltaic panels***

Wind and solar energy are extremely variable compared to geothermal, but complementary, so their aggregation is useful. With the help of a DC battery one can store the wind and the solar energy, supplying the heat pump and all the PG's electrical equipment needs. Besides charging the batteries, the solar panels may shade, at the same time, the plants, when solar radiation is excessive and the greenhouse effect would overheat the greenhouse. Because the secondary energy sources have to produce only a small part of the nominal power of the heat pump, their sizes and prices are correspondently low.

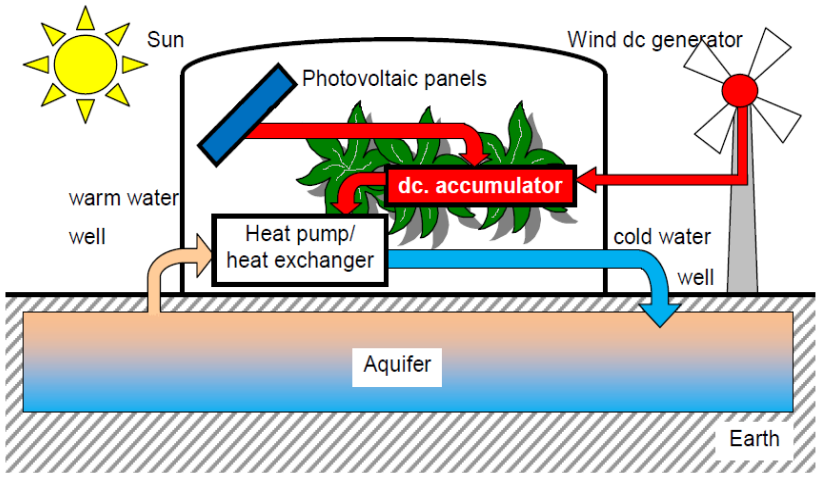

Figure 1
A generic Passive Greenhouse with aquifer

One of the first greenhouses equipped with a heat pump, working in parallel with a gas heat source, was mentioned in 2007 in one of the key works of the greenhouse theoretical domain [9]. Since then heat pumps are currently included in the offers of greenhouse producers. It is to remark that the first attempts to fit greenhouses with heat pumps were rather reserved, with tendency to oversize the heat pumps power output, which increase unnecessarily the investment costs.

PGs are proposing more than heat pumps connected to electricity or gas distribution networks, which means infrastructure investment costs. PG means a full independence of any energy or water utility infrastructure. This is cutting the umbilical cord that keeps greenhouses stuck to localities, and offers them an enormous development potential in remote areas.

It is to remark that PGs are directly using the energy, avoiding the costs associated with a grid connection, which charge the average renewable energy systems.

While the Fiwihex closed greenhouse concept implies great built surfaces and huge artificial aquifers that are used also as bioreactors, which altogether increase the costs, the manual labor and the system's ecological impact, PGs propose a minimalist yet effective architecture, suited to any possible user, starting with the small family or hobby solar greenhouse up to the largest farms.

The main PG's disadvantage is its high initial investment cost. The optimal sizing of the energy sources and appropriate tunings for the PG control algorithms may be achieved only under computer assistance and expert guidance.

3.2 The Computer Modeling of the Passive Greenhouse

Many greenhouses with heat pumps were built recently, in different countries, Romania included. The weights of heat pumps in their energy balance are different. The experience of the greenhouse builders is growing in this matter, and a large amount of specific knowledge about greenhouse construction and interaction with the environment is now being accumulated. The ultimate realization of this knowledge will be achieved when we can embed it into computers. Most of our previous PG studies used computer models that we began to develop since 2004, starting from the experimental data issued from the Experimental Greenhouse of the Southern University of Toulon-Var, France. When such a model originates out of experimental data, its validation is not a problem and its confidence degree is sufficiently high, allowing us to assume results of simulations following a large variety of scenarios. The models' parameters are tuned and optimized for the most significant operating points. After that, the models are able to interpolate the evolution of the greenhouses' variables when fed with new input data. The input data may consist of technical specifications for various types of equipment, including investment and exploitation costs, they may reproduce the behavior of the greenhouse under extreme climate conditions, etc.

Two main strategies were applied for the identification of the Toulon Greenhouse:

- *The synthetic approach*, consisting of identifying the models of the significant operating points by neural networks and aggregating the resulting models by a fuzzy fusion procedure [10]

- *The structural approach*, consisting of identifying the models of the significant operating points by structural models (differential equations of the main physical phenomena) and tuning the physical parameters of the models with genetic algorithms [11], neural networks or other optimization methods (see Fig. 2) [12]

Our own choice continues to be the structural ISO (input-state-output) deterministic model, like the one in Fig. 3, able to clearly and distinctly estimate the evolution of the state and output variables (inside temperature, ventilation, air and soil humidity, CO_2 concentration, etc.), under the influence of the input variables (external temperature, solar radiation, humidity, wind, heating/cooling power, etc.)

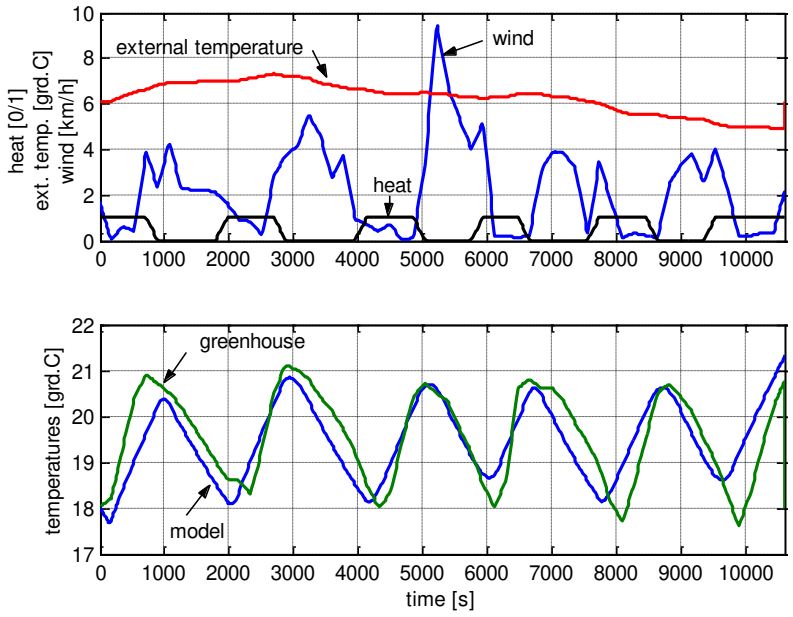

Figure 2
The identification of the greenhouse model starting from experimental data

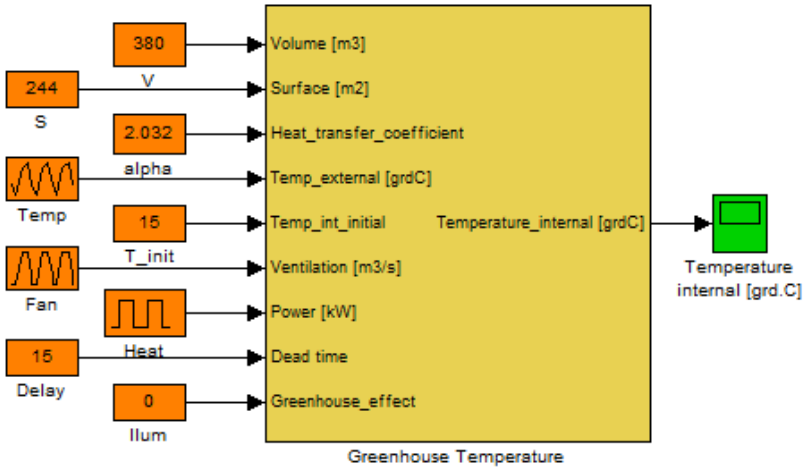

Figure 3
A Matlab implementation of the structural greenhouse model, for the inside temperature

3.3 The Passive Greenhouse Control

The PG automated control is necessarily depending of its construction. Greenhouses are highly nonlinear and variable. Many quantities must be taken into consideration, which is not a trivial task. Some of them are extremely uncertain, like for instance the estimation of the crop development, which is needed for a correct feeding of the plants with nutrients and water. In the PG case, a supplementary difficulty occurs: the high inertia of the heat pump, which is not able to change its power as fast as a gas burner device, for example. On the other hand, the precision asked when controlling all the greenhouse parameters is sufficiently weak. In other words, greenhouses are rather tolerant. This suggests the PG system as a perfectly compliant system with the application of intelligent control algorithms.

The usual greenhouse control equipment belongs to the PLC family, and in recent years, all the facilities demanded by remote PLC operation and networking became fully accessible.

Two strategies are bounding the greenhouse control algorithms field:

a) The *Optimal Control* [9], extremely precise and sharp, which is well suited for standardized greenhouses (namely Venlo)

b) The *Expert Control* [5] under its different versions, including the fuzzy-expert control, which is suboptimal, yet extremely robust, adaptive and flexible. The expert systems are able to embed heuristic solutions and can cope with the specific knowledge and specifications of each particular user

4 The Carbon and the Trophic Synergies

The property of the above generic PG, that is ensuring its individuality, is its total independence of any infrastructure, except transportation. That is why PGs may be associated in some points with the class of *the Portable Greenhouses*.

All the monitoring and automated control demanded by PGs may be executed by means of the Internet, or by any other telecommunication systems so human presence is necessary only during farming activity. As a matter of fact, even the human presence will be eventually made unnecessary, when applying another powerful concept that is emerging these days: *the Autonomous Greenhouse*.

This feature makes possible a new global agricultural system that has the potential to boost the performances of our food system and the quality of our natural environment, at a planetary scale. The previous papers containing the argumentation that supports the concept of the PG Agricultural System are recalled in [5] and detailed in its bibliographic references. In the following sections, we will provide a review of this matter.

4.1 The Passive Greenhouse Control

The *carbon footprint* is the total set of greenhouse gas GHG emissions, like CO_2, caused by a certain process. Our civilization produces a huge carbon footprint because of two specific activities:

- *Extremely rapid burning of the fossil fuels* accumulated during million years. The oxidations are extracting the atmospheric oxygen and replacing it with CO_2 and other chemical compounds

- *Deforestation*. Because of their great size compared to other plants, trees are able to compensate for the growth of CO_2 atmospheric concentration. Their metabolism demands great quantities of CO_2 and the release of oxygen O_2. The continuous reduction of the forest enhances our carbon footprint.

The processes that reduce the CO_2 concentration are known as *carbon offsets*. The most rightful carbon offset strategy would be the *reforestation*. Trees are storing carbon through photosynthesis, converting CO_2 and water into oxygen and plant matter. However, reforestation is expensive and long lasting.

As one can observe in the literature, the daily CO_2 consumption in greenhouses is very high (100-250 kg/ha), similar to a forest, due to the high density of the plants and to the ideal growing conditions.

Increasing the surface occupied by PGs is therefore more or less equivalent to reforestation. Besides their own carbon offset, greenhouses are also generating a collateral carbon offset, due to the consequential ecological reconstruction.

4.2 The Ecological Reconstruction

A land surface occupied by PGs produces a certain carbon offset but its surface is ecologically depreciated. However, the extensive use of PGs offers us the opportunity to reconsider the global structure of the agricultural lands and to reconstruct huge surfaces, in the proximity of our towns and villages. The price to be paid is to sacrifice some remote areas, where the PG farms are installed.

The following assumptions support this idea:

- Using the same surface area, greenhouses can feed at least 5-10 times more people than cereal cultivated lands;

- Sacrificing certain remote or inappropriate zones, for conventional agriculture in the favor of the PG farms, is feasible

- Replacing the cereal cultures with greenhouses, frees huge land surfaces

- The unshackled surfaces that result, may be converted into forests, pastures, orchards, pounds, etc.

We can formulate now a fourth synergy:

4) **The carbon offset synergy:** *Besides its own carbon offset effect, extending the PG surfaces creates a supplementary carbon offset thanks to the consequent ecological reconstruction of the newly liberated surfaces*

4.3 The Passive Greenhouses and the Trophic Chains

Feeding the human population can be accomplished by two food chains, supported by the capacity of the plants to produce vegetal matter by photosynthesis:

a) A three trophic levels chain: *plants → animals → humans*

b) A two trophic levels chain: *plants → humans*

A lot of energy is lost at each transfer from a trophic level to another. That is why the food chain **a**) needs much more agricultural surfaces than the food chain **b**. By the help of the greenhouses we can further reduce the surface demanded by the food chain **b**). However we fail to imagine a totally vegetarian population and we must find sustainable solutions to keep food chain **a**). The ecological reconstruction can sustain a new type of zootechny, that lets the common species of animals that are now fed with cereals (cattle, pigs, birds, etc.) to live in a natural way, like sheep for instance. The animals' quality will significantly improve in all senses, and their carbon footprint will decrease. We may think about cattle for instance: avoiding feeding them with corn and letting them out of the stables to pasture is perfectly suited to their nature and it will obviously decrease the DHG emissions.

We find here a fifth synergy:

5) **The trophic synergy:** *The PG agricultural system is directly reinforcing the two trophic levels chain and in the same time is increasing the quality of the three trophic levels chain*

Besides economical or technological advantages, a greenhouse based food system reduces the production uncertainties, the risks of bad weather and climate changes, pests, diseases, etc.

5 The Economic Synergies

Renewable energy sources are expensive. PGs are usually provided with three items, a heat pump, a wind turbine and solar panels. It is natural for an investor to ask for accurate investment analysis and business plans. The only way to make feasible such a structure is its size optimization associated with a smart control, in order to avoid over-sizing and energy or crop waste.

Each of the necessary energy sources has created and established its own market. The designer's task is just the correct choice of products. The nominal power of each component and the construction parameters of the greenhouse must be carefully balanced, taking into account the climatic features of the location and the exploitation characteristics, which may differ according to each user's specifications.

Our main tool is the computer modeling. Besides handling of the internal temperature, which is the key factor, the simulations can assist us in any particular optimization problem, as for instance the minimization of the investment costs.

A recent investment analysis performed by a Romanian company for the 2012 Romanian market, reveals the following encouraging facts, which prove the feasibility of the PG concept:

- The necessary equipment for building different PG configurations is available and a related market of builders that have experienced greenhouses provided with heat pumps is functioning

- Many greenhouse farmers have already successfully experienced heat pump greenhouses

- The evolution of the prices is favorable for all components

- A representative price of a fully equipped 1000 m^2 PG is about 285,000 RON (62,400 EURO) comparied to 220,000 RON (48,200 EURO) for the same greenhouse provided with gas burners (when growing tomatoes); the infrastructure prices (gas network connection) is not taken into account

- The estimated payback period is approximately seven years

The renewable energy market is now oriented towards passive houses. In great lines passive houses and PGs are sharing the same technological platform. If the PGs will create a new market, this will boost the whole renewable energy market (higher trade turnovers, lower prices, more jobs, etc.), with beneficial effects over the economies of the countries involved into the PG agricultural system development.

Therefore we can point the sixth synergy:

6) **The economical synergy:** *PGs are already feasible and use available technologies and homologated components, which are creating a fast growing market; they have the potential to boost the renewable energy market and to generate a sustainable economic growth*

6 The Political Synergy

A last, but perhaps the most important of the synergies, is related to some of the fundamental objectives of our society:

7) **The political synergy:** *PGs are appeasing some political goals that seemed contradictory so far: economical growing and efficiency, increasing the number of jobs, reducing the carbon footprint and increasing the carbon offset, improving the quality of life by a structural ecological reconstruction of our environment and removing many of the agricultural and alimentation risks*

Conclusions

The Passive Greenhouses main assets are 100% free renewable energy and the quality of being deployable virtually anywhere one can find or construct aquifers. A global Passive Greenhouses agricultural system is made possible by a chain of synergies that support its feasibility. We outlined seven synergies: the renewable energy, the water, the construction, the carbon offset, the trophic, the economical and the political synergies.

Such an agricultural system gives us the chance to repurpose a great deal of the existing agricultural terrain and to ecologically reconstruct our environment in a more efficient and ecologic way.

This approach relies exclusively on existing renewable energy sources and has no significant technological risks or ecological impacts.

The main obstacle to be removed in Passive Greenhouses is the high investment cost, which can be partially addressed by carefully optimizing the construction and the energy sources design, and using intelligent control algorithms.

References

[1] Gröndahl M., Gates G.: The Secrets of a Passive House, New York Times website, September 25, 2010, Retrieved October 4, 2012

[2] Heat Pump Statistics - Outlook 2012, European Heat Pump Association website, Retrieved October 4, 2012

[3] Renewable Energy Manual, Iowa Energy Center website. Retrieved Oct. 4, 2012

[4] Balas M. M., Cociuba N., Musca C.: The Energetic Passive Greenhouses, Analele Universităţii Aurel Vlaicu din Arad, Arad, 2004, pp. 524-529

[5] Balas M. M., Musca C., Musca S. V., The Passive Greenhouses, in *Paths to Sustainable Energy,* Editors: Nathwani J. J. and Ng, A. *InTech*, Dec. 30, 2010, pp. 75-92

[6] Nederhoff E. Closed Greenhouses and Heat Producing Greenhouses, The Grower, New Zealand, No. 61, 2006, pp. 67-69

[7] Watergy. Water and Energy Efficiency, Energy Efficiency Global Forum, Orlando, USA, March 27-29, 2012. *http://www.watergy.org/* Retrieved Oct. 8, 2012

[8] van Straten G.: Investment in Novel Closed Greenhouse Systems: the Watery design and other developments, First Workshop on Investment in Protected Cultivation in GCC Countries, Abu Dhabi, 2006

[9] van Ooteghem R. J. C.: Optimal Control Design for a Solar Greenhouse, Ph.D. thesis, Wageningen University, 2007. Wageningen UR site (Wageningen Dissertations). Retrieved Oct. 9, 2012

[10] Pessel N., Duplaix J., Balmat J. F., Lafont F.: A Multi-Structure Modeling Methodology, in Soft Computing-based Modeling in Intelligent Systems and Technologies, edited by Balas V., Fodor J. and Várkonyi-Kóczy A., Springer, 2009, Vol. 196, pp. 93-114

[11] Balas M. M., Duplaix J., Bouchouicha M., Balas S. V.: Modeling the Wind's Influence over the Heat Flow of the Greenhouses, Journal of Intelligent & Fuzzy Systems, 2008, Vol. 19, No. 1, pp. 29-40

[12] Balas M. M., Musca C., Musca S. V., The Passive Greenhouses, in Paths to Sustainable Energy, edited by Nathwani J. J. and Ng, A., InTechOpen, 30 Dec., 2010, pp. 75-92

Pros and Cons of the Renewable Energy Application

Péter Kádár

Power System Department Faculty of Electrical Engineering, Óbuda University, Bécsi út 96/B, H-1034 Budapest, Hungary
e-mail: kadar.peter@kvk.uni-obuda.hu

Abstract: Nobody questions the reason for existence of fossil power plants meanwhile the acceptance of the renewable tools is often problematic. Of course the rationales based on the experiences of decade long operation the picture is not clear. The world turns to the consciousness that well-ruled renewables contribute to the sustainability. We summarize dozens of pros and cons and we are going to suggest ways to fit the renewable resources into the power system.

Keywords: power system, renewable sources, integration to the power mix

1 Introduction

Immanuel Kant in his work „The Critique of Pure Reason" [1] had two controversial logical statements. He proved both of them right by pure logic. One is deduced on the left side page of his work the other on the right side page. It shows that the perception of the real word is done in different ways and only the logical (and honest) thinking don't obviously arrive at the unique conclusion. This dual situation characterizes the application of the renewable energies, too. These techniques move into the mature phase, there is not too much doubt about the operation. The long term effects are not yet cleared and this provides the basis for the eternal debate. Almost all the assumptions are reasonable, only the conclusion differs if they are good or not for our future. In the following presentation we describe a set of pros and cons of the most widely used renewable resources. Looking for the optimal power generation is a standard problem of energy policy. [2-8]

2 Hydro Energy

The hydro power application is one of the oldest technical solutions. For electricity generation it has been used almost for 140 years. During these years a huge amount of knowledge was accumulated. Through the construction and operation of the more than 100.000 establishments nearly all the possibilities and contingencies were experienced. There are no surprises all the effects can roughly be forecast. The hydro complex consists of the hydro power station and waterway/reservoir in large extension, e.g. dams. It is in the focus of debates.

Advantages of the damming

- Renewable energy source
- The operation is CO_2 free (theoretically)
- Energy source comes to the turbine, no external transport is required
- The running water slows down, doesn't wreck the bank
- The environment is not loaded by heat
- The dam can protect areas from flood
- Waterway transport is more secure
- The number of the personnel is low
- Fast starting, easy control
- Black start capability
- Efficiency above 80%
- High lifespan (over 100 years)
- New wild water areas are formed
- Touristic highlights, holiday environments

Risks

The longer list of the problems comes from the huge number of the detailed analyses of the last hundred years.

- The specific area usage is the worst in case of hydro energy. Large areas are flooded:
    - Sobradinho, Brasil – where 1.050 MW were harvested from 415.000 hectares – 0,25 W/ m^2!!
    - Venezuela Guri complex – where 10.300 MW run on 426.000 hectares – 2,4 W/ m^2). [1]
    - Balbina, Brasil – where 2500 km^2 Amazonian rain forest was flooded for 250 MW – 0,1 W/m^2. It became the symbol of the ecological destruction beyond reason.[2]
    - Gabcikovo, Slovakia – where 720 MW was built in with 5300 hectares – 13,5 W/ m^2

[1] Environmental criteria for site selection of hydroelectric projects, The world Bank, 2003
[2] http://ergobalance.blogspot.com/2007/07/hydro-not-so-green.html

  - Itaipu, Brasil – where 14.000 MW were harvested from 135.000 hectares – 10,3 W/ m^2
- The hydro energy is not really CO_2 free. In case of careful design the specific emission is low, but we can't forget the iron furnacing and cement burning emission. In a bad case the eutrophication produces million tons of methane.[3]
- If we project all the investment costs to the produced electricity, we get really high specific electricity price (we normally have other purposes too e.g. flood protection, irrigation, shipping, etc.)
- Construction takes 5-15 years
- No protection from flood and drought
- Significant cultural heritage has been devastated by the inundation (e.g. in Aswan, Egypt or at Merowe plant in Sudan.[4]
- An interesting specific number is the *displaced persons/MW*. At Mozambique/Cabora Bassa – 120 person/MW (total 249.000 persons), in China, Three Gorges – 66 person/MW (total 1.200.000 persons).[5]
- The dams are built with large heading in front of the former waterfalls. The Nile dams tuck away the ancient cataracts, the Iguacu dam the Guaira falls in Brasil[6].
- Vessel traffic is traversed
- The natural sandy bank is changed into rocky shore. Pay gravel never comes anymore.
- Level of the underground water rising.
- Due to the slowing down of the flow the floating drift subsides
- Beside the headwater channels the floodplains are going to be drained
- Below the dam the riverbed is deepened and the level of the underground water is sinking
- Large agricultural areas are taken out from the food production
- Masses of peoples must be resettled (e.g. China – Three Gorge Dam – more than 1,5 millions)
- The peak power operation erodes the bank
- The dynamic water level changes disturb the fish reproduction
- Earthquake, mud sliding and terrorist attacks cause dam break and catastrophe.[7]
- The excavation of the sediment in the upper reservoir hurts the natural drinking water filtering structures

[3] Vincent St. Louis: Hydro, not so Green?, Canadian University of Alberta, http://ergobalance.blogspot.com/2007/07/hydro-not-so-green.html

[4] http://www.meroe.hu

[5] IEEE power and energy magazine july/august 2008

[6] http://tourismplacesworld.blogspot.hu/2011/06/guaira-falls-brazil.html

[7] Epic Vajont Dam Disaster, Italy, 1963: Manmade or Natural? http://www.semp.us/publications

- The excavation work produces new sediments that can cover the previously clean gravel.
- The fish don't like the banks covered by concrete or asphalt.
- The shallow water is overheated in summer and the fish may perish
- The wastewater is cleaned biologically and mechanically into the natural rivers. The slow flowing results eutrophication, for enrichment of polluting materials.
- In North Canada in the frame of La Grande/James Bay project 2830 km^2 area was flooded. The decaying flooded forests produce toxins that mean high health risk for the aboriginal local Inuit people.[8]
- The damming in the desert (e.g. Nile – Aswan, Egypt or Merowe, Sudan) causes losses in three ways: evaporation in the hot air from the large surface, leaking in the large sandy riverbed and excessive irrigation.
- At high dams the new water level washes hillsides and slip into the water. The wandering wave may break the dam, too.
- An ethical question is the disturbance of aboriginals and the ecology of the flooded area. The eutrophication of the water (decaying forest) pollutes the lake and the drinking water reservoirs.
- Is it really necessary to exploit the renewable energy resources of black Africa (Congo river) and transmit the electricity to the „developed" Europe?
- Large dams retain the thousand year old water sources: Turkey <–> Syria on Euphrates river; USA <–> Mexico on Colorado River.

Figure 1. River Bistrica in Romania 2011

[8] James Bay – Where two worlds collide; National Geographics – Water 1993 November

Figure 2. Dried riverbed of deviated Bistrica River in Romania 2011

3 Wind Energy

Wind energy application in the last four decades has matured phase. The most widely emphasized pros and cons are the following.

Pros

- renewable energy
- low maintenance cost
- medium (not high) price
- few residual waste materials

Against

- volatile production
- hard to estimate (precisely)
- noise disturbs the environment
- birds are in danger
- drying of the soil

Since the wind application is quotidian practice nowadays more deemed problems and their solutions are known. Here we list some assumed but not real obstacles against wind based energy production. Fortunately there are satisfactory solutions.

We discuss the sudden loss of wind production (con), some theoretic integration methods and recommended manners. [10]

3.1 Sudden stops of wind power plants

Network problem

As the following record shows 500 MW of wind production dropped suddenly (and resumed to operation). Due to network faults (line, breaker or transformer problem) one or more turbines can be isolated which causes a stop. It is not a specialty of wind generation it can happen to any other plant.

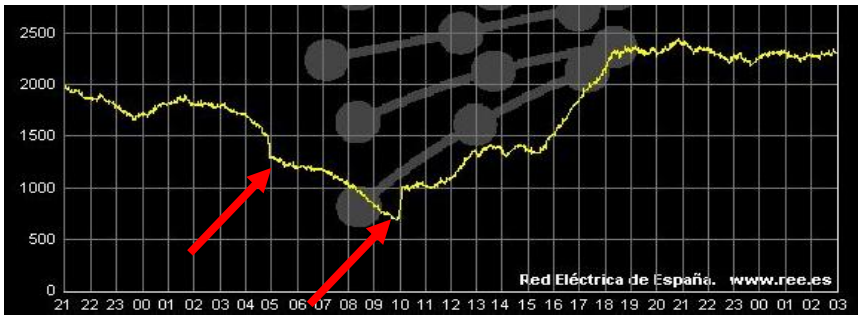

Figure 3. Outage of wind plants for network fault in Spain

Behavior in case of frequency deviation

The turbines have frequency protections that turn them off in case of under-frequency. It happened on 4th of November 2004 when the European power system split into three parts and the south-West part had under-frequency for the lack of production capacity. Similar protection operates in nuclear power plants, too. Nowadays the new frequency dependent wind turbine control can alleviate the load-frequency balance: in case of over-frequency (over 50 Hz) cuts back the output power, on the opposite side produces the appropriate maximum.

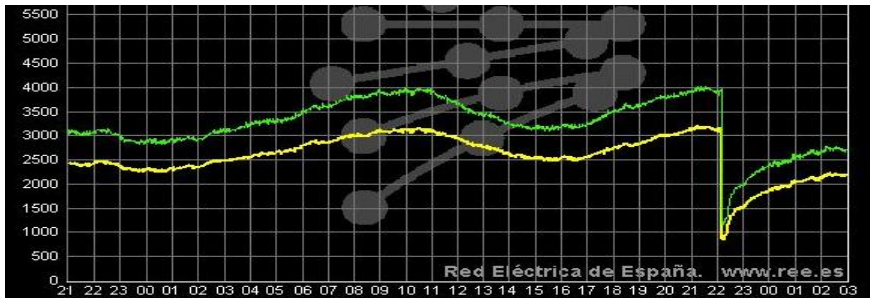

Figure 4. Fall out of wind plants for frequency problems in Spain on 2006.11.04.

Cut off by storm?

The individual wind turbine's cut off speed is between 25-30 m/s. In case of stormy wind each element of the plant makes an emergency stop. The total dropped power can reach some hundreds of MWs. – Is it a real problem to lose 200 MW? – NO. It is a normal daily event to lose any thermal power plant unit up to 1000 MW. The power system withstands it. On the other side the stormy weather can be well forecast, so this event doesn't reach the system unprepared.

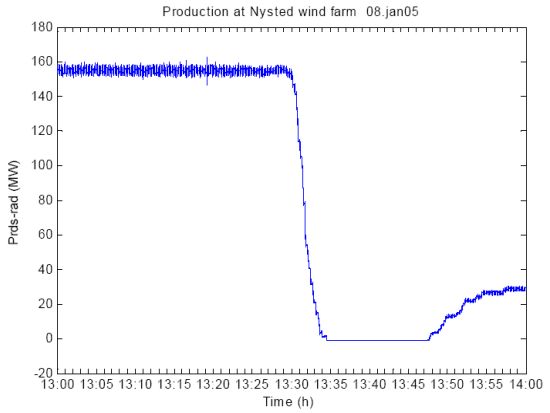

Figure 5. Windpark output during storm in Denmark[9]

Is the pumped storage plant an indispensable need to wind capacities?

There is an opinion that a high ratio of the hydro plants in the national power mix and/or the pumped storage plants would allow for large scale wind integration. We can state, that these energetic devices make the integration easier, but these are not indispensable elements of the system. Good examples are the German, Danish and the Dutch energy mix. The wind energy can be planned in the day-ahead energy portfolio. The deviation comes from the forecast errors it is generally controlled by oil, gas and coal fired plants, but as a curiosity can we mention that in Germany some nuclear plants participate in the wind generation balancing (e.g. Kernkraftwerk Isar). A Hungarian proposal is to realize small scale Pumped Storage systems too.

[9] Joana Rasmussen: System Protection Schemes in Eastern Denmark

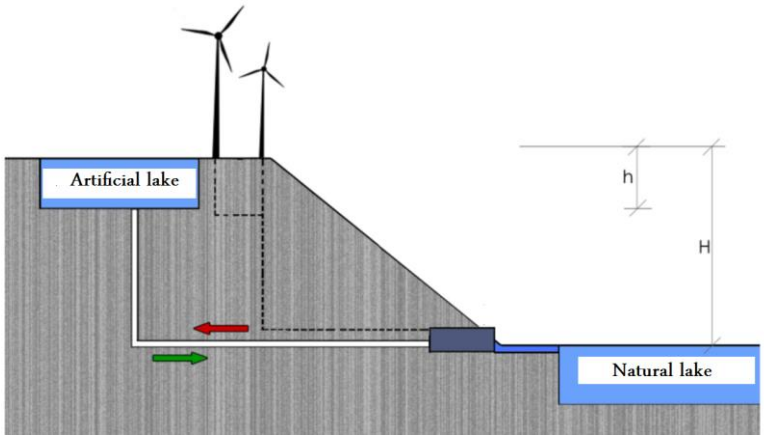

Figure 6. Micro pumped storage plant[10]

Generation volatility

Due to the steep operation characteristics of the turbines the wind speed changes are amplified in the power output in quadratic measure. The local turbulences equalize each other and the statistical sum of the individual productions is really smooth. The diversification in space helps also this smoothening. In case of bulk plants or branches of plants the individual upload and download gradients are also moderated.

3.2 Ideal solutions

Although there are many paper solutions for the integration, not all are viable.

Store the energy in form Hydrogen

As the load and wind generation peaks are really independent a good idea is to store the wind energy. A classic demonstration was made on Utsira Island in Norway[11], where the surplus wind energy was converted and stored in form of hydrogen and it was reformed into electricity by fuel cells. The system works, technically it is realistic. The only problem is that the total electrical efficiency of the loop (hydrogen generation, compression, storage, fuel cell, etc.) is not higher than 60%. So it closely doubles the wind energy price – without taking into account the really high investment cost.

[10] Courtesy of F&L Ltd.

[11] The Utsira wind –hydrogen project; IPHE ILC meeting, Rio de Janeiro, March22, 2005; Presentation on behalf of Hydro -Trygve Riis

A better option is to use the hydrogen directly in traffic by gas engines or by fuel-cells. Not only the surplus wind energy but the "early morning valley time" generated energy can be transformed into hydrogen form.

Co-control with gas engines

The widely used medium size (1-3 MW) cogeneration (CHP) gas engines can be involved in the wind-deviation control. A set of the micro CHPs through virtual power plants (VPP) can be co-controlled too.

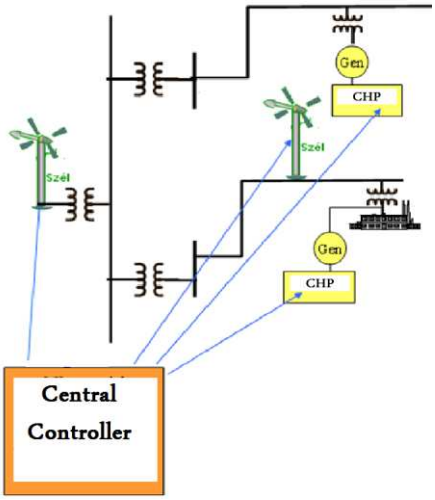

Figure 7. Fig. Co-control of different production characteristics

What capacities can be used for control?

In the power system more generation/consumption capacity is built in than are usage in a moment (actual power – built power). Almost all elements are controllable but practically only some parts, some large elements are involved into the power balance control. The exploitation and the connection of the up to this time not used control capacities are huge reserves how to balance the non planned deviations. The smart technology helps it. Unfortunately the present control practice is determined by financial interest and contracts that will not be easily changed without hurting interests of actual energy producer.

3.3 Real solutions

The DSM and the Smart grids

By the traditional paradigm we produce as much energy (power) as we need. We follow the need to have a balance between demand and production. The same result can be reached by controlling demand. The passive and active Demand Side Management (DSM) deals with it. New smart technics broadening the appliances included in this cooperation.

Aggregated control centers

In the last decade there appeared more and more aggregation centers where the small, non-scheduled, non-controlled rest capacities are handled as a whole. In the power market control centers act jointly, give bids for production, control or 'no run'. This logical solution is supported by developed info communication (smart system) but it was not made specifically for the renewables. It helps the integration (Virtual Power Plant) The VPP helps the work of the system operator, too. One of the earliest solutions is the Control Center for Renewable Energy (CORE), Iberdrola, Toledo, Spain[12], but there are 4 small VPPs in Hungary too.

Figure 8. Damaged turbine at Crete, Greece

Figure 9. Craning of Vertical Axe Wind Turbine (VAWT) at Óbuda University

[12] source: Iberdrola

The fuel saving approach

There is no power system based 100 percent on wind generation. The way of the technical development is to set up a system by traditional sources (coal, oil, gas, nuclear). It is followed by the wind and PV extension. The right approach: we have an operating system, and we use less fossil fuel if we have actually renewable production. This is the fuel saving approach.[13]

4 Photovoltaic solutions

Electricity production based on solar radiation is not a new idea but spread over only in the last decade. That is why we don't have so many best practices and bad experiences. Main solutions are the semiconductor based photovoltaics (PV) and the mirrored concentrated solar power (CSP). [11-13] Of course we have the pro-cons list:

The advantages

- renewable energy, no CO_2 emission during the operation
- low maintenance cost
- good daily characteristics (peak power generation)
- large industrial halls and „brown" areas can be reused
- the solar panels shielding against the heat on the roofs
- no noise production
- can be anticipated

Disadvantages

- high energy pay-back time (a lot of 'built in' energy needed to produce the devices)
- seasonal production (summer – more, winter – less)
- the reflected light is polarized and it victimizes millions of insects and birds. By mistake they take the solar panels for lakes.
- large areas may be used instead of agriculture
- lack of raw materials
- leaking of toxic materials during the semiconductor production
- dangerous waste must be deployed after dismounting the system
- birds can be burned over CSP
- weak mechanical resistance against ice fall in storm

[13] source: WWEA 2010

Figure 10. Broken PV amorphous PV panel (2010) [14]

Figure 11. PV panel testing on Sun tracking system at Óbuda University

[14] Photo of Ferenc Herbert

5 Recommendations

We listed a bunch of benefits and real problems of the renewable resources. We are convinced that the renewable approach is more than a fashion and it is more sustainable than the traditional fossil fuel operation. Some methods definitively help the promotion of these methods:

- prudent design of the systems
- enabling the remote control of the weather dependent production (limitation)
- diversification of sources in space
- development of the forecast precision
- VPP type aggregation centers
- cooperation with energy markets through developed info communication

Conclusion

The hydro, PV and wind energy production devices are off-the-shelf products that can be chosen from catalogues. The behavior of these tools really differs from the previous demand-controlled paradigm. It is high time for their application and integration. The good news is that several technical solutions exist for the large scale application of the weather dependent sources. The hot topics nowadays are the off-shore plants, the storage, the Demand Response Management.

References

[1] Immanuel Kant: Kritik der reinen Vernunft, 1781

[2] Peter Kadar: Seeking for the optimal market; 4th Slovakian – Hungarian Joint Symposium on Applied Machine Intelligence; Herl'any, Slovakia January 20-21, 2006, proceedings pp 234-246

[3] Peter Kadar: Scheduling of the generation of Renewable Power Sources; 5th Slovakian – Hungarian Joint Symposium on Applied Machine Intelligence, Poprad, Slovakia January 25-26, 2007, proceedings pp 255-263

[4] Peter Kadar: Storage optimization in a liberalized energy market; 7th International Symposium on Applied Machine Intelligence and Informatics; Herl'any, Slovakia January 30-31, 2009

[5] Hugo Morais, Péter Kádár, Pedro Faria, Zita A. Vale, H.M. Khodr: Optimal scheduling of a renewable micro-grid in an isolated load area using mixed-integer linear programming; Elsevier Editorial System(tm) for Renewable Energy Magazine Volume 35, Issue 1, Pages 151-156; April, 2010

[6] Khodr, H.M.; Vale, Zita A.; Ramos, Carlos; Soares, J.P.; Morais, H.; Kadar, Peter: Optimal methodology for renewable energy dispatching in islanded operation; Transmission and Distribution Conference and

Exposition, 2010 IEEE PES Digital Object Identifier: 10.1109/TDC.2010.5484411

[7] Peter Kadar: Power generation portfolio optimization by externality minimization; Acta electrotechnica et informatica; Faculty of Electrical Engineering and Informatics, Technical University of Kosice, SK; April-June 2010, vol.10. No.2, 2010, ISSN 1335-8243, pp5-9

[8] Peter Kadar: Multi Objective Power Mix Optimization; 8th International Symposium on Applied Machine Intelligence and Informatics (SAMI 2010) Herl'any, Slovakia January 28-30, 2010

[9] Zita Vale: "Computational Intelligence Applications for Future Power Systems", Computational Intelligence for Engineering Systems, 2011

[10] P. Kádár: Large Scale Wind Turbines and Their Application in Renewable energy systems Editor: Socrates Kaplanis – Eleni Kaplanis pp 405-452; Nova Science Publisher Inc. New York, 2013 ISBN: 978-1-62417-744-6

[11] Tiberiu Tudorache, Liviu Kreindler: Design of a Solar Tracker System for PV Power Plants; Acta Polytechnica Hungarica Vol. 7, No. 1, 2010

[12] Zerhouni et al,: Proposed Methods to Increase the Output; Efficiency of a Photovoltaic (PV) System; Acta Polytechnica Hungarica Vol. 7, No. 2, 2010

[13] P. Kadar, A. Varga: Measurement of spectral sensitivity of PV cells; Intelligent Systems and Informatics (SISY), 2012 IEEE 10th Jubilee International Symposium Subotica, Serbia, pp. 549 – 552, Sept 20-22, 2012

Implementation of Immunological Algorithms in Solving Optimization Problems

Petar Čisar

Academy of Criminalistic and Police Studies, Cara Dušana 196, 11080 Zemun, Serbia, petar.cisar@kpa.edu.rs

Sanja Maravić Čisar

Subotica Tech, Marka Oreškovića 16, 24000 Subotica, Serbia, sanjam@vts.su.ac.rs

Branko Markoski

Technical Faculty "Mihajlo Pupin", University of Novi Sad, Đure Đakovića bb, 23000 Zrenjanin, Serbia, markoni@uns.ac.rs

Abstract: This paper gives a global review of artificial immune systems in computer science and their implementation. The performance of the immunological algorithm in solving optimization problems is analysed using the Optimization Algorithm Toolkit, with emphasis on determining the impact of parameter values. It is shown that these types of algorithms are particularly sensitive to the choice of parameters that affect the functioning of the algorithm.

Keywords: immunological algorithm; implementation; Optimization Algorithm Toolkit; travelling salesman problem; function optimization, parameters

1 Introduction

The contribution of this paper is its use of the Optimization Algorithm Toolkit (OAT) environment to examine the impact of immunological algorithm parameters on accuracy and speed of calculations in solving optimization problems.

The paper consists of three sections. The first section is the introduction, which shows the analogy between biological and artificial immune systems (AIS) and explains the categorization of immunological algorithms. The second section

presents an overview of implementation possibilities of artificial immune systems. The third section concentrates on one specific type of implementation, which is optimization, and its various aspects in an adequate software environment. Lastly, this paper offers a conclusion based on the analysed cases.

We begin with a detailed background necessary for understanding the immunological algorithms.

Humans, similar to other living organisms, are constantly exposed to a wide range of micro-organisms such as bacteria, viruses, parasites and other harmful molecules (called antigens) that can damage the human body. In order to prevent this, the human body has developed an immune system. The immune system is a very complex defence system that is composed of different cells (B and T lymphocytes) that prevent foreign objects from damaging the body. The T-cell is a special type of white blood cell that is of key importance to the immune system. It has so-called T-cell receptors on its surface with which it can detect antigens. Normally, the receptors of a T-cell do not match the body's own substances.

In the above context, it is possible to formulate a definition of a clone. A clone is a propagating population of organisms, either single cell or multi cellular, derived from a single progenitor cell. Such organisms should be genetically identical, though mutation events may abrogate this [1].

Each human body has an innate immune system. This system has a major role in the development of a complete immune system. Namely, over the years as the body is attacked by certain antigens, the immune system does not just have the goal of destroying these antigens, but also to memorize them. It has the important property of pattern recognition that may be used to differentiate between outer cells entering the body (antigens) and the body cells. Immune systems have several crucial characteristics such as uniqueness, autonomy, memory and recognition of foreigners, distributed detection, and noise tolerance [2].

Artificial Immune Systems (AIS) are adaptive systems, inspired by theoretical immunology and observed immune functions, principles and models, which are applied to problem solving [3]. The general principle of functioning of the immune algorithm is presented in the following figure.

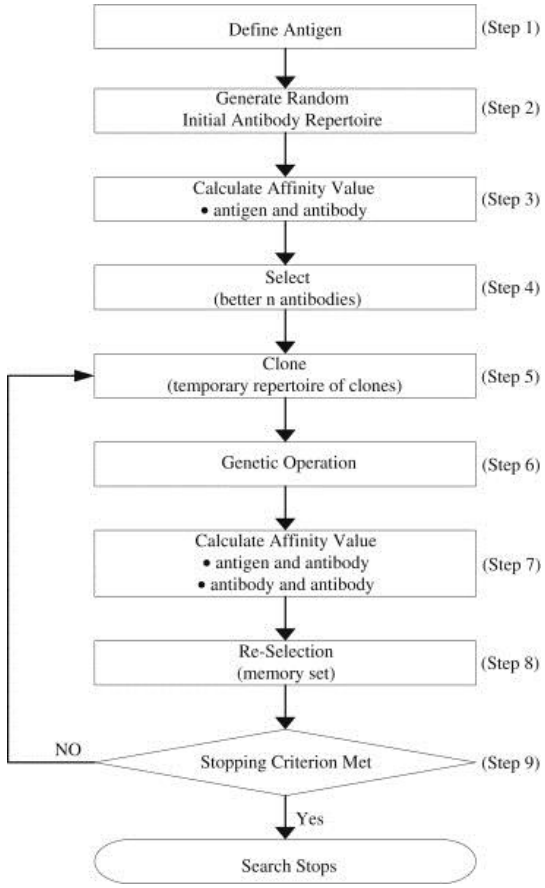

Figure 1
Flowchart of the immune algorithm [4]

The research of the artificial immune system began in the 1990s, and until now a significant number of algorithms have been developed which have different applications. Existing algorithms can be divided into four categories, according to the functioning principle of the used immune system: negative selection, clonal selection, immune network algorithm and dendritic cell.

Negative Selection Algorithm – The inspiration for this type of algorithm can be found in the mechanism in the thymus whose task it is to generate a set of mature T-cells that can only bind to non-self antigens. The thymus, which is a lymphoid organ, can be found in the middle of the upper chest right behind the sternum (breastbone). The thymus is where lymphocytes mature, multiply and become T-cells. Forrest et al [5] introduced the first negative selection algorithm in order to detect data manipulation which was caused by a computer virus. The algorithm's primary task is to produce a set of self strings that are characteristic of the

system's normal state. The following task is to generate so-called detectors that exclusively recognize the complement of these strings. Then the given detectors are applied to new data in order to categorize them as being self or non-self, specifying the situation that data was changed.

Clonal Selection Algorithm - The clonal selection approach inspired the development of the AIS that executes optimization and pattern recognition problems. This stems from the antigen controlled maturation of B-cells, with associated hyper mutation process. These immune systems also implement the concept of memory cells to continue to provide excellent solutions to the problem in question. De Castro and Timmis [3] highlight two important features of affinity maturation in B-cells, the first being that the increase of B-cells is in proportion to the affinity of the antigen which binds to it, therefore the higher the affinity, the more clones created. Furthermore, the mutations resulting through the antibody of a B-cell are inversely proportional to the affinity of the antigen to which it binds. De Castro and Von Zuben [6] developed a frequently used clonal selection based-AIS (CLONALG) by implementing these two features, which has been applied to executing pattern matching and multi-modal function optimization tasks.

Immune Network Algorithms – These algorithms originated from Jerne [7] who described the immune network theory in order to provide an explanation for some of the observed vital characteristics of the immune system (learning and memory). The basis of the network approach states that any lymphocyte receptor can be identified by a subset of the receptors. The receptors of this recognizing set have their own similar set, creating a network of interactions [8]. Immune networks are usually called idiotypic networks. If there is no foreign antigen, Jerne summarized that the immune system has to present a behaviour or activity resulting from interactions with itself, resulting in tolerance and memory, among others, from the immunological behaviour of these reactions.

Dendritic Cell Algorithms - Matzinger [9] created the danger theory, which has met with widespread acceptance in the circle of immunologists as a manner of explaining the development of peripheral tolerance (tolerance to external agents). This algorithmic approach states that antigen – presenting cells (APC) are actually activated by signals of danger. The activated APCs can then provide the needed co-stimulatory signal to the T cells which in turn control the immune reaction. The danger signals originate from normal cells of the human body which have been injured by an attack.

The performance of the immunological algorithm in solving optimization problems is analysed in this paper using the Optimization Algorithm Toolkit (OAT). The OAT is a workbench and toolkit for developing, evaluating and experimenting with classical and state-of-the-art optimization algorithms on standard benchmark problem domains. This open source software includes reference algorithm implementations, graphing, visualizations and other options. The OAT provides a functional computational intelligence library for

investigating existing algorithms and problems, as well as implementing new problems and algorithms. Built on top of this library is a simple explorer and experimenter graphical user interface that provides a basic understanding of the functionality in the library. The goal of the library is to facilitate the best practice of algorithm, problem, and experiment design and implementation, as well as software engineering principles. The graphical user interface provides non-technical access for configuring and visualizing existing techniques on standard benchmark problem instances [10].

2 Implementation of Artificial Immune Systems

Using the historical chronology of research and existing division of applications [11], the basic implementations of artificial immune systems can be classified into the following main areas and corresponding sub-areas [12]:

Anomaly Detection

- Fault detection
- Computer and network security

Recognition and detection of anomalies in data include, among other areas, discriminative analysis, error estimation, feature extraction, grammatical inference, image analysis, sign recognition, speech recognition and identification mechanisms. Applications are extremely diverse and range from the recognition of spectrum reactants in chemical analysis, prediction of infectious diseases and analysis of medical data. The area of detecting anomalies in time data is based on the detection of new or unexpected patterns. Their applications include the area of early detection of potential hardware failures (for example, the detection of temperature and pressure fluctuations and detection of defects in different devices). Fault detection in software and hardware is extended to distributed systems such as sensor networks and nodes of wireless networks, where it can affect the flexibility and routing of traffic.

Machine Learning

- Clustering and classification
- Robotics
- Pattern recognition
- Control (planning)

The domain of machine learning is very general and includes various forms of pattern recognition, conceptual learning, controlled and uncontrolled learning, clustering and classification data. The earliest applications were in the area of unmonitored learning to identify clusters of data while further implementations are in the area of supervised learning in systems with limited resource classifiers,

the model of immune network for clustering and filtering unmarked sets of numerical data, adaptation of intelligent systems and conceptual learning.

In the field of robotics, there are several directions of implementation of artificial immune systems, which can generally be divided into the collective management of robot groups and adaptive management of an individual robot.

The domain of control also contains examples of artificial immune systems in processes of adaptive, sequential and feedback control, which are applicable in manufacturing systems, planning tasks and workflow, process planning and planning of software and hardware support.

Optimizations

- Optimization of numerical functions
- Combinatorial optimization

Numerous algorithms have been developed in this area, mainly based on the principle of clonal selection, for example, the CLONALG clonal selection algorithm [6], the immunological network optimization opt-aiNET [13], an algorithm with the B-cells [14] and the immune optimization algorithm opt-IA [15]. In order to display the elements, the popular and often exploited CLONALG algorithm uses binary strings, implements affinity maturation and is also suitable for pattern recognition. The application of these algorithms and systems is explained in numerous papers involving optimization functions, multi-target optimization, optimization of multimodal functions, combinatorial and time-independent optimization, and offer a range of solutions in the field of route management (e.g. the travelling salesman problem), planning tasks, and storage optimization. The clonal algorithm and the algorithm with B-cells are applied to the optimization of dynamic function, which is analogous to the task of the human immune system.

Other Implementation Areas

- Computational immunology
- Data and Web mining

One of the applications of the AIS lies in computer immunology and the areas of bio-informatics and immuno-informatics, where the first computer simulations of immune networks have evolved into modern stochastic models of the immune system. However, they do not necessarily use an immune network and are used for educational and scientific purposes. Although this area is often related to the problem of clustering, further research is progressing in different directions, from the study of evolution of antibody libraries to the behaviour of ecosystems.

The area of data mining, which involves classification and anomaly detection, covers a wide spectrum of applications from data and web mining, but also different applications, such as the detection of fraud in financial systems, detection

of potential customers, discovering disjunctive rules, data filtering, computer supported cooperative work, and information processing.

3 Examples - Optimization

In the fields of mathematics, statistics, empirical sciences, computer science, mathematical optimization refers to the selection of the best element (with regard to some criteria) from the set of available alternatives [16]. An optimization problem involves finding the minimum and maximum of a real function by systematically changing the input values from within a pre-defined set and calculating the corresponding values of the function. More generally, optimization includes finding extreme values of some objective function given a defined domain, including a variety of objective functions and domains.

Solving optimization problems by means of appropriate software will be examined through several examples: route management and function optimization.

The optimization problem as a route management problem can be considered as follows. If one takes a set of cities and the travel costs between each pair of them, the Travelling Salesman Problem (TSP) comprises the problem of identifying the shortest possible route that passes through every city exactly once and returns to the initial city. The standard version of this problem assumes symmetric travel costs, meaning that the travel cost from city X to city Y is equal to the travel cost from the city Y to X. A large problem in graph theory is to minimize the total distance and determine the route for the salesman so that he travels through each city only once. This problem is categorized as NP (nondeterministic polynomial)-hard and NP-complete.

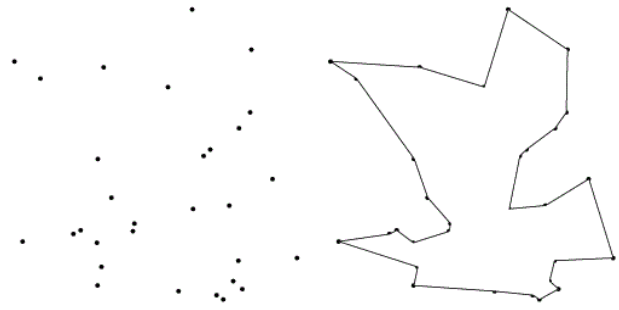

Figure 2
Travelling salesman problem - illustration

The dots in the figure above represent geographic locations of given cities, with known distances between each pair of them.

The simplicity of the statement of the problem is apparent. This makes the TSP one of the most closely examined problems in computational mathematics, though a method for a suitable solution for the general case has yet to be found [17]. It is also used as a benchmark for many optimization methods.

The practical part of this paper will present the testing of immune algorithm in solving the TSP using the OAT as a working environment.

Within this category, the CLONALG algorithm was chosen. The basic principle of operation of the CLONALG algorithm is shown in the following figure.

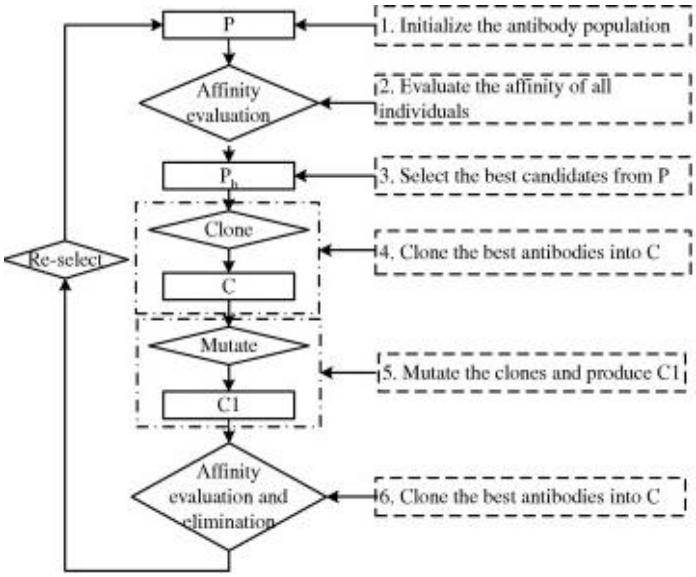

Figure 3

Steps of clonal selection method [18]

As shown in the figure above, the clonal selection algorithm contains three basic parameters:

- antibody population size
- clone factor
- mutate factor

As stated before, the aim of this paper is to present the implementation of the OAT environment, to examine the influence of these parameters on accuracy in determining the optimal tour and speed of calculations. In this sense, the ability to configure the algorithm will be used, as shown in the figure below.

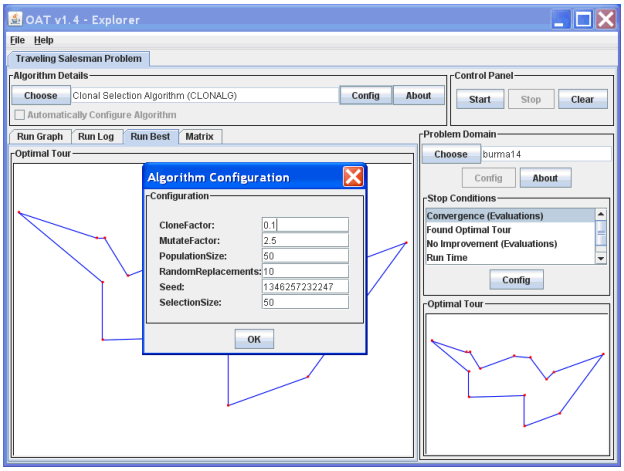

Figure 4
CLONALG algorithm configuration

The problem domain with 14 dots and the known optimal tour (shown in the bottom right corner of the figure above) were analysed. The optimization is considered finished when the same graphic form is obtained as the optimal tour. The influence of the analysed parameters (population size, clone and mutate factor) on the solving time is given in the following table.

Table 1
Influence of Parameters

Population size	20	30	40	50	60	70	80
Solving time (sec)	25	95	1	80	2	20	37

Clone factor	0.1	0.2	0.3	0.4	0.5	0.6	0.7
Solving time (sec)	83	1	3	1	1	1	1

Mutate factor	2	2.5	3	3.5	4	4.5	5
Solving time (sec)	< 1	80	< 1	420	170	< 1	> 600

After thoroughly analysing the above values obtained for the solving time, it can be concluded that the CLONALG algorithm is extremely sensitive to the choice of parameters. This means that the performance of this algorithm must be checked with several different parameters, and based on the results, the optimal value will be chosen. This procedure is known in the literature as tuning parameters and directly affects the speed of convergence of the algorithm (i.e. solving time) to the solution. Also, it can be noticed that the CLONALG maintains a diverse set of local optimal solutions, which is mainly due to the selection and reproduction schemes. Another important characteristic is the fact that CLONALG takes into

account the cell affinity, corresponding to an individual's fitness, in order to define the mutation rate applied to each member of the population.

The optimization problem as a continuous function optimization problem can be summarized as follows. It is logical that the increase of the population size directly influences the algorithm to find the optimum quickly, but it also increases the processor computation time. These parameters, the clone and mutate factor, are important because they affect the algorithm to find more optima or a faster global optimum. These parameters also affect the CPU time so they need to be precisely set in order to achieve the desired result in a satisfactory time. The function that was tested in research [19] is:

$$f = x \cdot \sin(4\pi x) - y \cdot \sin(4\pi y + \pi) + 1 \tag{1}$$

The mutate factor affects the number of clones of each individual. In this way it affects the CPU time of execution of the algorithm.

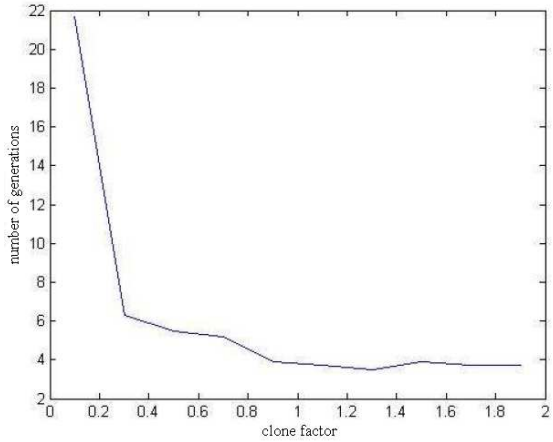

Figure 5

Influence of clone factor on convergence of algorithm [19]

Figure 5 shows that for very small values of clone factor, the algorithm is not able to find the global optimum, whereas increasing the parameter above 1 does not contribute to the improvement of convergence. Also, large values of mutate factor inhibit the algorithm to find the global optimum (Figure 6).

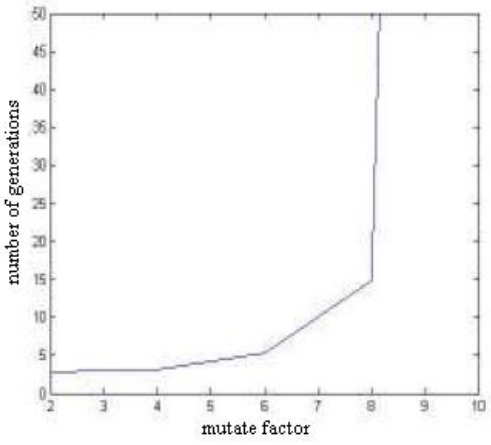

Figure 6
Rate of convergence [19]

Another example of function optimization will be shown in the OAT environment. The Shubert function was analysed, with the help of the optimized artificial immune network (opt-aiNET) algorithm. This is a multimodal test function given by the following relation:

$$f(x_1, x_2) = -\sum_{i=1}^{5} i\cos((i+1)x_1 + 1)\sum_{i=1}^{5} i\cos((i+1)x_2 + 1) \tag{2}$$

The test range is usually limited to: $-5.12 \leq x_1 \leq 5.12$, $-5.12 \leq x_2 \leq 5.12$. This function has several local minima and 18 global minima. In this case, the optimization implies minimization of the function, i.e. finding the minima.

The convergence of solutions around extremes (global minima) is easy to recognize in the next figure – the left side. Single solutions are shown in the form of numerous dots deployed around the points of the minima. The right side of Figure 7 represents the Shubert function in 3D.

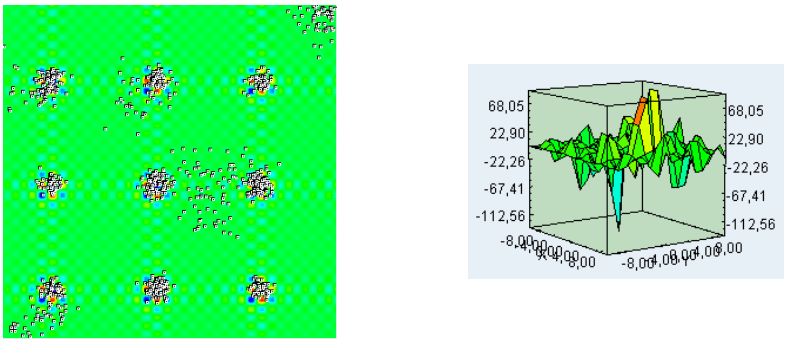

Figure 7
Shubert function optimization – optimized artificial immune network algorithm

The parameter of this algorithm that predominantly affects the final result is the total number of clones per cell. It is important to emphasize that the performed testing has shown that when this number is greater than 90, 1-2 minima always remain unidentified (unclustered).

Also, it was found that using other immunological algorithms offered by the OAT (adaptive clonal selection (ACS) [20] and optimization immune algorithm (opt-IMMALG) [21]) do not give a satisfactory result, i.e. it does not generate clustering solutions.

The next example of optimization is the optimization of binary functions. A binary function, or function of two variables, is the type of function which takes two inputs. A binary function may also be defined as a function from $X \times Y$ to Z (X, Y inputs, Z output). Out of the offered functions in the OAT environment, a simple trapdoor function is chosen. The trapdoor function is a function that is easy to compute in one direction, but it is difficult to compute in the opposite direction without the secret trapdoor information (for given $f(x)$ and y it is easy to compute x). Trapdoor functions are widely used in cryptography. An example of a trapdoor one-way function is the factorization of a product of two large primes. While selecting two large primes and multiplying them is relatively easy, factoring the resulting product is rather difficult. This is the basis of the RSA encryption, which is conjectured to be trapdoor one-way. The graphical result of the optimization is shown in the figure below. The black dot represents the logical zero, while the white dot is the logical one. Binary string length was set to 100, the number of total evaluations was 1000, and the run time 33 ms.

Figure 8
Trapdoor function optimization – optimization immune algorithm

The algorithm used in the above case was the optimization immune algorithm. It has several parameters: maximum age, mutation (static or inversely proportional), number of clones and population size. It has been shown that these parameters do not affect the final result, but only the run time.

It was also found that other offered algorithms in the OAT (B-cell algorithm (BCA), Cloning, Information Gain, Aging (CLIGA), CLONALG and simple immune algorithm (SIA)) also generate correct results. They differ only in run time.

Conclusions

The practical part of the paper is focused on examining the impact of parameters of immunological algorithms on processing time needed to determine the optimal values. In all of the analysed cases of route management, only the spent times of the algorithms that led to the optimal solution were different for the different parameter values. In this sense, the existence of multiple optimal values was found, as well as extremely unacceptable values. This means that great attention must be paid to the selection of parameter values (it is not to be disregarded which values are applied) and it is vital to test the behaviour of the algorithm in practice with several different parameters. Also, it was confirmed that all of the immune algorithms are not equally suitable for certain situations of function optimization. Namely, it has been shown that some of the analysed algorithms did not identify local extremes of examined test function.

References

[1] Biology Online, www.biology-online.org

[2] L. de Castro, F. Zuben: Artificial Immune Systems: Part I – Basic Theory and Applications, TR – DCA 01/99, 1999

[3] L. de Castro, J. Timmis: Artificial Immune Systems: A New Computational Intelligence Approach, Springer, pp. 57–58. ISBN 1-85233-594-7, 9781852335946, 2002

[4] C. Chu, M. Lin, G. Liu, Y. Sung: Application of immune algorithms on solving minimum-cost problem of water distribution network, Mathematical and Computer Modelling, Volume 48, Issues 11-12, pp. 1888-1900, 2008

[5] S. Forrest, A. Perelson, L. Allen, R. Cherukuri: Self-nonself discrimination in a computer, in Proceedings IEEE Symposium on Research in Security and Privacy, pp. 202–212, 1994

[6] L. de Castro, F. Von Zuben: Learning and optimization using the clonal selection principle, IEEE Transactions on Evolutionary Computation, 2002 Jun, 6(3):239-251. ISSN: 1089-778X

[7] N. Jerne: Towards a network theory of the immune system, Annals of Immunology (Inst.Pasteur). 125C. pp. 373-389, 1974

[8] AISWeb, The Online Home of Artificial Immune Systems, http://www.artificial-immune-systems.org/algorithms.shtml

[9] P. Matzinger: Tolerance, Danger and the Extended Family, Annual Review of Immunology. 12, pp. 991-1045, 1994

[10] Optimization Algorithm Toolkit, http://optalgtoolkit.sourceforge.net/

[11] E. Hart, J. Timmis: Application areas of AIS: The past, the present and the future, Journal of Applied Soft Computing, vol. 8, No. 1, pp.191-201, 2008

[12] B. Mihaljević: Područja primjene umjetnih imunoloških sustava i teorije opasnosti, Fakultet elektrotehnike i računarstva, Zagreb, www.fer.unizg.hr/_download/repository/Kvalifikacijski_doktorski_ispit_-_Branko_Mihaljevic.pdf

[13] L. de Castro, J. Timmis: An artificial immune network for multimodal function optimization, Proceedings of the 2002 Congress on Evolutionary Computation (CEC '02), Honolulu, HI, USA, USA: IEEE Computer Society, 2002, 699-704. ISBN: 0-7803-7282-4

[14] J. Timmis, C. Edmonds, J. Kelsey: Assessing the Performance of Two Immune Inspired Algorithms and a Hybrid Genetic Algorithm for Function Optimisation, Proceedings of the Congress on Evolutionary Computation (CEC04), Potland, Oregon. USA. USA: IEEE Press; 2004: 1044-1051

[15] V. Cutello, G. Narzisi, G. Nicosia, M. Pavone, G. Sorace: How to Escape Traps using Clonal Selection Algorithms, The First International Conference on Informatics in Control, Automation and Robotics, ICINCO 2004,Setubal, Portugal. INSTICC Press; 2004: 322-326

[16] "The Nature of Mathematical Programming", Mathematical Programming Glossary, INFORMS Computing Society, http://glossary.computing.society.informs.org

[17] Travelling Salesman Problem, www.tsp.gatech.edu

[18] I. Aydin, M. Karakose, E. Akin: Chaotic-based hybrid negative selection algorithm and its applications in fault and anomaly detection, Expert Systems with Applications, Volume 37, Issue 7, pp. 5285–5294, 2010

[19] K. Đuretec: Umjetni imunološki sustavi, Projekt: Algoritmi zasnovani evolucijskom računanju, Fakultet elektrotehnike i računarstva, Zagreb, www.zemris.fer.hr/~golub/ga/studenti/projekt2008/ais/umjetni_imunoloski_sustavi.pdf

[20] S. Garrett: Parameter-free, adaptive clonal selection, Congress on Evolutionary Computing (CEC 2004), Portland Oregon, USA. USA: IEEE Press; 2004: 1052-1058. ISBN: 0-7803-8515-2

[21] V. Cutello, G. Nicosia, M. Pavone, G. Narzisi: Real Coded Clonal Selection Algorithm for Unconstrained Global Numerical Optimization using a Hybrid Inversely Proportional Hypermutation Operator, 21st Annual ACM Symposium on Applied Computing (SAC), Dijon, France, 2006: 950-954. ACM

Informal Post-Experiential Learning

Ágnes Szeghegyi

Óbuda University, Keleti Faculty of Business and Management, Institute of Enterprise Management, Tavaszmező u. 15-17, 1084 Budapest, Hungary, szeghegyi.agnes@kgk.uni-obuda.hu

Viktória Szoboszlai

Budapest University of Technology and Economics, Department of Management and Corporate Economics, Magyar tudósok körútja 2, 1117 Budapest, Hungary, viktoria.szoboszlai@flemingeurope.com

Jolán Velencei

Óbuda University, Keleti Faculty of Business and Management, Institute of Enterprise Management, Tavaszmező u. 15-17, 1084 Budapest, Hungary, velencei.jolan@kgk.uni-obuda.hu

Abstract: In this paper, we emphasize the unprecedented problems that the age of shallow knowledge offers. We investigate how navigating in the world of information and communication technology (ICT) innovations and influencing the spreading of memes are affecting those who make the decisions about how we should behave in the "ICT labyrinth". Drawing on the role of key influencers and communities of practice, we offer an alternative framework of emerging learning tools in the post-experiential informal learning ecosystem and investigate the ways of some implementations in corporate practice.

Keywords: informal learning; learning ecosystems; learning tools

1 The New Age of Shallow-Knowledge

Today it is unnecessary to convince organizations to buy computers since they have already bought them. Today it is unnecessary to convince people to buy computers since they have already bought them. Today it is unnecessary to convince anyone to use computers, as everyone is using them. They are using

them more or less in order to be faster in something: in mailing, in browsing, etc. Somehow everyone has learned it through much practice. Nevertheless, we should not forget about the generational differences, the different approach of digital natives and digital immigrants. No one had been taught in school how to use Facebook. No lectures were given either on the glorified pros or on the dangerous cons. Today this is a challange, people seem to be concerned more about the cons as the usage of Facebook has been banned at some workplaces. In post-experiential learning, the emphasis needs to be put also on how to become competent in the application of tools. These applications are going viral and memes are being created. Further research is much needed today in how the user gets to know the validation mechanisms of the tools.

The new tools of social communication have necessarily brought an era where all of us (including those who are not using online social platforms) have to rethink learning, knowledge sharing and collaboration in a fundamentally different way than ever before. Instead of deeply thinking in a narrow area, having only superficial knowledge of many things will become more dominant. In 2011, the writer and blogger Nicolas Carr gave his newest book the title ”The Shallows: What the Internet Is Doing to Our Brains”. He describes how the newest achievements of information technology are distracting us and don't let us focus on one thing at a time and sustain concentration longer. The information overload is urging us to continually browse and “scan” its contents [1]. In knowledge refreshing – which is not the same as educating – the rigid curriculum and formal learning are replaced by cross-functional content that can satisfy curiosity and thus, informal learning can occur. From this mash-up content everyone can take and deal with what they really need; the rest is optional. This new type of learning is more and more loosely-structured, adapting itself in time, space and in tools to the “here and now needs” of the passionate learners. In a post-experiential learning process the participants need to have the opportunity – based on their knowledge levels and preferences – to step up in this “flood-gate-like” process.

Recent reports found that mobiles will outnumber people next year [2]. The question is simple: is there anything that needs to be done today? We can believe the prognosis but we don't have to. We can say now “let's wait and see”, and deal with it later. What we cannot do is bury our heads in the sand. This result in the absurd situation that we don't know what those people should know who are refreshing their knowledge in a post-experiential learning process. This reality is what makes the planning of this learning process interesting. In the course of post-experiential learning, having wide but superficial knowledge can be acceptable. It is worth to get away from the world of ”deep knowledge superspecialists” who cannot make themselves understood.

That leads us to two problem areas for further investigation:

1. Navigating in the world of ICT innovations
2. Influence on the spreading of memes.

In the ”ICT labyrinth” the challenge is about how to see through this blizzard of information and knowledge, to recognize and filter the junk from the internet. Those whose decisions can affect our behaviour in the ”ICT labyrinth” should be protected from two extremes. The first extreme is that on the internet nothing is true as it is not proven, so there is no pre-control. The other extreme is to blindly believe everything which is available on the internet.

The communities of practice (CoPs) [3] and self-organized learning environments (SOLEs) [4] are formed, and the expeditors and promoters of organizational changes are from the members of these communities. They don't believe in the concepts of the majority, they are the minority who are sustaining the momentum of development. “The key people have disproportionately high influence. They are like the kingpins, in bowling, when we hit them, they topple all the other pins” argue Kim and Mauborgne [5]. Malcolm Gladwell writes about the key influencers as *connectors* who are important not just because they know large number of people. Their importance lies in who they know [6]. In this paper we argue that it might be useful to show the role of key influencers in dissemination of ICT achievements to those who make the decisions how we should behave in the “ICT labyrinth”. In the ICT world the “make or buy” dilemma has long survived. It's a fact by now that the software needs to be bought from one of its major producers. It does not really matter from which one, as the reliability of the major producer's software is guaranteed exactly by their existence on the market. It is obvious that each costumer has his preferences that drive his decision.

Sugata Mitra shared in his TED talk that he left a computer in a slum, 500 kms away from Delhi and the kids started using it and playing with it even in the absence of any supervision or formal teaching. A few months later, when he returned the kids wanted a faster processor and a better mouse [3]. This story can be perhaps an example for the informal learning process. In one sense it is not remarkable that the kids learn to use computers as they learn to use mobile phones without any training. What is remarkable is how much they can learn and with how little guidance if their self-motivation, self-discipline and self-organization are encouraged and enabled. Efficient and independent learning means that one is able to learn persistently, to plan his own learning path - individually and in groups as well - and that includes effective time management and information management.

Preferred patterns of learning strategies typical of the individual are interpreted as learning style and can be regarded as an individual characteristic. Certain learning strategies (the method of information acquisition, sense modality) show some sort of stability while others (the method of information processing and its application) show continuous changes [7]. The learner is able to recognize his needs and opportunities, he knows the process of learning which means the acquisition, procession and integration of new knowledge on the one hand, as well as the search and application of guidelines on the other. Efficient and independent learning is encouraging the learner to build his knowledge upon former learning-

and life-experience and to apply his ability, which is supported by the set of his skills, in the most different of situations.

Efficient and independent learning is characterized by motivation and confidence. Further conditions of independent learning are the creation of a personal learning strategy, the continuous maintenance of motivation, the ability to focus, the critical reflection on the willingness and purpose of learning, and the acquisition, procession and integration of new knowledge. A learner has to be able to work in groups, to share his knowledge, to evaluate objectively his own work and to ask for advice, information, support, if needed. To maintain continuously the positive attitude and the intrinsic motivation to learn, it is indispensable to use the former learning- and life-experience, to explore new learning opportunities and to widely apply what had been learned.

Formal learning is no longer enough, there is a need for informal as well. In the course of informal learning, the learning content – and the knowledge as such – learns "on the go". This is a knowledge refresher process whilst not a subject, people are becoming more educated. In this process, the passionate learner can increase his knowledge, while he can frame up new contents as well (learner-generated content). There are a lot of talks about the anachronism of the informal education, however, it does not seem to become totally unnecessary. Although in the digital world it needs to find a new place and a new role. Today, the digital culture is having a profound effect on the world just like the disruptive technologies of previous eras and new solutions often have an impact on each other as well as on human behaviour. The development of the internet is advanced not only by the technological innovations but also the evolving imagination and desires of millions which give again new momentum to the technological innovations, argues one of the world's top thought-leaders, Sir Ken Robinson who elaborates on weaknesses of informal education in his books and lectures [8]. His thoughts contribute largely to clarify the "formal vs. informal education" dilemma.

2 Emerging Tools in the Learning Ecosystem

According to IBM's Survey of 1,709 CEOs, 16% of organizations say today they are committed to building a social organization and looking for opportunities to increase communication, collaboration and innovation. Tomorrow, 57% of them say they will be committed to being a social organization [9]. Workplaces can't avoid to become environments that provide an intensely personalized, social experience to attract, develop and engage employees across all generations and nationalities. One of the major forces that will dramatically affect employers is social networking, social media and social learning. Thinking of the 90s and 2000s as the "e"decade, as in e-books, e-libraries and e-learning, we can envision 2010 to 2020 as the "s" decade [10].

“Games are the new normal” were the exact words of Al Gore in his iconic keynote speech at the Games for Change Festival back in 2011 [11] and since then, the trend has become even more significant. By 2014, Gartner predicts that over 70 percent of the Forbes Global 2,000 organizations will have at least one "gamified" application, and that "gamification is positioned to become a significant trend in the next five years" [12]. In addition, reports found that gamification market is estimated to grow from $421.3 million in 2013 to $2.8 billion by 2016 [13] and to $5.5 billion by 2018. This represents a compound annual growth rate (CAGR) of 67.1% from 2013 to 2018 [14].

A natural ecosystem is a biological community of interacting organisms and their physical environment. Conversely, a learning ecosystem is a self-organizing infrastructure aimed at creating a learning environment for networked members that supports the cooperation, the knowledge sharing, the development of open and adaptive technologies and evolutionary business models. Personal ownership of technologies and devices coupled with access to social software means that all kind of learning-related activity can be e-enabled today and the main challenge lies in the real transition to a less tutor-led approach to learning, becoming competent in the application of these tools and getting to know their validation mechanisms.

The goal of this paper is to describe emerging learning tools within learning networks and the broader learning ecosystem, and to map out the validation mechanisms. To do this, we need to explore in which forms can these learning tools occur and how they are situated within the learning ecosystem (1) as well as what kind validation mechanisms are effective based on the possible use in practice (2). Drawing on the authors’ theoretical and empirical research, prior expert advisor feedbacks, and the content analysis of delivered presentations at two consecutive summits with the highest corporate university and academy leader attendance in Europe (Brussels, 2013; Paris, 2012), we will attempt to develop a framework for the emerging tools in corporate learning ecosystems. In 2012, out of 21 sessions 13 indicated the prevalence of social learning and 2 sessions the popularity of gamification. In 2013, this number increased further, up to 15 and 5 respectively, proving how these tools continue gaining momentum.

2.1 Social Learning Tools as the Engine of CoPs

Social learning is collaborative, immediate, relevant, and presented in the context of the individual’s unique work environment [10]. Social learning tools are distinguished here based on the main purpose of either Community of Practice (CoP)-building or CoP-maintaining.

2.1.1 Social Learning Tools for Building CoPs

"Employees of 2013 initiate their own learning more and more" pointed out the dean of a leading corporate learning institute, Caterpillar University and in this process the importance of being surrounded by CoPs is critical. The question was if we were ready to support social networking tools i.e. Linkedin or Facebook; synchronous and asynchronous communication; shared workspaces and shared media on the changing learning landscape [15]. AGFA Academy underlined this with their approach of linking structured learning and on the job learning, thus linking Learning Management Systems (LMS) to building up CoPs. In the section "What should be in your Educator Toolbox?" AGFA shared how they are disseminating *user-generated* content via blogs, wikis, the "AGFA Training Community" forum and knowledgebase, while they are using self-paced e-learning sessions, virtual classroom sessions and video sharing to *deliver content generated by subject matter experts* (SMEs). They are using social bookmarking and social tagging - tagging courses so they appear in search results - and allow for communication with coaches, mentors and CoPs via tools like instant messaging, live webcasts and message boards [16].

2.1.2 Social Learning Tools for Maintaining CoPs

Social learning should be enabled not only by facilitating the CoP frameworks where this type of learning can occur; there is a need for community "gardening" so that social learning can flourish. Amongst the most powerful CoP-maintaining social learning tools, we would point out blogging (text, audio/video or micro-blogging i.e. Twitter) and mobile/location-based technologies.

Maintaining a blog gives a permanent presence on the web and serves as a jumping-off point for deeper professional discussions. Employees can get connected and ask for informal peer reviews. In communities of practice, the influence of Gladwell's connectors and the impact of "who" becomes greater than the sum of their parts, knowing who to contact becomes more important than having the right answer.

A geographically dispersed business like Philips, might have a CoP in several functions. Today, tech-savvy employees are using a geo-locator app that allows them to see an expert in a particular function "checked in" at a given location. If it is nearby, users then can contact each other to meet for lunch or to shadow an on-the-job task, making these mobile applications a good way to maintain relationships and share knowledge. Philips Lighting University is particularly strong in maintaining communities and keeping its learners engaged. In 2012, their community's site became the 7th most successful, with 5 webpages in the top 20 most viewed sites, 30,131 unique visitors and an average of 14 minutes per visit from Philips employees who accessed the site based on focus areas, business or functions [17]. ArcelorMittal University created functional academies and introduced collaborative learning that is guided by a virtual network of experts in

each topic and nurtured by social networks of peers at each location. This strengthened the power of its communities and set the foundations of the ArcelorMittal University's first internal massive open online course (MOOC) [18].

Another real-life validation of a community-enhancing social learning tool is PwC's Spark story about an internal social network embedded in the workflow with the ambitious goals to connect 180,000 employees in 154 countries, to create an attractive work environment for younger employees, and to make a large firm feel small. Spark, a PwC business network using Jive software was launched in spring, 2012. Adoption grew virally as Jive became the hub for PwC employees to collaborate and create value for themselves and their clients. Within six months 90,000 people used Spark and growth continued as PwC people found innovative ways to derive value from the solution. Since then, PwC is using Spark to engage employees, locate experts, share knowledge and hold powerful conversations on key strategic issues [19].

2.2 Gamified Tools as Amplifiers of the Learning Ecosystem

Gamification is a business strategy which applies game design techniques to non-game experiences. The goals are to achieve higher levels of engagement, change behaviors, and stimulate innovation. Opportunities for employers are great: gaining more engaged customers, improving employee performance, and crowdsourcing internally are all among the benefits gamification can offer. In this paper we argue that game design techniques and game mechanics can be applied in two domains: *employer branding* and *people management*.

Employer branding, the desire of most employees to have on their CV a company name that gives a sense of pride ties this type of *branding* to talent attraction, talent acquisition, and recruiting as such, while *people management* includes learning and development related, assessment related as well as reward and recognition related policies.

2.2.1 Branding

Many organizations now weave employee engagement and learning into the employee life cycle from beginning to end and they create an employment brand to engage people even before they are hired. Marriott was among the pioneers in the industry with the introduction of a gamified platform called "My Marriott Hotel" to generate interest in hospitality careers. Gamers on Facebook had to first manage a virtual hotel restaurant kitchen before moving on to other areas of hotel operations. Ultimately, they were rewarded when their operation turned into profit. Recently, danish shipping and logistics giant Maersk Group made a unique effort with its game "Quest for Oil" to improve transparency in the industry, encourage the interest of school children and university graduates in the energy

industry, and recruit new talents. Several other examples could be listed amongst the adopters such as HAYS' "Hays Challenge" or PwC's "Multipoly" popularizing recruiting or tax and advisory services and strengthening the brand, which generated a significant increase in candidate numbers and new hires. The most important achievement is to put gamers in virtual immersive environments, virtual worlds such as Siemens' "Plantville" and simulate job tasks in order to become the "employer of choice" for top talents.

The research of this field provides a vast background in terms of game design techniques and game mechanics particularly aligned with employer branding and recruiting goals, which is not the aim of this paper explicitly, rather, we focus more on the People Management part.

2.2.2 People Management

An average gamer plays 10,000 hours of games by age 21. That's about the same number of hours that students spend from 5th grade to graduation of high school. This 10,000 hours ties in with Malcolm Gladwell's theory of success [20] that if we can spend 10,000 effortless hours of study we have a chance to become masters in our area. So what are the gamers becoming masters at? Collaboration, virtual teaming, influencing, problem solving and critical thinking – all core values of the future workplace [19].

In the learning and development field, practice-based insights were provided by a couple of early game-based learning implementations, including Philips Ligthing University's edu-games, Nestlé University's board games combining experiential learning, engagement and fun [21], as well as Yapi Kredi Bank Academy's game-based trainings and simulations. This latter example is what we would like to elaborate more on in terms of validation mechanisms.

Yapi Kredi Bank had to meet new employee time-to-competency goals and maintain proficiency for 17,000 employees at 900 branches throughout Turkey with this alternative, gamified learning delivery method. "YKB City" was developed with the academy's partners (including Koc University, IMD, INSEAD) and with gaming product vendors. At the conclusion of the game, the top successful employees and top branches were determined and rewarded. Short films about their achievements were then broadcasted on the bank's portal. Enjoyable to play and convenient to use, "YKB City" had become also a popular resource for employees to readily consult learning content by visiting the game's virtual library. As a result, cross-selling performance had improved steadily and YKB City proved to be a cost-saving training tool as well. By delivering the training during off-duty hours via e-learning, Yapi Kredi saved three days - 89,460 man hours - that would otherwise have been devoted to classroom training with the same content. Comparing the cost of the game with that of three-day classroom training, the academy realized a savings equal to 5 percent of its annual budget. The impact on job results was also significant. The "incomplete job ratio"

i.e. for the topic “retail credits” dropped from 53 percent to 18 percent, while the average job waiting time decreased by 25 percent [22].

Over and abover all of these success stories, according to Gartner, 80% of current gamified applications will fail to meet business goals by 2015 and poor game design is one of the key failings of many gamified applications today. For a gamified application to truly engage its audience three key design ingredients must be present and correctly positioned: motivation, momentum, and meaning (collectively known as "M³") [23]. Motivation and momentum are also provided by continuous feedback, rewards, and recognitions that are applied as must-have elements in the game-based learning apps of the corporate learning practice. Their design has to provide incentives to learn. Leaderboards and badges are two ways that games engage and reward learners by recognizing their achievements and making them visible to others. Taking the simple example of social media platforms, such as Facebook and LinkedIn, they use badging too, in the form of “likes” and “endorsements”, to drive participation.

Massive open online courses, better known as MOOCs, are at the forefront of a movement to revolutionizre what we call “traditional learning environments”. In our technology-enabled era when anyone anywhere anytime can access high quality higher education at little to nocost, MOOCs are also facing challenges where gamification-based course design might be the answer.

Learners (people anwhere at any point in their lives who want to learn) in the “ICT labyrinth” are increasingly being guided by “content curational advice” and consructing their own educational “playlists”.

However, while MOOC enrollments are stratospheric, their completion rates are extremely low.

Table 1 depicts information on the world’s largest three MOOC platforms today. Stanford-born Coursera leads the way with over 4,000,000 total enrolments, the Stanford University spin-off Udacity has mounted the second highest number with over 1,500,000 enrollments and the Harvard-MIT collaboration edX is in in third place, with only about a quarter the enrollments of Coursera [24].

According to Coursera’s information on completion rates given to partner universities, out of the 3,4 million registrants in Coursera’s first year 55% never completed one lesson and 3-5% of those who started a class actually completed it [24].

Table 1
Top 3 MOOC Platforms

	Foundation	**Number of Students**	**Number of Universities**	**Number of Courses**
Coursera	April 2012	Over 4 million	83	393
Udacity	February 2012	Over 1,5million	2	25
edX	May 2012	Over 1 million	28	44

MOOC or not, the not-for-profit Khan Academy (launched in 2006) did plant a seed to help MOOCs grow into the phenomenon they are in today. While a MOOC can be classified as a "transplantation" of a traditional course, the on-demand capabilities of the Khan Academy's more than 4,000 videos, interactive challenges and assessments as elements cannot be found with a standard MOOC. This organization seems to lead the way also in how to address the issue of low completion rates. The Khan Academy with a mission to make education more accessible by providing free world-class resources to anyone, anywhere, is using now gamification to drive learners through the learning journey, rewarding them with badges as they complete classes.

More information on standard MOOCs where game design elements and game mechanics are embedded in the course design would help us to establish a greater degree of accuracy on this matter. Therefore further investigation would be needed to identify a more exact definition for gamification-based MOOC design and to determine the correlation between game-based learning paths and MOOC completion rates.

Discussion

As learning moves out of the classroom and into the "ICT labyrinth" and the hands of learners, the roles of those who make the decisions about how we should behave in this labyrinth are shifting. These decisions are either programmable [25] operating through various forms of self-discipline and control, or non-programmable but need a certain level of conducting [26]. We argue that these processes can be increasingly associated with self-disciplined decisions adapting itself in time, space, and tools to the "here and now needs" of the passionate learners.

In this paper, we have first described an alternative framework of emerging learning tools in the post-experiential informal learning process, based on the building blocks of social learning and gamification, then we have identified and situated these tools within the broader learning ecosystem. Secondly, we have tried to map out the effective validation mechanisms based on the possible use in practice. There is a need to link and embed these tools in a "more pluralistic" learning ecology in which both prescriptive and emergent application domains and modes of learning have their place [27]. Self-motivated, self-organized and self-disciplined informal post-experiential learning should be recognized as a vital part of learning ecosystems in which the application of emerging tools of social learning and gamification can be applied based on the described validation mechanisms.

References

[1] Carr, N.: The Shallows: What the Internet Is Doing to Our Brains, W. W. Norton & Company, NY, USA, 2010

[2] ITU's World in 2013 Report: ICTs Facts and Figures http://www.itu.int/en/ITU-D/Statistics/Documents/facts/ICTFactsFigures2013.pdf [Accessed at 22 October, 2013]

[3] Wenger, E.: Communities of Practice. Meaning, Learning and Identity, Cambridge University Press, Cambridge, UK, 1998

[4] Mitra, S., & Dangwal, R. Limits to Self-Organising Systems of Learning – The Kalikuppam Experiment. British Journal of Educational Technology, London, UK, 2012

[5] Kim, W. C., Mauborgne, R.: Tipping Point Leadership, Harvard Business School Publishing Company, MA, USA, 2003

[6] Gladwell, M.: The Tipping Point: How Little Things Can Make a Big Difference, Little, Brown and Company, NY, 2000

[7] Tóth P.: Learning Strategies and Styles in Vocational Education, Acta Polytechnica Hungarica, 9(3), pp. 195-216, Budapest, Hungary, 2012

[8] Robinson, R.: Out of Our Minds: Learning to be Creative, Capstone, MN (Minnesota), 2011

[9] IBM: IBM 2012 Global CEO Study http://www.slideshare.net/ArtilleryMarketing/ibm-global-ceo-study [Accessed at 22 October, 2013]

[10] Meister, J., Willyerd, K.: The 2020 Workplace, HarperColling Publishers, USA, NY, 2010

[11] Gore, A.: Games for the Environment, Games for Change Festival, NY, 2011

[12] Gartner. Gartner Gamification Report 2011, http://www.gamification.org/wiki/Gartner_Gamification_Report_2011 [Accessed at 24 October, 2013]

[13] Meloni, W., Gruener, W.: M2 Report - Gamification in 2012, Market Update Consumer and Enterprise Market Trends, 2012 http://www.m2research.com/gamification-2012.htm [Accessed at 24 October, 2013]

[14] Markets and Markets. Gamification Market [(Consumer Gamification, Enterprise Gamification) by Deployment (On-Premise, On-Demand); Application (Marketing, Sales, Hr, Support, and Development); Size (SMB, Enterprise)]: Worldwide Market Forecasts and Analysis (2013 - 2018), 2013 http://www.marketsandmarkets.com/Market-Reports/gamification-market-991.html [Accessed at 24 October, 2013]

[15] Kronenburg, R.: Running a Corporate University: Right Learning, Right People, Right Time…All The Time! - Caterpillar University, Proceedings of the 3rd Corporate Universities and Ac@demies Summit Brussels, 2013

[16] Hove, B.: A Cost Effective Global Learning Strategy with High Impact-What Should Be in Your Educator Toolbox? - AGFA Academy, Proceedings of the 3rd Corporate Universities and Ac@demies Summit Brussels, 2013

[17] Hooydonk, S.: Learning @Philips Lighting - Philips Lighting University, Proceedings of the 3rd Corporate Universities and Ac@demies Summit Brussels, 2013

[18] Standaert, C.: Guiding the Corporate University through Turbulent Times – ArcelorMittal University, Proceedings of the 3rd Corporate Universities and Ac@demies Summit Brussels, 2013

[19] Mangelsdorf, M.: Learning Design Futurology and the Learning Function 3.0. – 2020 Future Workplace Network, Proceedings of the 3rd Corporate Universities and Ac@demies Summit Brussels, 2013

[20] Gladwell, M.: Outliers: The Story of Success; Little Brown and Company, NY, USA, 2008

[21] Rajon, B: The Rive-Reine Experience – How Corporate T&L can make the difference – Nestlé University, Proceedings of the 3rd Corporate Universities and Ac@demies Summit Brussels, 2013

[22] Önen, S.: Integrating Talent Management Programs with the Corporate Academy Vision – Yapi Kredi Banking Academy, Proceedings of the 3rd Corporate Universities and Ac@demies Summit Brussels, 2013

[23] Brian Burke, research vice president at Gartner - Future of Gamification at Gartner Portals, Content and Collaboration Summit, March 12-14, 2012 in Orlando, FL, USA In: Gartner. Press Release https://www.gartner.com/newsroom/id/1844115?brand=1 [Accessed at 24 October, 2013]

[24] Gallagher, S., Garrett, G.: Disruptive Education – Technology-enabled Universities, The United States Studies Centre at the University of Sydney, 2013

[25] Simon, H.: The Sciences of the Artificial (second edition; first edition 1969) MIT Press, Cambridge, MA, USA, 1981

[26] Mintzberg, H.: Covert Leadership: Notes on Managing Professionals, Harvard Business School Publishing Company, MA, USA, 1998

[27] Williams, R., Karosousou, R., Mackness, J.: Emergent Learning and Learning Ecologies in Web 2.0, International Review of Research in Open and Distance Learning, Alberta, Canada, 2011